SYNERGETICS OF NUCLEAR BREEDING SYSTEMS

by

Charles W. Gordon, B.A.Sc., M.Eng.

A Thesis

Submitted to the School of Graduate Studies

in Partial Fulfillment of the Requirement

for the Degree

Doctor of Philosophy

McMaster University

1979

SYNERGETICS OF NUCLEAR BREEDING SYSTEMS

DOCTOR OF PHILOSOPHY (1979)
(Nuclear Engineering)

MCMASTER UNIVERSITY
Hamilton, Ontario

TITLE: Synergetics of Nuclear Breeding Systems

AUTHOR: Charles William Gordon, B.A.Sc. (University of Toronto)
M.Eng. (McMaster University)

SUPERVISOR: Professor A.A. Harms

NUMBER OF PAGES: xxiii, 259

ABSTRACT

The role of nuclear energy systems which produce fissile materials has become an important and essential part of scenarios for the future development of nuclear energy. Definitive analyses and nucleonic comparisons of these breeder systems have been impeded by the lack of a rigorous and consistent methodology for describing fissile fuel production and fertile fuel utilization. The research reported here therefore addresses itself to this problem and is based on a synthesis of three concepts: (1) the lumped parameter formulation of reactor physics, (2) the establishment of symbiotic relationships between breeders and converters and (3) the use of material stockpile inventories.

In the lumped parameter synergetic analysis the temporal variation of stockpile inventories and net electrical output of a selected system are established. The system is taken to consist of a general breeder reactor coupled to a fission converter reactor and fuel reprocessing-fabrication plant. By including the converter and processing plant and examining the temporal and nuclear behaviour of the entire system, various types of nuclear breeders can be analysed and subjected to a comparative analysis in a consistent manner. The use of lumped parameters, based on the integration of detailed space and energy dependent effects into single-valued parameters, has facilitated survey calculations and analysis of the conceptual systems defined herein. The temporal variation of the stockpile inventory is used to describe fissile

fuel production and fertile fuel utilization since information, such as minimum inventory requirements and material replacement times, is provided. This approach eliminates the ambiguities involved in a single figure of merit description, such as, for example, the doubling time, and includes pre-steady-state effects and reprocessing lags and losses. To assess the net electrical production of the system, the consumption of electricity by the reactors and the processing plant is explicitly included.

The synergetics of fast-fission, symbiotic fusion, hybrid fusion and spallation breeders are then investigated. In these analyses, the fissile and fertile inventories and power output are calculated over the system lifetime for a specific breeder power. The effects on the system inventories of varying breeder thermal power are also examined. Since the mathematical-physical formulations are specified in terms of lumped parameters, the results of changing these on the system can be easily dealt with. Four fissile fuel breeding systems are then compared using current economic data.

On the basis of this study, it is evident that there exists no single breeder system which consistently outperforms the others in all aspects. The fast-fission breeder, while not a good fissile fuel producer, has the best power generating efficiency and, due to its relatively low capital costs, can produce electricity at the lowest cost. The symbiotic fusion breeder system has the shortest fissile fuel replacement time and requires less initial fuel investment but it produces electricity at the highest cost. For combined fissile fuel production and electrical generation, the hybrid fusion breeder excells and

it is also a good conserver of fertile fuel. The spallation breeder outranks all others in fissile fuel production.

While no single breeder was found to be superior in a general sense, the synergetics method of analysis has been shown to be effective in several specific respects. The temporal variations of the stockpile inventories and net power derived here have a physically reasonable basis and are mathematically tractable. The pre-steady-state effects can be described with great accuracy by two functions determined by the fuel management scheme. Processing lags and losses are also explicitly incorporated. The flexibility and usefulness of the developed methodology are enhanced by the fact that any material stockpile inventory in the system can be calculated. Essential to this procedure is the inclusion at the outset of all system components in a synergetic analysis.

ACKNOWLEDGEMENTS

The author would like to acknowledge and thank all those who helped produce this thesis. In particular, the author would like to thank Dr. A.A. Harms who has provided much direction and help, Dr. J. Robinson and Dr. Volkov members of his supervising committee and Dr. M. Heindler of the Institute for Theoretical Physics and Reactor Physics, Technical University of Graz, Austria, with whom he has had many useful discussions. The author would also like to thank Ms. Georgina Savin for typing this thesis and Ms. A. de Fiesta for doing the drawings. Lastly, the author gratefully acknowledges his patient wife for her support and help without which this thesis could not have been written.

SYNERGETICS OF NUCLEAR BREEDING SYSTEMS

Table of Contents

List of Figures

List of Figures (continued)

List of Figures (continued)

List of Figures (continued)

List of Tables

List of Tables (continued)

List of Symbols

Symbol	Description	Page Introduced
a	Fraction of DT fusion energy possessed by neutrons	48
$a_{M,J,i}(\underline{r},t)$	Element of depletion matrix $\underline{a}_i(\underline{r},t)$ defined in Section 3.2	55
a_1, a_2, a_3	Coefficients in an equation for the system replacement time of material M	90
A_M	Atomic weight of material M	75
$A^D_{M,J,i}(t)$	Element of space integrated (over discharged volume) depletion matrix $\underline{A}^D_i(t)$ defined in Section 3.2	56
b	Fraction of DD reactions which produce tritium	61
$b_{M,J,K,i}(\underline{r},t)$	Element of depletion matrix $\underline{b}_i(\underline{r},t)$ defined in Section 3.2	55
b_1, b_2, b_3	Coefficients in an equation for the value of the minimum value of the system replacement time for material M	92
C_i	Specific capital cost of component i	232
C	Capitalized cost of the system	231
$(dN_{M,R}/dt)^-$	Rate at which material M is discharged from reactor R	70

List of Symbols (continued)

Symbol	Description	Page Introduced
$(dN_{M,S}/dt)_{SS}$	Steady-state rate of change of the stockpile inventory of material M	84
$(dN_{M,S}(t)/dt)^{R}$	Net rate of change of the stockpile inventory of material M due to reactor R	68
$(dN_{M,S}(t)/dt)^{R\pm}$	Rate of increase (+) or decrease (-) of the stockpile inventory of material M due to reactor R	68
$D_{M,i}(t)$	Specific rate of change function for reactor i and material M	76
E	Energy of incident protons, neutrons	39
$E_{M,i}(t)$	Specific rate of discharge of material M from reactor i	99
$f_{M,i}(\underline{v}_M,t)$	Normalized distribution function for ion M in velocity space of reactor i	47
F(t)	Fuel cycle expenses	231
$g_i(t)$	Function describing pre-steady-state net generation ratio variation in reactor i	71
G	Total fusion blanket net generation ratio	23
G_J	Net generation ratio of material J in a fusion reactor blanket	23

List of Symbols (continued)

Symbol	Description	Page Introduced
$G_{M,i}$	Net generation ratio of material M in reactor i	58
$h_i(t)$	Function describing pre-steady-state refuelling rate in reactor i	70
$H(t)$	Heaviside unit step function	75
I_i	Incident particle current in spallation reactor i	51
$I(t)$	Interim capital replacement costs	231
K	Parameter used to evaluate the characteristic reaction rate which gives a minimum stockpile inventory minimum value	92
ℓ_M	Fraction of material M entering reprocessing-fabrication which is lost	71
LF_i	Load factor for reactor i	104
M	Fusion blanket energy multiplication factor	23
$M(t)$	Nuclear material costs	231
$n_{M,i}(\underline{r},t)$	Atom density of material M in reactor i, an element of the material density array $\underline{n}_i(\underline{r},t)$	46
$n_{p,i}(\underline{r},E,t)$	Energy dependent density of particles of type p in reactor i	46

List of Symbols (continued)

Symbol	Description	Page Introduced
N_{AV}	Avagadro's number	75
$N_{M,i}(t)$	Number of atoms of material M in reactor i	45
$N_{M,S}(t)$	Number of atoms of material M in the inventory stockpile	68
$N^{D}_{M,i}(t)$	Number of atoms of material M in discharged volume of reactor i	56
$N^{SS}_{M,R}$	Number of atoms of material M in reactor i at steady-state	70
$O(t)$	Operational costs	231
P	Plant capital cost	231
$P_R(t)$	Power consumed by reprocessing-fabrication plant	97
P^{C}_{i}	Circulating power for reactor i	94
P^{G}_{i}	Gross electrical power output of reactor i	94
P^{I}_{i}	Power injected to reactor i core	96
P^{N}_{i}	Nuclear power generated in reactor i	96
P^{NET}_{i}	Net electrical power of reactor i	97
P^{T}_{i}	Thermal power of reactor i	94
$P^{NET}_{S}(t)$	Net electrical power output of system	97

List of Symbols (continued)

Symbol	Description	Page Introduced
$(P_B^T)_M^{MIN}$	Thermal power of breeder which minimizes the value of the minimum stockpile inventory of material M	181
q_p	Charge on incident spallation particle	51
Q_i^P	Plasma amplification factor for reactor i	142
Q_i^T	Total amplification factor for reactor i	96
r	Discount factor in economic analysis	231
$\underline{r}$	Position vector	46
R_i	Characteristic reaction rate of reactor i	47
$(R_B)_M^{MIN}$	Breeder characteristic reaction rate which minimizes the value of the minimum stockpile inventory of material M	79
$R_{M,i}^{r,p}(t)$	Rate of reaction of type [r,p] for material M in reactor i	45
s_p	Price of electrical power	233
$s_{N,J}$	Price of nuclear fuel of type J	233
S	Revenues from the system operation	233
t	Time	45
t_o	Time of startup after refuelling	56
$t_{M,i}(\underline{r},t)$	Rate at which material M is transferred into position about $\underline{r}$ in reactor i	54
T	Temperature	50

List of Symbols (continued)

Symbol	Description	Page Introduced
$T^{D}_{M,i}(t)$	Rate at which material M is transferred into the discharged volume in reactor i	56
$\bar{T}^{D}_{M,i}$	Rate at which material M is transferred into the discharged volume in reactor i averaged over the mean residence period	57
U_J	Energy released in spallation of material J by incident protons	39
$U^{r,p}_M$	Energy released by reaction of type [r,p] in material M	45
v	Speed of neutrons	46
v_p	Speed of incident spallation particles	51
$\underline{v}_M$	Velocity of ions of material M	47
$v_{A,B}$	Relative speed between ions of type A and B	47
V_i	Volume of reactor or domain i	46
V_{pi}	Volume of plasma in reactor i	50
V^{D}_i	Volume of fuel discharged from reactor i	56
W_M	Energy needed to reprocess-fabricate material M per atom	99
Y_J	Yield of neutrons by spallation with incident protons in material J	37

List of Symbols (continued)

Symbol	Description	Page Introduced
α_i	Fraction of injected energy recovered in reactor i	96
β	Ratio of plasma kinetic pressure to the magnetic field pressure	20
$\gamma_{M,J}^{r,p}(E)$	Probability that a reactor of type [r,p] in material J will result in the production of material M	54
$\delta_{K,L}$	Kronecker delta	54
$\Delta N_{M,i}^{D}(\tau_i^D)$	Change in number of nuclei of type M in the discharge volume after time τ_i^D	57
ϵ_i	Circulating energy for fraction for reactor i	94
η_i^I	Injector efficiency for reactor i	96
η_s^N	Nuclear-electrical conversion efficiency	100
$\eta_s^{NET}(t)$	Net system electrical conversion efficiency	100
$\eta_s^R(t)$	Reprocessing-fabrication electrical energy efficiency	100
η_i^T	Thermal-electric conversion efficiency of reactor i	94
Θ_M	Isotope weight factor for material/ isotope M	65

List of Symbols (continued)

Symbol	Description	Page Introduced
λ_M^P	Decay constant of material M decaying to material P	45
μ_i	Coefficient in decay chain equations	62
$\rho_{M,i}^{r,p}(t)$	Ratio of reaction rate of type [r,p] in material M in reactor i to the characteristic reaction rate of reactor i	50
$\sigma_M^{r,p}(E)$	Microscopic cross section of material M for a reaction of type [r,p]	44
τ_i^D	Mean residence period of fuel in reactor i	56
τ^{EOL}	Reactor-system lifetime	86
τ_R^{EOL}	Lifetime of reactor R	70
τ_S^{EOL}	System lifetime	115
τ_i^F	Time between refuellings in reactor i	56
τ_M^{MIN}	Time to reach the minimum value of the system inventory of material M	79
τ_M^D	System replacement time for material M	90
τ_M^R	Time needed to reprocess-fabricate material M	71
τ_R^{SS}	Time needed to reach steady-state in reactor R	70
$(\tau_M^{MIN})_{MIN}$	Minimum time to reach the minimum value of the system inventory for material M	88

List of Symbols (continued)

Symbol	Description	Page Introduced
$(\tau_M^0)_{MIN}$	Minimum value for system replacement time for material M	92
$\phi_i(\underline{r},E,t)$	Energy dependent neutron flux in reactor i	46
$\omega_{M,i}$	Steady-state specific inventory of material M in reactor i	74
$\omega_{M,i}^0$	Initial specific inventory of material M in reactor i	75

CHAPTER I

INTRODUCTION

1.1 Motivation

The role of nuclear energy systems which produce fissile fuels has in recent years become an important part of scenarios for the future of nuclear energy. These systems, referred to as breeders, transmute fertile isotopes into fissile isotopes using neutrons generated by various nuclear processes and in so doing make more efficient use of resources than current fission reactors. It is the method of generating neutrons which distinguishes the proposed types of breeders: fast-fission, fusion and spallation.

Comparison and analysis of different breeding systems have been impeded by the absence of a rigorous and comprehensive methodology. For example, the doubling time, a figure of merit for fast-fission breeders, gives a measure of the time needed for the breeder to produce enough fuel to startup an identical breeder reactor. If a reactor requires no initial fissile fuel, such as a symbiotic fusion breeder, then it will have a zero doubling time even though such a reactor may be generating less fissile fuel than a fast-fission breeder with a longer doubling time. Similarly, it should be possible to distinguish a system which breeds fissile fuel by consuming vast amounts of fertile material from one which conserves these resources. A further complication results from the production or consumption by breeder systems of energy

and hence it is not only the breeding capabilities but also the total power balance of a given reactor, which must be considered.

It is the aim of this thesis to investigate fissile fuel breeding systems in such a manner that the above deficiencies are avoided or minimized. Specifically, a combined system consisting of a fissile fuel breeder coupled by isotope and power linkages to a separate fission converter reactor will be considered. Such a configuration lends itself to an energy park where, with on-site fuel reprocessing and fabrication, only fertile material and electrical power would cross the boundaries.

The coupling of breeder and converter reactors has been labelled symbiosis[1] by analogy to the biological term describing the union of different organisms for mutual benefits. In the case of breeder-converter symbiosis, the breeder would supply fuel to the converter while receiving, if necessary, electrical power. Synergetics is a related term which literally means working together[2] but it is used here to refer to the study of an entire system as opposed to the components separately. It is this synergetic analysis which will allow us to analyse nuclear breeding systems consistently by including, from the outset, the converter reactor which will be fuelled by breeder produced fissile material.

The method which will be used is based on the stockpile inventory concept[3,4] and will be extended to include the symbiotic coupling of the breeder and converter reactors[5,6]. Temporal variation of an artificial stockpile and a system power balance are calculated using applicable system parameters. The reprocessing-fabrication plant is also included since it will be an integral part of the complete fuel

cycle. One of the features of this representation is the description of the temporal variation of any material in the system. This allows the tritium and lithium inventories to be evaluated which will be important to fuel cycle economics of a fusion reactor as well as the fertile inventory which will be necessary in economic and resource utilization studies.

The use of the stockpile inventory as a means of expressing fissile fuel production offers several advantages. This approach allows material generation rate transients to be found using analytical expressions thus eliminating the necessity for detailed computer simulations. Characteristics, such as the maximum amount of fissile or fertile fuel required can be derived which would not be possible using a single figure of merit. In addition, the effects of reprocessing, such as time lags and losses, and of pre-steady-state reactor cores are explicitly incorporated in this approach.

Lumped reactor parameters which are based on space and energy integrated values are used. Because these lumped parameters can be found from the existing literature or reliably estimated there is no need for repeated, detailed analyses of each reactor. Thus, survey calculations can be considerably simplified without the need to specify exact geometric and material changes. This approach also allows us to study efficiently conceptual designs for proposed breeding systems.

The type of fissile fuel breeding systems which will be considered here are designated as fast-fission, fusion and spallation breeder reactors. Essentially, the distinction among these is the method by which the neutrons used in transmutation are produced. In a

fast-fission breeder reactor, a critical core is constructed and maintained in such a way that more neutrons are produced than are lost in parasitic and fission events. These excess neutrons are then used in a breeding blanket surrounding the core. In contrast, fusion of deuterium and tritium in a plasma is the source of high energy neutrons in a fusion breeder. These neutrons interact in a blanket surrounding the fusion plasma to produce fissile fuel, tritium and heat. In the spallation breeder, neutrons are emitted when high energy protons strike target nuclei. These neutrons are used for breeding and heat generation in a blanket similar in design to fast-fission or fusion breeding blankets.

Although fission reactor technology is well developed and the fast-fission breeder is at the prototype stage, the use of other methods for producing fissile fuel has been proposed. Some of the reasons which have been advanced for introducing fusion breeders are:

1) fusion breeder reactors could be introduced earlier than pure fusion devices due to relaxation of plasma conditions[7-10];

2) breeding capabilities and resource utilization could be enhanced over fast-fission breeders[7,10,11];

3) the ^{232}Th-^{233}U fuel cycle could be used in advanced converter reactors without the use of ^{235}U or ^{239}Pu[1,12,13];

4) design options are expanded so that environmental effects might be minimized and safety enhanced[7,9,14].

The spallation breeder also offers utilization of thorium and uranium ores by efficient breeding[15,17], introduction of different fuel cycles[15,18] and added safety during operation[16]. In addition, the technological problems involved with implementing a spallation breeder appear to be less formidable than for a fusion breeder[15,18]. With such a wide range of breeding systems which will be available, it is essential that the fissile fuel and power producing capacities of the various systems be treated uniformly.

1.2 Development of Concepts

Three major concepts have been synthesized to produce the system model used here: breeder-converter symbiosis, lumped parameter analysis and the stockpile inventory. In this section we will present a brief summary of previous work germane to the development of our representation.

The first work on fusion breeder-fission converter symbiosis was by Lidsky and reported on in a paper to the British Nuclear Energy Society Fusion Conference at the Culham Laboratories in 1969[1]. The system considered consisted of a DT fusion breeder which produced fissile fuel and tritium in its blanket coupled to a molten salt converter reactor. Tritium produced in the breeder and fissile material in the fuel discharged from the converter reactor were recycled back into the respective reactors. In addition, fissile fuel produced in the fusion blanket was used in the converter reactor. The rates of changes of the tritium and fissile inventories were set equal to constants involving conversion ratios and specific inventories. From these

equations and by introducing a system time constant, an expression for the relative sizes of the components and a value for the doubling time were found. In his analysis, Lidsky did not consider reprocessing and, in fact, instantaneous reprocessing without losses was assumed. By fixing the doubling time and converter thermal power, he was able to determine the size of the breeder necessary to maintain the constant fissile-to-tritium inventory ratio which was assumed in the analysis. With the sizes of both reactors known, the power balance and economics could be calculated.

This type of lumped parameter analysis was extended by Gordon and Harms[5,19,20] to allow for processing losses and tritium production within the fission converter. In their analysis, equations for the rates of change of the fissile and tritium inventories of the combined system were found in terms of constant conversion ratios, specific inventories and loss fractions. By setting a boundary condition on one of the inventories, the reaction rate ratio for the two reactors could be found leading to the determination of the doubling time and power output of the system. Their numerical results included different breeder and converter reactors in a parametric analysis to identify potential efficient breeder-converter pairs. Although losses were included, processing was assumed to be instantaneous with respect to the doubling time; however, for very short doubling times, this was a poor assumption. Also, no pre-steady-state considerations were included in this constant coefficient analysis. This method was later extended to spallation breeders[6] and to dense plasma focus devices[21]

thus further illustrating the flexibility of the lumped parameter formulation.

An alternate method of dealing with symbiotic systems was used by Fortescue[22] to analyse both fusion and fission breeder systems. In his analysis, an atom balance for the annual fuelling rate of the fission converter including an allowance for expanding the fissile inventory or the converter power, was equated to the breeder output. Thus, an equation relating the breeder-to-converter power ratio and the annual growth rate of the fissile fuel was found. In this analysis, external inventories and delay times due to reprocessing and fabrication were included although pre-steady-state was not. This method was used to study gas-cooled fusion and fission reactors to compare their fissile fuel and electrical power producing capabilities.

The stockpile approach to analysing the fissile fuel breeding characteristics of a reactor was first proposed by Hardie et al[3] as a means of rigorously defining a doubling time. This method was later extended by the same group to include pre-steady-state in a fast-fission breeder[23]. They used an external stockpile as a means of accounting for fissile material passing into and out of a fast-fission breeder reactor. In this way it was possible to include in an expression for the fissile fuel doubling time factors to account for out-of-reacto. inventories and the losses associated with reprocessing and fabrication. Using the same procedure, a factor to account for the approach to steady-state in the reactor was also formulated.

The stockpile method of Hardie et al[3,23] was extended by Heindler and Harms[4] so that the temporal variation of the stockpile

inventory could be calculated in terms of analytical expressions. To do this, two stockpiles were set up, one which accounted for reactor fuelling and the other which accounted for discharged material. A piecewise continuous expression for the complete variation was found by adding the rates of change of these two stockpiles. The effects of reprocessing lags and losses was well as pre-steady-state in the core and blanket were explicitly included in their model.[9] The method was used to analyse a fast-fission breeder reactor and showed that significant errors can result from neglecting reprocessing lags and pre-steady-state terms. It was also found that the first doubling time for breeders, that is, the time needed for the stockpile to reach the pre-startup level, is not longer than the reactor lifetime plus the processing lag at which time the final core and blanket are returned to the stockpile. Subsequent doubling times, the time necessary to produce an additional amount of fissile material equal to the pre-startup level, may be less than the first; the cause for this has been attributable to the pre-steady-state effects.

1.3 Outline

Before developing the conceptual basis for the method, some nuclear energy systems to be analysed will be briefly described. An overview of types and conceptual designs for fission, fusion and spallation reactors will be given in order to introduce the relevant physics, engineering and data which will be used later. Fusion breeding blankets which are representative of other reactor blankets will

be discussed in some detail and conversion ratio and energy multiplication data introduced. In addition to the reactor systems, fuel reprocessing and fabrication will be presented.

The model of the breeder-converter system will be developed in Chapter III beginning with the nuclear reactions of interest and the notation for their description. A general isotope balance for a reactor will be used to define the net generation ratio. In addition, a relationship between the fissile and fertile net generation ratios will be found from the breeding-decay chain equations. The stockpile inventory concept will be described and an expression in terms of lumped system parameters for the temporal variation of the material stockpile established. From this will be obtained expressions for such characteristics as the minimum inventories and material replacement times. A power balance, including the energy for fuel processing, will be set up and used to extract relationships among the various parameters and efficiencies which describe the electrical power generation.

In the next three chapters, fission, fusion and spallation breeders will be described using this approach. In each case, a reference system will be used as a basis for comparison. The criteria which will be used in selecting the reference systems are comparable technologies and realistic engineering values. Chapter IV will contain the analysis of a gas-cooled fast-fission breeder reactor coupled to a high-temperature gas-cooled converter reactor. After defining the reference system, the stockpile characteristics will be described for the case where the breeder and converter thermal powers are equal.

Following this, the effects of changing the breeder power and some parameters will be investigated. In Chapter V, a similar analysis will deal with a symbiotic and hybrid fusion breeder; in Chapter VI a spallation breeder will be discussed.

The four reference breeder-converter systems will be compared in Chapter VII. The systems in which the breeder and converter thermal powers are equal will be discussed followed by a comparison of the effects of changing the breeder size. Finally, economics and how this representation could fit in will be introduced. A summary with conclusions will be given in Chapter VIII. A graphical depiction of this outline is shown in Fig. 1.3-1.

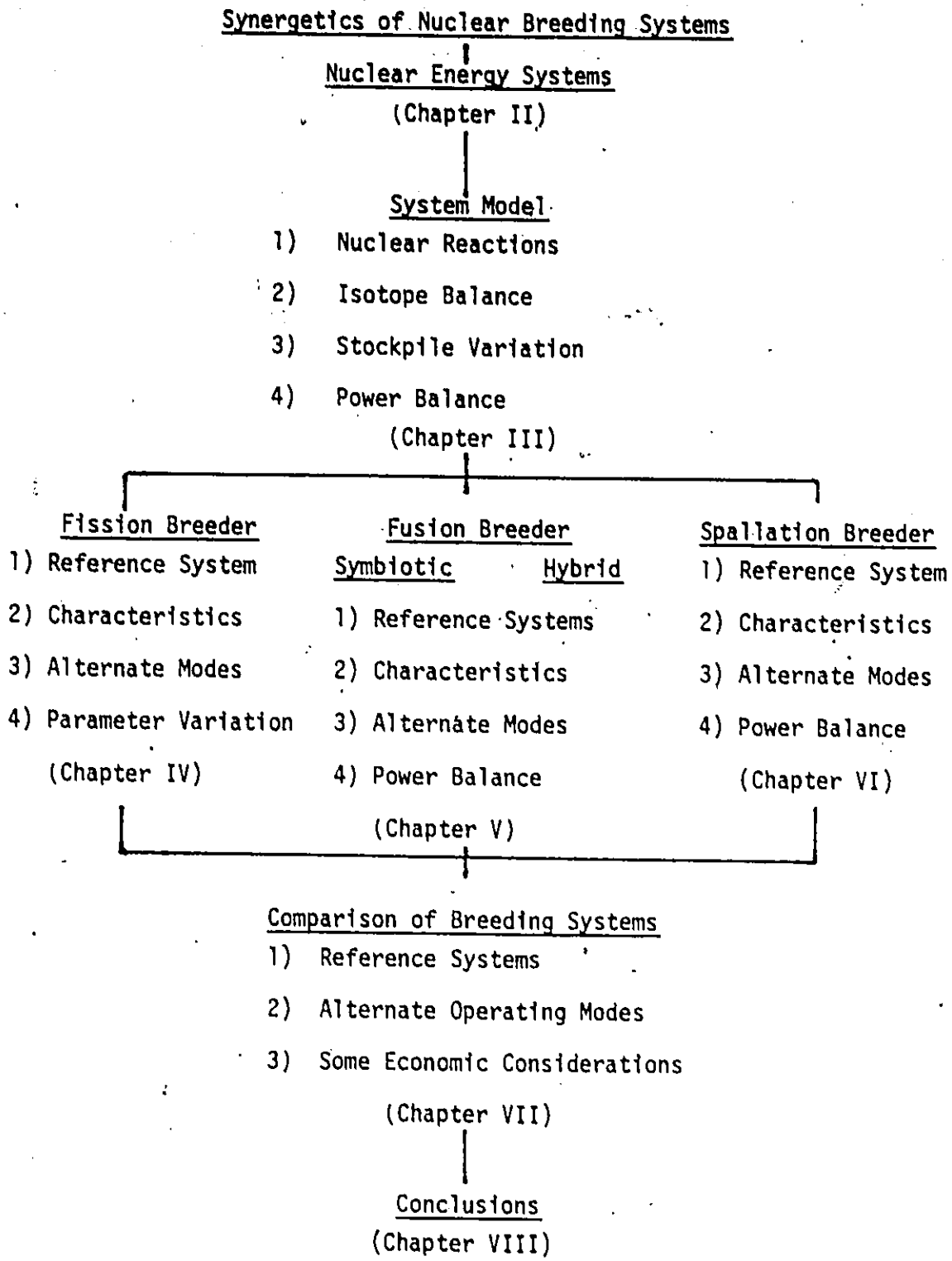

Fig. 1.3-1 Outline of study of nuclear breeding systems.

CHAPTER II

NUCLEAR ENERGY SYSTEMS

In this chapter fission, fusion and spallation reactors and fuel processing plants will be discussed. The aim here is to introduce the necessary physics and engineering to describe these in the model developed in Chapter III. Also, data used in sample calculations will be presented.

2.1 Fission Systems

Power in a fission reactor is produced from the fission of neutron multiplying fissile isotopes. Some of the neutrons released will be absorbed in parasitic capture, some may undergo radiative capture in fertile material to produce new fissile nuclei and at least one must induce another fission to maintain the chain reaction. Power reactors can be classified most conveniently for our purposes by the energy of the neutrons which cause the majority of the fissions and the coolant used. We will discuss some features of several fission reactor types with emphasis on fertile to fissile conversion, fissile inventory and thermal efficiency of each type.

For a fission reactor, the conversion, or breeding, ratio is defined as the number of fissile atoms produced per fissile atom destroyed. The specific inventory of a material is used here to refer to the initial mass in the core or blanket divided by the thermal power. Since these parameters will be important in the analysis to follow, some

values for various types of fission reactors are presented in Table 2.1-1 and Table 2.1-2. In Fig. 2.1-1, the approximate domains of reactor types are shown in a fissile specific inventory-conversion ratio plot. The spread of the data is due to the variety of designs possible within each grouping.

There is a continuum of designs in Fig. 2.1-1 for conversion ratio values between 0.4 and 1.6. The reactor type designated HWR (Heavy Water Reactor) refers to a class of reactors with a thermal neutron spectrum, moderated by heavy water and cooled by either heavy water, boiling light water or an organic coolant. Because of the good neutron economy associated with the low neutron absorption cross section of D_2O, natural uranium or low fissile enrichment fuels can be used. This neutron economy also allows future HWRs to have conversion ratios between 0.7 and 0.9[35] with a fissile specific inventory as low as 0.3 kg/MW_t. These reactors can be refuelled on power with the fuel having a mean residence period of 1.1 years for uranium or 3.5 years for thorium fuels[36]. The net thermal efficiency is in the range of 0.28 to 0.30[24]. This net efficiency includes the requirements of auxiliary systems, such as pumps and control units, which is about 5-10% of the gross electrical output[29].

Light Water Reactors (LWR), including both Pressurized Water Reactors (PWR) and Boiling Water Reactors (BWR), are cooled and moderated by light water and hence have a thermal neutron spectrum. In PWRs, the coolant-moderator is under a pressure of ~2200 psia to inhibit boiling in the core; for BWRs the pressure is lower, ~1000 psia, so that steam is produced within the core[29]. Because the neutron

Reactor Type	Conversion Ratio	Fissile Specific Inventory (kg/MW_t)	(Reference)
Heavy Water Reactors			
PHW(U)	0.45	0.36	(24)
PHW(U)	0.59-0.70	0.24	(25)
PHW(Th)	--	0.89	(25)
PHW(Th)	--	0.79	(25)
UCR(Th)	0.8	0.75	(12)
BLW(U)	0.85	0.65	(26)
Light Water Reactors			
PWR	0.5	0.69	(24)
PWR	0.5	0.77	(24)
PWR	0.5	0.65	(24)
PWR	0.6	0.80	(27)
BWR	0.5	0.95	(24)
BWR	0.7	1.04	(27)
High Temperature Gas Cooled Reactors			
	0.9	1.28	(11)
	0.7	--	(24)
	0.65	0.51	(27)
	0.65-0.90	--	(28)
Molten Salt Reactors			
	0.96	0.66	(11)
	1.049	0.35	(11)
	1.068	0.42	(29)

Table 2.1-1 Fission reactor conversion ratio and fissile specific inventory data.

Reactor Type	Conversion Ratio	Fissile Specific Inventory (kg/MW_t)	(Reference)
Liquid Metal Fast Breeder Reactors			
	1.3	0.99	(24)
	1.18	1.19	(25)
	1.20	0.92	(27)
	1.32	1.48	(29)
	1.42	0.46	(29)
	1.25	0.92	(29)
	1.57	1.47	(29)
	1.29	0.66	(30)
	1.50	0.56	(30)
Gas Cooled Fast Reactors			
	1.5	1.38	(24)
	1.39	1.28	(27)
	1.47	1.18	(28)
	1.50	0.91	(31)
	1.45	1.25	(31)
	1.45	1.00	(31)
	1.45	1.11	(31)
	1.47	1.15	(32)
	1.47	1.11	(32)
	1.5	0.83	(33)

Table 2.1-1 Fission reactor conversion ratio and fissile specific inventory data (continued)

Reactor	Power (MW_t)	Inventory (te)	Fissile Enrichment (%)	Fissile Specific Inventory (kg/MW_t)
Heavy Water Reactors				
Pickering	1744	92.6	natural	0.39
Gentilly 1	840	65.	natural	0.56
Bruce	2855	114.	natural	0.29
Gentilly 2	2131	85.5	natural	0.29
Cirene	120	10.2	0.71-1.1	0.60-0.94
Pressurized Light Water Reactors				
Cherokee County 1	3000	102.8	3.32	1.14
Davis Besse 3	2772	81.	2.5	0.73
Surry 4	2631	66.	2.8	0.70
Wyhl 2	3765	102.7	2.49	0.68
St. Lucie 2	2560	87.	2.4	0.82
Boiling Light Water Reactors				
Borts 2	3579	156.3	2.07	0.90
Phipps Bend 2	3579	138.	2.0	0.77
Leibstadt	3012	118.3	2.72	1.07
Browns Ferry 3	3293	169.	2.2	1.13
Dresden 2	2527	152.	2.1	1.26
Graphite Moderated-Helium Cooled				
Julich AVR	55	0.03U:0.40Th	93.	0.51
THTR Ventrop	750	0.28U:6.52Th	93.	0.35
Summit 1	2000	1.1U:27.32Th	93.	0.51
St. Rosalie 1	3210	1.88U:40.Th	93.	0.55
Fulton 1	3000	1.72U:37.5Th	93.15	0.53

Table 2.1-2: Specific inventory data for some fission reactors[34].

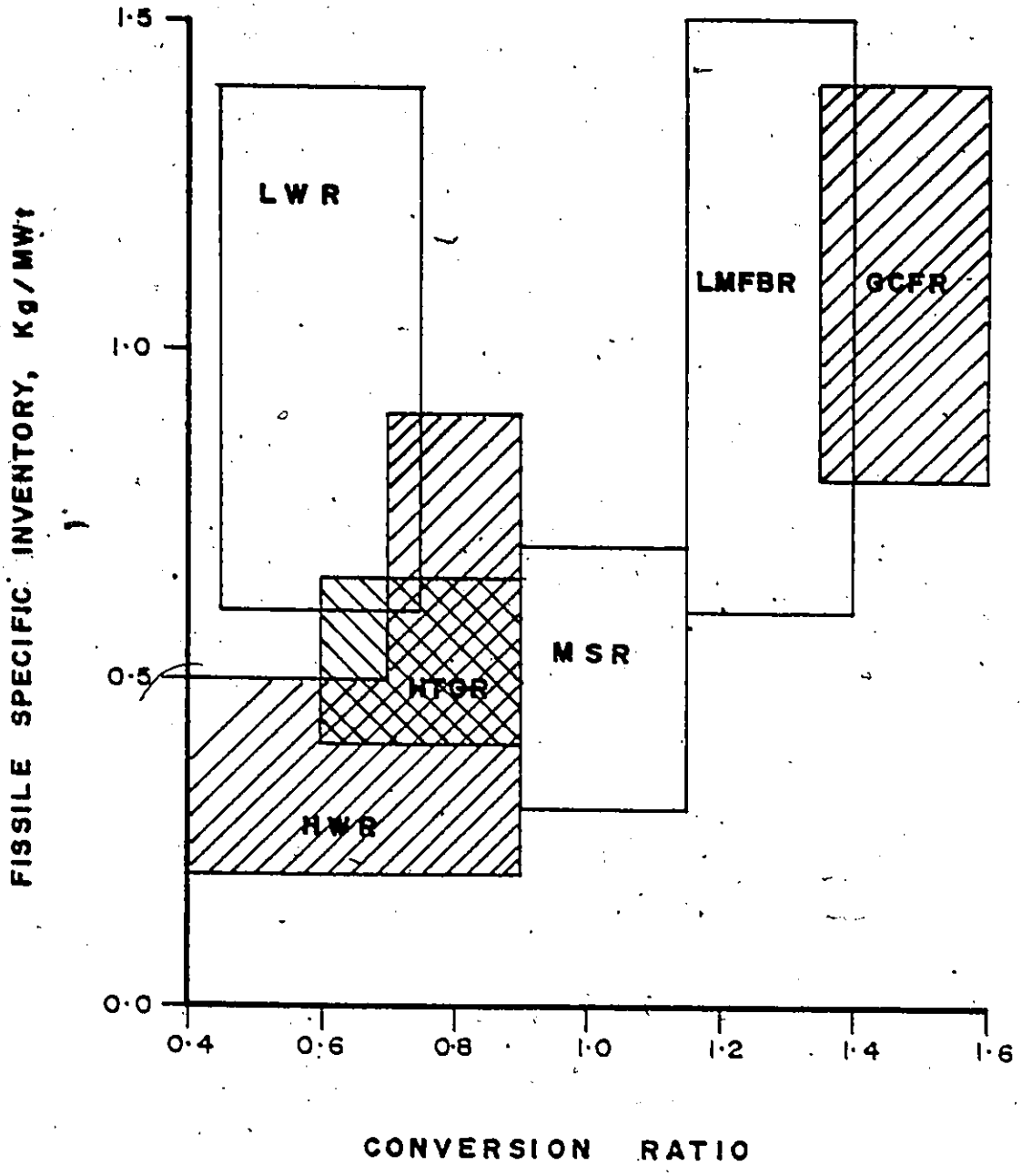

Fig. 2.2-1: Approximate fissile specific inventory-conversion ratio domains for several fission reactor concepts.

absorption cross section for light water is higher than for heavy water, the reactor fuels must be enriched with fissile material, typically to 2-3%[24]. The core is refuelled such that approximately one third of the entire core is replaced each year[24]. The thermal efficiencies of LWRs are typically 30-33%[29].

High Temperature Gas-cooled Reactors (HTGR) have a thermal neutron spectrum, are helium cooled and graphite moderated. The low neutron absorption cross sections of helium and graphite provide good neutron economy so that conversion ratios of 0.6-0.9 are possible. Most HTGRs are fuelled with pellets of highly enriched UC_2 mixed with ThC_2 in a graphite matrix and, as with the LWRs, about one third of the core is replaced each year[37]. With a gas coolant, higher temperatures are possible and thermal efficiencies of 39-40% are attained[28]. The transition between converter and breeder reactors, those which have conversion ratios greater than unity, is bridged by Molten Salt Reactors (MSR). These reactors are fuelled with a molten salt of LiF, BeF_2, ThF_4 and UF_4 which is pumped through a graphite moderated core at high temperatures.

Two types of fast-fission breeder reactor designs have been considered for future use: liquid metal and gas cooled. In these reactors, the energy of those neutrons inducing the majority of fissions is 200-500 keV rather than 0.025 ev as in thermal reactors. The Liquid Metal Fast Breeder Reactor (LMFBR) is cooled by liquid sodium and operates on a U-Pu fuel cycle. Here, a core enriched to 13-20%[38] in fissile material is surrounded by a blanket of natural or depleted uranium. Breeding ratios of 1.15-1.40 are projected with thermal-to-

electric conversion efficiencies of about 32%[29]. In Gas Cooled Fast Reactors (GCFR), the core is enriched to ~12% and a thorium blanket is used[31]. As with the HTGR, thermal efficiencies of 38-40% are possible due to the high temperatures available with the pressurized helium coolant[28]. In fast-fission breeder reactors, breeding is divided between the core (50%), the radial blanket (32%) and the axial blanket (18%)[38] with the refuelling scheme such that about one third of the core and one sixth of the blanket fuel elements are replaced each year[39].

2.2 Fusion Systems

The first generation of fusion reactors will most likely be fuelled with a deuterium-tritium mixture because, of the possible fusion reactions, the plasma temperature required for net energy production is lowest; concurrently, the energy gain per reaction is high. The condition for energy breakeven, that is, when the electrical power produced equals the electrical power input required to maintain the plasma, is generally called the Lawson criterion[40] and is expressed in terms of the product of plasma density and confinement time. To attain the Lawson criterion, the plasma must be contained either by magnetic fields or the inertia of the plasma.

In magnetic confinement, the charged particles of the plasma are held in orbits about the magnetic field lines, thus, the kinetic pressure of the plasma is constrained by the magnetic pressure of the applied field. In this confinement scheme, densities of 10^{14} - 10^{16} cm^{-3} and confinement times of 10 - 0.1 sec are required[41]. Magnetic confine-

ment schemes can be characterized as follows:

1) open or closed, depending upon whether the magnetic field lines leave the confinement region;

2) high (>10%) or low (<10%) β, where β is the ratio of plasma kinetic pressure to the magnetic field pressure;

3) pulsed or steady-state.

To achieve fusion temperatures, some means of heating the plasma is required. One form of heating is by neutral beam injection whereby fuel ions are created outside the reactor, accelerated to 200 - 1000 keV, neutralized by charge exchange and injected into the plasma. Because they are initially neutral, the particles can cross the magnetic field lines but are then rapidly ionized in the plasma adding energy and new fuel particles. Radio-frequency fields can be utilized as another method of heating. Other sources include thermalization of the 3.5 MeV alpha particles which are formed by DT fusion once the fuel starts to burn, ohmic heating if a current is present in the plasma and compression. For long burn time or steady-state devices, the spent fuel, ash and impurities must be removed and new fuel added. Open systems have a means of removing these by end losses while for closed systems, magnetic field lines near the wall can be diverted to a separate chamber. These diverters allow for the removal of fusion products and also reduce the flux of plasma to the wall and impurities from the wall into the plasma. New fuel can be added by neutral beam injection or by the injection of frozen pellets of fuel.

The TOKAMAK fusion reactor is a low β, toroidal device. The ionized plasma forms the secondary of a set of transformer cores whose

primaries are driven by a pulse of current which induces a toroidal current in the plasma. This current heats the plasma by ohmic heating and sets up the poloidal magnetic field which contains the plasma. A second, toroidal magnetic field is induced by a set of windings to stabilize the plasma. A TOKAMAK may operate as a steady-state or quasi-steady-state reactor with diverters for removing ash and neutral beam injection for heating and refuelling.

The mirror type fusion device is an open system with a high β which operates at steady-state. In the mirror, the stronger fields at the ends reflect the ions back into the plasma region so that only ions with a trajectory parallel to the magnetic field lines can escape. This provides a natural means of removing ash; however, it also represents a loss of a large amount of energy from the plasma. Direct conversion of the energetic charged particle energy to electrical power is usually included in conceptual designs in order to recover some of this energy. Neutral beams are used to supply both energy and fuel. Because the device operates at steady-state, the magnetic field coils must be superconducting to minimize ohmic heating losses.

Inertial confinement is based on the finite time needed for a rapidly heated mass of plasma to disassemble. Energy either from laser light, relativistic electrons or high energy ions is deposited on the surface of a fuel pellet, ablating the outer layers and causing a radially converging compression wave in the remaining pellet. Atom densities at the centre of the pellet may reach 10^{26} cm^{-3}; at these densities disassembly times of 10^{-9} sec still allow a net production of energy[42]. In a laser-induced inertial-confinement reactor, pellets

of solid deuterium-tritium are injected into a chamber, irradiated by a laser beam and the resultant energy released by fusion is absorbed and multiplied in a blanket. Because of the pellet injection, the inertial confinement device is inherently a pulsed reactor.

2.3 Fusion Blankets

The neutrons produced by DT fusion devices do not interact strongly in the plasma, thus, 80% of the energy per fusion reaction could potentially be lost from the system energy balance. To extract this energy, an envelope or blanket is placed around the plasma in which the neutrons will interact to release their kinetic energy and, by suitable choice of materials, produce tritium and fissile isotopes. The heat generated will be removed by a coolant and used to produce electricity; the nuclear fuels will be used in fusion and fission reactors.

The design of a breeding blanket is constrained by mechanical and nuclear considerations. Integrity of the device must be maintained at all times but with minimum parasitic neutron absorptions. The blanket has to conform to the geometry of the magnetic coils and be as thin as possible since capital costs of superconducting magnets are strongly influenced by the blanket thickness. Penetrations and asymmetries in the blanket can reduce the production of fuel and energy[43] but nevertheless, allowances are required for vacuum integrity, coolant couplings, blanket replacement and maintenance. The radiation from the plasma and nuclear reactions within the blanket could cause structural damage, particularly in the first wall. Also, in DT fusion devices, the tritium production rate must exceed the consumption and loss rates.

Subcritical operation is essential at all times in breeding blankets. The fissile fuel production and/or energy production must be maximized within these constraints.

There are many ways to classify the conceptual blankets which have been proposed. We choose to characterize them by the fissile isotope(s) produced, that is;

1) blankets which breed ^{233}U;

2) blankets which breed ^{239}Pu;

3) blankets which breed both ^{233}U and ^{239}Pu.

For these blankets, the parameters of interest are those which describe the energy and fuel production. The parameter related to energy production is the blanket energy multiplication factor denoted by M. Here, M is defined as the total energy released in the blanket divided by the energy of the incident neutrons. Fuel production, both fissile and tritium, is given by the net generation ratio. For a material of type J, the net generation ratio for a DT fusion blanket is defined as the net number of nuclei of type J produced in the blanket per DT fusion reaction. Thus, G_{U3} refers to ^{233}U production; G_{Pu9}, to ^{239}Pu production and G_T, to tritium production. Two other parameters will be derived from these: the total blanket generation ratio, G,

$$G = G_{U3} + G_{Pu9} + G_T \; ; \qquad (2.3\text{-}1)$$

and the ratio of tritium production to total generation, G_T/G. A representative example of each of the three blanket types will be presented below followed by a discussion of some data selected from the literature.

For thorium containing blankets, those described by Cook et

al[44] for a laser-induced fusion reactor have been chosen. Their neutronic analysis was performed using the TART Monte Carlo code; for each run, 10^4 histories were followed yielding a theoretical standard deviation of ~2%. Two types of thorium blankets were investigated: fissioning and non-fissioning; the difference being higher neutron energies in the thorium region in a fissioning blanket. The fuel region of lithium-cooled, stainless-steel-clad fuel pins consisted of thorium metal, lithium coolant, cladding and structure. For the fissioning blanket, it was found that M = 2.3, G_{U3} = 0.84 and G_T = 1.0 while for the non-fissioning blanket, M = 1.3, G_{U3} = 0.33 and G_T = 1.05. The number of fission events in the non-fissioning case was reduced to 15% of the fissioning blanket result but the fissile fuel production was reduced to 39%. Clearly, a penalty must be paid if neutron multiplication by fission is suppressed.

The Lawrence Livermore Laboratory mirror hybrid blankets investigated by Bender et al[45,46] have been selected as representative of uranium containing blankets. This analysis was also performed using the TART Monte Carlo code. A nearly spherical modular blanket consisting of an outer and an inner pressure vessel of stainless-steel containing two fuel regions was used. The region nearest the plasma was fuelled with uranium and 7% molydenum and the other region fuelled with lithium aluminate and graphite. Both fuel zones are helium cooled and have stainless-steel structure.

A blanket composed of concentric spherical shells with each shell containing a homogeneous mixture of materials was assumed for the neutronic analysis. With the first wall 10 m from the centre of the

plasma, the blanket thickness was maintained at 1.0 m while the thicknesses of the two fuel zones were varied. For a fission zone thickness of 25 cm, the values of M, G_{Pu9} and G_T were estimated to be 10.2, 1.75 and 1.1 respectively. As the thickness of the fission zone is decreased, both plutonium production and energy multiplication decrease due to the decrease in fission produced neutrons; however, more neutrons can penetrate the second zone so the tritium production increases. An estimate of the effects of exposure were also calculated; first wall neutron wall loadings of 5 MW·yr/m^2 or less were recommended for this blanket. At the end of such an exposure, the blanket energy multiplication was found to be doubled, the plutonium net generation ratio decreased by ~9% and the tritium net generation ratio increased by ~40%. The fissile concentration reached 2.5% at the end of the exposure but the blanket remained well subcritical with the neutron multiplication factor less than 0.5.

The final blanket design we present is for a blanket with both thorium-uranium and uranium-plutonium conversion as designed by Su et al[47]. The design has a neutron converter region containing ^{238}U enriched with ^{239}Pu to an equilibrium value of 8% next to the vacuum wall. The uranium-plutonium mixture was used because it is more effective for neutron multiplication than thorium-uranium in fast neutron spectra, hence, a thinner converter region could be used.

A one-dimensional cylindrical geometry was used in the ANISN transport code model with a uniformly distributed, isotropic 14 MeV fusion neutron source. Niobium was used throughout because of its superior fabrication characteristics, low sputtering ratio, stability

against structural failure and its relatively high (n,2n) reaction cross section. The neutron converter containing ^{238}U and ^{239}Pu fuel pins cooled by helium precedes the 40 cm breeding region of ThC fuel pins cooled by liquid lithium. This was followed by 30 cm of graphite moderator and 10 cm of lithium absorber to capture escaping thermal neutrons. Thorium carbide was chosen because of the possibility of using the irradiated fuel pins in a gas-cooled fission reactor without reprocessing.

For the fresh blanket, they found $G_{U3} = 3.54$, $G_{Pu9} = 0.59$ and $G_T = 1.05$. The blanket energy multiplication factor was 80.9 and the neutron multiplication factor, 0.944. A time dependent depletion calculation was performed to simulate a two year irradiation. It was found that the tritium production was increased ~40%, the production of ^{233}U increased ~16% while the production of ^{239}Pu decreased by ~85% due to the increase in the plutonium fission rate. The combined fissile generation ratio, $G_{U3} + G_{Pu9}$, increased only 1.5%. The neutron multiplication factor was 0.958 at the end of the irradiation.

In Tables 2.3-1, 2.3-2 and 2.3-3, a selection of some conceptual blanket design data are presented for blankets with ^{232}Th - ^{233}U conversion, ^{238}U - ^{239}Pu conversion and mixed ^{232}Th - ^{233}U and ^{238}U - ^{239}Pu conversion, respectively. The data in these tables gives the fissile net generation ratio, G_T, the total blanket generation ratio, G, the ratio of tritium production to total generation, G_T/G, and the blanket energy multiplication, M. Fig. 2.3-1 shows a blanket energy multiplication-blanket generation ratio plot. Points on the diagram joined by a solid line represent continuous variation of some variable. The thorium blankets tend to have both a low total generation ratio, $1.2 < G < 2.1$, and

Net Generation Ratios				Energy Multiplication	(Reference)
G_{U3} (a)	G_T (a)	G (b)	G_T/G	M(c)	
0.33	1.13	1.45	0.78	1.59	(1)
0.89	0.93	1.82	0.51	12.3	(48)
0.69	1.27	1.98	0.65	33.2	(48)
0.23	1.35	1.58	0.85	32.2	(49)
0.02	1.44	1.45	0.99		(12)
0.07	1.39	1.45	0.95		(12)
0.19	1.26	1.45	0.87		(12)
0.30	1.15	1.45	0.79		(12)
0.22	1.28	1.50	0.85		(12)
0.09	1.37	1.46	0.94		(12)
0.24	1.24	1.48	0.84		(12)
0.13	1.35	1.48	0.91		(12)
0.22	1.28	1.50	0.85		(12)
0.08	1.35	1.43	0.94		(12)
0.27	1.02	1.29	0.79		(12)
0.14	1.30	1.44	0.90		(12)
0.11	1.36	1.47	0.92		(12)
0.22	1.28	1.50	0.85		(12)
0.18	1.30	1.48	0.88		(12)
0.73	1.00	1.73	0.58	2.28	(50)
0.84	1.00	1.84	0.54	2.3	(51)

Table 2.3-1: Listing of selected characteristics of thorium blankets.

Net Generation Ratios				Energy Multiplication	(Reference)
G_{U3} (a)	G_T (a)	G (b)	G_T/G	M (c)	
0.14	1.12	1.26	0.89	1.1	(51)
0.48	1.0	1.48	0.68	1.9	(51)
0.55	1.0	1.55	0.64	1.9	(51)
0.56	1.0	1.56	0.64	2.1	(52)
0.49	1.0	1.49	0.67	1.8	(52)
0.71	1.17	1.88	0.62	2.2	(52)
0.50	1.05	1.55	0.68	2.0	(44)
0.72	1.17	1.89	0.62	2.3	(44)
0.84	1.0	1.84	0.54	2.3	(44)
0.55	1.07	1.62	0.66	1.6	(44)
0.33	1.05	1.38	0.76	1.3	(44)
0.29	1.00	1.29	0.82	1.3	(44)
0.14	1.12	1.26	0.89	1.1	(44)
0.56	1.02	1.58	0.64	2.1	(44)
0.45	1.0	1.45	0.69	1.8	(44)
0.45	1.0	1.45	0.69	1.8	(44)
0.49	1.02	1.51	0.67	1.8	(44)
0.71	1.13	1.84	0.61	2.2	(44)
0.71	1.17	1.88	0.62	2.2	(44)
0.83	0.8	1.48	0.44	1.6	(44)
1.78	0.25	2.03	0.12	2.8	(44)

Table 2.3-1: Listing of selected characteristics of thorium blankets. (continued)

Net Generation Ratios				Energy Multiplication	(Reference)
G_{U3} (a)	G_T (a)	G (b)	G_T/G	M (c)	
0.75	1.1	1.85	0.60	2.5	(52)
↓	↓	↓	↓	↓	
0.5	1.2	1.7	0.71	5.0	(52)
0.61	1.05	1.66	0.63	2.2	(53)
0.62	1.08	1.70	0.63	1.16	(54)
0.84	0.71	1.55	0.46	1.0	(54)
1.23	0.39	1.62	0.24	0.8	(54)
0.93	0.57	1.50	0.38	0.45	(54)

Table 2.3-1: Listing of selected characteristics of thorium blankets. Arrows joining data points indicate continuous variation of some parameter (continued).

(a) G_J is the net number of nuclei of type J produced per DT fusion reaction;

(b) $G = G_{U3} + G_T$;

(c) M is the total energy released in the blanket divided by the incident neutron energy.

Net Generation Ratios				Energy Multiplication	(Reference)
G_{Pu9} (a)	G_T (a)	G (b)	G_T/G	M (c)	
1.70	0.99	2.69	0.37	8.94	(48)
1.97	1.09	3.06	0.36	13.83	(48)
2.12	1.18	3.30	0.36	18.51	(48)
2.67	1.38	4.05	0.34	30.57	(48)
1.66	1.18	2.84	0.41	21.7	(48)
0.93	1.26	2.19	0.57	22.4	(48)
1.06	1.50	2.56	0.59	34.3	(48)
0.67	1.27	1.93	0.65	22.2	(48)
0.57	1.26	1.83	0.69	17.2	(48)
0.18	1.57	1.75	0.90	28.4	(48)
0.29	1.27	1.56	0.81	22.2	(48)
0.57	1.14	1.71	0.67	37.0	(48)
4.56				14.6	(55)
5.03				20.0	(55)
5.52				27.2	(55)
7.91				56.5	(55)
3.92				12.8	(55)
4.11				14.5	(55)
4.18				16.9	(55)
4.55				22.8	(55)
7.44				50.9	(55)

Table 2.3-2: Listing of selected characteristics of uranium blankets.

Net Generation Ratios				Energy Multiplication	(Reference)
G_{Pu9} (a)	G_T (a)	G (b)	G_T/G	M (c)	
1.1	1.3	2.4	0.54	9.0	(56)
2.15	0.64	2.79	0.23		(57)
0.59	2.41	3.00	0.80		(57)
1.30	1.83	3.13	0.58		(57)
1.95	1.02	2.97	0.43	10.0	(51)
0.41	1.92	2.33	0.82	5.3	(51)
0.91	1.2	2.11	0.57	5.9	(51)
1.34	1.0	2.34	0.43	7.0	(51)
1.0	1.1	2.1	0.52	6.0	(51)
1.95	1.02	2.97	0.34	10.0	(44)
0.41	1.92	2.33	0.82	5.3	(44)
1.0	0.8	1.8	0.44	5.2	(58)
2.25	0.15	2.4	0.06	7.2	(58)
1.45	0.75	2.20	0.34	6.4	(58)
1.43	0.82	2.25	0.36	6.40	(58)
1.31	0.91	2.22	0.41	6.43	(58)
1.30	1.02	2.32	0.44	6.54	(58)
1.27	0.96	2.23	0.43	6.40	(58)
1.25	1.08	2.33	0.46	6.42	(58)
1.38	0.85	2.33	0.38	6.43	(58)

Table 2.3-2: Listing of selected characteristics of uranium blankets (continued).

Net Generation Ratios				Energy Multiplication	(Reference)
G_{Pu9} (a)	G_T (a)	G (b)	G_T/G	M (c)	
1.82	1.14	2.96	0.38	10.0	(52)
↓	↓	↓	↓	↓	
0.74	1.39	2.13	0.65	5.9	(52)
1.8	1.1	2.9	0.38	10.0	(52)
1.7	1.8	3.5	0.51	21.0	(52)
1.95	1.02	2.97	0.34	10.0	(53)
1.99	1.07	3.06	0.35	10.4	(53)
1.96	1.04	3.0	0.35	11.4	(53)
1.34	1.06	2.4	0.44	7.0	(53)
4.58	1.16	5.74	0.20	80.2	(53)
1.04	1.06	2.1	0.50	25.0	(53)
1.05	1.03	2.08	0.49	23.6	(53)
0.94	1.16	2.10	0.55	25.1	(53)
1.03	1.00	2.03	0.49	18.7	(53)
1.05	1.18	2.23	0.53	35.4	(53)
0.33	1.0	1.33	0.75	39.8	(53)
2.24	1.1	3.34	0.33	8.7	(59)
2.65	0.28	2.93	0.10	10.7	(60)

Table 2.3-2: Listing of selected characteristics of uranium blankets. Arrows joining data points indicate continuous variation of some parameter (continued).

(a) G_J is the net number of nuclei of type J produced per DT fusion reaction;

(b) $G = G_{Pu9} + G_T$;

(c) M is the total energy released in the blanket divided by the incident neutron energy.

Net Generation Ratios				Energy Multiplication	(Reference)
$G_{U3} + G_{Pu9}$ (a)	G_T (a)	G (b)	G_T/G	M (c)	
1.54	1.07	2.61	0.40	6.6	(51)
2.08	0.94	3.02	0.31	7.0	(54)
1.05	1.09	2.14	0.51	2.57	(54)
1.32	0.99	2.31	0.43	4.32	(54)
2.08	0.23	2.31	0.10	4.32	(54)
2.14	0.88	3.02	0.29	6.81	(54)
1.54	1.07	2.61	0.41	6.6	(44)
1.90	1.05	2.95	0.36	10.0	(44)
2.21	0.29	2.50	0.12	5.4	(44)
1.38	1.12	2.5	0.45	6.2	(44)
2.08	0.89	2.97	0.30	32.2	(47)
1.88	0.55	2.44	0.23	14.7	(47)
3.01	2.34	5.35	0.44	107.9	(47)
3.65	1.45	5.10	0.28	79.2	(47)
3.56	1.73	5.30	0.33	79.2	(47)
3.78	1.47	5.35	0.28	79.9	(47)
4.13	1.05	5.18	0.20	80.9	(47)
4.03	0.92	4.95	0.19	83.0	(60)

Table 2.3-3: Listing of selected characteristics of thorium-uranium blankets.

(a) G_J is the net number of nuclei of type J produced per DT fusion reaction;

(b) $G = G_{U3} + G_{Pu9} + G_T$;

(c) M is the total energy released in the blanket divided by the incident neutron energy.

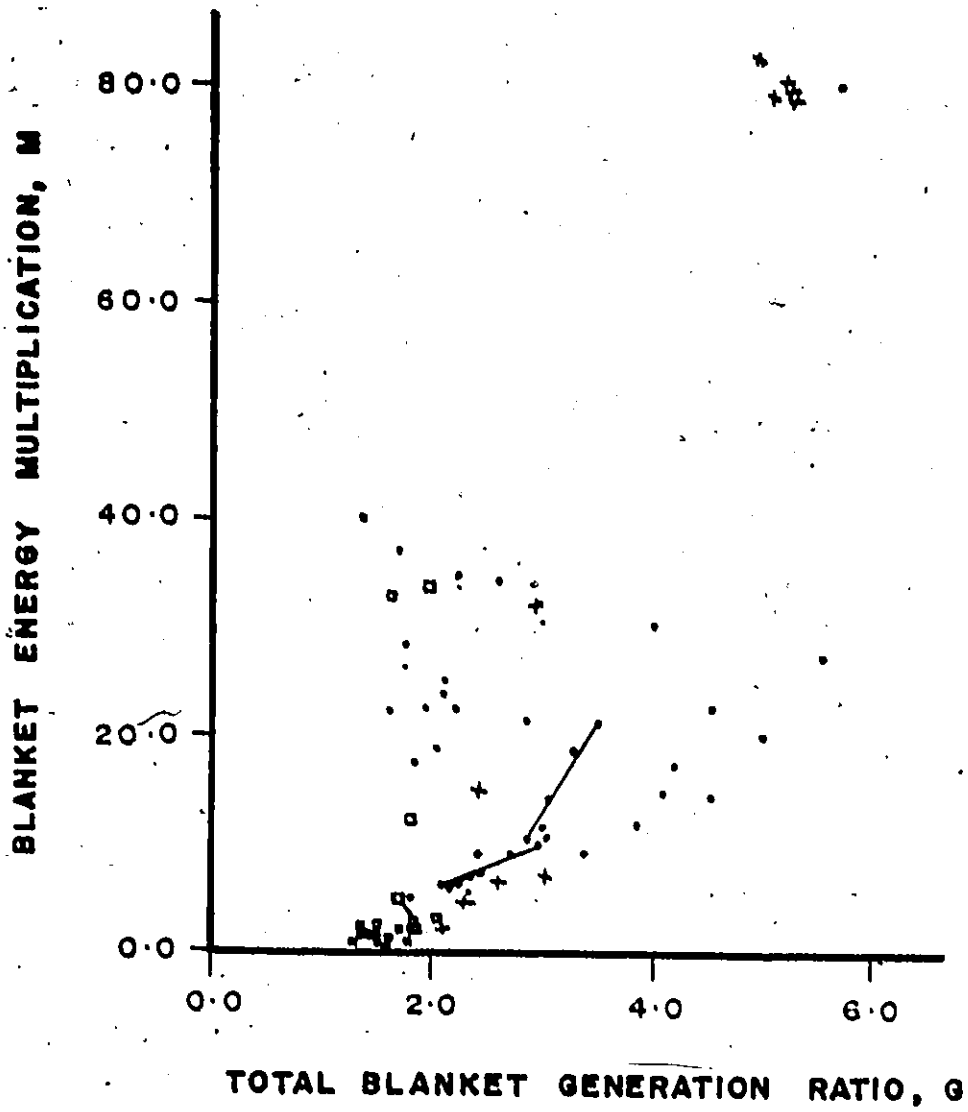

LEGEND:
- • BLANKETS WITH U-Pu CONVERSION
- □ BLANKETS WITH Th-U CONVERSION
- + BLANKETS WITH U-Pu and Th-U CONVERSION

Fig. 2.3-1: Blanket energy multiplication-blanket conversion ratio plot for three blanket types.

a low energy multiplication, M<5.0. There are, however, some blankets which have a higher energy multiplication due to increased fissile enrichment. The uranium blankets are scattered throughout the plot but generally are within 1.5<G<5.5 and 5.0<M<40.0. This domain is higher than the thorium regime since uranium is a better neutron multiplier and these blankets tend to be enriched more than those using thorium. The mixed blankets, due to the lack of data, are difficult to bound; however, they tend to fall into two groups: one group within the uranium blanket regime and a second group with M~80.0 and G~5.5. This wide range is due to the increased design operations available and a tendency to make these blankets near critical. In Fig. 2.3-2, the data is plotted with G_T/G versus the total generation ratio, G. This plot shows the wide range of design possibilities available for the split between tritium and fissile fuel production.

2.4 Spallation Systems

The production of neutrons by accelerator techniques has been under consideration since the Material Testing Accelerator at the Lawrence Livermore Laboratory in the early 1950's[18,61]. Use of these neutrons for the production of fissile fuel has been referred to as a spallation breeder[18], an electro-nuclear breeder[15], a clean breeder[61] and an accelerator breeder[16]. In the spallation breeder, high energy ions, either protons, deuterons or tritons, are accelerated toward a material which has a high atomic number; neutrons are then generated in the resultant spallation and evaporation events. These neutrons are used for fertile to fissile conversion in a blanket surrounding the target.

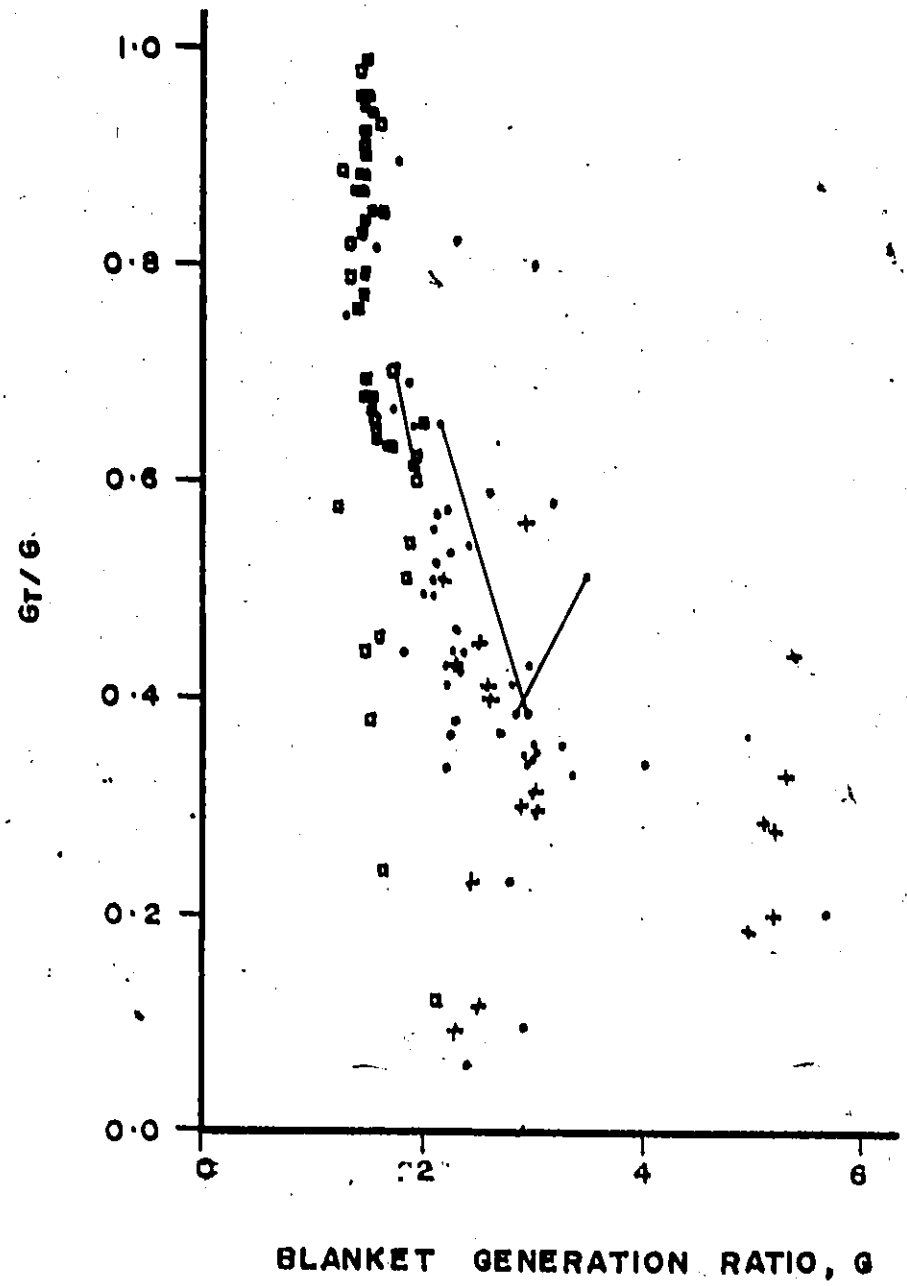

LEGEND:
- • BLANKETS WITH U-Pu CONVERSION
- ▫ BLANKETS WITH Th-U CONVERSION
- + BLANKETS WITH U-Pu and Th-U CONVERSION

Fig. 2.3-2: Ratio of tritium to total generation ratio plot for three blanket types.

Typically, a proton linear accelerator would be used to obtain a continuous, ~300 mA current of 1 GeV protons which strike a lead-bismuth or uranium target[18]. Lead-bismuth is preferred because its heat transfer qualities are superior to those of uranium and because the power density in a uranium target may be excessive due to the fissioning of ^{238}U and ^{239}Pu. The blanket for a spallation breeder is similar to the fast-fission or fusion breeder blankets as to choice of fuel cycle, coolant and form of the fuel.

An accelerator used in a spallation breeder should have a high average beam power, a high efficiency in converting electrical energy to proton energy at 100% duty factor, a high reliability (>90%) and a low beam spill to minimize losses. To achieve the necessary 1 GeV proton energy, a linear accelerator approximately 1.0 km long[18] is anticipated which will put severe constraints on beam handling systems. The conversion of electricity to proton energy can be accomplished presently with 6-10% efficiency[18] but improvements to 50-75% are possible and not far beyond current technology[61].

The neutrons generated by cascade or evaporation processes undergo reactions similar to those that occur in fast-fission and fusion breeder blankets but the higher energies possessed by spallation neutrons tend to decrease parasitic absorptions and enhance neutron multiplication reactions. Neutron yield data from various references are displayed in Fig. 2.4-1 for protons striking lead and uranium targets. For 1 GeV protons incident on ^{238}U, the expected number of spallation neutrons released varies from 20 to 40 and the total number of neutrons released per proton ranges from 25 to 100[61]. For deuterons, there is an

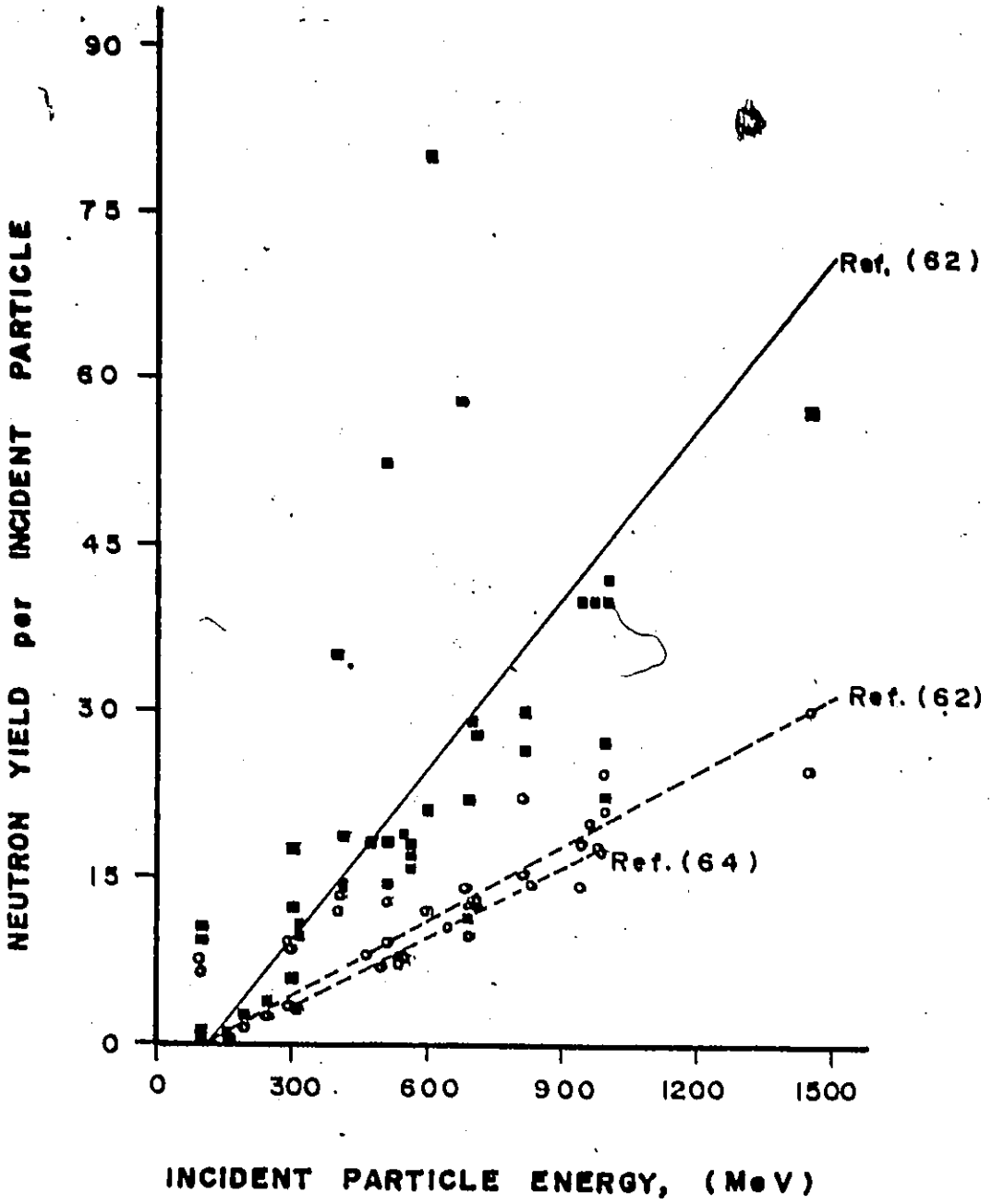

Fig. 2.4-1: Neutron yield in lead and uranium targets bombarded by protons. (experiment and calculation) (16,18,62-66)

increase in the neutron yield of about 20%[61,63] over proton yields at 1 GeV; however, there is the added problem associated with accelerating the heavier ions. Also in Fig. 2.4-1, empirical linear curves to fit some data are shown. For uranium targets, Steinberg et al[61] found the neutron yield, Y_U, could be approximated by

$$Y_U = 0.0516(E-120), \quad 170 \text{ MeV} < E < 1500 \text{ MeV}, \tag{2.4-1}$$

for proton energy E in MeV; for lead targets, Y_{Pb} is given by

$$Y_{Pb} = 0.0227(E-120), \quad 120 \text{ MeV} < E < 1000 \text{ MeV}. \tag{2.4-2}$$

West and Wood[63] found a linear fit to the neutron yields in lead to be

$$Y_{Pb} = 0.02113(E-167), \quad 300 \text{ MeV} < E < 1000 \text{ MeV} \tag{2.4-3}$$

The energy released per proton is shown in Fig. 2.4-2 with two linear curves fitted to the Tunnicliffe data[18]. For uranium, the heat released, U_U, is given by

$$U_U = 2.99(E-130) \text{ MeV}, \quad 130 \text{ MeV} < E < 1000 \text{ MeV}, \tag{2.4-4}$$

and for lead, U_{Pb} is given by

$$U_{Pb} = 0.630E \text{ MeV}, \quad 130 \text{ MeV} < E < 1000 \text{ MeV}. \tag{2.4-5}$$

In choosing these relations, data from Barashenkov et al[64,65] has not been included because their computations, which excluded meson production, are applicable only for low proton energies[61].

Mynatt et al[16] have simulated three proposed blanket types coupled to an accelerator delivering 1 GeV protons with a continuous current of 300 mA. For a LMFBR type blanket using U-Pu fuel and a molten lead target, 2.4-2.6 kg/d ^{239}Pu could be produced depending upon

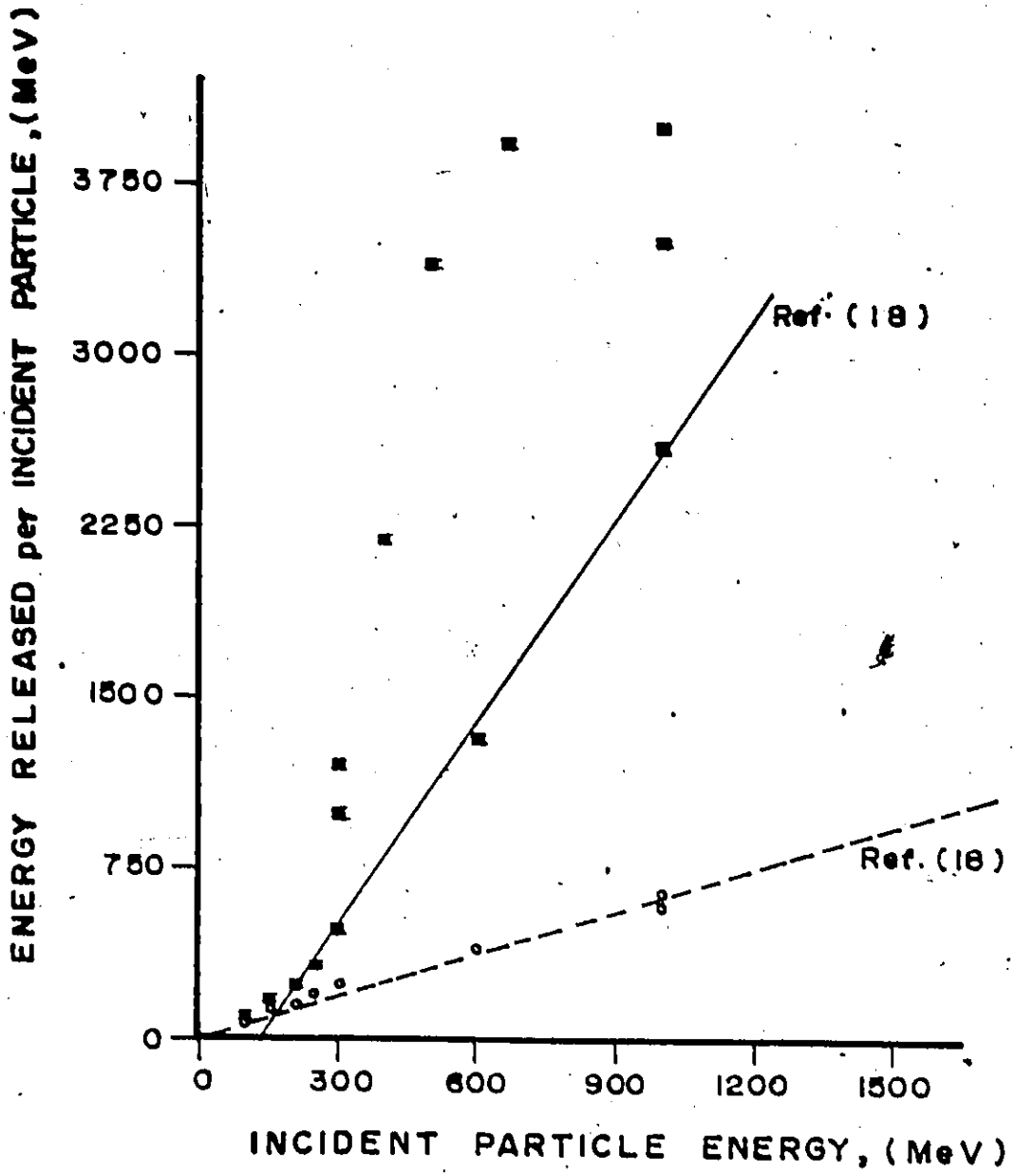

Fig. 2.4-2: Energy released in lead and uranium targets bombarded with protons[16,18,62,65,66].

the plutonium enrichment. This is equivalent to 37.4 to 40.6 atoms of ^{239}Pu per proton. The energy released ranged from 460 MW_t (1533 MeV per proton) at 0% enrichment to 1400 MW_t (4667 MeV per proton) at 4% enrichment. Blanket elements were projected to have a 200 day irradiation period. A molten salt blanket design which would allow for continuous extraction of fissile fuel, was also considered with a Th-U fuel cycle and a molten lead target. They found such a blanket could produce from 1.20 kg/d at 0% ^{233}U to 1.14 kg/d at 4% enrichment, that is, 19.2 and 18.2 atoms of ^{233}U per proton. A gas-cooled combined blanket-target was found to produce 4.0 kg/d (62.0 atoms of ^{239}Pu per proton) or 2.8 kg/d (44.8 atoms of ^{233}U per proton) at 1% fissile enrichment. Other groups studying spallation breeders have found similar results[18,61].

2.5 Fuel Processing

Fuel fabrication and reprocessing form an important link in the fuel cycle of nuclear reactors. For our purposes, the exact nature of the reprocessing is not important but the time delays introduced, the fissile fuel which becomes unavailable for use in the fuel cycle due to the processing and the energy consumed are.

For the fertile-fissile fuel cycle, the time delay between removal from the reactor and reinsertion is about 1.5 yr[25] as shown in Table 2.5-1. The losses estimated by various groups range from 0.5-3.0%[25,67-69] of the input fissile material. Fabrication and reprocessing of fuels require electrical and thermal power which will come from the output of the reactors if these processes are carried out on-site. For LWRs, this energy has been estimated at 3.35×10^3 $kW_e \cdot h/kg$

External Reactor Fuel Cycle Delay Periods	Current (LWR) (months)	Future (LMFBR) (months)
Holdup after removal from the core	3	1
Shipping to reprocessing facility	-	-
Reprocessing	1	0.25
Pin Fabrication	8	3
Complete assembly of fuel elements	6	1-2
Storage	-	-
Total	18-19	6-8

Table 2.5-1: External fuel cycle delay periods for fission reactors[66].

of fissile fuel handled[70]. It will be assumed that this value will be applicable to other reactor fuel types.

For fusion reactors, the tritium handling systems will be contained within the plant itself. Since the extraction is expected to be essentially continuous, there will be only a short holdup. Due to the reduced amount of processing, the loss of tritium will be small, <1%. The energy required to extract the tritium ranges from 3.1×10^2 $kW_e \cdot h/kg$ to 1.4×10^4 $kW_e \cdot h/kg$ handled[71] depending upon the concentration of the tritium in the lithium.

CHAPTER III

SYSTEM MODELLING

In this chapter, a method of describing fissile fuel production, resource utilization and electrical power generation capabilities of various types of fissile fuel breeders will be developed. The relevant nuclear reactions are introduced and used to derive a general isotope balance for a reactor core or blanket in terms of lumped parameters. Using this general equation and introducing the concept of stockpile inventories, the temporal variation of any isotope or material in the system is described. Finally, the power balance of a breeder-converter system is presented.

3.1 Nuclear Reactions of Interest

The types of reactions which will occur in breeder reactors can be divided into four categories: neutron-nucleus, fusion, spallation and decay. The microscopic cross section of an isotope or material M for a reaction of type [r,p] will be denoted by $\sigma_M^{r,p}(E)$. Here, r is used to identify the reaction:

$$r = \begin{cases} n, \text{ neutron-nucleus,} \\ f, \text{ fusion,} \\ s, \text{ spallation,} \\ d, \text{ nuclear decay;} \end{cases}$$

and p is used to identify the particular reaction. For neutron-nucleus

reactions the following convention[72] will be followed:

$$p = \begin{cases} n, \text{ elastic scattering, } (n,n), \\ n', \text{ inelastic scattering, } (n,n'), \\ \gamma, \text{ radiative capture, } (n,\gamma), \\ f, \text{ fission, } (n,f), \\ t, \text{ tritium production, } (n,t). \end{cases}$$

In fusion reactions, [f,p], p will refer to a fusion reactant; for example, $\sigma_D^{f,D}(E)$ is the cross section for DD fusion. Spallation reactions, [s,p], use p to identify the incident particle; thus, $\sigma_{Pb}^{s,d}(E)$ represents the cross section of lead by deuterons. Nuclear decay of an isotope M can be described by

$$\frac{dN_{M,i}(t)}{dt} = -N_{M,i}(t)\lambda_M^P, \tag{3.1-1a}$$

$$= -R_{M,i}^{d,P}(t), \tag{3.1-1b}$$

where $N_{M,i}(t)$ is the number of nuclei of the M in a given domain i at time t; λ_M^P is the decay constant for material M decaying to a material P, that is,

$$M \longrightarrow P, \tag{3.1-2}$$

and $R_{M,i}^{d,P}(t)$ is the nuclear decay rate of material M to P. Using this notation for decay allows both the decaying isotope and its daughter product to be readily identified. For example, the beta decay of ^{233}Pa,

$$^{233}_{91}Pa \xrightarrow{\beta^-} {}^{233}_{92}U, \tag{3.1-3}$$

will be described by the decay constant λ_{Pa3}^{U3}. Also, $U_M^{r,p}$ will be used to represent the energy released by a reaction of type [r,p] in material M.

The atomic density of isotope M in a reactor i about position $\underline{r}$ at time t will be denoted by $n_{M,i}(\underline{r},t)$. The inventory, or total number of nuclei, in the reactor, $N_{M,i}(t)$, is defined by

$$N_{M,i}(t) = \int_{V_i} n_{M,i}(\underline{r},t)d\underline{r}, \tag{3.1-4}$$

where V_i is the volume of reactor i. For neutrons and incident spallation particles, the following notation will be used: $n_{n,i}(\underline{r},E,t)$ refers to the energy dependent neutrons density while $n_{p,i}(\underline{r},E,t)$ refers to the energy dependent incident-particle density. The energy dependent neutron flux in reactor i will be written as $\phi_i(\underline{r},E,t)$ where

$$\phi_i(\underline{r},E,t) = vn_{n,i}(\underline{r},E,t), \tag{3.1-5}$$

and v is the speed of neutrons with energy E.

In fissile fuel breeding systems, neutron-nucleus reactions are of primary importance since breeding is initiated by neutron capture events,

$$^{232}_{90}Th + n \longrightarrow {}^{233}_{90}Th \xrightarrow{\beta^-} {}^{233}_{91}Pa \xrightarrow{\beta^-} {}^{233}_{92}U, \tag{3.1-6a}$$

$$^{238}_{92}U + n \longrightarrow {}^{239}_{92}U \xrightarrow{\beta^-} {}^{239}_{93}Np \xrightarrow{\beta^-} {}^{239}_{94}Pu. \tag{3.1-6b}$$

Also, the tritium production reactions,

$$^{6}_{3}Li + n \longrightarrow {}^{3}_{1}H + {}^{4}_{2}He, \tag{3.1-7a}$$

$$^{7}_{3}Li + n \longrightarrow {}^{3}_{1}H + {}^{4}_{2}He + n', \tag{3.1-7b}$$

involve neutron interactions. The rate of neutron-nucleus reactions, [n,p], in material M in reactor i is given by

$$R^{n,p}_{M,1}(t) = \int_{V_1} \int_0^\infty n_{M,1}(\underline{r},t)\sigma^{n,p}_M(E) \times \phi_1(\underline{r},E,t)d\underline{r}dE. \quad (3.1\text{-}8)$$

In fission reactors, a characteristic reaction rate, R_1, will be defined as the neutron absorption rate in fissile material,

$$R_1(t) = \sum_M \int_{V_1} \int_0^\infty n_{M,1}(\underline{r},t)\sigma^{n,abs}_M(E) \times \phi_1(\underline{r},E,t)d\underline{r}dE, \quad (3.1\text{-}9)$$

where the summation is over all fissile isotopes and the microscopic neutron absorption cross section is given by

$$\sigma^{n,abs}_M(E) = \sum_P \sigma^{n,p}_M(E) - [\sigma^{n,n}_M(E) + \sigma^{n,n'}_M(E)]. \quad (3.1\text{-}10)$$

Fusion reactions between two ions A and B will be described by the reaction rate

$$R^{f,B}_{A,1}(t) = \int_{V_1} \int_{\underline{v}_A} \int_{\underline{v}_B} n_{A,1}(\underline{r},t)f_{A,1}(\underline{v}_A,t) \times n_{B,1}(\underline{r},t)f_{B,1}(\underline{v}_B,t)\, v_{A,B} \times \sigma^{f,B}_A(v_{A,B})d\underline{r}d\underline{v}_A d\underline{v}_B, \quad (3.1\text{-}11)$$

where $\underline{v}_M$ is the velocity of ion M; $f_{M,1}(\underline{v}_M,t)$ is the normalized distribution function for ion M in velocity space of reactor 1 and $v_{A,B}$ the relative speed between ions of types A and B. For fusion between ions of the same species, Eq(3.1-11) must be rewritten as

$$R^{f,A}_{A,1}(t) = 1/2 \int_{V_1} \int_{\underline{v}_A} \int_{\underline{v}_{A'}} n_{A,1}(\underline{r},t)f_{A,1}(\underline{v}_A,t) \times n_{A',1}(\underline{r},t)f_{A',1}(\underline{v}_{A'},t)\, v_{A,A'} \times \sigma^{f,A}_A(v_{A,A'})d\underline{r}d\underline{v}_A d\underline{v}_{A'}, \quad (3.1\text{-}12)$$

otherwise interactions will be counted twice by the integration. The blanket energy multiplication factor introduced in Section 2.3 can thus be defined by

$$M_1 = \left\{ \sum_{[n,p]} \sum_M \int_{V_1} \int_0^\infty n_{M,1}(\underline{r},t)\sigma_M^{n,p}(E)\phi_1(\underline{r},E,t) \right. \\ \left. \times U_M^{n,p} d\underline{r} dE \right\} \times \left\{ \int_{V_1} \int_{\underline{v}_D} \int_{\underline{v}_T} n_{D,1}(\underline{r},t) f_{D,1}(\underline{v}_D,t) \right. \quad (3.1\text{-}13)$$
$$\left. \times n_{T,1}(\underline{r},t) f_{T,1}(\underline{v}_T,t) v_{D,T} \sigma_D^{f,T}(v_{D,T}) U_T^{f,D} a d\underline{r} d\underline{v}_D d\underline{v}_T \right\}^{-1},$$

where a is the fraction of the DT fusion energy possessed by the neutrons. Here, the summations are over all neutron-nucleus reaction types and all materials in the blanket.

In our analysis, deuterium-tritium fuelled fusion reactors will be considered. Hence, the reactions of interest are[73]:

$$^2_1H + {}^3_1H \longrightarrow {}^4_2He\ (3.52\ MeV) + n\ (14.06\ MeV), \quad (3.1\text{-}14a)$$

$$^2_1H + {}^2_1H \longrightarrow {}^3_1H\ (1.01\ Mev) + p\ (3.03\ MeV), \quad (3.1\text{-}14b)$$

$$^2_1H + {}^2_1H \longrightarrow {}^3_2He\ (0.82\ MeV) + n\ (2.45\ MeV), \quad (3.1\text{-}14c)$$

$$^2_1H + {}^3_2He \longrightarrow {}^4_2He\ (3.67\ MeV) + p\ (14.67\ MeV), \quad (3.1\text{-}14d)$$

where n refers to a neutron and p, to a proton. Of these, the most important is the DT fusion reaction, Eq(3.1-14a), since, from Fig. 3.1-1, the cross section for this reaction is much larger than for the other two and the peak of the DT reaction is at a lower energy than either DD or DHe^3 fusion. It is for these reasons that the DT fuel cycle has been chosen for the first generation of fusion reactors.

In a DT fuelled fusion reactor, some DD fusions and, since the

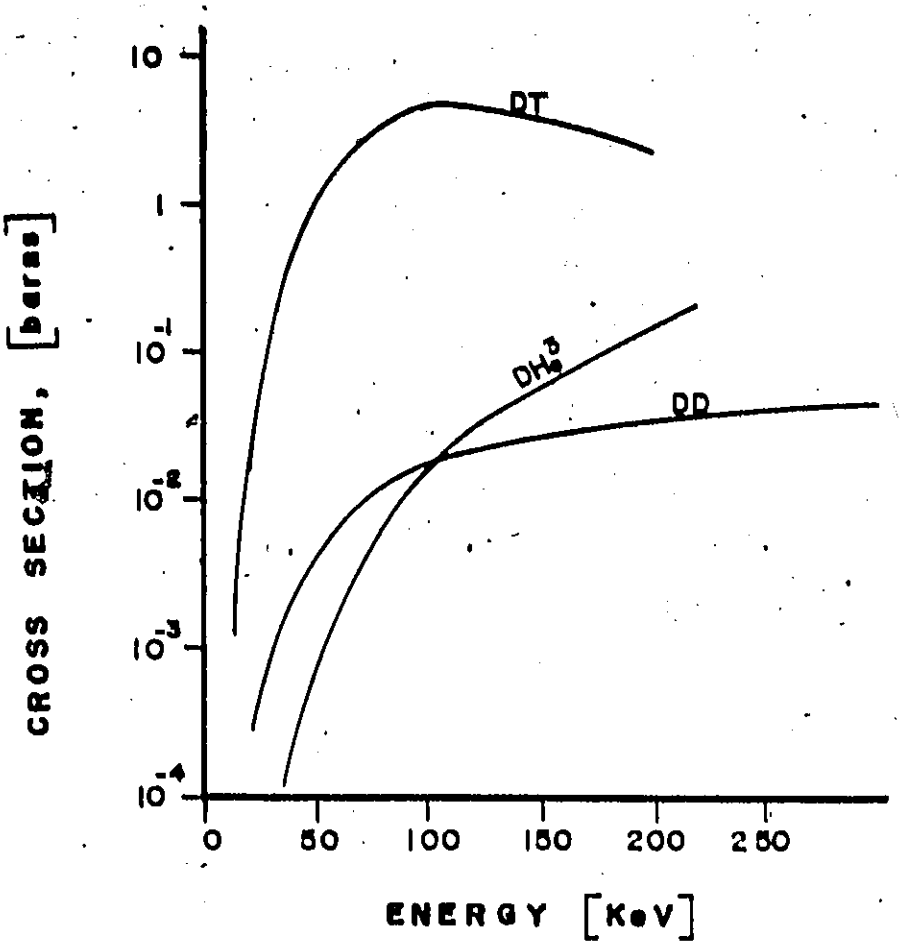

Fig. 3.1-1: Cross-sections for DT, DD and DHe^3 fusion as a function of ion energy after Rose et al.[74]

DD fusion reaction Eq(3.1-14c) produces ^3He, some DHe^3 fusions will occur. To estimate the effects of these, an approximate value of the reaction rate ratio $\rho_{D,1}^{f,D}$ will be found with the DT fusion rate as the characteristic reaction rate. We have then,

$$\rho_{D,1}^{f,D} = R_{D,1}^{f,D} / R_1 \ , \tag{3.1-15a}$$

$$R_{D,1}^{f,D} = 1/2 \int_{V_{p1}} \int_{\underline{v}_D} \int_{\underline{v}_{D'}} n_{D,1}(\underline{r},t) f_{D,1}(\underline{v}_D,t) \times n_{D',1}(\underline{r},t) f_{D',1}(\underline{v}_{D'},t) v_{D,D'} \times \sigma_D^{f,D}(v_{D,D'}) d\underline{r} d\underline{v}_D d\underline{v}_{D'} \ , \tag{3.1-15b}$$

$$R_1 = R_{D,1}^{f,T} \ , \tag{3.1-15c}$$

$$R_1 = \int_{V_{p1}} \int_{\underline{v}_T} \int_{\underline{v}_D} n_{T,1}(\underline{r},t) f_{T,1}(\underline{v}_T,t) \times n_{D,1}(\underline{r},t) f_{D,1}(\underline{v}_D,t) v_{T,D} \times \sigma_D^{f,T}(v_{D,T}) d\underline{r} d\underline{v}_T d\underline{v}_D \ . \tag{3.1-15d}$$

Assuming, for simplicity, $n_{D,1}$ and $n_{T,1}$ are constant within the plasma volume, V_{p1}, and the distribution of the ions is Maxwellian, then an expression for the fusion reaction rates can be found[74] from

$$R_{D,1}^{f,D} = 2.3 \times 10^{-14} (n_{D,1})^2 \left(\frac{1}{T}\right)^{2/3} \exp\left(-\frac{18.8}{T^{1/3}}\right) V_{p1} , \tag{3.1-16a}$$

$$R_{D,1}^{f,T} = 3.7 \times 10^{-12} (n_{D,1} n_{T,1}) \left(\frac{1}{T}\right)^{2/3} \times \exp\left(-\frac{20.0}{T^{1/3}}\right) V_{p1} \ ; \tag{3.1-16b}$$

hence

$$\rho_{D,1}^{f,D} = 6.22 \times 10^{-3} \frac{n_{D,1}}{n_{T,1}} \exp\left(\frac{1.2}{T^{1/3}}\right) \ . \tag{3.1-17}$$

Fusion reactor temperatures are typically 20-40 keV[40]. Using a temperature of 30 keV and assuming equal densities for deuterium and tritium, we get

$$\rho_{D,1}^{f,D} \approx 9.14 \times 10^{-3} \, . \tag{3.1-18}$$

In Section 2.3, it was stated that blanket Monte Carlo simulations are normally carried out to an accuracy of ~2%[44] but nuclear data and model idealizations may increase the uncertainty to 10-20%[41]. Clearly, the neutron, energy and fuel balances will not be greatly affected by neglecting DD and DHe^3 fusions.

Here, spallation processes of interest involve high energy particles, such as protons or deuterons, striking target nuclei as illustrated in Fig. 3.1-2. The primary interaction causes a cascade of energetic nucleons to be ejected from the struck nucleus. These nucleons can have energies well in excess of 100 MeV. The nuclei left in an excited state may de-excite by boiling off several evaporation neutrons which possess energies of 3-10 MeV or the nuclei may occasionally spall off larger fragments[18]. For our purposes, we choose to describe the spallation rate by

$$\sum_M R_{M,1}^{s,p} = \int_{V_1} \int_0^\infty n_{M,1}(\underline{r},t) n_{p,1}(\underline{r},E,t) \times v_p \sigma_M^{s,p}(E) \, d\underline{r} \, dE, \tag{3.1-19a}$$

$$= R_1 \, . \tag{3.1-19b}$$

where v_p is the speed of incident particles with energy E. The cross section $\sigma_M^{s,p}(E)$ is defined such that the characteristic reaction rate of the breeder, R_1, is equal to the rate at which the particles strike the target. Thus, if the particle current in a spallation reactor is I_1 amperes, then

$$R_1 = I_1/q_p \, . \tag{3.1-20}$$

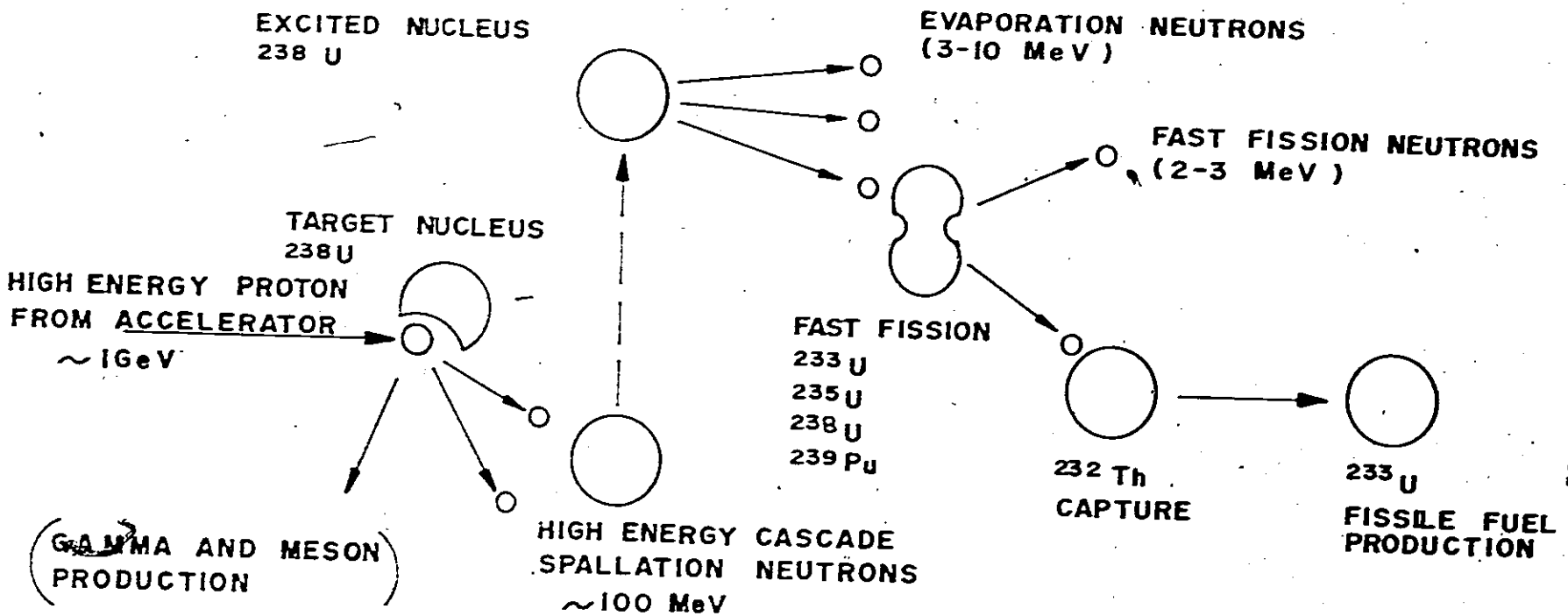

Fig. 3.1-2: Schematic of some spallation breeder reactions after Steinberg et al.[62]

where q_p is the charge on the incident particles.

We are now in a position to write an isotope balance for any material in a reactor using the notation introduced in the preceding. This will be accomplished in the following section.

3.2 Isotope Balance in a Reactor

To analyse material production and consumption rates in a reactor, the inventory at any time must be described. The number of nuclei in a reactor can be increased or decreased by neutron absorptions, fusion reactions, spallation events and/or decays. Not all of these events will necessarily occur concurrently, but, for convenience, all nuclear processes of interest will be considered for the derivation of a general isotope balance. However, after this equation has been obtained, the fusion reactor plasma equations will be treated separately. This general isotope balance will be used to define the net generation ratio of a material in the reactor.

In a generalized reactor i, the rate of change of the number of nuclei of isotope M in a differential volume about position $\underline{r}$ at time t can be described by

$$\frac{\partial n_{M,i}(\underline{r},t)}{\partial t}\, d\underline{r} = \begin{pmatrix}\text{net production rate of material M}\\ \text{by neutron-nucleus reactions}\end{pmatrix} + \begin{pmatrix}\text{net production rate of material M}\\ \text{by fusion reactions}\end{pmatrix} + \begin{pmatrix}\text{net production rate of material M}\\ \text{by spallation reactions}\end{pmatrix} + \begin{pmatrix}\text{net production rate of material M}\\ \text{by decay}\end{pmatrix} + \begin{pmatrix}\text{net transfer rate of material M}\\ \text{into position about } \underline{r}\end{pmatrix}, \tag{3.2-1}$$

Using the definitions from Section 3.1, Eq(3.2-1) can be written as

$$\frac{\partial n_{M,\ell}(\underline{r},t)}{\partial t} = \sum_J \int_0^\infty n_{J,\ell}(\underline{r},t)\sigma_J^{n,abs}(E)\phi_\ell(\underline{r},E,T)\gamma_{M,J}^{n,abs}(E)dE$$
$$+ \sum_{(K,L)} (1-\delta_{K,L}/2)\int_{\underline{v}_K}\int_{\underline{v}_L} n_{K,\ell}(\underline{r},t)f_{K,\ell}(\underline{v}_K,t)$$
$$\times n_{L,\ell}(\underline{r},t)f_{L,\ell}(\underline{v}_L,t)v_{K,L}\sigma_K^{f,L}(v_{K,L})\gamma_{M,K}^{f,L}(v_{K,L})d\underline{v}_K d\underline{v}_L$$
$$+ \sum_J \int_0^\infty n_{J,\ell}(\underline{r},t)n_{p,\ell}(\underline{r},E,t)v_p\sigma_J^{s,p}(E)\gamma_{M,J}^{s,p}(E)dE \quad (3.2\text{-}2)$$
$$+ \sum_J n_{J,\ell}(\underline{r},t)\lambda_J^M$$
$$+ t_{M,\ell}(\underline{r},t) \quad ,$$

where the following additional notation has been introduced. The probability that a reaction of type [r,p] in material J will result in the production of material M is denoted by $\gamma_{M,J}^{r,p}(E)$ where

$$\gamma_{J,J}^{r,p}(E) = -1 \text{ for } [r,p] = \begin{cases} [n,abs] \\ [f,p] \\ [s,p] \end{cases} , \quad (3.2\text{-}3)$$

For example, the probability of neutron absorption in ^{233}U forming ^{234}U will be $\gamma_{U4,U3}^{n,abs}(E)$ where this is the ratio of the capture cross section to the total neutron absorption cross section of ^{233}U. The decay constant λ_M^J defined in Eq(3.1-1) is extended here such that

$$\lambda_M^M = -\sum_J \lambda_M^J \quad . \quad (3.2\text{-}4)$$

The rate at which material M is transferred to position $\underline{r}$ is denoted by $t_{M,\ell}(\underline{r},t)$. In Eq(3.2-2) and Eq(3.2-4), the summations with respect to J are over all isotopes and the summation with respect to (K,L) is over all fusion reactant pairs. In addition, $\delta_{K,L}$, the Kronecker delta, has been used.

We can cast Eq(3.2-2) into a matrix form in terms of the com-

position vector, $\underline{n}_i(\underline{r},t)$ which has as elements $(n_{1,i}(\underline{r},t), n_{2,i}(\underline{r},t), \ldots)$, and the transfer vector $\underline{t}_i(\underline{r},t)$ which has as elements $(t_{1,i}(\underline{r},t), t_{2,i}(\underline{r},t), \ldots)$. Using these we find

$$\frac{\partial \underline{n}_i(\underline{r},t)}{\partial t} = \underline{a}_i(r,t)\cdot\underline{n}_i(\underline{r},t) + \underline{b}_i(\underline{r},t)\cdot\underline{n}_i(\underline{r},t)\cdot\underline{n}_i(\underline{r},t) + \underline{t}_i(\underline{r},t) \ , \tag{3.2-5}$$

where the elements of $\underline{a}_i(\underline{r},t)$ are given by

$$a_{M,J,i}(\underline{r},t) = \int_0^\infty \sigma_J^{n,abs}(E)\phi_i(\underline{r},E,t)\gamma_{M,J}^{n,abs}(E)dE + \int_0^\infty \sigma_J^{s,p}(E)n_{p,i}(\underline{r},E,t)v_p\gamma_{M,J}^{s,p}(E)dE + \lambda_J^M \ , \tag{3.2-6}$$

and the elements of $b_i(\underline{r},t)$ are given by

$$b_{M,J,K,i}(\underline{r},t) = (1-\delta_{J,K}/2)\int_{\underline{v}_J}\int_{\underline{v}_K} f_{J,i}(\underline{v}_J,t)f_{K,i}(\underline{v}_K,t) \times v_{J,K}\sigma_J^{f,K}(v_{J,K})\gamma_{M,J}^{f,K}(v_{J,K})d\underline{v}_J d\underline{v}_K \ . \tag{3.2-7}$$

The term describing fusion reactions, $\underline{b}_i\cdot\underline{n}_i\cdot\underline{n}_i$, involves the product of two isotope densities. In the following analysis, only deuterium and tritium will undergo fusion reactions, hence, this term will be neglected although the isotope balance for a fusion reactor plasma will be discussed later. For a reactor which has no fusion reactions, Eq(3.2-5) can be written as

$$\frac{\partial \underline{n}_i(\underline{r},t)}{\partial t} = \underline{a}_i(\underline{r},t)\cdot\underline{n}_i(\underline{r},t) + \underline{t}_i(\underline{r},t) \ . \tag{3.2-8}$$

This equation can be used to describe the time behaviour of the isotope densities in a fission reactor core, fission reactor blanket, fusion reactor blanket, spallation reactor target or a spallation reactor blanket.

Two reasons for discharging fuel from any of the above systems are: (1) to maintain criticality in a fission core or sub-criticality in a blanket and (2) to extract the fissile material and tritium produced. When the reactor is refuelled, either the entire core or blanket (or a part) is unloaded and new fuel added. First fuel loadings will not be typical since, in a fresh core, fission products will buildup and a fuel management scheme different from the long term one will be used. For a reactor which has already passed through this transitional stage, fuel loadings will be more uniform. Here, the reactor starts up after a refuelling at time t_o and the fuel is irradiated. The reactor is shut down at a time $t_o + \tau_i^F$ (except reactors with on-power refuelling such as the CANDU or pebble bed reactors), fuel discharged, new fuel added and the cycle begins again.

If a volume V_i^D is discharged during refuelling, then, after the reactor has passed through the transitional stage,

$$\frac{V_i^D}{V_i} = \frac{\tau_i^F}{\tau_i^D} \quad , \tag{3.2-9}$$

will hold where τ_i^D is the mean residence period of the fuel and V_i is the volume of the reactor. For example, if 1/3 of the core is discharged every year, the mean residence period will be 3 years. It has been assumed in Eq(3.2-9) that all materials in the reactor will have the same mean residence period; however, the extension to separate mean residence periods for different materials is straight forward.

Integrating Eq(3.2-8) over the discharged volume, we find

$$\frac{d\underline{N}_i^D(t)}{dt} = \underline{\underline{A}}_i^D(t) \cdot \underline{N}_i^D(t) + \underline{I}_i^D(t) \tag{3.2-10}$$

where

$$N^D_{M,i}(t) = \int_{V_i^D} n_{M,i}(\underline{r},t)\, d\underline{r} \,, \tag{3.2-11}$$

is the number of atoms of isotope M in the discharged volume;

$$A^D_{M,J,i}(t)N^D_{J,i}(t) = \int_{V_i^D} a_{M,J,i}(\underline{r},t)n_{J,i}(\underline{r},t)d\underline{r} \,, \tag{3.2-12}$$

describes the net production rate of material M due to reactions in material J within the discharge volume and

$$T^D_{M,i}(t) = \int_{V_i^D} t_{M,i}(\underline{r},t)\, d\underline{r} \,, \tag{3.2-13}$$

is the rate of transfer of material M into the discharge volume. To find the amount of material discharged, Eq(3.2-10) is integrated with respect to time over one mean residence period yielding

$$\underline{N}^D_i(t_o+\tau^D_i) = \underline{N}^D_i(t_o) + \int_{t_o}^{t_o+\tau^D_i} \underline{\underline{A}}^D_i(t')\cdot\underline{N}^D_i(t')dt' + \tau^D_i\, \underline{\bar{T}}^D_i \tag{3.2-14}$$

where the average rate of transfer of material M into the discharge volume is defined by

$$\bar{T}^D_{M,i} = \frac{1}{\tau^D_i}\int_{t_o}^{t_o+\tau^D_i} T^D_{M,i}(t')dt' \,. \tag{3.2-15}$$

The change in the number of nuclei of type M in the discharge volume after a time τ^D_i is defined by

$$\Delta N^D_{M,i}(\tau^D_i) = N^D_{M,i}(t_o+\tau^D_i) - N^D_{M,i}(t_o) \,. \tag{3.2-16}$$

Substituting this into Eq(3.2-14), we have

$$\Delta\underline{N}^D_i(\tau^D_i) = \int_{t_o}^{t_o+\tau^D_i} \underline{\underline{A}}^D_i(t')\cdot\underline{N}^D_i(t')dt + \tau^D_i\underline{\bar{T}}^D_i \,. \tag{3.2-17}$$

We have defined $\underline{\bar{T}}^D_{M,i}$ as the average rate of transfer of material M into the discharge volume during the mean residence period. For

reactors with solid fuel, this term will be zero since the fuel is fixed within the discharge volume. By choosing a material volume for reactors with fluid fuel, this term can be set to zero since, by definition, mass does not cross the surface of a material volume. Neglecting this term, we will have

$$\Delta \underline{N}_i^D(\tau_i^D) = \int_{t_o}^{t_o + \tau_i^D} \underline{A}_i^D(t') \cdot \underline{N}_i^D(t') dt' , \qquad (3.2\text{-}18)$$

or, using Eq(3.2-6), a space and energy integrated value for the change in the number of nuclei in a volume V_i^D during a period τ_i^D will be given by

$$\begin{aligned} \Delta N_{M,i}^D(\tau_i^D) = \int_{t_o}^{t_o + \tau_i^D} \int_{V_i^D} \Big\{ & \Sigma n_{J,i}(\underline{r},t) \\ & \times \int_0^\infty \sigma_J^{n,abs}(E) \phi_i(\underline{r},E,t) \gamma_{M,J}^{n,abs}(E) dE \qquad (3.2\text{-}19) \\ & + \int_0^\infty \sigma_J^{s,p}(E) n_{p,i}(\underline{r},E,t) \nu_p \gamma_{M,J}^{s,p}(E) dE \\ & + \lambda_J^M \Big\} d\underline{r} dt \end{aligned}$$

The net generation ratio for a material M in reactor i, $G_{M,i}$, will be defined by

$$G_{M,i} R_i = \frac{\Delta N_{M,i}^D(\tau_i^D)}{\tau_i^F} , \qquad (3.2\text{-}20)$$

that is, the product of the net generation ratio for material M in reactor i and the characteristic reaction rate of reactor i gives the change in the number of atoms of type M in the volume discharge divided by the time between refuellings. In a steady-state reactor with R_i and τ_i^F constant, the change in the number of nuclei, $\Delta N_{M,i}^D(\tau_i^D)$, will be

constant at each refuelling; hence, G_i will also be constant. We can write Eq(3.2-20) in vector form,

$$\underline{G}_i = \frac{\Delta \underline{N}_i^D(\tau_i^D)}{\tau_i^F R_i} , \qquad (3.2\text{-}21)$$

or, substituting in Eq(3.2-18) and Eq(3.2-12), we find

$$\underline{G}_i = \frac{1}{\tau_i^F R_i} \int_{t_o}^{t_o + \tau_i^D} \int_{V_i^D} \underline{a}_i(\underline{r},t') \cdot \underline{n}_i(\underline{r},t') dt' d\underline{r} . \qquad (3.2\text{-}22)$$

Discontinuous refuelling schemes can be replaced for mathematical convenience by a continuous "refuelling-interval-averaged" description[14] in which

$$\tau_i^F \longrightarrow d\tau_i^F , \qquad (3.2\text{-}23a)$$

$$V_i^D \longrightarrow dV_i^D , \qquad (3.2\text{-}23b)$$

in such a way that Eq(3.2-9) continues to hold. Applying this to Eq(3.2-22), we have

$$\underline{G}_i = \frac{1}{\tau_i^F R_i} \int_{t_o}^{t_o+\tau_i^D} \underline{a}_i(\underline{r},t') \cdot \underline{n}_i(\underline{r},t') dt' dV_i^D , \qquad (3.2\text{-}24a)$$

$$\underline{G}_i = \frac{V_r}{\tau_i^D R_i} \int_{t_o}^{t_o+\tau_i^D} \underline{a}_i(\underline{r},t') \cdot \underline{n}_i(\underline{r},t') dt' . \qquad (3.2\text{-}24b)$$

For a reactor which has passed through the transitional stage described earlier, the refuelling is uniform. Thus, the inventory of the reactor can be said to be periodic in time with a period of τ_i^F. Using Eq(3.2-23) we have

$$\underline{N}_i(t) = \underline{N}_i(t + d\tau_i^F) , \qquad (3.2\text{-}25)$$

or, the number of atoms in the volume V_i will be constant. Similarly, we have

$$\underline{A}_i(t)\cdot\underline{N}_i(t) = \underline{A}_i(t + d\tau_i^F)\cdot\underline{N}_i(t + d\tau_i^F) , \qquad (3.2\text{-}26)$$

or, the reaction rate will be constant in the volume V_i. If Eq(3.2-24b) is integrated over the reactor volume, then we get

$$\int_{V_i}\underline{G}_i d\underline{r} = \frac{V_i}{\tau_i^D R_i}\int_{V_i}\int_{t_o}^{t_o + \tau_i^D}\underline{a}_i(\underline{r},t')\cdot\underline{n}_i(\underline{r},t')d\underline{r}dt', \qquad (3.2\text{-}27)$$

but, since $\underline{G}_i$ is constant and using Eq(3.2-26), the net generation ratio vector can be written

$$\underline{G}_i = \underline{A}_i\cdot\underline{N}_i/R_i . \qquad (3.2\text{-}28)$$

Using the definition of $\underline{a}_i(\underline{r},t)$, Eq(3.2-6), and the reaction rate ratio $\rho_{M,i}^{r,p}(t)$, the net generation ratio can also be written as

$$G_{M,i} = \sum_J(\rho_{J,i}^{n,abs}\gamma_{M,J}^{n,abs} + \rho_{J,i}^{s,p}\gamma_{M,J}^{s,p} + \rho_{J,i}^{d,M}) , \qquad (3.2\text{-}29)$$

where $\gamma_{M,J}^{r,p}$ has been obtained by suitable averaging. For example, for neutron absorption we have

$$\gamma_{M,J}^{n,abs}\rho_{J,i}^{n,abs} = \frac{1}{\tau_i^D R_i}\int_{V_i}\int_{t_o}^{t_o + \tau_i^D}\int_0^\infty n_{J,i}(\underline{r},t)\sigma_J^{n,abs}(E) \qquad (3.2\text{-}30)$$

$$\times\ \phi_i(\underline{r},E,t)\gamma_{M,J}^{n,abs}(E)d\underline{r}dtdE.$$

The ratio of the decay rate, Eq(3.1-1b), to the characteristic reaction rate, R_i, is denoted by $\rho_{M,i}^{d,J}$. From Eq(3.2-26), these reaction rate ratios will be constant in a steady-state core.

The definition of $G_{M,i}$ using reaction rate ratios also holds for a fusion reactor operating in a steady-state mode or for a batch fuelled

reactor where Eq(3.2-23) has been applied. For a DT fusion plasma, the tritium net generation ratio will be given by

$$G_{T,1} = -\rho_{T,1}^{f,D} + (1-b)\rho_{D,1}^{f,D} \quad , \tag{3.2-31}$$

where tritium production by a fraction b of the DD fusions has been included. From Eq(3.1-18), $\rho_{D,1}^{f,D} \ll 1$ and since the DT fusion reaction rate is also the characteristic reaction rate, the tritium net generation ratio in a DT fusion plasma can be reduced to

$$G_{T,1} = -1 \quad , \tag{3.2-32}$$

with an error of less than 1%.

The data presented in Chapter II for the various breeder and converter reactors will give only the fissile and tritium net generation ratios. However, since fuel costs for the breeder-converter systems will be proportional to the fertile fuel consumption, relationships between the fertile and fissile, and tritium and lithium, net generation ratios are necessary.

Neglecting spallation and fusion events since they will not take place in the relevant volume, the fertile net generation ratio, $G_{FE,1}$, can be written using Eq(3.2-29) as

$$G_{FE,1} = -\rho_{FE,1}^{n,abs} \quad , \tag{3.2-33}$$

where it has been assumed that no fertile fuel is produced and the decay of fertile material can be neglected on the time scales of interest (the half-life of $^{232}Th \sim 10^{10}$ years and $^{238}U \sim 10^{9}$ years). Similarly, the fissile net generation ratio, $G_{FI,1}$, can be written as

$$G_{FI,1} = -\rho_{FI,1}^{n,abs} + \gamma_{FI,FE}^{n,abs}\rho_{FE,1}^{n,abs} \quad , \tag{3.2-34}$$

if the decay of fissile material is neglected (the half life of $^{233}U \sim 10^5$ years and $^{239}Pu \sim 10^4$ years) and where $\gamma_{FI,FE}^{n,abs}$ is the probability that neutrons absorbed in fertile material will result in fissile nuclei. The fissile net generation ratio defined by Eq(3.2-34) is the same as the breeding gain, the breeding ratio minus one, used in fission reactor physics.

To find $\gamma_{FI,FE}^{n,abs}$, it is necessary to consider the breeding decay chains, Eq(3.1-7). Since the decay chain for the Th-U and U-Pu cycles are similar, the decay chain

$$(1) + n \longrightarrow (2) \xrightarrow{\lambda_2^3} (3) \xrightarrow{\lambda_3^4} (4) \ , \qquad (3.2\text{-}35)$$

can be used to describe both. In Eq(3.2-35), (1) represents the fertile isotope, ^{232}Th or ^{238}U, (4), the fissile isotope ^{233}U or ^{239}Pu, and (2) and (3), the intermediate isotopes, ^{233}Th or ^{233}Pa or ^{239}U and ^{239}Np. The equations describing the decay chain are

$$dN_1(t)/dt = -u_1 N_1(t) \ , \qquad (3.2\text{-}36a)$$

$$dN_2(t)/dt = -u_2 N_2(t) + \gamma_{2,1}^{n,abs}\, \sigma_1^{n,abs}\, \phi N_1(t), \qquad (3.2\text{-}36b)$$

$$dN_3(t)/dt = -u_3 N_3(t) + \lambda_2^3 N_2(t) \ , \qquad (3.2\text{-}36c)$$

$$dN_4(t)/dt = -u_4 N_4(t) + \lambda_3^4 N_3(t) \ ; \qquad (3.2\text{-}36d)$$

where

$$u_1 = \sigma_1^{n,abs}\, \phi + \sum_J \lambda_1^J \ , \qquad (3.2\text{-}37)$$

and $(\sigma_1^{n,abs}\, \phi)$ and $(\gamma_{2,1}^{n,abs}\, \sigma_1^{n,abs}\, \phi)$ are averaged over the relevant space and energy domains. By sequentially integrating each equation in the system and substituting the result in the equation which follows it, we find the fissile production term in Eq(3.2-36d) is given by

$$\lambda_3^4 N_3(t) = \frac{\lambda_3^4 \lambda_2^3 \gamma_{2,1}^{n,abs} \sigma_1^{n,abs}}{\mu_2 - \mu_1} N_1(t)$$

$$\times \frac{(1-e^{-(\mu_3-\mu_1)t})}{(\mu_3-\mu_1)} - \frac{(e^{-(\mu_2-\mu_1)t} - e^{-(\mu_3-\mu_1)t})}{(\mu_3-\mu_2)} , \quad (3.2\text{-}38)$$

for $N_2(0) = 0$ and $N_3(0) = 0$. From Table 3.2-1, it can be seen that for the flux levels of interest, $10^8 < \phi < 10^{17}$ $(cm^{-2} \cdot s^{-1})$,

$$\mu_2 >> \mu_3 >> \mu_1 . \quad (3.2\text{-}39)$$

If the time t is long, $t >> 1/\mu_3$, then Eq(3.2-28) reduces to

$$\lambda_3^4 N_3(t) = \frac{\lambda_3^4 \lambda_2^3 \gamma_{2,1}^{n,abs}}{\mu_3 \mu_2} \sigma_1^{n,abs} \phi N_1(t) . \quad (3.2\text{-}40)$$

Equating Eq(3.2-40) with the fissile production term in Eq(3.2-34), an expression for the probability that neutron absorption in fertile material will result in fissile nuclei is found:

$$\gamma_{FI,FI}^{n,abs} = (\lambda_3^4 \lambda_2^3 \gamma_{2,1}^{n,abs})/(\mu_3 \mu_2) . \quad (3.2\text{-}41)$$

If the neutron absorption in intermediate nuclei is small, then we find

$$\gamma_{FI,II}^{n,abs} = \gamma_{2,1}^{n,abs} = \rho_{FI,1}^{n,\gamma} / \rho_{FI,1}^{n,abs} . \quad (3.2\text{-}42)$$

From Eq(3.2-33) and Eq(3.2-34), the following will hold

$$G_{FI,1} = -(\rho_{FI,1}^{n,abs} + G_{FI,1})/\gamma_{FI,FI}^{n,abs} , \quad (3.2\text{-}43)$$

or, if $G_{FI,F}$ is not zero and by substituting Eq(3.2-42) into Eq(3.2-43), we will have

$$\frac{G_{FI,1}}{G_{FI,1}} = \frac{\rho_{FI,1}^{n,abs}}{\rho_{FI,1}^{n,abs} + \rho_{FI,1}^{n,\gamma}} . \quad (3.2\text{-}44)$$

For lithium and tritium in a blanket we have from Eq(3.2-29)

Isotope	$\sigma_f^{n,abs}$ (b)	Half-life	λ_f (sec^{-1})
^{232}Th	7.4	1.4×10^{10} a	1.6×10^{19}
^{233}Th	1400.	22.1 m	5.2×10^{-4}
^{233}Pa	522.	27.4 d	2.9×10^{-7}
^{233}U	579.	1.6×10^{5} a	1.4×10^{-13}
^{234}U	96.	2.5×10^{5} a	8.8×10^{-14}
^{235}U	681.	7.1×10^{8} a	3.1×10^{-17}
^{238}U	2.7	4.5×10^{9} a	4.9×10^{-18}
^{239}U	22.	23 m	5.0×10^{-4}
^{239}Np	30.	56 hr	3.4×10^{-6}
^{239}Pu	1011.	2.4×10^{4} a	9.2×10^{-13}
^{240}Pu	286.	6.6×10^{3} a	3.3×10^{-12}
^{241}Pu	1377.	13.2 a	1.66×10^{-9}

Table 3.2-1 Some nuclear data relevant to fissile fuel breeding; after Henry[76]. Cross sections are evaluated at thermal neutron energies (0.025 ev).

$$G_{T,1} = \rho_{Li,1}^{n,abs} \gamma_{T,Li}^{n,abs} \quad . \tag{3.2-45}$$

and also

$$G_{Li,1} = -\rho_{Li,1}^{n,abs} \quad . \tag{3.2-46}$$

Combining these we find the following relationship between the tritium and lithium net generation ratios:

$$G_{Li,1} = -G_{T,1}/\rho_{T,Li}^{n,abs} \quad . \tag{3.2-47}$$

where the probability of neutron absorption in lithium will lead to the production of tritium, Eq(3.1-7), is given by

$$\gamma_{T,Li}^{n,abs} = \rho_{Li,1}^{n,t}/\rho_{Li,1}^{n,abs} \quad . \tag{3.2-48}$$

Since a reactor could contain more than one fissile isotope, the fissile material inventory will be defined by

$$N_{FI,1}(t) = \sum_M O_M N_{M,1}(t) \quad , \tag{3.2-49}$$

where O_M is an isotope weight[76] for material M and the summation is over all fissile nuclei. Similarly, the fertile inventory will be given by

$$N_{FE,1}(t) = \sum_M O_M N_{M,1}(t) \quad . \tag{3.2-50}$$

where the summation is over fertile isotopes. It will be assumed that an equation of the form of Eq(3.2-44) will hold to relate the fertile and fissile net generation ratios.

3.3 Temporal Variation of the Stockpile Inventory

The temporal variation of the system inventory is considered here rather than the usual measure of breeding capacity, the doubling

time, due to the ambiguity in defining precisely the doubling time[3,76] and the fact that the doubling time can be time dependent[4]. In addition, more information can be extracted from the inventory variation than from a single figure of merit. For these reasons, the stockpile inventory during the entire system lifetime will be calculated and the characteristics of this used to describe the breeding capabilities of the system.

The system model we will consider, shown schematically in Fig. 3.3-1, consists of a fission, fusion or spallation type breeder reactor coupled by isotope and power linkages to a neutronically and thermally efficient fission converter reactor. Referring to the isotope flows for one reactor, material is received from an external source and placed in the stockpile. In this case the stockpile is an artificial device included solely for the purpose of accounting for material flows within the system[3,4]. From the stockpile, material is transferred to the reactor where it is irradiated. Then, the material goes to the reprocessing-fabrication plant and finally back to the stockpile. By examining the stockpile inventory, it is possible to account for the amount of material produced or consumed by the system at any time throughout the lifetime of the system. This method also allows for the explicit incorporation of pre-steady-state conditions in the reactor and reprocessing-fabrication lags and losses.

In the following, there will be no decay or losses of material from the stockpile since the stockpile is an artifice. Also, the discrete fuelling of the reactors will be averaged over a refuelling period[4] as described by Eq(3.2-23). Intermediate decays in the breeding chains, Eq(3.1-6), can be neglected so that Eq(3.2-40) will

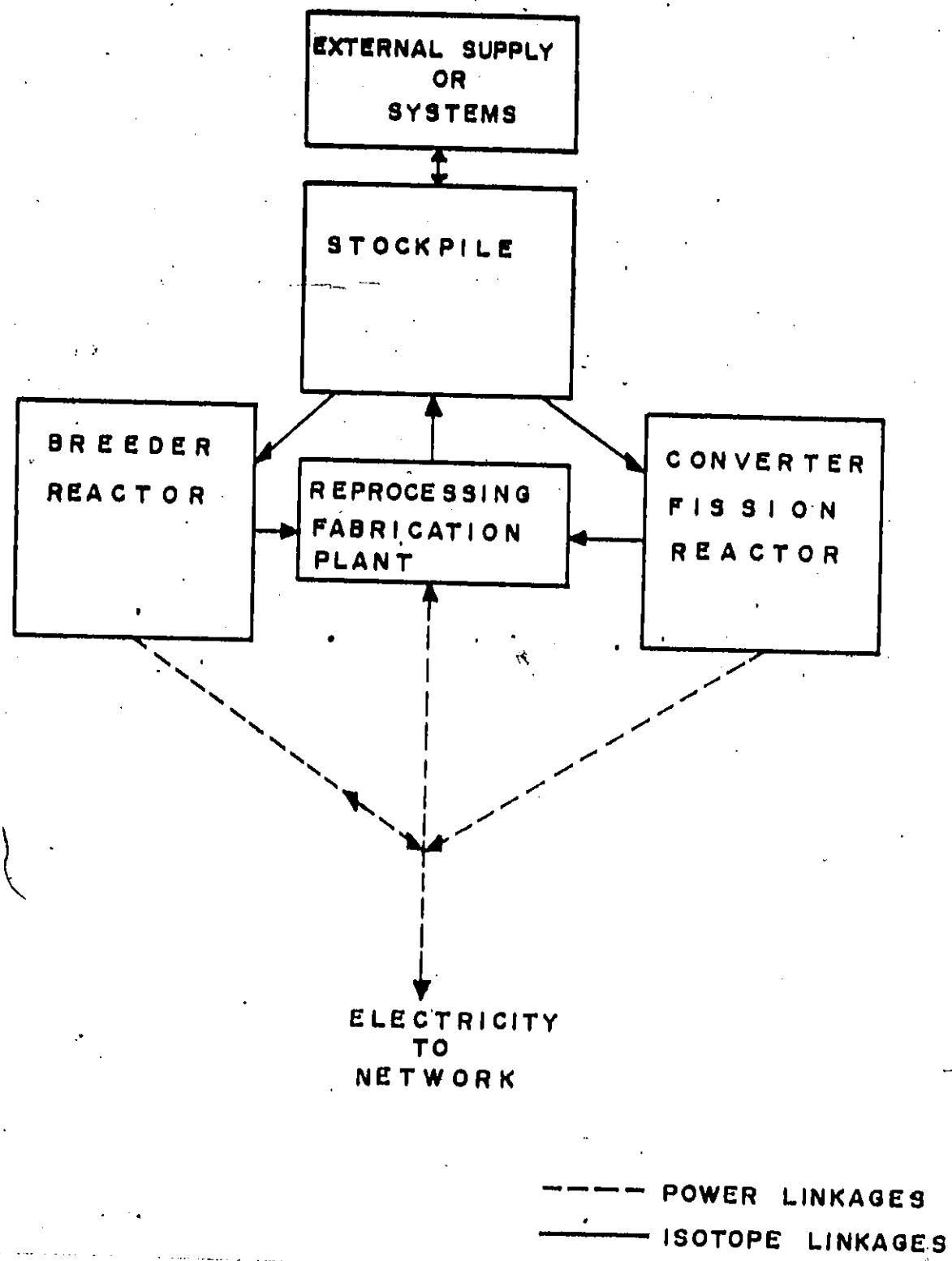

Fig. 3.3-1: Schematic showing the coupling of the breeder-converter system.

hold. The initial buildup of the reprocessing-fabrication plant inventories will be excluded and processing losses will be directly proportional to the amount of material handled. As in the previous section, $G_{M,1}$, R_1 and all refuelling, residence and lag periods are constant.

Changes in the stockpile inventory can be separated into the changes due to the individual reactors; thus, the system shown in Fig. 3.3-1 can be sub-divided so that the interaction of the stockpile and the reprocessing-fabrication plant with one reactor can be examined as shown in Fig. 3.3-2. The total change in the stockpile inventory will be the sum of the changes due to each reactor in the system plus that due to the external source. The inventory of material M in the stockpile will be denoted by $N_{M,S}(t)$ and the inventory of a typical reactor R, $N_{M,R}(t)$. From Fig. 3.3-2, the rate of change of the stockpile in this subsystem can be written as

$$\left(\frac{dN_{M,S}(t)}{dt}\right)^{R} = \left(\frac{dN_{M,S}(t)}{dt}\right)^{R+} - \left(\frac{dN_{M,S}(t)}{dt}\right)^{R-} , \qquad (3.3\text{-}1)$$

where $(N_{M,S}(t)/dt)^{R+}$ is the rate of increase of the stockpile inventory of material M due to material processed by the reprocessing-fabrication plant which came from reactor R and $(N_{M,S}(t)/dt)^{R-}$ is the rate of decrease of the stockpile inventory of material M due to fuelling the reactor.

For reactor refuelling, we consider a reactor at steady-state with a refuelling interval τ_R^F and with a fuel mean residence period of τ_R^D. Thus, from Eq(3.2-9), the fraction τ_R^F/τ_R^D is replaced at each refuelling. If $N_{M,R}^D$ is the amount added at each refuelling, then the

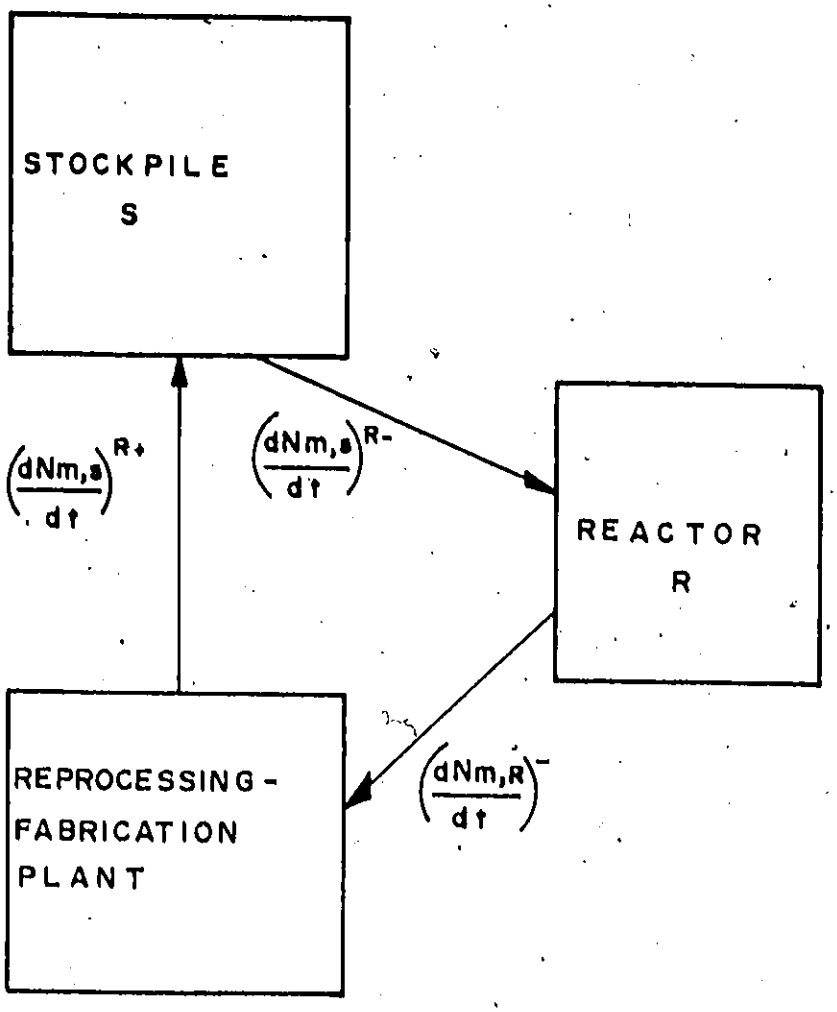

Fig. 3.3-2: Schematic showing the isotope coupling of a sub-system for reactor R.

total reactor steady-state inventory of fresh fuel, $N^{SS}_{M,R}$, will be given by

$$N^{SS}_{M,R} = (\tau^D_R/\tau^F_R)\, N^D_{M,R} \,. \tag{3.3-2}$$

After steady-state has been attained, the averaged rate at which material is added to the reactor from the stockpile will be given by

$$\left(\frac{dN_{M,S}(t)}{dt}\right)^{R-} = \begin{cases} N^{SS}_{M,R}/\tau^D_R, & \tau^{SS}_R < t \leq \tau^{EOL}_R \,, \quad (3.3\text{-}3a) \\ 0, & t > \tau^{EOL}_R \,, \quad (3.3\text{-}3b) \end{cases}$$

where τ^{SS}_R is the time needed to attain steady-state and τ^{EOL}_R, the lifetime of the reactor. Here, the reactor was started up at t = 0. Steady-state is reached when the inventory at any time during the refueling satisfies

$$N_{M,R}(t) = N_{M,R}(t + \tau^F_R), \quad \tau^{SS}_R < t \leq \tau^{EOL}_R \,. \tag{3.3-4}$$

For the transitional period, $0 < t \leq \tau^{SS}_R$, a function $h_R(t)$ is defined such that

$$\left(\frac{dN_{M,S}(t)}{dt}\right)^{R-} = \left(\frac{N^{SS}_{M,R}}{\tau^D_R}\right) h_R(t), \quad 0 < t \leq \tau^{SS}_R \,. \tag{3.3-5}$$

This will account for pre-steady-state reactor fuel management.

The rate at which material M is discharged from the reactor for $t > \tau^{SS}_R$ will be given by

$$\left(\frac{dN_{M,R}(t)}{dt}\right)^{-} = \frac{N^D_{M,R}(t-\tau^D_R) + \Delta N^D_{M,R}(\tau^D_R)}{\tau^F_R} \,, \tag{3.3-6}$$

where $\Delta N^D_{M,R}(\tau^D_R)$ is defined by Eq (3.2-19). The rate of change, $(dN_{M,R}/dt)^-$, will vary during the lifetime of the reactor. After steady-state has been attained, using Eq(3.3-2) and Eq(3.2-21), the rate of

discharge will be found from

$$\left(\frac{dN_{M,R}(t)}{dt}\right)^{-} = \begin{cases} N_{M,R}^{SS}/\tau_R^D + G_{M,R}R_R, & \tau_R^{SS} < t \leq \tau_R^{EOL} , \quad (3.3\text{-}7a) \\ 0, & t > \tau_R^{EOL} . \quad (3.3\text{-}7b) \end{cases}$$

Here, Eq(3.3-7a) gives the rate at which the fuel is loaded into the reactor plus the change due to irradiation. After shutdown, no fuel will be removed from the reactor and Eq(3.3-7b) will hold. Between startup and steady-state, the amount of material discharged will depend upon the fuel management scheme, so, by analogy with Eq(3.3-5), a function $g_R(t)$ will be defined such that

$$\left(\frac{dN_{M,R}(t)}{dt}\right)^{-} = \left(\frac{N_{M,R}^{SS}}{\tau_R^D}\right) h_R(t) + (G_{M,R}R_R) g_R(t) , \quad 0 < t \leq \tau_R^F . \quad (3.3\text{-}8)$$

This function will describe the pre-steady-state net generation ratio and hence the rate at which material M is discharged from the reactor. The rate at which material M is added to the stockpile from the reprocessing-fabrication plant due to reactor R will be given by

$$\left(\frac{dN_{M,S}(t)}{dt}\right)^{R+} = \left(\frac{dN_{M,R}(t-\tau_M^R)}{dt}\right)^{-} (1-\ell_M) , \quad (3.3\text{-}9)$$

where the processing lags and losses have been accounted for. Here, τ_M^R is the amount of time needed to reprocess and fabricate the material and ℓ_M is the fraction of the material entering the plant which is lost.

Using Eq(3.3-1), the rate of change of the stockpile inventory for all t due to reactor R will be given by

$$\left(\frac{dN_{M,S}(t)}{dt}\right)^{R} = \begin{cases} -N^{SS}_{M,R}/\tau^{D}_{R}\, h_R(t), \quad 0<t\leq\tau^{R}_{M}, & (3.3\text{-}10a) \\ -N^{SS}_{M,R}/\tau^{D}_{R}\, h_R(t) + [N^{SS}_{M,R}/\tau^{D}_{R} h_R(t-\tau^{R}_{M}) & (3.3\text{-}10b) \\ \quad +G_{M,R}R_R g_R(t-\tau^{R}_{M})]\,(1-\ell_M), \tau^{R}_{M}<t\leq\tau^{SS}_{R}, & \\ -N^{SS}_{M,R}/\tau^{D}_{R} + [N^{SS}_{M,R}/\tau^{D}_{R} h_R(t-\tau^{R}_{M}) & (3.3\text{-}10c) \\ \quad +G_{M,R}R_R g_R(t-\tau^{R}_{M})]\,(1-\ell_M), \tau^{SS}_{R}<t\leq\tau^{SS}_{R}+\tau^{R}_{M}, & \\ -N^{SS}_{M,R}/\tau^{D}_{R} + [N^{SS}_{M,R}/\tau^{D}_{R} + G_{M,R}R_R]\,(1-\ell_M), & (3.3\text{-}10d) \\ \quad \tau^{SS}_{R}+\tau^{R}_{M} < t \leq \tau^{EOL}_{R}, & \\ [N^{SS}_{M,R}/\tau^{D}_{R} + G_{M,R}R_R]\,(1-\ell_M), & (3.3\text{-}10e) \\ \quad \tau^{EOL}_{R}<t\leq\tau^{EOL}_{R}+\tau^{R}_{M}, & \\ 0, \quad t>\tau^{EOL}_{R}+\tau^{R}_{M}. & (3.3\text{-}10f) \end{cases}$$

The various time domains in Eq(3.3-10) are graphically displayed in Fig. 3.3-3. Between startup and the time at which material first reaches the stockpile, $0<t\leq\tau^{R}_{M}$, Eq(3.3-10a) describes the refuelling of the reactor at a pre-steady-state rate. After a time equal to the reprocessing-fabrication period, material begins to reach the stockpile. During the next period, $\tau^{R}_{M}<t\leq\tau^{SS}_{R}$, the reactor is refuelled and material discharged at the pre-steady-state rate, Eq(3.3-10b). After steady-state is reached, the reactor is refuelled at the rate Eq(3.3-3a) but material added to the stockpile from the processing plant is from a pre-steady-state core; hence, Eq(3.3-10c) describes steady-state refuelling and pre-steady-state discharge. Steady-state discharge material begins to reach the stockpile at $t = \tau^{SS}_{R} + \tau^{R}_{M}$, thus, until the reactor is shut down at $t = \tau^{EOL}_{R}$,

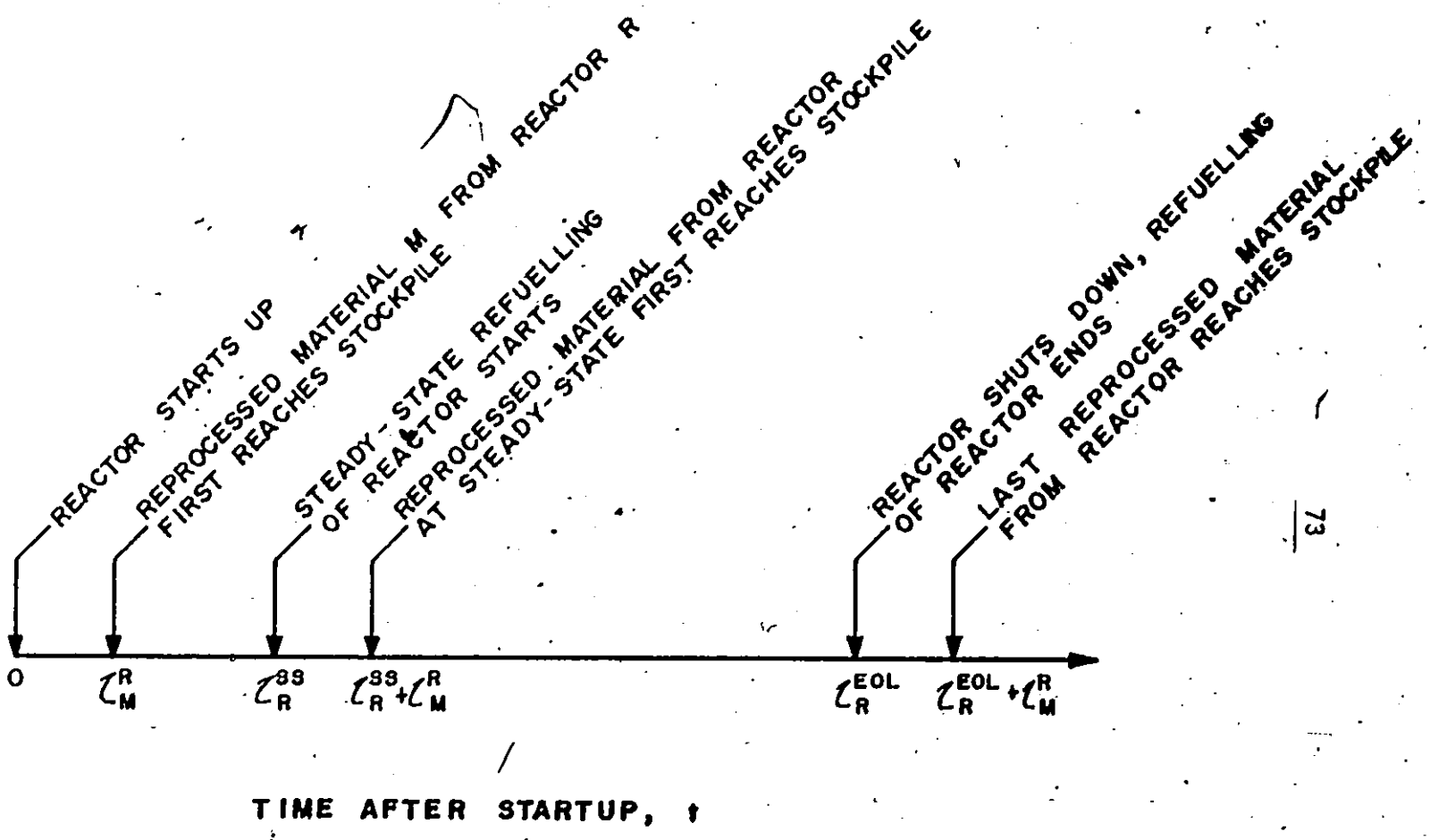

Fig. 3.3-3: Schematic of time domains during the system lifetime.

Eq(3.3-10d) is applicable. After the reactor is shutdown, there will be no refuelling or material discharged, but for the next τ_M^R years, the material already in the reprocessing-fabrication plant will be added to the stockpile. During this period, $\tau_R^{EOL} < t \leq \tau_R^{EOL} + \tau_M^R$, Eq(3.3-10e) describes the addition to the stockpile. After this material is processed, there will be no change in the inventory and Eq(3.3-10f) holds.

In addition to this continuous variation, two discontinuous changes in the stockpile inventory will occur. At startup, an initial loading of reactor R must take place which is given by

$$(\Delta N_{M,S}(0^+))^R = -N_{M,R}(0^+), \quad t = 0^+ \tag{3.3-11}$$

At the end of the reactor life, the core will be discharged; the amount added to the stockpile will be

$$(\Delta N_{M,S}(\tau_R^{EOL} + \tau_M^R))^R = (N_{M,R}^{SS} + 1/2 G_{M,R} R_R \tau_R^D)(1-\ell_M) , \tag{3.3-12}$$
$$t = \tau_R^{EOL} + \tau_M^R$$

which includes the steady-state fresh fuel loading and a term to account for changes due to irradiation. The factor of $1/2\tau_R^D$ in Eq(3.3-12) is the average exposure during the mean residence period,

$$\frac{1}{\tau_R^D} \int_0^{\tau_R^D} t'dt' = \frac{1}{2}\tau_R^D \tag{3.3-13}$$

Specific inventory of reactor i will be defined as

$$\omega_{M,i} = N_{M,i}^{SS}/R_i , \tag{3.3-14}$$

and, as stated in Chapter II, will be constant. A specific inventory

with units of kg/MW_t is related to a specific inventory with units of nuclei second, as in Eq(3.3-14), by a factor $(U_i\ N_{AV}\ 10^{-3})/A_M$ where U_i is the energy released per characteristic reaction in MW s, N_{AV} is Avagadro's number and A_M is the atomic weight of the material in grams/mole. The stockpile inventory of material M due to reactor R including discontinuous changes can be written as

$$(N_{M,S}(t))^R = -\omega^o_{M,R} R_R H(t) + \int_0^t (dN_{M,S}(t')/dt')dt' + (\omega_{M,R} R_R + 1/2 G_{M,R} R_R \tau^D_R)(1-\ell_M) H(t-\tau^{EOL}_R-\tau^R_M) , \quad (3.3\text{-}15)$$

where $\omega^o_{M,i}$ is defined by

$$\omega^o_{M,i} = N_{M,i}(0^+)/R_i , \quad (3.3\text{-}16)$$

and H(t) is the Heaviside unit step function.

By extending the ranges of $g_i(t)$ and $h_i(t)$ to cover the period $t \geq 0$, Eq(3.3-10) can be reduced to one equivalent equation. Using the following definitions

$$g_i(t) = \begin{cases} 0, \ t \leq 0 , & (3.3\text{-}17a) \\ g_i(t), \ 0 < t \leq \tau^{SS}_i , & (3.3\text{-}17b) \\ 1, \ \tau^{SS}_i < t \leq \tau^{EOL}_i , & (3.3\text{-}17c) \\ 0, \ t > \tau^{EOL}_i ; & (3.3\text{-}17d) \end{cases}$$

and

$$h_i(t) = \begin{cases} 0, \ t \leq 0 , & (3.3\text{-}18a) \\ h_i(t), \ 0 < t \leq \tau^{SS}_i , & (3.3\text{-}18b) \\ 1, \ \tau^{SS}_i < t \leq \tau^{EOL}_i , & (3.3\text{-}18c) \\ 0, \ t > \tau^{EOL}_i , & (3.3\text{-}18d) \end{cases}$$

and substituting these into Eq(3.3-10),

$$\left(\frac{dN_{M,S}(t)}{dt}\right)^R = \left\{\frac{\omega_{M,R}}{\tau_R^D}\left[h_R(t-\tau_M^R)(1-\ell_M)-h_R(t)\right] + G_{M,R}g_R(t-\tau_M^R)(1-\ell_M)\right\}R_R \quad , \quad t\geq 0 \quad , \tag{3.3-19}$$

will describe the rate of change of the stockpile inventory of material M due to reactor R.

To consider the complete system model of a breeder-converter, separate parameters will be used for the breeder core and blanket as illustrated in Fig. 3.3-4. Letting C refer to the converter reactor, BC to the breeder core, BB to the breeder blanket and S to the stockpile, the rate of change of the system stockpile of material M will be given by the sum

$$\left(\frac{dN_{M,S}(t)}{dt}\right) = \left(\frac{dN_{M,S}(t)}{dt}\right)^C + \left(\frac{dN_{M,S}(t)}{dt}\right)^{BC} + \left(\frac{dN_{M,S}(t)}{dt}\right)^{BB} . \tag{3.3-20}$$

Here, the effects of the external source have been excluded. A function $D_{M,i}(t)$ for each component is defined by

$$D_{M,i}(t) = \left(\frac{dN_{M,S}(t)}{dt}\right)^i /R_i \quad . \tag{3.3-21}$$

Using this definition, Eq(3.3-20) can be rewritten as

$$\frac{dN_{M,S}(t)}{dt} = D_{M,C}(t)R_C + [D_{M,BC}(t) + D_{M,BB}(t)]R_B \quad . \tag{3.3-22}$$

The stockpile inventory, including startup and end-of-life changes, will be described by

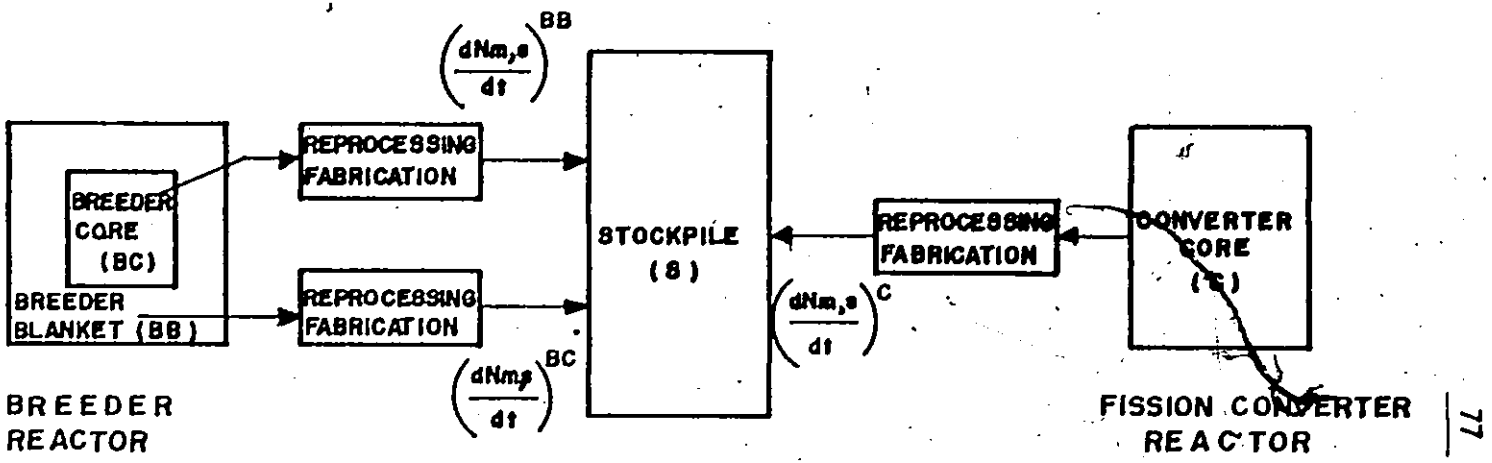

Fig. 3.3-4: Schematic of the breeder-converter reactor showing the isotope couplings.

$$
\begin{aligned}
N_{M,S}(t)-N_{M,S}(0) = & -[\omega^{o}_{M,C}R_C + (\omega^{o}_{M,BC} + \omega^{o}_{M,BB})R_B]H(t) \\
& + \int_o^t [D_{M,C}(t')R_C + (D_{M,BC}(t') + D_{M,BB}(t'))R_B]dt' \\
& + (\omega_{M,C} + \frac{\tau^{D}_{C}}{2} G_{M,C})R_C(1-\ell_M)H(t-\tau^{EOL}_{C}-\tau^{R}_{M}) \qquad (3.2\text{-}23) \\
& + (\omega_{M,BC}+\omega_{M,BB}+\frac{\tau^{D}_{BC}}{2}G_{M,BC}+\frac{\tau^{D}_{BB}}{2}G_{M,BB}) \\
& \times R_B(1-\ell_M)H(t-\tau^{EOL}_{B}-\tau^{R}_{M}) \ ,
\end{aligned}
$$

The initial stockpile inventories are set to zero, thus $N_{M,S}(t)$ will be the amount of material M available to external reactors if $N_{M,S}(t)>0$ or the amount of material required from the external source if $N_{M,S}(t)<0$. If the parameters describing the reactors and the reprocessing-fabrication plant are known, then only R_C and R_B are needed to completely determine the stockpile inventories. It will be shown in Section 3.4 that the power of a reactor is proportional to the characteristic reaction rate. Since it is our aim to study primarily breeder reactors, R_C will be fixed in the following; hence, only R_B will need to be specified.

The specification of the breeder thermal power, one inventory or the rate of change of only one inventory will determine R_B. For example, if for some arbitrary material, $N_{1,S}(t_o)$ is fixed, then we want R_B such that at time t_o the value of the stockpile inventory of material 1 is $N_{1,S}(t_o)$. Using Eq(3.3-23), the breeder size necessary to achieve this will be given by

$$R_B = \{N_{1,S}(t_o)+\omega^o_{1,C}R_C H(t_o)-\int^{t_o}_0 D_{1,C}(t')dt'R_C$$
$$-(\omega_{1,C}+1/2\tau^D_C G_{1,C})R_C(1-\ell_M)H(t_o-\tau^{EOL}_C-\tau^R_1)\}$$
$$X\{-(\omega^o_{1,BC}+\omega^o_{1,BB})H(t_o)+\int^{t_o}_0(D_{1,BC}(t')+D_{1,BB}(t'))dt'$$
$$+(\omega_{1,BC}+\omega_{1,BB}+1/2\tau^D_{BC}G_{1,BC}+1/2\tau^D_{BB}G_{1,BB})(1-\ell_M) \qquad (3.3\text{-}24)$$
$$X\ H(t_o-\tau^{EOL}_B-\tau^R_1)\}^{-1}\ .$$

Similarly, if a certain value, $dN_{1,S}(t_o)/dt$, is required, then using Eq(3.3-22), the characteristic reaction rate of the breeder will be found using

$$R_B = \left\{\frac{dN_{1,S}(t_o)}{dt} - D_{1,C}(t_o)R_C\right\}\left\{D_{1,BC}(t_o)+D_{1,BB}(t_o\int\right\}^{-1} \quad .(3.3\text{-}25)$$

An interesting condition to fix R_B is to find the breeder size such that $N_{M,S}(\tau^{MIN}_M)$, that is, the minimum value of the stockpile of material M, is minimized. To do this, Eq(3.3-21) is set to zero to find the value of τ^{MIN}_M and this is substituted into Eq(3.3-23). The derivative with respect to R_B of this new equation for $N_{M,S}(\tau^{MIN}_M)$ is taken and set to zero in order to find the value of $(R_B)^{MIN}_M$. To fix R_B by this method, the time dependence of $g_1(t)$ and $h_1(t)$ must be explicitly known.

Exact specification of $g_1(t)$ and $h_1(t)$ will require knowledge of the fuel management scheme during the transitional period which, for most breeders, is unknown. To avoid such a detailed treatment, a simplified but physically reasonable approximation will be presented. The function $h_1(t)$ was defined by Eq(3.3-5) to account for the pre-steady-state fuel loading scheme. If the components are consistently fuelled throughout their lifetime, then

$$h_i(t) = \begin{cases} 0, & t \leq 0 , \quad (3.3\text{-}26a) \\ 1, & 0 < t \leq \tau_i^{EOL} , \quad (3.3\text{-}26b) \\ 0, & t > \tau_i^{EOL} , \quad (3.3\text{-}26c) \end{cases}$$

$$i = C, BC \text{ or } BB .$$

Thus, there will be no pre-steady-state refuelling in this case. The function $g_i(t)$ is used to describe the pre-steady-state net generation ratio, Eq(3.3-8). Since a core, fission or fusion, must be maintained in some critical state, it is reasonable to expect that

$$g_i(t) = \begin{cases} 0, & t \leq 0 , \quad (3.3\text{-}27a) \\ 1, & 0 < t \leq \tau_i^{EOL} , \quad (3.3\text{-}27b) \\ 0, & t > \tau_i^{EOL} , \quad (3.3\text{-}27c) \end{cases}$$

$$i = C \text{ or } BC .$$

Here then, we have excluded pre-steady-state conditions in a critical core. For the breeder blanket however, we postulate that the rate at which a material is discharged at a time t will be proportional to the fraction of the core discharged, τ_i^F/τ_i^D, and the length of time it has been irradiated, t. This is equivalent to assuming a linear variation in the change $\Delta N_{M,i}^D$ during the discharge period. Thus, steady-state is reached in the blanket after one mean residence period and the function $g_i(t)$ is given by

$$g_i(t) = \begin{cases} 0, & t \leq 0 , \quad (3.3\text{-}28a) \\ t/\tau_i^D, & 0 < t \leq \tau_i^D , \quad (3.3\text{-}28b) \\ 1, & \tau_i^D < t \leq \tau_i^{EOL} , \quad (3.3\text{-}28c) \\ 0, & t > \tau_i^{EOL} , \quad (3.3\text{-}28d) \end{cases}$$

$$\text{for } i = BB .$$

As a result of this, τ_{BB}^{SS} for the breeding blanket is reached at τ_{BB}^{D}.

These pre-steady-state functions have been compared with two more exact treatments. In Fig. 3.3-5, data from the Clinch River Breeder Reactor project[38,39] is shown without reprocessing. The solid line was calculated using the above assumptions while the points are values for an exact fuel management scheme proposed for the reactor. It can be seen that, although the curve does not follow exactly the data points and the zero cross over is underestimated by approximately 1.5 years, the general shape and steady-state slope are reproduced. Fig. 3.3-6 shows the detailed treatment by Heindler and Harms[4] for a fission breeder reactor over the lifetime of the reactor. The major discrepancy between their analysis and our analysis is the assumption that $\omega_{FI,BC}^{o} = \omega_{FI,BC}$ which introduced a constant error of ~5%. The only other difference in shape between the two is during the first 1.5 years where a constant load factor and power have been assumed in this model as opposed to a more detailed treatment. Overall however, the simplifications introduced reproduce the same trends as the exact analyses. In view of the fact that conceptual blanket designs for breeder systems will have uncertainties of ~20%[41], the errors introduced as a result of the assumptions seem acceptable for parametric studies.

The rate of change functions defined in Eq(3.3-21) can be found by substituting Eq(3.3-26), Eq(3.3-27) and Eq(3.3-28) into Eq(3.3-19):

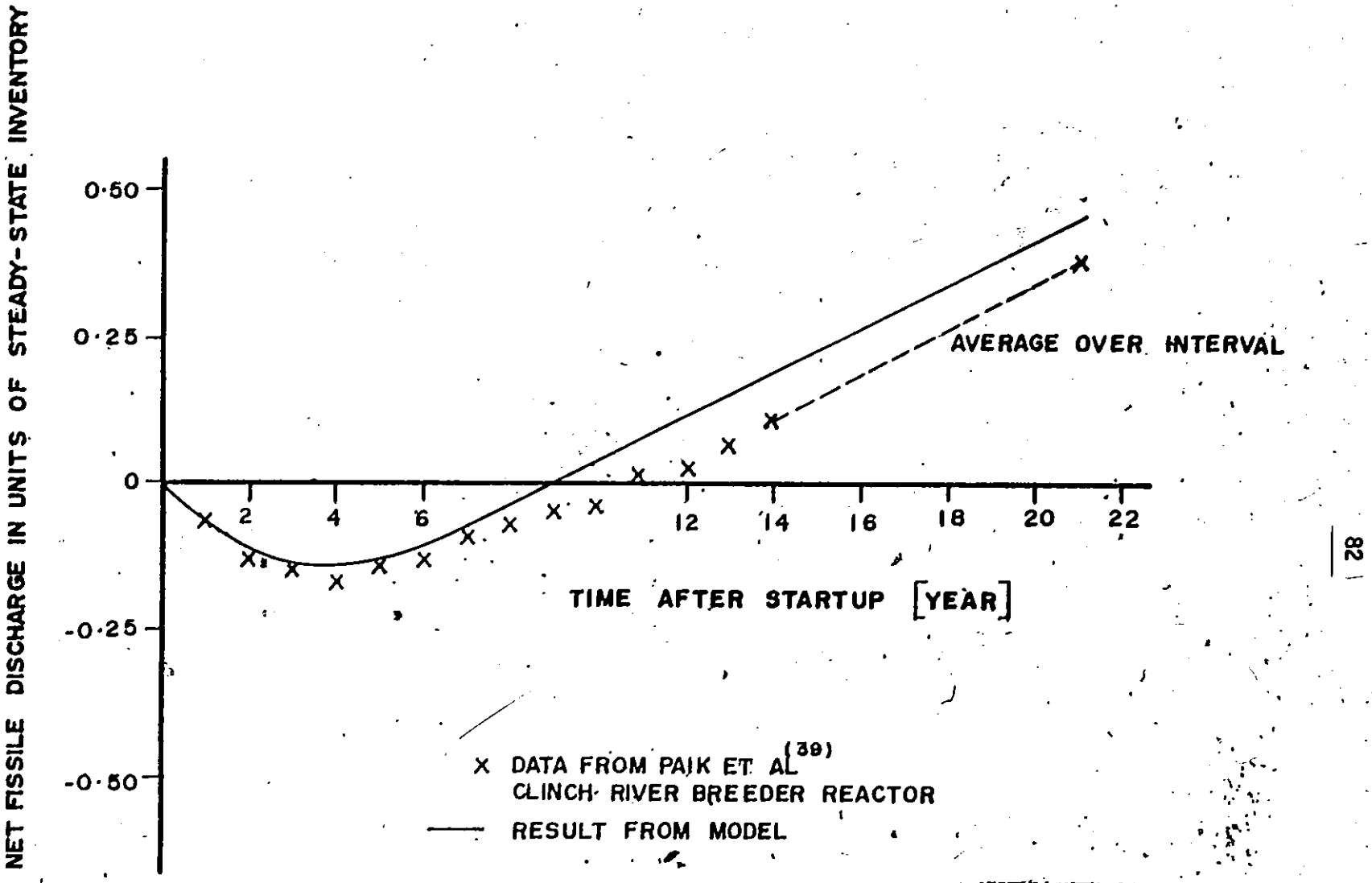

Fig. 3.3-5: Comparison of fissile discharge calculated using model developed in text with an exact fuel management scheme. (No reprocessing). An alternative approach, if the exact fuel management scheme is known, would be to use g(t) and h(t) to fit the data.

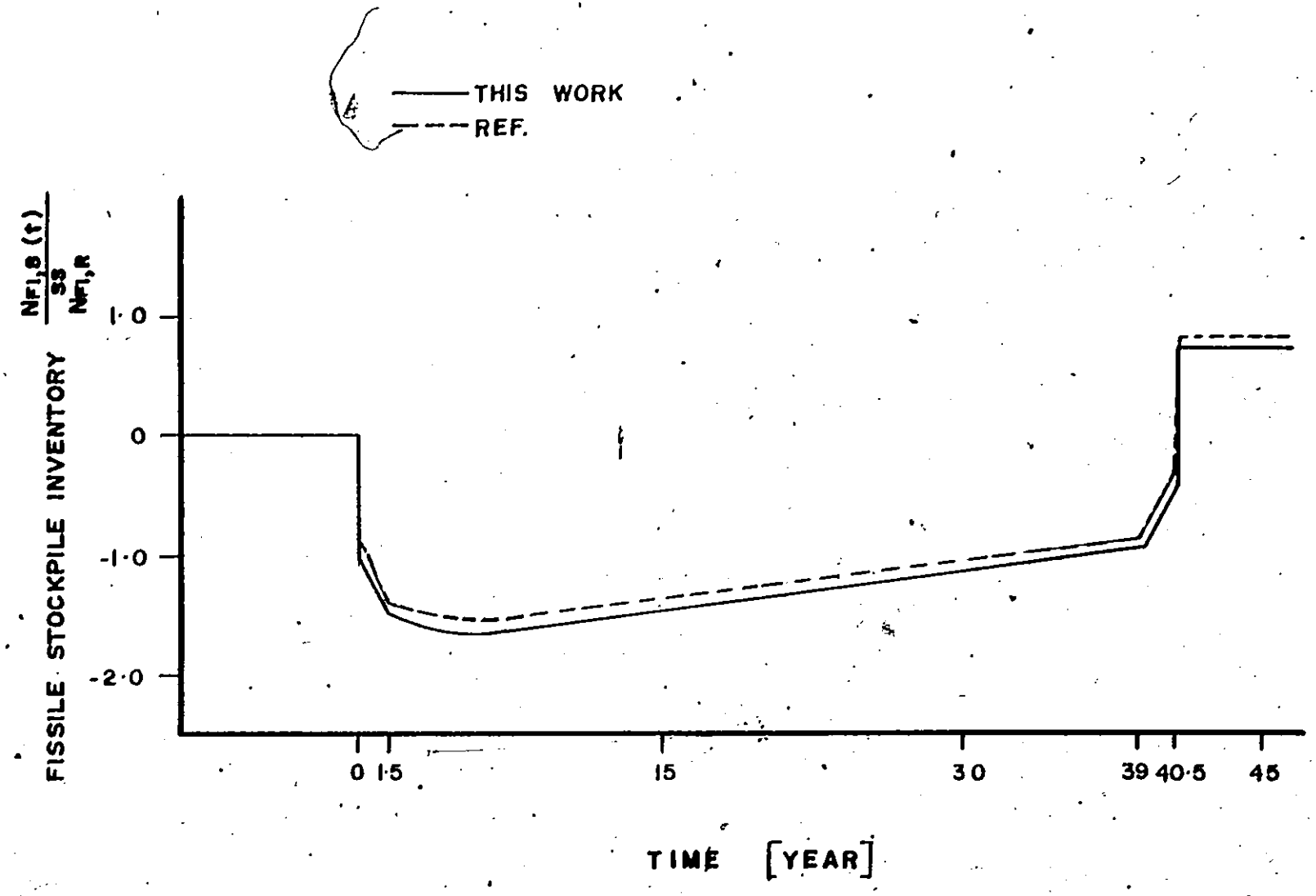

Fig. 3.3-6: Comparison of the variation of stockpile inventory as calculated here with a detailed integration.

$$D_{M,C}(t) = \begin{cases} 0, \ t \le 0 , & (3.3\text{-}29a) \\ -\omega_{M,C}/\tau_C^D, \ 0 < t \le \tau_M^R , & (3.3\text{-}29b) \\ -\omega_{M,C}/\tau_C^D \ell_M + G_{M,C}(1-\ell_M), \ \tau_M^R < t \le \tau_C^{EOL} , & (3.3\text{-}29c) \\ (\omega_{M,C}/\tau_C^D + G_{M,C})(1-\ell_M), \ \tau_C^{EOL} < t \le \tau_C^{EOL} + \tau_M^R , & (3.3\text{-}29d) \\ 0, \ t > \tau_C^{EOL} + \tau_M^R ; & (3.3\text{-}29e) \end{cases}$$

$$D_{M,BC}(t) = \begin{cases} 0, \ t \le 0 , & (3.3\text{-}30a) \\ -\omega_{M,BC}/\tau_{BC}^D, \ 0 < t \le \tau_M^R , & (3.3\text{-}30b) \\ -\omega_{M,BC}/\tau_{BC}^D \ell_M + G_{M,BC}(1-\ell_M), \ \tau_M^R < t \le \tau_B^{EOL} , & (3.3\text{-}30c) \\ (\omega_{M,BC}/\tau_B^D + G_{M,BC})(1-\ell_M), \ \tau_B^{EOL} < t \le \tau_B^{EOL} + \tau_M^R , & (3.3\text{-}30d) \\ 0, \ t > \tau_B^{EOL} + \tau_M^R ; & (3.3\text{-}30e) \end{cases}$$

and

$$D_{M,BB}(t) = \begin{cases} 0, \ t < 0 , & (3.3\text{-}31a) \\ -\omega_{M,BB}/\tau_{BB}^D, \ 0 < t \le \tau_M^R , & (3.3\text{-}31b) \\ -\omega_{M,BB}/\tau_{BB}^D \ell_M + G_{M,BB}(t-\tau^R)(1-\ell_M)/\tau_{BB}^D , & (3.3\text{-}31c) \\ \tau_M^R < t < \tau_{BB}^D + \tau_M^R , & \\ -\omega_{M,BB}/\tau_{BB}^D \ell_M + G_{M,BB}(1-\ell_M), \ \tau_{BB}^D + \tau_M^R < t \le \tau_B^{EOL} , & (3.3\text{-}31d) \\ (\omega_{M,BB}/\tau_{BB}^D + G_{M,BB})(1-\ell_M), \ \tau_B^{EOL} < t \le \tau_B^{EOL} + \tau_M^R , & (3.3\text{-}31e) \\ 0, \ t > \tau_B^{EOL} + \tau_M^R . & (3.3\text{-}31f) \end{cases}$$

These can be substituted into Eq(3.3-22) to find the rate of change of the stockpile inventory or Eq(3.3-23) to find the stockpile inventory at any time.

The temporal variation of stockpile inventories calculated using the above will exhibit similar overall trends. In Fig. 3.3-7, we show the temporal variation of two inventories, $N_{1,S}(t)$ with $(dN_{1,S}/dt)_{SS}>0$

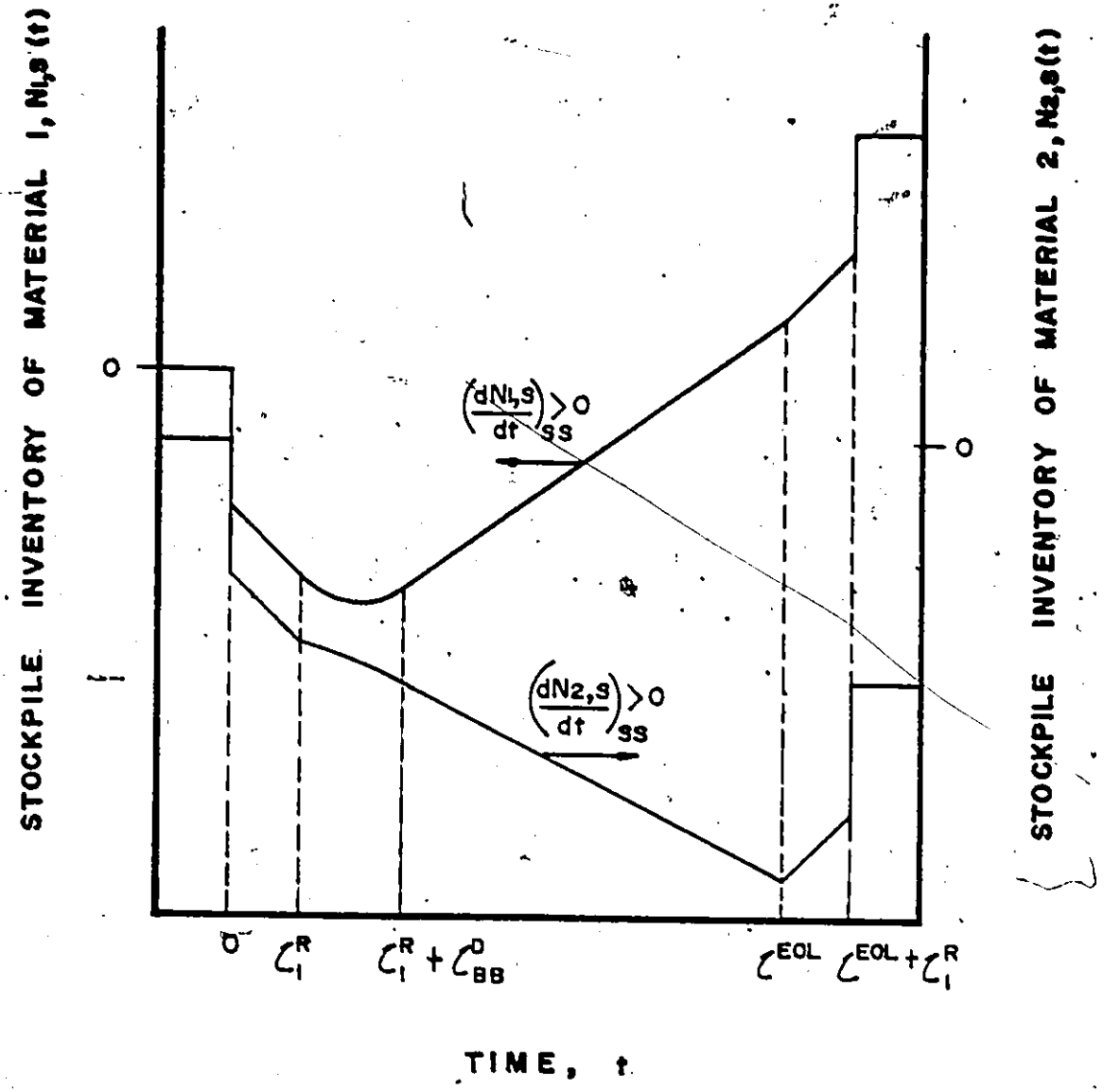

Fig. 3.3-7: Schematic showing stockpile trends for two materials. Scales have been offset for clarity and $\tau_1^R = \tau_2^R$, $\tau_C^{EOL} = \tau_B^{EOL} \neq \tau^{EOL}$.

and $N_{2,S}(t)$ with $(dN_{2,S}/dt)_{SS<0}$, to illustrate these trends. Here, τ_1^R and τ_2^R, and τ_B^{EOL}, τ_C^{EOL} and τ^{EOL} are set equal. Both inventories start out at zero and have a discontinuous first loading which is given for each component by Eq(3.3-11). Following this, there is a period of τ_1^R years during which both inventories decrease linearly with time. It is during this period that the reactors are fuelled without any processed material reaching the stockpile. In the period $\tau_1^R<t\leq\tau_{BB}^R+\tau_1^R$, the inventories undergo a quadratic variation due to the increase in processed material. This is an effect attributable to pre-steady-state in the breeder blanket. Steady-state occurs for $\tau_{BB}^R+\tau_1^R<t\leq\tau^{EOL}$ and during this period both inventories have a constant rate of change. Between τ^{EOL} and $\tau^{EOL}+\tau_1^R$, material in the reprocessing-fabrication plant is added to the stockpile, hence both inventories increase. At $\tau^{EOL}+\tau_1^R$, there is another discontinuous change in the stockpile as the processed final core and blankets are added to the inventory. For $t>\tau^{EOL}+\tau_1^R$, the inventories are constant.

The minimum inventory of a material gives the maximum amount which must be supplied by external sources, as illustrated in Fig. 3.3-8. To find the time to reach the minimum, τ_M^{MIN}, we note that if the steady-state rate of change of the inventory, $(dN_{M,S}/dt)_{SS}$, is negative then

$$\tau_M^{MIN} = \tau^{EOL} , \qquad (3.3\text{-}32)$$

where it has been specified that τ_C^{EOL} and τ_B^{EOL} are equal to τ^{EOL}. Otherwise, the minimum will occur in the period $\tau_M^R<t\leq\tau_{BB}^D+\tau_M^R$ where explicit time dependence occurs in $D_{M,BB}(t)$. Combining Eq(3.3-29),

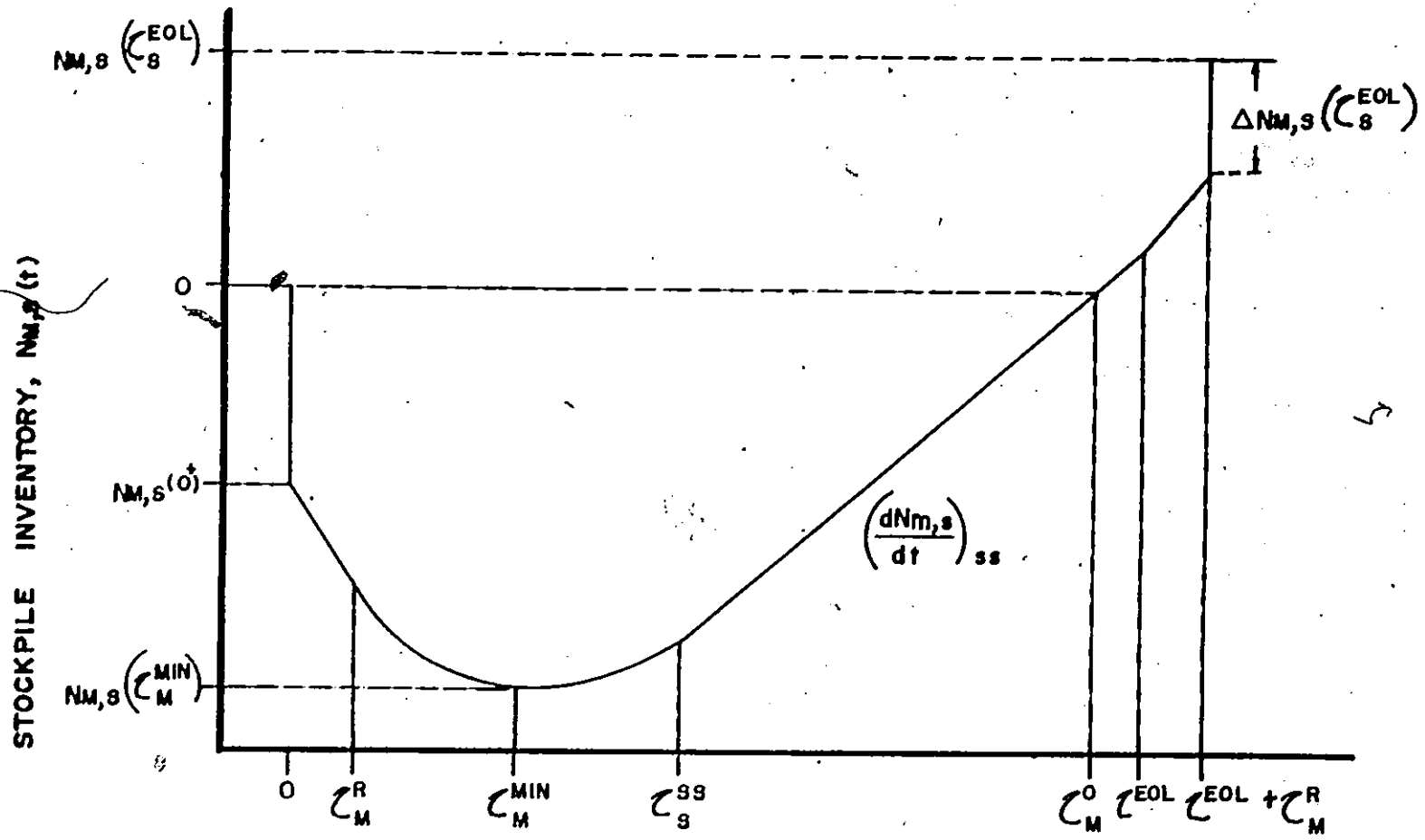

Fig. 3.3-8: Schematic showing some stockpile inventory characteristics.

Eq(3.3-30) and Eq(3.3-31) with Eq(3.3-22) and setting the derivative to zero, the time for the minimum to occur will be given by

$$\tau_M^{MIN} = \tau_M^R + \left\{ \left(\frac{\omega_{M,C}}{\tau_C^D} R_C + \frac{\omega_{M,BC}}{\tau_{BC}^D} R_B + \frac{\omega_{M,BB}}{\tau_{BB}^D} R_B \right) \ell_M \right. \qquad (3.3\text{-}33)$$
$$\left. -(G_{M,C} R_C + G_{M,BC} R_B)(1-\ell_M) \right\} \left\{ G_{M,BB} R_B (1-\ell_M)/\tau_{BB}^D \right\}^{-1} ,$$
$$\tau_M^R < \tau_M^{MIN} \leq \tau_{BB}^D + \tau_M^R .$$

If the breeder size is increased to infinity, a minimum value of τ_M^{MIN} can be found which depends only on breeder and system parameters:

$$(\tau_M^{MIN})_{MIN} = \tau_M^R + \tau_{BB}^D \frac{\left\{ (\omega_{M,BC}/\tau_{BC}^D + \omega_{M,BB}/\tau_{BB}^D)\ell_M - G_{M,BC}(1-\ell_M) \right\}}{G_{M,BB}(1-\ell_M)} . \qquad (3.3\text{-}34)$$

The minimum stockpile inventory, $N_{M,S}(\tau_M^{MIN})$ is found by substituting Eq(3.3-32) or Eq(3.3-33) into Eq(3.3-23). If the steady-state rate of change is negative, then Eq(3.3-32) applies and the minimum stockpile is given by

$$\begin{aligned} N_{M,S}(\tau_M^{MIN}) = & -(\omega_{M,C}^o R_C + (\omega_{M,BC}^o + \omega_{M,BB}^o) R_B) \\ & -(\omega_{M,C}/\tau_C^D R_C + (\omega_{M,BC}/\tau_{BC}^D + \omega_{M,BB}/\tau_{BB}^D) R_B)\tau_M^R \\ & -(\omega_{M,C}/\tau_C^D R_C + (\omega_{M,BC}/\tau_{BC}^D + \omega_{M,BB}/\tau_{BB}^D) R_B)\ell_M(\tau^{EOL} - \tau_M^R) \\ & +(G_{M,C} R_C + (G_{M,BC} + G_{M,BB}) R_B)(1-\ell_M)(\tau^{EOL} - \tau_M^R) \\ & -1/2 G_{M,BB} R_B (1-\ell_M)\tau_{BB}^D , \qquad (3.3\text{-}35) \\ \tau_M^{MIN} = & \tau^{EOL} . \end{aligned}$$

Examining this equation term by term, we find that the first term represents the initial loading of material M. The next gives the amount of material taken from the stockpile during the first τ_M^R years when no

processed material is added to the stockpile. In the third term, the loss of material due to processing for a period of $(\tau^{EOL}-\tau_M^R)$ years and the final term gives a correction factor due to pre-steady-state in the breeder blanket. If, however, Eq(3.3-33) is applicable, then the minimum stockpile inventory of material M will be given by

$$\begin{aligned} N_{M,S}(\tau_M^{MIN}) = & -(\omega_{M,C}^o R_C + (\omega_{M,BC}^o + \omega_{M,BB}^o)R_B) \\ & -(\omega_{M,C}/\tau_C^D R_C + (\omega_{M,BC}/\tau_{BC}^D + \omega_{M,BB}/\tau_{BB}^D)R_B)\tau_M^R \\ & -1/2\left\{(\omega_{M,C}/\tau_C^D R_C + (\omega_{M,BC}/\tau_{BC}^D + \omega_{M,BB}/\tau_{BB}^D)R_B)\ell_M \right. \\ & \left. -(G_{M,C}R_C + G_{M,BC}R_B)(1-\ell_M)\right\}^2 \\ & \times \left\{G_{M,BB}(1-\ell_M)R_B/\tau_{BB}^D\right\}^{-1}, \\ & \tau_M^R < \tau_M^{MIN} \leq \tau_{BB}^D + \tau_M^R . \end{aligned} \tag{3.3-36}$$

As mentioned previously, there will be a value of R_B, $(R_B)_M^{MIN}$, for which $N_{M,S}(\tau_M^{MIN})$ is minimum. This can be found by differentiating Eq(3.3-36) with respect to R_B and setting the result to zero yielding

$$\begin{aligned} (R_B)_M^{MIN} = & R_C\{\omega_{M,C}/\tau_C^D\ell_M - G_{M,C}(1-\ell_M)\}\left\{\frac{2G_{M,BB}(1-\ell_M)}{\tau_{BB}^D}\right. \\ & \times (\omega_{M,BC}^o + \omega_{M,BB}^o + \omega_{M,BC}\tau_M^R/\tau_{BC}^D + \omega_{M,BB}\tau_M^R/\tau_{BB}^D) \\ & \left. + [(\omega_{M,BC}/\tau_{BC}^D + \omega_{M,BB}/\tau_{BB}^D)\ell_M - G_{M,BB}(1-\ell_M)]^2\right\}^{-1/2} \\ & \tau_M^R < \tau_M^{MIN} \leq \tau_{BB}^D + \tau_M^R . \end{aligned} \tag{3.3-37}$$

This is applicable only if $(dN_{M,S}/dt)_{SS}$ is greater than zero. If this is not the case, then the value of $(R_B)_M^{MIN}$ will be given by

$$(R_B)_M^{MIN} = R_C\{-\omega_{M,C}/\tau_C^D\ell_M + G_{M,C}(1-\ell_M)\}\{-(\omega_{M,BC}/\tau_{BC}^D + \omega_{M,BB}/\tau_{BB}^D)\ell_M + (G_{M,BC} + G_{M,BB})(1-\ell_M)\}^{-1} , \quad (3.3\text{-}37)$$

$$\tau_{BB}^D + \tau_M^R < \tau_M^{MIN} \leq \tau^{EOL} ,$$

which gives a zero steady-state rate of change of the stockpile inventory.

An important measure of the breeding capabilities of the system is the material replacement time, τ_M^0. This is the time needed by the breeder-converter to replace the material which has been supplied from the external source, as shown in Fig. 3.3-8. The value of τ_M^0 will be defined by

$$N_{M,S}(\tau_M^0) = 0 , \quad (3.3\text{-}38)$$

and can be calculated using Eq(3.3-23). There are five regimes which must be accounted for. Clearly for a producing system, τ_M^0 must be longer than the reprocessing-fabrication lag since, prior to $t = \tau_M^R$, no material is added to the stockpile. During the transitional phase, we obtain

$$\tau_m^0 = \tau_M^R + [-a_2 + (a_2^2 - 4a_1a_3)^{1/2}]/(2a_1) , \quad (3.3\text{-}40)$$

$$\tau_M^R < \tau_M^0 \leq \tau_M^R + \tau_{BB}^D ,$$

where the coefficients a_1, a_2 and a_3 are given by

$$a_1 = G_{M,BB}(1-\ell_M)R_B/(2\tau_{BB}^D) , \quad (3.3\text{-}41a)$$

$$a_2 = -[\omega_{M,C}/\tau_C^D R_C + (\omega_{M,BC}/\tau_{BC}^D + \omega_{M,BB}/\tau_{BB}^D)R_B]\ell_M + (G_{M,C}R_C + G_{M,BC}R_B)(1-\ell_M) , \quad (3.3\text{-}41b)$$

$$a_3 = -(\omega_{M,C}^o R_C + (\omega_{M,BC}^o + \omega_{M,BB}^o)R_B) - (\omega_{M,C}/\tau_C^D R_C + (\omega_{M,BC}/\tau_{BC}^D + \omega_{M,BB}/\tau_{BB}^D)R_B)\tau_M^R . \quad (3.3\text{-}41c)$$

At steady-state, the material replacement time will be given by

$$\tau_M^o = \{\omega_{M,C}^o R_C + (\omega_{M,BC}^o + \omega_{M,BB}^o)R_B + (\omega_{M,C}/\tau_C^D R_C + (\omega_{M,BC}/\tau_{BC}^D + \omega_{M,BB}/\tau_{BB}^D)R_B)\ \tau_M^R + G_{M,BB}(1-\ell_M)R_B\tau_{BB}^D/2\} \quad (3.3\text{-}42)$$
$$X\{-(\omega_{M,C}/\tau_C^D R_C + (\omega_{M,BC}/\tau_{BC}^D + \omega_{M,BB}/\tau_{BB}^D)R_B)\ell_M$$
$$+(G_{M,C}R_C + (G_{M,BC} + G_{M,BB})R_B)(1-\ell_M)\}^{-1} + \tau_M^R ,$$
$$\tau_M^R+\tau_{BB}^D<\tau_M^o\leq\tau^{EOL} .$$

After the reactor has been shut down, there is a period of τ_M^R years during which the reprocessing-fabrication plant is adding material to the stockpile. When τ_M^o occurs within this period, it is given by

$$\tau_M^o = \{\omega_{M,C}^o R_C + (\omega_{M,BC}^o + \omega_{M,BB}^o)R_B + (\omega_{M,C}/\tau_C^D R_C + (\omega_{M,BC}/\tau_{BC}^D + \omega_{M,BB}/\tau_{BB}^D)R_B)\tau^{EOL} + G_{M,BB}(1-\ell_M)R_B\tau_{BB}^D/2\} \quad (3.3\text{-}43)$$
$$X\{-[\omega_{M,C}/\tau_C^D R_C + (\omega_{M,BC}/\tau_{BC}^D + \omega_{M,BB}/\tau_{BB}^D)R_B]\ell_M$$
$$+[G_{M,C}R_C + (G_{M,BC} + G_{M,BB})R_B](1-\ell_M)\}^{-1} + \tau_M^R ,$$
$$\tau^{EOL}<\tau_M^o\leq\tau^{EOL} + \tau_M^R .$$

If the material M is replaced only after the final cores and blanket have been processed, then τ_M^o will be found using

$$\tau_M^o = \tau^{EOL} + \tau_M^R , \quad (3.3\text{-}44)$$

but if, even after the final reprocessing, $N_{M,S}(\tau^{EOL} + \tau_M^R)$ is less than zero, we will set τ_M^o to zero.

From Eq(3.3-24), a value of R_B can be found for a given $N_{M,S}(t_o)$. If we set t_o equal to τ_M^o, then for a finite positive R_B to be found such

that $N_{M,S}(\tau_M^O) = 0$, the following inequality must be satisfied,

$$\int_0^{\tau^{EOL}+\tau_M^R} (D_{M,BC}(t) + D_{M,BB}(t))dt > \omega_{M,BC}^o + \omega_{M,BB}^o - (\omega_{M,BC} + \omega_{M,BB} + 1/2\tau_{BC}^D G_{M,BC} + 1/2\tau_{BB}^D G_{M,BB})(1-\ell_M) \quad (3.3\text{-}45)$$

If Eq(3.3-45) is not satisfied then for all breeder powers, τ_M^O will be zero. The minimum value of the material replacement time can be found for R_B tending to infinity. There are two possible values for $(\tau_M^O)_{MIN}$:

$$(\tau_M^O)_{MIN} = \tau_M^R + [-b_2 - (b_2^2 - 4b_1 b_3)^{1/2}]/(2b_1) , \quad (3.3\text{-}46)$$

where the coefficients b_1, b_2 and b_3 are given by

$$b_1 = 1/2 G_{M,BB}(1-\ell_M)/\tau_{BB}^D , \quad (3.3\text{-}47a)$$

$$b_2 = G_{M,BC}(1-\ell_M) - (\omega_{M,BC}/\tau_{BC}^D + \omega_{M,BB}/\tau_{BB}^D)\ell_M , \quad (3.3\text{-}47b)$$

$$b_3 = -(\omega_{M,BC}/\tau_{BC}^D + \omega_{M,BB}/\tau_{BB}^D)\tau_M^R - (\omega_{M,BC}^o + \omega_{M,BB}^o) ; \quad (3.3\text{-}47c)$$

or

$$(\tau_M^O)_{MIN} = \tau_M^R + \left\{\omega_{M,BC}^o + \omega_{M,BB}^o + (\omega_{M,BC}/\tau_{BC}^D + \omega_{M,BB}/\tau_{BB}^D)\tau_M^R + 1/2 G_{M,BB}(1-\ell_M)\tau_{BB}^D\right\}\left\{(G_{M,BC} + G_{M,BB})(1-\ell_M) - (\omega_{M,BC}/\tau_{BC}^D + \omega_{M,BB}/\tau_{BB}^D)\ell_M\right\}^{-1} , \quad (3.3\text{-}48)$$

$$\tau_{BB}^D + \tau_M^R < (\tau_M^O)_{MIN} \leq \tau^{EOL} .$$

The value of $(R_B)_M^{MIN}$ is found from Eq(3.3-37) or Eq(3.3-38). We can use $(\tau_M^O)_{MIN}$ to decide which equation is applicable. The equations for $(R_B)_M^{MIN}$ can be combined into an equivalent equation using the coefficients defined by Eq(3.3-47),

$$(R_B)_M^{MIN_K} = -\omega_{M,C}\ell_M/\tau_C^D + G_{M,C}(1-\ell_M) , \quad (3.3\text{-}49)$$

where

$$K = \begin{cases} 2[(\tau_M^O)_{MIN} - \tau_M^R]b_1 + b_2 , & \\ \tau_M^R < \tau_M^{MIN}, \ (\tau_M^O)_{MIN} \leq \tau_{BB}^D + \tau_M^R , & (3.3\text{-}50a) \\ (-b_3 + b_1)/[(\tau_M^O)_{MIN} - \tau_M^R] , & \\ \tau_M^R + \tau_{BB}^D < \tau_M^{MIN}, \ (\tau_M^O)_{MIN} \leq \tau^{EOL} . & (3.3\text{-}50b) \end{cases}$$

Thus, if $(\tau_M^O)_{MIN} > \tau_{BB}^D + \tau_M^R$, Eq(3.3-50b) or Eq(3.3-38) is applicable and if $(\tau_M^O)_{MIN} < \tau_{BB}^D + \tau_M^R$, then Eq(3.3-50a) or Eq(3.3-37) is used.

To summarize then, we have developed an analytical expression, Eq(3.3-23), which yields the system stockpile inventory at any time. This equation is based on the system isotope balance and incorporates pre-steady-state fuel management, pre-steady-state net generation ratios and reprocessing lags and losses. In order to evaluate the explicit time dependence of the $g_i(t)$ and $h_i(t)$ functions which were introduced, we specified no special pre-steady-state fuelling schemes, Eq(3.3-26), no pre-steady-state effects on the net generation ratio in a critical core, Eq(3.3-27), and a linear variation of the pre-steady-state breeding-blanket net generation ratio, Eq(3.3-28). Once the explicit time dependence was known, some characteristics of the system were described. We emphasize that the equations developed in this section are applicable to any material in the system. In the next section, the relationship between the thermal power and the characteristic reaction rate referred to earlier will be developed.

3.4 System Power Balance

The power produced by the combination of the two reactors in the system will determine revenues from the sale of electricity. In addition, the capital costs of many components are proportional to the thermal power. The thermal power of a reactor is a measure of its size but, in this analysis, the power of the system component need not be limited to one reactor. For example, if a converter thermal power of 10,000 MW_t is specified, this value may be the result of the combined output of five, identical, converter reactors each with a thermal power of 2000 MW_t. As with the isotope balance, the power balance of one reactor will be considered first followed by the system power balance.

The reactor will consist of three components as shown in Fig. 3.4-1: the reactor, the energy converter and the reactor operating equipment. This component approach was developed by Darvas et al[77] for tokamaks but is applicable to all fusion[74], spallation[61] and fission reactors. The total thermal power of the reactor, P_i^T, is converted to electricity with a thermal efficiency, η_i^T, so that the gross electrical power, P_i^G, is given by

$$P_i^G = \eta_i^T P_i^T . \qquad (3.4\text{-}1)$$

Some of the gross electrical power is used to maintain operation of the reactor, that is, to operate pumps, control systems, particle accelerators or laser beams and other necessary auxiliary systems. This circulating electrical power, P_i^C, will be related to the gross electrical power by the circulating energy fraction, ε_i, where

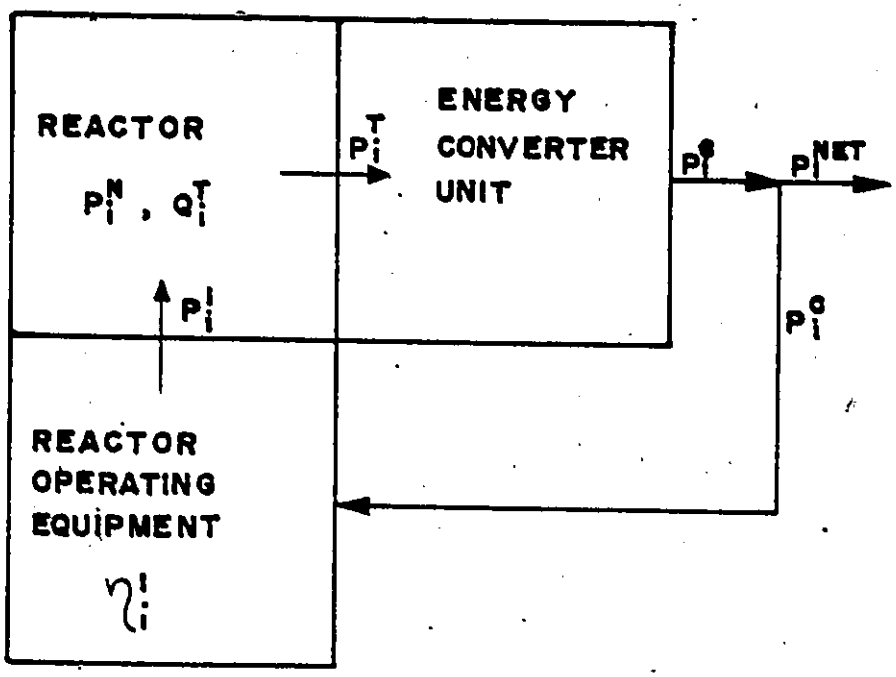

Fig. 3.4-1: Schematic showing the components of a reactor relevant to a reactor power balance.

$$\varepsilon_i = P_i^C / P_i^G \quad . \tag{3.4-2}$$

If $\varepsilon_i > 1$, then power must be added to drive the reactor. For fusion and spallation reactors, energy must be injected to ionize and confine a plasma or to accelerate protons. The injected power, P_i^I, is related to the circulating power by an overall injector efficiency defined by

$$\eta_i^I = P_i^I / P_i^C \quad , \tag{3.4-3}$$

where the efficiency here includes an amount for auxiliary power as well as the actual injector efficiency. For a fission reactor, η_i^I will be zero since no energy is injected into the core, however, ε_i will not be zero since some auxiliary power will be needed to operate the reactor.

The total thermal power will come from two sources: the nuclear reactions and the recovered injected power, hence

$$P_i^T = P_i^N + \alpha_i P_i^I \quad . \tag{3.4-4}$$

The nuclear source, P_i^N, is given by

$$P_i^N = R_i U_i \quad , \tag{3.4-5}$$

where U_i is the energy released per characteristic reaction. The second source is the fraction α_i of the injected energy which can be recovered. Following the example of fusion reactor analysis[74], the total amplification factor, Q_i^T, will be defined by

$$Q_i^T = P_i^T / P_i^I \quad . \tag{3.4-6}$$

Note that for a fission reactor, Q_i^T will be infinite since P_i^I will be

zero. The net electrical output of the reactor, P_i^{NET}, will be given by the difference between the gross and circulating electrical power,

$$P_i^{NET} = P_i^G - P_i^C \quad . \tag{3.4-7}$$

Using the above equations, P_i^{NET} can be expressed in terms of any other power in the system but, for our purposes,

$$P_i^{NET} = P_i^N \eta_i^T (1-\epsilon_i) Q_i^T / (Q_i^T - \alpha_i) \quad , \tag{3.4-8}$$

will prove convenient. The reactor thermal power can be related to the nuclear power by

$$P_i^T = P_i^N Q_i^T / (Q_i^T - \alpha_i) \quad , \tag{3.4-9}$$

and to the characteristic reaction rate by

$$P_i^T = R_i U_i Q_i^T / (Q_i^T - \alpha_i) \quad . \tag{3.4-10}$$

By sequential substitution, the following relationship is found among the parameters,

$$Q_i^T \epsilon_i = 1/(\eta_i^T \eta_i^I) \quad . \tag{3.4-11}$$

In the system power balance, Fig. 3.4-2, the net electrical output of the system, $P_S^{NET}(t)$, is equal to the sum of the net reactor powers less any power used in the reprocessing-fabrication of the fuels,

$$P_S^{NET}(t) = P_B^{NET} + P_C^{NET} - P_R(t) \quad . \tag{3.4-12}$$

Although it is not usual to include the energy used for processing in the system power balance, it is included here since, as stated in

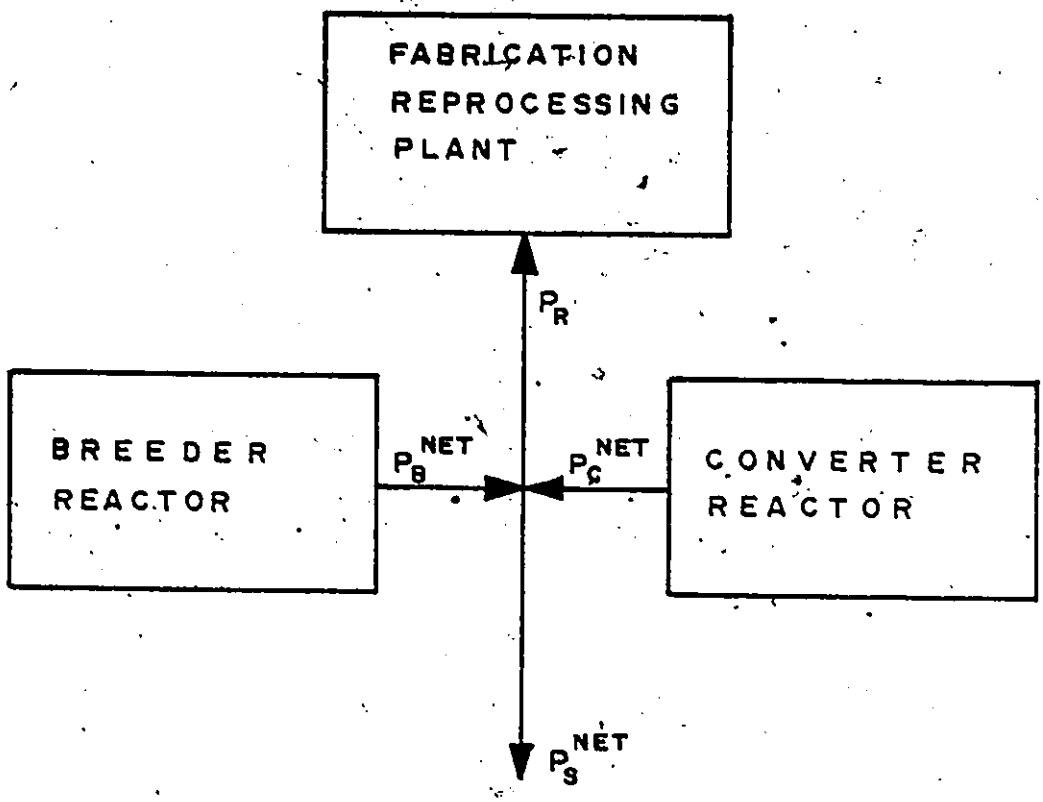

Fig. 3.4-2: Schematic showing the electrical coupling of the system components relevent to a system power balance.

Chapter I, an energy park with on-site processing is envisioned. The energy per atom needed to reprocess and fabricate a material M will be denoted by W_M and the rate of processing for a reactor defined by Eq(3.3-8), that is,

$$(dN_{M,i}(t)/dt)^{-} = \{\omega_{M,i}/\tau_i^D h_i(t) + G_{M,i} g_i(t)\}R_i \ . \qquad (3.4\text{-}13)$$

By analogy with the function $D_{M,i}(t)$, we define a function $E_{M,i}(t)$ such that

$$(dN_{M,i}(t)/dt)^{-} = E_{M,i}(t)\ R_i \ . \qquad (3.4\text{-}14)$$

Thus, the power needed for reprocessing-fabrication will be given by

$$P_R(t) = \Sigma_M W_M[E_{M,C}(t)R_C + (E_{M,BC}(t) + E_{M,BB}(t))R_B] \ . \qquad (3.4\text{-}15)$$

Here, we have neglected any discontinuous fuel reprocessing but include only the continuous variation during the reactor lifetime. Substituting Eq(3.4-5) into Eq(3.4-15), the processing power can be expressed in terms of the nuclear powers,

$$P_R(t) = \Sigma_M W_M[E_{M,C}(t)P_C^N/U_C + (E_{M,BC}(t) + E_{M,BB}(t))P_B^N/U_B] \ . \qquad (3.4\text{-}16)$$

Combining Eq(3.4-12) with Eq(3.4-8) and Eq(3.4-16), the net system electrical power will be given by

$$P_S^{NET}(t) = P_C^N\left\{\eta_C^T(1-\varepsilon_C) - \Sigma_M W_M E_{M,C}(t)/U_C\right\} \qquad (3.4\text{-}17)$$
$$+ P_B^N\left\{\eta_B^T(1-\varepsilon_B)Q_B^T/(Q_B^T-\alpha_B) - \Sigma_M W_M(E_{M,BC}(t)+E_{M,BB}(t))/U_B\right\}.$$

The net system efficiency is defined as the ratio of net electrical

power output to the total nuclear thermal power generated,

$$\eta_S^{NET}(t) = P_S^{NET}(t)/(P_C^N + P_B^N) \quad . \tag{3.4-18}$$

Using Eq(3.4-17), the net efficiency can be separated into a nuclear and a processing term such that

$$\eta_S^{NET}(t) = \eta_S^N - \eta_S^R(t) \quad . \tag{3.4-19}$$

The electrical generating efficiency, or net nuclear efficiency, η_S^N, is then defined by

$$\eta_S^N = \left\{ \frac{\eta_C^T(1-\varepsilon_C) + \eta_B^T(1-\varepsilon_B)Q_B^T/(Q_B^T-\alpha_B)P_B^N/P_C^N}{1 + P_B^N/P_C^N} \right\}, \tag{3.4-20}$$

and the fuel processing energy efficiency is given by

$$\eta_S^R(t) = \left\{ \frac{\Sigma_M W_M(E_{M,C}(t)/U_C + (E_{M,BC}(t) + E_{M,BB}(t))/U_B P_B^N/P_C^N}{1 + P_B^N/P_C^N} \right\} \tag{3.4-21}$$

This processing efficiency can be regarded as a penalty associated with including reprocessing-fabrication in the power balance. Because the processing rate is not constant due to the effects of pre-steady-state, the net station efficiency and the processing efficiency will be time dependent.

In this section, the power producing capabilities of the system have been described in terms of lumped parameters based on reactor and processing plant data. In particular, the power of the reactor has been related to the characteristic reaction rate and the net electrical power

was described using a net nuclear efficiency and a processing efficiency. This will be important in the following chapters.

We have, in this chapter, developed a series of equations which describe the variation of the system stockpile and power balance of the combined system. From these, we have derived characteristics describing fissile fuel production, fertile fuel utilization and electrical conversion efficiency. These characteristics include the replacement time τ_M^0, the time to reach minimum τ_M^{MIN} and the depth of the minimum $|N_{M,S}(\tau_M^{MIN})|$, the nuclear conversion efficiency η_S^N and the net station efficiency $\eta_S^{NET}(t)$. In the following chapters, we will use the data from Chapter II in the equations developed in Chapter III to evaluate the combined systems. Here, fast-fission, fusion and spallation breeders coupled to a fission converter reactor will be considered in the next three chapters followed by a comparison in Chapter VII. Since all systems will be evaluated using the same set of equations, such comparisons will be valid and provide a consistent means of characterizing breeders.

CHAPTER IV

FAST-FISSION BREEDER

As outlined in Chapter I, the production of fissile material by nuclear breeders is often considered in nuclear energy strategies for the future. This is particularly true for thorium cycles since no naturally occurring fissile isotopes of thorium exist. Of the types of breeder reactors which have been considered, the fast-fission breeder is the most advanced in development with operating prototypes in several countries. For these reasons, a Gas Cooled Fast Reactor operating on the thorium cycle will be studied. As the converter, a thorium-uranium fuelled High Temperature Gas-Cooled Reactor will be used. Of importance here is the fissile and power producing capabilities of the system and the efficiencies of conversion, that is, fertile to fissile and thermal to electric. The stockpile method described above will provide detailed information about the time dependence of the fissile fuel production (Section 3.3) and hence, an unambiguous definition of these capabilities[4].

In the following, a reference system will first be described and the procedure developed in Chapter III used to determine its characteristics. These characteristics including the initial inventory, the minimum inventory, the time to reach the minimum, the fissile replacement time, the fertile inventory at the fissile replacement time, the steady-state rates of change, the end-of-system-life inventories, the net

power output and the nuclear and processing efficiencies. Following this, some parameters describing the reference system will be varied in order to observe the effects on the system characteristics.

4.1 Reference System

Since there is a wide range of reactor parameter values to choose from, a reference system will be chosen. A high-temperature gas-cooled fission reactor fuelled with thorium and uranium has been chosen as the reference converter reactor because of its good neutron economy and high thermal conversion efficiency. The parameters necessary to describe the converter for this analysis are listed in Table 4.1-1. For any fission reactor, the following will hold as explained in Section 3.4:

$$P_i^I = 0 \ , \tag{4.1-1a}$$

$$n_i^I = P_i^I / P_i^C = 0 \ , \tag{4.1-1b}$$

$$Q_i^I = P_i^T / P_i^I = \infty \ , \tag{4.1-1c}$$

The fraction of injected energy which can be recovered, α_i, is undefined since no energy is injected, hence, α_i will be set to zero. We also specify

$$\omega_{M,i}^o = \omega_{M,i} \ , \tag{4.1-2}$$

that is, the initial specific inventory and the steady-state specific inventory are equal. In Section 3.3, it was assumed that the fission reactor core will reach steady-state at startup, thus Eq(4.1-2), although in error by ~5%[4], is consistent.

Parameter	Value
Fissile Net Generation Ratio, $G_{FI,C}$	-0.20
Fertile Net Generation Ratio, $G_{FE,C}$	-0.80
Fissile Specific Inventory, $\omega_{FI,C}$	0.50 kg/MW_t
Fertile Specific Inventory, $\omega_{FE,C}$	11.0 kg/MW_t
Mean Fuel Discharge Period, τ_C^D	3.0 years
Energy Released per Characteristic Reaction, U_C	170 MeV
Thermal-Electric Conversion Efficiency, η_C^T	0.40
Injector Efficiency, η_C^I	0.0
Circulating Energy Fraction, ε_C	0.05
Total Amplification Factor, Q_C^T	∞
Fraction of Injected Energy Recovered, α_C	0.0
Load Factor, LF_C	0.75
Thermal Power, P_C^T	3000 MW_t

Table 4.1-1: Reference converter reactor data necessary for this analysis.

Referring to Fig. 2.1-1, the reference converter reactor with a conversion ratio of 0.8, or a fissile net generation ratio of -0.2, and with a fissile specific inventory of 0.5 kg/MW_t can be regarded as a typical HTGR. In arriving at the values listed in Table 4.1-1, $\gamma^{n,abs}_{FI,FE}$ has been set to unity which implies that no neutron absorption occurs in the intermediate decay products while in fertile isotopes the total neutron cross section is dominated by the capture cross section. The energy released per fissile absorption was based on data for ^{233}U and taken to be 190 MeV per fission[78]; also a capture to fission ratio of 0.093[78] has been used. An average core enrichment of 4.4% (Table 2.1-2) has been used to find the fertile specific inventory. The thermal power of the reference converter reactor has been fixed at 3000 MW_t and the load factor, at 0.75. These values are typical for large power reactors.

As a reference fast-fission breeder reactor, a gas-cooled fast reactor which will couple easily with the HTGR was chosen. The GCFR which has a Th-U fuel in the blankets and a U-Pu fuel in the core is capable of a high thermal efficiency, 40%. Table 4.1-2 lists the relevant reference breeder reactor parameters and, as with the converter reactor, Eq(4.1-1) and Eq(4.1-2) will hold. The total breeding ratio 1.45, is split between the core and axial blankets, 60% and the radial blankets, 40%[31,38]; thus, the net fissile generation ratio of the core is -0.13 and of the blanket, 0.58. It has been assumed that there is no neutron absorption in the fissile material produced in the blanket so that Eq(3.2-44) reduces to

$$G_{FE,BB} = -G_{FI,BB} \,, \qquad (4.1\text{-}3)$$

Parameter	Value
Net Fissile Generation Ratio, Core, $G_{FI,BC}$	-0.13
Net Fissile Generation Ratio, Blanket, $G_{FI,BB}$	0.58
Net Fertile Generation Ratio, Core, $G_{FE,BC}$	-0.87
Net Fertile Generation Ratio, Blanket, $G_{FE,BB}$	-0.58
Fissile Specific Inventory, Core, $\omega_{FI,BC}$	1.10 kg/MW_t
Fissile Specific Inventory, Blanket, $\omega_{FI,BB}$	0.0 kg/MW_t
Fertile Specific Inventory, Core, $\omega_{FE,BC}$	8.07 kg/MW_t
Fertile Specific Inventory, Blanket, $\omega_{FE,BB}$	9.17 kg/MW_t
Mean Fuel Discharge Period, Core, τ^D_{BC}	3.0 years
Mean Fuel Discharge Period, Blanket, τ^D_{BB}	6.0 years
Energy Release per Characteristic Reaction, U_B	164 MeV
Thermal-Electric Conversion Efficiency, η^T_B	0.40
Injector Efficiency, η^I_B	0.0
Circulating Energy Fraction, ε_B	0.05
Total Amplification Factor, Q^T_B	∞
Fraction of Injected Energy Recovered, α_B	0.0
Load Factor, LF_B	0.75
Thermal Power, P^T_B	3000 MW_t

Table 4.1-2: Reference fission breeder reactor data necessary for this analysis.

where here $\gamma_{FI,FE}^{n,abs}$ is unity. The specific fissile inventory of the reactor is 1.1 kg/MW_t which, from Fig. 2.1-1, is a representative value for GCFR. The average initial enrichment for the core is 12% and for the radial blanket, 0% since it is fuelled with thorium. To find the specific fertile inventory of the blanket, the number of blanket and core fuel elements were set equal[28]. The energy per fissile absorption was calculated using 200 MeV per fission and a capture to fission ratio of 0.22[31].

To complete the specification of the breeder-converter system, the reprocessing-fabrication plant and the operating life of the system must be known. These data are listed in Table 4.1-3. The processing times and loss fractions for both fertile and fissile material are equal and have value of 1.5 years and 1.5% respectively. The energy needed to reprocess and fabricate the fuel was fixed at 3.35×10^3 $kW_e \cdot h/kg$ of fissile material handled with equal amounts of ^{239}Pu and ^{233}U processed. The breeder and converter reactors have a 40 year operating life.

4.2 Characteristics of the Reference System

The variation of the reference system fissile and fertile stockpile inventories has been calculated using the system model described in Chapter III. Since we have set the pre-startup stockpile inventory to zero, the value of $N_{M,S}(t)$ will determine the amount of material required from the external source if $N_{M,S}(t)<0$ or the amount of material supplied to an external system if $N_{M,S}(t)>0$. In the calculation, a breeder thermal power of 3000 MW_t, equal to that of the converter, has been used.

Parameter	Value
Reprocessing-Fabrication Lag, Fissile, τ_{FI}^{R}	1.5 years
Reprocessing-Fabrication lag, Fertile, τ_{FE}^{R}	1.5 years
Loss Fraction, Fissile, ℓ_{FI}	0.015
Loss Fraction, Fertile, ℓ_{FE}	0.015
Energy to Process Fuel, W_{FI}	3.35×10^{3} $kW_e \cdot h/kg$
System Reactor Lifetime, τ^{EOL}	40.0 years

Table 4.1-3: Balance of system data necessary for this analysis.

The value of the stockpile inventory of material M at time t was found using Eq(3.3-23) which reduces to

$$\begin{aligned} N_{M,S}(t) = &-[\omega_{M,C}R_C + (\omega_{M,BC} + \omega_{M,BB})R_B]H(t) \\ &+ \int_0^t \{D_{M,C}(t')R_C + [D_{M,BC}(t') + D_{M,BB}(t')]R_B\}dt' \\ &+ \{(\omega_{M,C} + 1/2\tau_C^D G_{M,C})R_C(1-\ell_M)+(\omega_{M,BC} + \omega_{M,BB} \\ &+ 1/2\tau_{BC}^D G_{M,BC} + 1/2\tau_{BB}^D G_{M,BB})R_B(1-\ell_M)\}\, H(t-\tau^{EOL}-\tau_M^R) , \end{aligned} \tag{4.2-1}$$

for the reference system. The rate of change functions, $D_{M,i}(t)$ are given by

$$D_{M,C}(t) = \begin{cases} 0, \ t\leq 0 , & (4.2\text{-}2a) \\ -\omega_{M,C}/\tau_C^D, \ 0<t\leq\tau_M^R , & (4.2\text{-}2b) \\ -\omega_{M,C}/\tau_C^D\ell_M + G_{M,C}(1-\ell_M), \ \tau_M^R<t\leq\tau^{EOL} , & (4.2\text{-}2c) \\ (\omega_{M,C}/\tau_C^D + G_{M,C})(1-\ell_M), \ \tau^{EOL}<t\leq\tau^{EOL}+\tau_M^R , & (4.2\text{-}2d) \\ 0, \ t>\tau^{EOL}+\tau_M^R , & (4.2\text{-}2e) \end{cases}$$

for the converter reactor;

$$D_{M,BC}(t) = \begin{cases} 0, \ t\leq 0 , & (4.2\text{-}3a) \\ -\omega_{M,BC}/\tau_{BC}^D, \ 0<t\leq\tau_M^R , & (4.2\text{-}3b) \\ -\omega_{M,BC}/\tau_{BC}^D\ell_M+G_{M,BC}(1-\ell_M), \ \tau_M^R<t\leq\tau^{EOL} , & (4.2\text{-}3c) \\ (\omega_{M,BC}/\tau_{BC}^D + G_{M,BC})(1-\ell_M), \ \tau^{EOL}<t\leq\tau^{EOL}+\tau_M^R , & (4.2\text{-}3d) \\ 0, \ t>\tau^{EOL}+\tau_M^R , & (4.2\text{-}3e) \end{cases}$$

for the breeder core and

$$D_{M,BB}(t) = \begin{cases} 0, \ t \leq 0 , & (4.2\text{-}4a) \\ -\omega_{M,BB}/\tau^D_{BB}, \ 0 < t \leq \tau^R_M & (4.2\text{-}4b) \\ -\omega_{M,BB}/\tau^D_{BB}\ell_M + G_{M,BB}(t-\tau^R_M)/\tau^D_{BB}(1-\ell_M) , & (4.2\text{-}4c) \\ \qquad \tau^R_M < t \leq \tau^D_{BB} + \tau^R_M , & \\ -\omega_{M,BB}/\tau^D_{BB}\ell_M + G_{M,BB}(1-\ell_M), \ \tau^D_{BB}+\tau^R_M \leq \tau^{EOL} , & (4.2\text{-}4d) \\ (\omega_{M,BB}/\tau^D_{BB} + G_{M,BB})(1-\ell_M), \tau^{EOL} < t \leq \tau^{EOL}+\tau^R_M , & (4.2\text{-}4e) \\ 0, \ t > \tau^{EOL} + \tau^R_M , & (4.2\text{-}4f) \end{cases}$$

for the breeder reactor blanket. The fissile inventory, $N_{FI,S}(t)$, and the fertile inventory, $N_{FE,S}(t)$, calculated using the above are shown in Fig. 4.2-1.

At $t = 0^+$, material is taken from the stockpile and loaded into the reactors. Since $\omega_{FI,BB}$ is zero, we have

$$N_{FI,S}(0^+) = -(\omega_{FI,C}R_C + \omega_{FI,BC}R_B) , \quad (4.2\text{-}5a)$$

$$= -4.71 \times 10^3 \text{ kg}; \quad (4.2\text{-}5b)$$

and the initial fertile loading will be

$$N_{FE,S}(0^+) = -\omega_{FE,C}R_C + (\omega_{FE,BC} + \omega_{FE,BB})R_B , \quad (4.2\text{-}6a)$$

$$= -8.41 \times 10^4 \text{ kg}. \quad (4.2\text{-}6b)$$

These values are negative indicating that material must be brought into the system from an external source. Following this, both inventories decrease linearly with time until material from the reprocessing-fabrication plant begins to reach the stockpile at $t = \tau^R_{FI}$. The rate

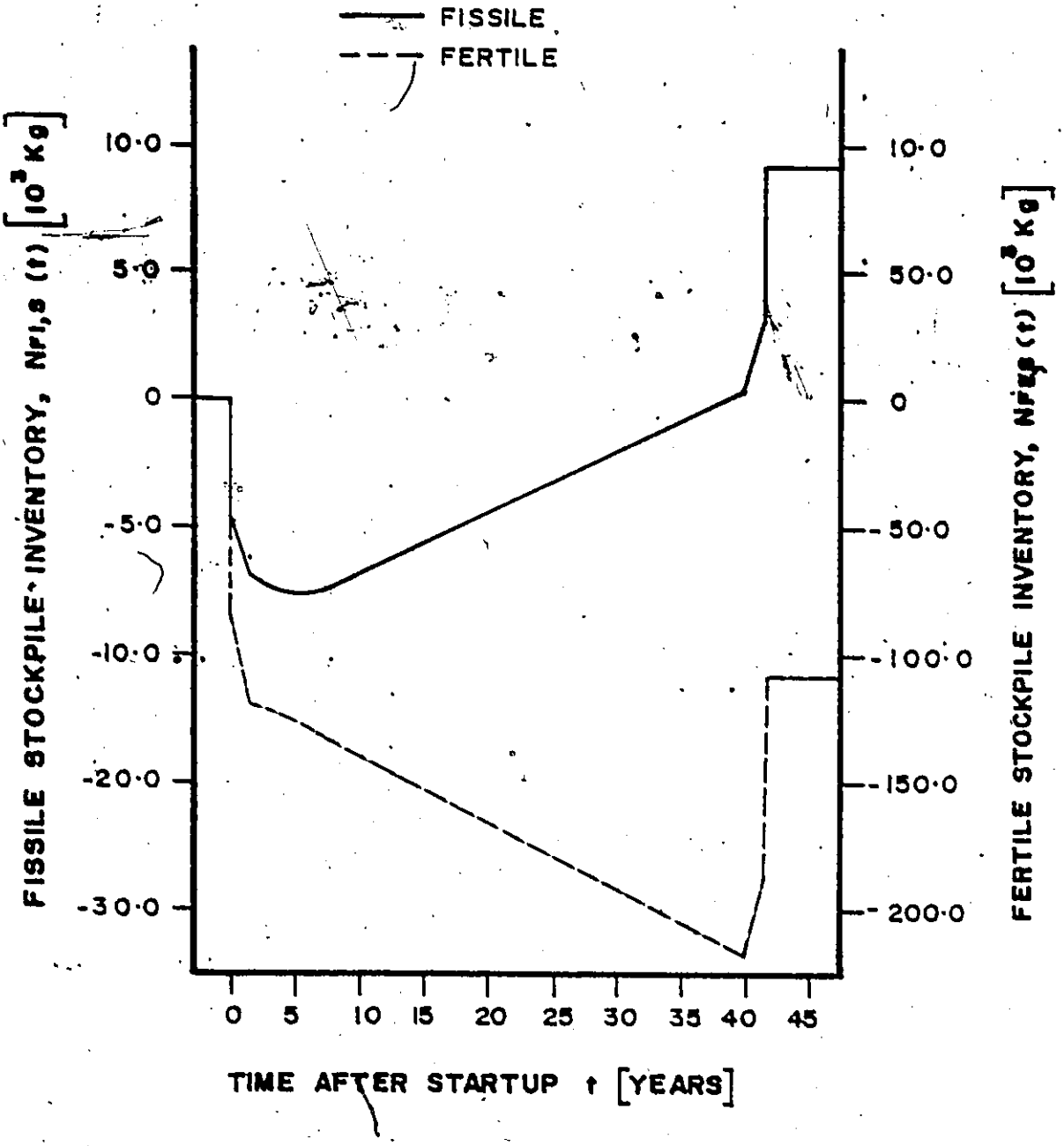

Fig. 4.2-1: Time variation of the fissile and fertile stockpile inventories for the reference fast fission breeder system with P_B^T = 3000 MWt.

of change of the fissile stockpile during this decrease is described by

$$\frac{dN_{FI,S}(t)}{dt} = -(\omega_{FI,S}/\tau_C^D R_C + \omega_{FI,BC}/\tau_{BC}^D R_B) , \qquad (4.2\text{-}7a)$$

$$= -1.6 \times 10^3 \text{ kg}, \qquad (4.2\text{-}7b)$$

$$0<t\leq\tau_{FI}^R ,$$

and, of the fertile stockpile, by

$$\frac{dN_{FE,S}(t)}{dt} = -[\omega_{FE,C}/\tau_C^D R_C + (\omega_{FE,BC}/\tau_{BC}^D + \omega_{FE,BB}/\tau_{BB}^D)R_B] \qquad (4.2\text{-}8a)$$

$$= -1.8 \times 10^4 \text{ kg} , \qquad (4.2\text{-}8b)$$

$$0<t\leq\tau_{FE}^R .$$

In this period, $\tau_{FI}^R<t\leq\tau_{FI}^R+\tau_{BB}^D$ (1.5 years$<t\leq$7.5 years), there is a quadratic variation of the stockpile. This is due to the pre-steady-state effects in the breeder blanket. The rate of change can be found using

$$\frac{dN_{M,S}(t)}{dt} = -[\omega_{M,C}/\tau_C^D R_C + (\omega_{M,BC}/\tau_{BB}^D + \omega_{M,BB}/\tau_{BB}^D)R_B]\ell_M$$

$$+(G_{M,C}R_C + G_{M,BC}R_B)(1-\ell_M) \qquad (4.2\text{-}9)$$

$$+G_{M,BB}R_B(1-\ell_M)(t-\tau_M^R)/\tau_{BB}^D , \quad \tau_M^R<t\leq\tau_{BB}^D+\tau_M^R .$$

The first term on the right gives the loss rate of fresh material due to processing neglecting irradiation; next, the effects of irradiation in the two cores and the third term gives the linear variation of the net generation ratio in the pre-steady-state breeder blanket. It is during this quadratic variation period that the fissile inventory reaches its minimum value. Using Eq(3.3-33), we find

$$\tau_{FI}^{MIN} = \tau_{FI}^{R} + \{[\omega_{FI,C}/\tau_{C}^{D}R_{C} + (\omega_{FI,BC}/\tau_{BC}^{D} + \omega_{FI,BB}/\tau_{BB}^{D})R_{B}]\ell_{FI} - (G_{FI,C}R_{C} + G_{FI,BC}R_{B})(1-\ell_{FI})\}\{G_{FI,BB}R_{B}(1-\ell_{FI})/\tau_{BB}^{D}\}^{-1} ,$$

$$\tau_{FI}^{R} < \tau_{FI}^{MIN} \leq \tau_{BB}^{D} + \tau_{FI}^{R} , \qquad (4.2\text{-}10a)$$

$$= 5.08 \text{ years.} \qquad (4.2\text{-}10b)$$

Substituting this into Eq(4.2-1) or using Eq(3.3-36) yields

$$N_{FI,S}(\tau_{FI}^{MIN}) = -7.71 \times 10^{3} \text{ kg.} \qquad (4.2\text{-}11)$$

This is the maximum amount of fissile material which must be supplied to the system from an external source; 64% more than the initial system loading.

Steady-state is reached at 7.5 years after which the fissile inventory increases linearly with time and the fertile inventory decreases linearly with time until the reactors are shut down at τ^{EOL}. The steady-rate of change of an inventory is given by

$$\left(\frac{dN_{M,S}}{dt}\right)_{SS} = -[\omega_{M,C}/\tau_{C}^{D}R_{C} + (\omega_{M,BC}/\tau_{BC}^{D} + \omega_{M,BB}/\tau_{BB}^{D})R_{B}]\ell_{M} + [G_{M,C}R_{C} + (G_{M,BC} + G_{M,BB})R_{B}](1-\ell_{M}) , \qquad (4.2\text{-}12)$$

$$\tau_{BB}^{D} + \tau_{M}^{R} < t \leq \tau^{EOL} .$$

Using this equation, we find the reference system produces 240 kg/yr fissile material while consuming 2.63×10^{3} kg/yr fertile. During the steady-state period, the system replaces the fissile deficit. The fissile replacement time, τ_{FI}^{0}, is found using

$$\tau^{0}_{FI} = \tau^{R}_{FI} + \{\omega_{FI,C}(1+\tau^{R}_{FI}/\tau^{D}_{C})R_{C}+\omega_{FI,BC}(1+\tau^{R}_{FI}/\tau^{D}_{BC})R_{B}$$
$$+1/2G_{FI,BB}R_{B}\tau^{D}_{BB}(1-\ell_{FI})\}\{-(\omega_{FI,C}/\tau^{D}_{C}R_{C}+\omega_{FI,BC}/\tau^{D}_{BC}R_{B})\ell_{FI}$$
$$+[G_{FI,C}R_{C}+(_{FI,BC} + G_{FI,BB})R_{B}](1-\ell_{FI})\}^{-1} ,$$
$$\tau^{R}_{FI} + \tau^{D}_{BB} \leq \tau^{0}_{FI} \leq \tau^{EOL} , \qquad (4.2\text{-}13a)$$
$$= 38.3 \text{ years.} \qquad (4.2\text{-}13b)$$

At $t = \tau^{0}_{FI}$, the system has consumed 2.14×10^{5} kg of fertile material.

The reactors are shut down at $t = \tau^{EOL}$ which, for this case, is 40 years. At this time, the maximum amount of fertile fuel has been supplied to the system, 2.19×10^{5} kg. For the next τ^{R}_{FI} years, there is a linear increase in the fertile and fissile inventories as seen in Fig. 4.2-1. During this period, the rate of change of the stockpile inventory is given by

$$\frac{dN_{M,S}(t)}{dt} = [\omega_{M,C}/\tau^{D}_{C}R_{C} + (\omega_{M,BC}/\tau^{D}_{BC} + \omega_{M,BB}/\tau^{D}_{BB})R_{B}](1-\ell_{M})$$
$$+[G_{M,C}R_{C} + (G_{M,BC} + G_{M,BB})R_{B}](1-\ell_{M}) , \qquad (4.2\text{-}14)$$
$$\tau^{EOL} < t \leq \tau^{EOL} + \tau^{R}_{M} .$$

The similarity between this linear increase and the linear decrease during the first τ^{R}_{M} years can be seen by comparing Eq(4.2-14) with Eq(4.2-7a) or Eq(4.2-8a).

At $t = \tau^{EOL} + \tau^{R}_{M}$, there will be an increase in the inventories as the final, processed, cores and blanket are added. This increase, which parallels the initial loading, is given by

$$\Delta N_{M,S}(\tau^{EOL}+\tau_M^R) = [\omega_{M,C}R_C+(\omega_{M,BC}+\omega_{M,BB})R_B](1-\ell_M) \qquad (4.2\text{-}15)$$
$$+1/2[\tau_C^D G_{M,C}R_C+(\tau_{BC}^D G_{M,BC}+\tau_{BB}^D G_{M,BB})R_B](1-\ell_M) .$$

For fissile material, we find $\Delta N_{FI,S}(\tau^{EOL}+\tau_{FI}^R)$ is 5.6×10^3 kg and for fertile material, $\Delta N_{FE,S}(\tau^{EOL} + \tau_{FE}^R)$ is 7.9×10^4 kg. The end-of-system-life is defined by

$$\tau_S^{EOL} = \max_{\{i,M\}} (\tau_i^{EOL} + \tau_M^R) , \qquad (4.2\text{-}16)$$

that is, when all material has been returned to the stockpile,

$$(dN_{M,S}/dt) = 0 , \quad t>\tau_S^{EOL} . \qquad (4.2\text{-}17)$$

The reference system produced 9.1×10^3 kg fissile and consumed 1.1×10^5 kg fertile during the system lifetime. Although $|N_{FE,S}(\tau_S^{EOL})|$ is less than $|N_{FE,S}(\tau^{EOL})|$, it is the later which will be important for fuelling supplies since it is the maximum amount of fuel which must be supplied to the system. The value of $N_{FI,S}(\tau_S^{EOL})$ is 17.6% more than $|N_{FI,S}(\tau_{FI}^{MIN})|$ so that at the end-of-system-life this system is capable of supplying enough fissile fuel to startup and operate an identical system.

For the reference system, both the breeder and converter reactors have a thermal power of 3000 MW_t. The net electrical power generated by the combined system at steady-state is 2279 MW_e. Since for this case η_C^T and η_B^T, and ε_C and ε_B are equal, Eq(3.4-20) will reduce to

$$\eta_S^N = \eta_C^T(1-\varepsilon_C) = 0.38 . \qquad (4.2\text{-}18)$$

At steady-state, the functions describing the fuel processing defined in Eq(3.4-14) are

$$E_{FI,C}(t) = \omega_{FI,C}/\tau_C^D + G_{FI,C}, \quad 0<t\leq\tau^{EOL} , \tag{4.2-19a}$$

$$E_{FI,B}(t) = \omega_{FI,BC}/\tau_{BC}^D + G_{FI,BC} + G_{FI,BB}, \tau_{BB}^D < t \leq \tau^{EOL} . \tag{4.2-19b}$$

If this is used in the following equation for the processing efficiency,

$$\eta_S^R(t) = W_{FI}(E_{FI,C}(t)/U_C + E_{FI,B}(t)/U_B) , \tag{4.2-20}$$

it is found that η_S^R at a steady-state is 0.01% or the system requires only 0.71 MW_e for fuel reprocessing and fabrication.

4.3 Alternate Operating Modes

In Section 4.2, the breeder thermal power was set equal to the converter thermal power to study the stockpile variations. By choosing different reactor powers, a different set of inventory characteristics will result; alternatively, by demanding the system satisfy a specific criterion, a certain thermal power will be required. In the following, the converter thermal power, P_C^T, will be fixed at 3000 MW_t; hence, setting one of the characteristics, for instance, $N_{M,S}(t)$ as in Eq(3.3-24) or $dN_{M,S}(t)/dt$ as in Eq(3.3-25), will serve to fix the breeder thermal power.

The effects of changing the breeder thermal power on some characteristics of the reference system are shown in Fig. 4.3-1. The initial fissile stockpile decrease, $N_{FI,S}(0^+)$, given by Eq(4.2-5a) is a linear function of R_B and by differentiating we find

$$\partial N_{FI,S}(0^+)/\partial R_B = -\omega_{FI,BC} . \tag{4.3-1}$$

For this case, using Eq(3.4-10), $(\partial N_{FI,S}(0^+)/\partial P_B^T)$ is -1.1 kg/MW_t. The end-of-system-life inventory is also a linear function of P_B^T. From

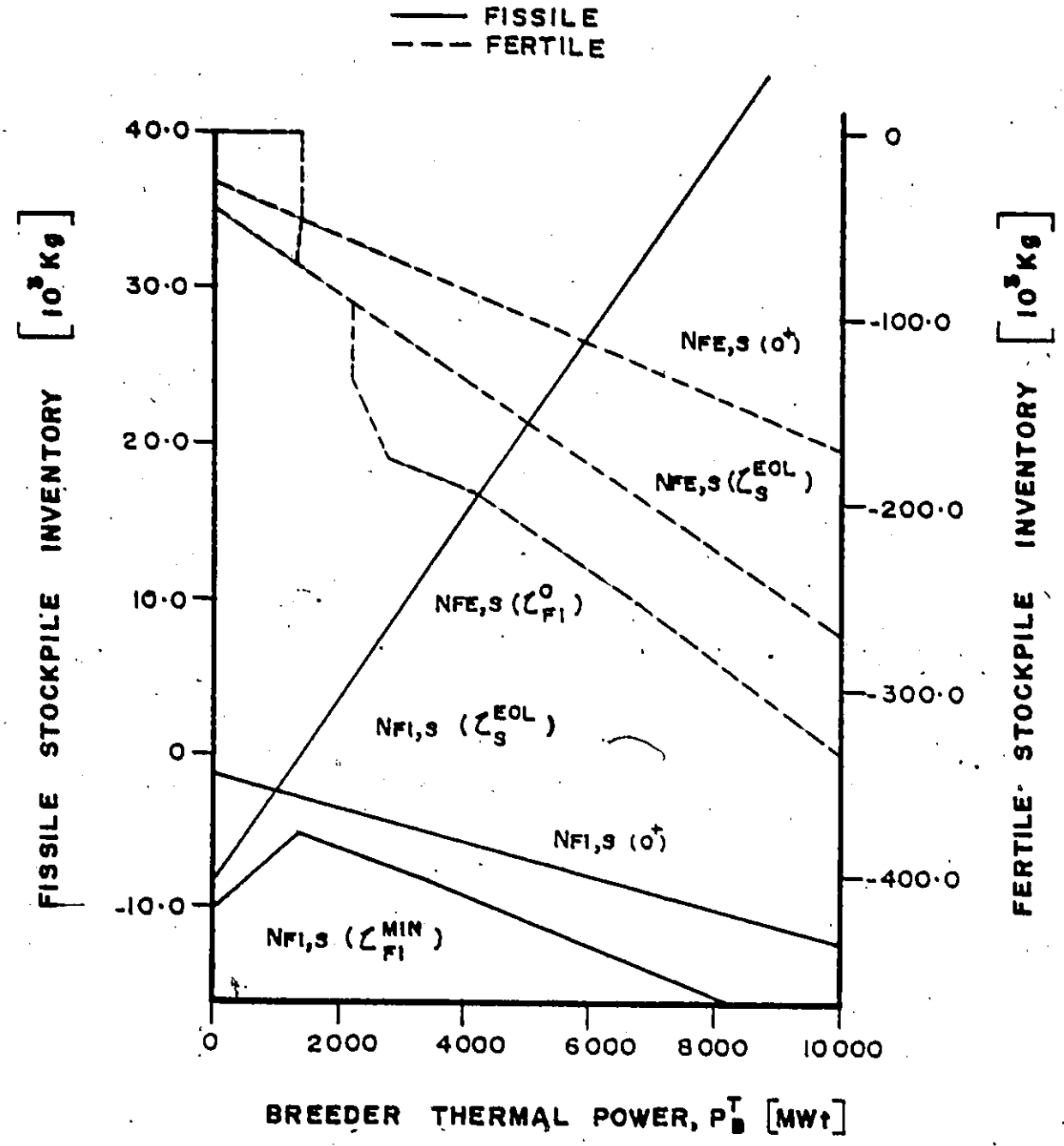

Fig. 4.3-1: The variation of some reference system characteristics with breeder thermal power.

Eq(4.2-1), the slope of $N_{FI,S}(\tau_S^{EOL})$ with respect to R_B is given by

$$(\partial N_{FI,S}(\tau_S^{EOL})/\partial R_B) = -\omega_{FI,BC}\ell_{FI}+1/2(\tau_{BC}^D G_{FI,BC}+\tau_{BB}^D G_{FI,BB})$$

$$X\ (1-\ell_M) + \int_0^{\tau_S^{EOL}} [D_{FI,BC}(t')+D_{FI,BB}(t')]dt' \ . \qquad (4.3\text{-}2)$$

The first term here represents losses of initial fissile loading; the next, the effects of irradiation on the final loading of the breeder; and the last represents the effects of fuelling and irradiation during the system lifetime. Evaluating Eq(4.3-2), we find $(\partial N_{FI,S}(\tau_S^{EOL})/\partial P_B^T)$ is 6.0 kg/MW_t. The reference HTGR will have an end-of-system-life fissile deficit of -8.6×10^3 kg. Consequently, the breeder thermal power at which $N_{FI,S}(\tau_S^{EOL})$ is zero can be found using

$$(\partial N_{FI,S}(\tau_S^{EOL})/\partial P_B^T)P_B^T = 8.6 \times 10^3 \text{ kg} \ , \qquad (4.3\text{-}3)$$

which leads to a value of 1429 MW_t; a breeder with a thermal power greater than 1429 MW_t will produce a surplus of fissile material.

The minimum fissile inventory, $N_{FI,S}(\tau_{FI}^{MIN})$, as a function of P_B^T is also shown in Fig. 4.3-1. This curve can be divided into two distinct regions with the dividing point occurring at 1383 MW_t. From Fig. 4.3-2 which gives the values of $(dN_{FI,S}/dt)_{SS}$ and $(dN_{FE,S}/dt)_{SS}$ as a function of P_B^T, we see that at P_B^T = 1383 MW_t, the steady-state rate of change of the fissile inventory is zero. In Section 3.3 we found that if the steady-state rate of change of an inventory is negative, then

$$\tau_M^{MIN} = \tau^{EOL} \ . \qquad (4.3\text{-}4)$$

For a breeder thermal power less than 1383 MW_t, Eq(3.3-35) will apply and can be reduced to

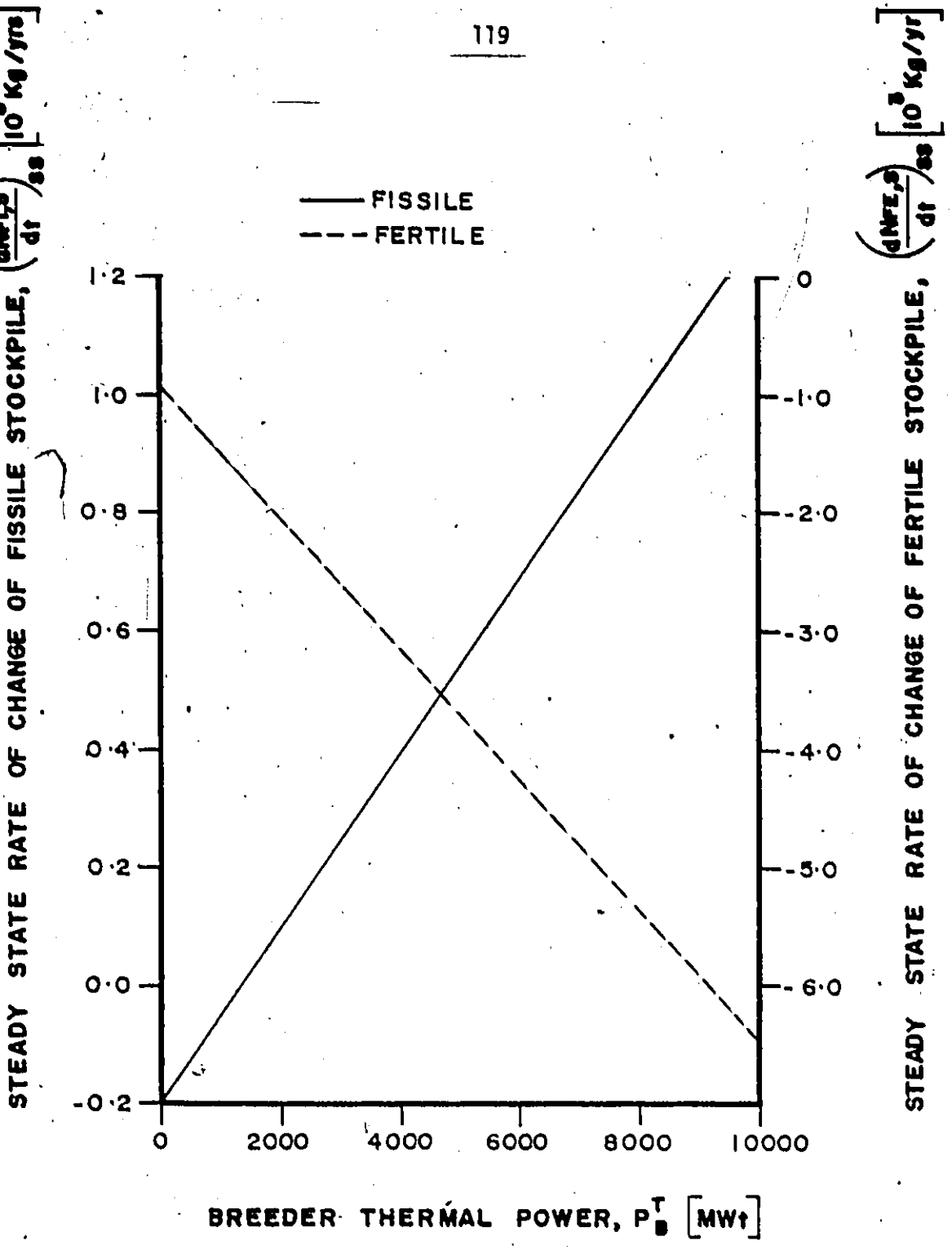

Fig. 4.3-2: Variation of the steady-state rates of change of the fissile and fertile stockpile inventories with breeder thermal power for the reference fission breeder system. The reference converter reactor requires 210 kg/year of fissile material.

$$N_{FI,S}(\tau_{FI}^{MIN}) = -[\omega_{FI,C}R_C+\omega_{FI,BC}R_B] - [\omega_{FI,C}/\tau_C^D R_C$$
$$+\omega_{FI,BC}/\tau_{BC}^D R_B][\tau_{FI}^R+\ell_{FI}(\tau^{EOL}-\tau_{FI}^R)] \qquad (4.3\text{-}5)$$
$$+[G_{FI,C}R_C+(G_{FI,BC}+G_{FI,BB})R_B](1-\ell_{FI})(\tau^{EOL}-\tau_{FI}^R)$$
$$-G_{FI,BB}R_B(1-\ell_{FI})\tau_{BB}^D/2 \ ,$$
$$P_B^T<1383 \ MW_t$$

The minimum inventory in this region is a linear function of R_B. For $P_B^T>1383$ MW_t, Eq(3.3-36) is applicable and the minimum fissile inventory will be given by

$$N_{FI,S}(\tau_{FI}^{MIN}) = -\omega_{FI,C}(1+\tau_{FI}^R/\tau_C^D)R_C-\omega_{FI,C}(1+\tau_{FI}^R/\tau_{BC}^D)R_B$$
$$-\{(\omega_{FI,C}/\tau_C^D R_C+\omega_{FI,BC}/\tau_{BC}^D R_B)\ell_{FI} \qquad (4.3\text{-}6)$$
$$+(G_{FI,C}R_C + G_{FI,BC}R_B)(1-\ell_{FI})\}^2$$
$$\times\{G_{FI,BB}(1-\ell_{FI})R_B/\tau_{BB}^D\}^{-1}, \ P_B^T=1383 \ MW_t \ .$$

Because τ_{FI}^{MIN} is a function of R_B as shown in Fig. 4.3-3, $N_{FI,S}(\tau_{FI}^{MIN})$ is not a linear function of the breeder thermal power. The minimum value of the minimum fissile inventory occurs at a breeder thermal power of 1383 MW_t. As stated above, at this value of P_B^T, $(dN_{FI,S}/dt)_{SS}$ is zero and, combining Eq(3.3-37) and Eq(3.4-10), we find

$$P_B^T = R_C U_B\{-\omega_{FI,C}/\tau_C^D\ell_{FI}+G_{FI,C}(1-\ell_{FI})\} \qquad (4.3\text{-}7)$$
$$\times\{-\omega_{FI,BC}/\tau_{BC}^D\ell_{FI} + (G_{FI,BC}+G_{FI,BB})(1-\ell_{DI})\}^{-1} \ .$$

The minimum value of fissile material required, 5.3×10^3 kg, will occur at this breeder thermal power. There is an asymptote for τ_{FI}^{MIN} ,

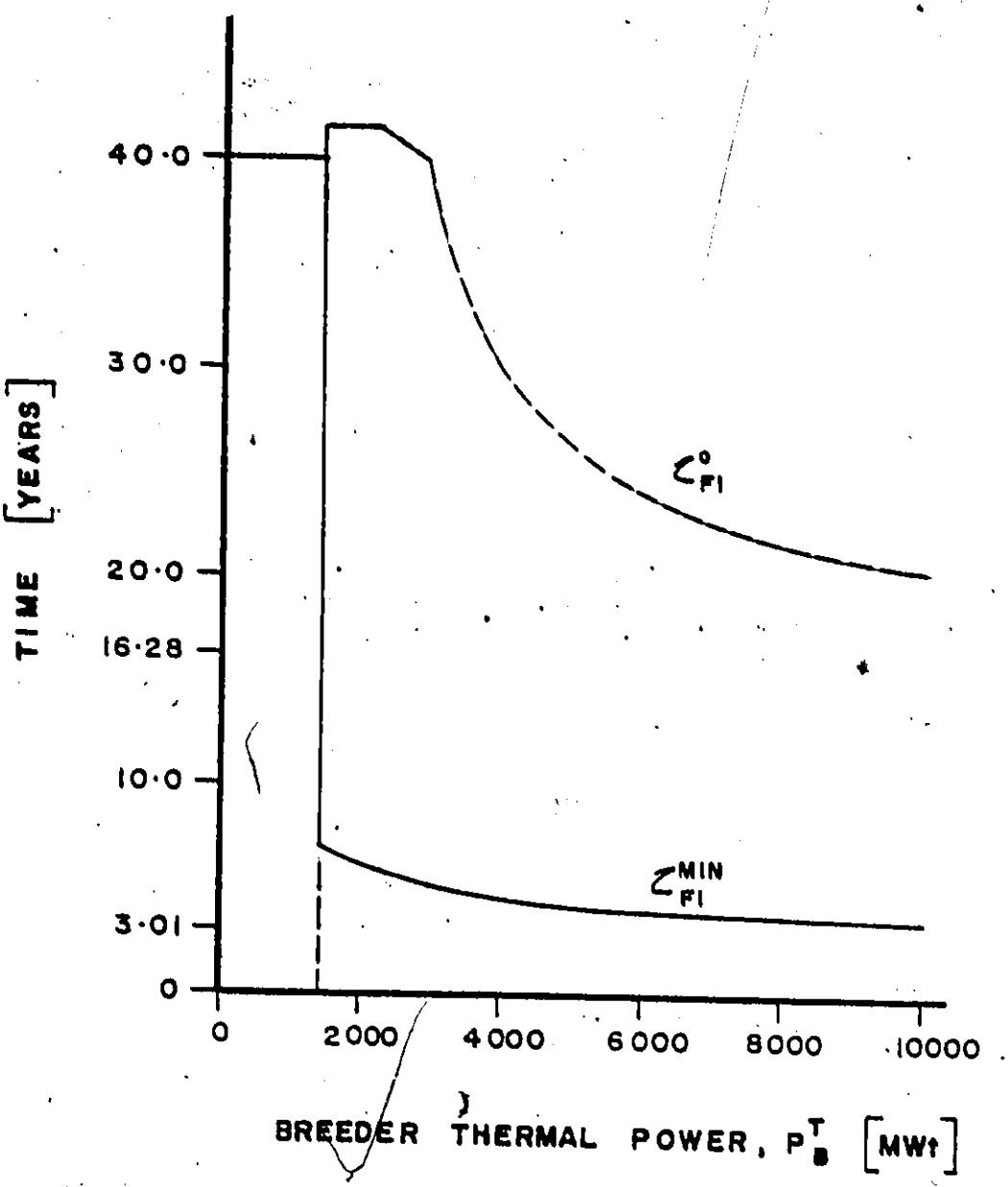

Fig. 4.3-3: The variation of the fissile replacement time and the time to reach the minimum fissile inventory with breeder thermal power for the reference fission breeder system.

$(\tau_{FI}^{MIN})_{MIN}$, found from Eq(3.3-34) which reduces here to

$$(\tau_{FI}^{MIN})_{MIN} = \tau_{FI}^{R} + \tau_{BB}^{D}\{\omega_{FI,BC}/\tau_{BC}^{D}\ell_{FI} - G_{FI,BC}(1-\ell_{FI})\}$$

$$X\{G_{FI,BB}(1-\ell_{FI})\}^{-1} , \qquad (4.3\text{-}8a)$$

$$= 3.01 \text{ years.} \qquad (4.3\text{-}8b)$$

This is the shortest possible time for the system to reach the minimum value of $N_{FI,S}(t)$.

Also displayed in Fig. 4.3-1 are three fertile inventory characteristics: the initial loading, the end-of-system-life inventory and the fertile inventory at the fissile replacement time. Both $N_{FE,S}(0^+)$ and $N_{FE,S}(\tau_S^{EOL})$ are linear functions of P_B^T as were $N_{FI,S}(0^+)$ and $N_{FI,S}(\tau_S^{EOL})$. In fact, from Eq(4.2-1), the inventory of any material at a fixed time will be a linear function of R_B and P_B^T. The slope of the initial loading with respect to the breeder size is given by

$$(\partial N_{FE,S}(\tau_S^{EOL})/\partial R_B) = -(\omega_{FE,BC}+\omega_{FE,BB})\ell_{FE}+1/2(\tau_{BC}^{D}G_{FE,BC} \qquad (4.3\text{-}10a)$$

$$+\tau_{BB}^{D}G_{FE,BB})(1-\ell_{FE}) + \int_0^{\tau_S^{EOL}} [D_{FE,BC}(t')+D_{FE,BB}(t')]dt' ,$$

$$(\partial N_{FE,S}(\tau_S^{EOL})/\partial P_B^T) = -22.8 \text{ kg/MW}_t. \qquad (4.3\text{-}10b)$$

The third fertile inventory characteristic displayed in Fig. 4.3-1 is the fertile inventory at the fissile replacement time. This curve has four regions due to the variation of τ_{FI}^{0} with P_B^T as shown in Fig. 4.3-3. For P_B^T less than 1429 MW_t, the fissile replacement time is zero since, from Eq(4.3-3), the system can not replace the fissile

deficit even after the final cores and blanket are processed. If the breeder thermal power is 1429 $MW_t < P_B^T \leq 2255$ MW_t, then the fissile deficit is replaced only after the final loading has been processed and added to the stockpile, thus,

$$\tau_{FI}^{0} = \tau_{S}^{EOL} \quad , \quad 1429 \text{ MW}_t < P_B^T \leq 2255 \text{ MW}_t \quad . \tag{4.3-11}$$

Within this domain of breeder thermal powers, the fertile inventory at the fissile replacement time and at the end-of-system-life coincide. When the breeder power is increased to a value such that 2875 $MW_t > P_B^T \geq 2255$ MW_t, the system fissile replacement time will be $\tau^{EOL} < \tau_{FI}^{0} < \tau^{EOL} + \tau_{FI}^{R}$. It is within this range of breeder power that the fissile deficit is replaced by material added to the stockpile after the reactors have been shut down. Here, Eq(3.3-43) is applicable,

$$\begin{aligned} \tau_{FI}^{0} = \tau_{FI}^{R} + \{ & \omega_{FI,C}(1+\tau^{EOL}/\tau_{C}^{D})R_C + \omega_{FI,BC}(1+\tau^{EOL}/\tau_{BC}^{D})R_B \\ & + 1/2 G_{FI,BB}(1-\ell_{FI})R_B \tau_{BB}^{D} \}\{-(\omega_{FI,C}/\tau_{C}^{D}R_C + \omega_{FI,BC}/\tau_{BC}^{D}R_B)\ell_{FI} \\ & + [G_{FI,C}R_C + (G_{FI,BC}+G_{FI,BB})R_B](1-\ell_{FI})\}^{-1} , \\ & \tau^{EOL} < \tau_{FI}^{0} \leq \tau^{EOL} + \tau_{FI}^{R} \quad . \end{aligned} \tag{4.3-12}$$

Since τ_{FI}^{0} in this region is a function of R_B, the variation of $N_{FE,S}(\tau_{FI}^{0})$ will not be linear. For the breeder thermal power greater than 2875 MW_t, the fissile replacement time will be less than 40 years. The system while operating at steady-state will replace the fissile deficit as in Eq(3.3-42),

$$\tau_{FI}^{O}=\tau_{FI}^{R}+\{\omega_{FI,C}(1+\tau_{FI}^{R}/\tau_{C}^{D})R_C+\omega_{FI,BC}(1+\tau_{FI}^{R}/\tau_{BC}^{D})R_B$$

$$+1/2G_{FI,BB}(1-\ell_{FI})R_B\tau_{BB}^{D}\}\{-(\omega_{FI,C}/\tau_{C}^{D}R_C+\omega_{FI,BC}/\tau_{BC}^{D}R_B)\ell_{FI}$$

$$+[G_{FI,C}R_C+(G_{FI,BC}+G_{FI,BB})R_B](1-\ell_{FI})\}^{-1} , \qquad (4.3\text{-}13)$$

$$\tau_{BB}^{D}+\tau_{FI}^{R}<\tau_{FI}^{O}\leq\tau^{EOL} .$$

This equation is similar to Eq(4.3-14).

As the breeder size approaches infinity, there is a limiting value of τ_{FI}^{O}. This asymptote has a value of 16.3 years and is the shortest possible time for the breeder to replace the fissile inventory deficit. From Eq(3.3-48), the asymptotic value is given by

$$(\tau_{FI}^{O})_{MIN}=\{\tau_{FI}^{R}+\{\omega_{FI,BC}(1+\tau_{FI}^{R}/\tau_{BC}^{D})+G_{FI,BC}(1-\ell_{FI})\tau_{BB}^{D}/2\} \qquad (4.3\text{-}14)$$

$$X\{(G_{FI,BC}+G_{FI,BB})(1-\ell_{FI})-\omega_{FI,BC}/\tau_{BC}^{D}\ell_{FI}\}^{-1} .$$

In Section 3.3 it was stated that if $(\tau_{FI}^{O})_{MIN}>\tau_{FI}^{R}+\tau_{BB}^{D}$, then the value of $(R_B)_{FI}^{MIN}$ will be given by Eq(3.3-38). Since 16.3 years > (6.0 + 1.5) years, Eq(3.3-38) should be used and, in fact, was used to find P_B^T in Eq(4.3-17).

Four cases to further illustrate the effects of changing the breeder thermal power and to illustrate the various modes described in Section 3.3 are shown in Fig. 4.3-4. In addition to the reference case described in Section 4.2, Case A, the following examples have been included: Case B, the system was required to have a fissile replacement time of 25 years or a power growth of 2.8% per year; Case C, the steady-state rate of increase of the fissile inventory was required to be equal to the fissile consumption rate of a reference HTGR,

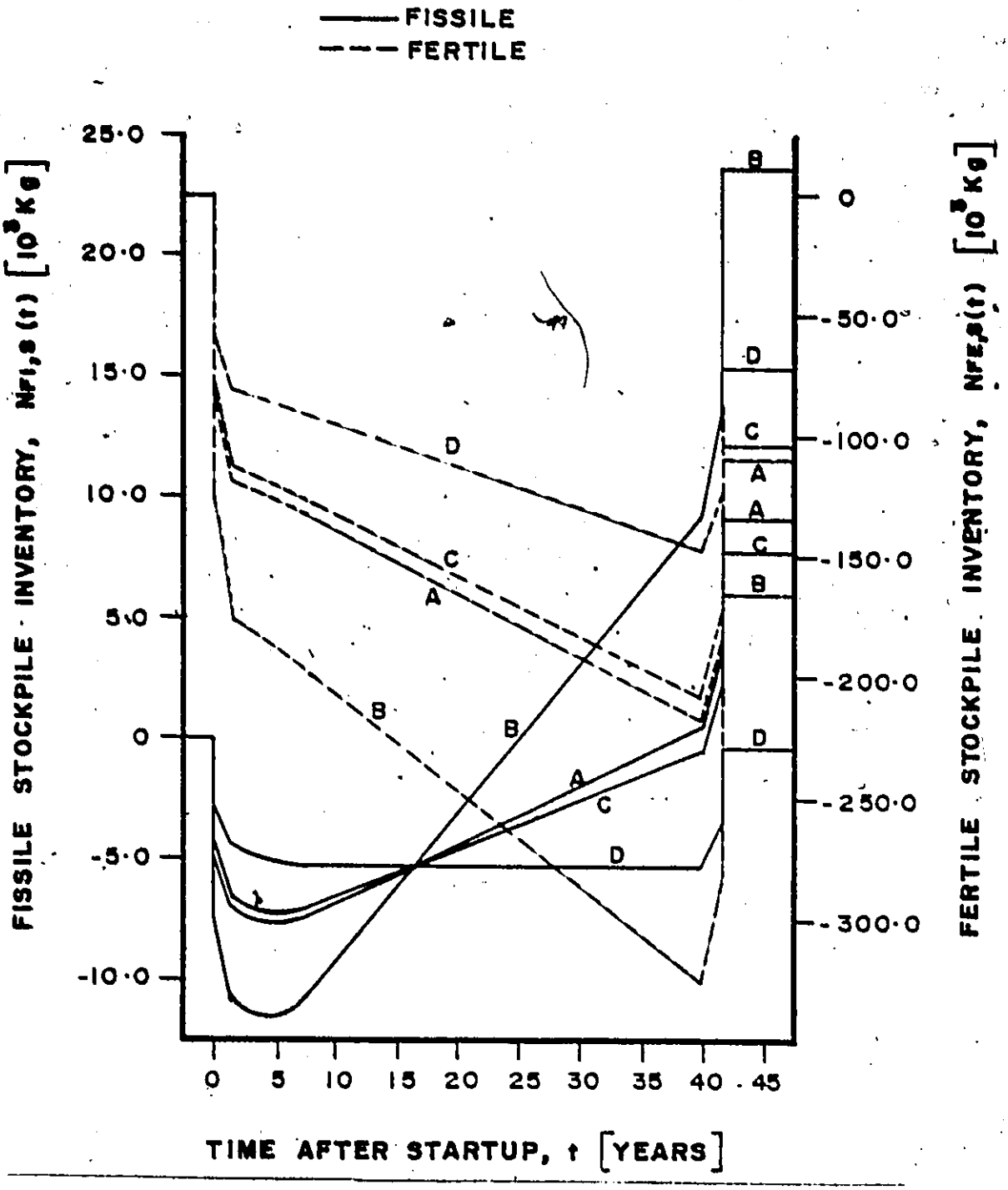

Fig. 4.3-4: The temporal variation of the fissile and fertile stockpile inventories for the reference fission breeder-system operating in four modes described in the text.

210 kg/year; and Case D, the system was to operate in a minimum fissile inventory mode. In Case B, the system will be capable of starting up another similar system after 25 years while in Case C, the system at steady-state will produce sufficient fissile material to fuel an external HTGR. Case D required the least amount of fissile material to operate and would be useful in a limited fissile resource scenario. Some characteristics of these four cases are listed in Table 4.3-1.

The breeder thermal power necessary to achieve a fissile replacement time of τ_{FI}^{0} will be calculated using Eq(3.3-24). For the reference breeder system, this reduces to

$$P_B^T = U_B\{\omega_{FI,C}(1+\tau_{FI}^R/\tau_C^D) + [\omega_{FI,C}/\tau_C^D\ell_{FI} - G_{FI,C}(1-\ell_{FI})] X(\tau_{FI}^0-\tau_{FI}^R)\}R_C\{-\omega_{FI,BC}(1+\tau_{FI}^R/\tau_{BC}^D)+[-\omega_{FI,BC}/\tau_{BC}^D\ell_{FI} + (G_{FI,BC} + G_{FI,BB})(1-\ell_{FI})] (\tau_{FI}^0-\tau_{FI}^R)\}^{-1} \quad (4.3\text{-}15a)$$

$$= 5462 \text{ MW}_t. \quad (4.3\text{-}15b)$$

In operating mode C, the steady-state rate of change of the system is to be such that one HTGR is supplied, that is,

$$(dN_{FI,S}/dt)_{SS} = -\{-\omega_{FI,C}/\tau_C^D\ell_{FI}+G_{FI,C}(1-\ell_{FI})\}R_C . \quad (4.3\text{-}16)$$

From Eq(3.3-25), the required breeder thermal power will be

$$P_B^T = -2U_BR_C\{-\omega_{FI,C}/\tau_C^D\ell_{FI}+G_{FI,C}(1-\ell_{FI})\} X\{-\omega_{FI,BC}/\tau_{BC}^D\ell_{FI}+(G_{FI,BC}+G_{FI,BB})(1-\ell_{FI})\}^{-1} , \quad (4.3\text{-}17a)$$

$$= 2767 \text{ MW}_t.$$

The power to operate in a minimum fissile inventory mode, Case D, has

Parameter	Case A	Case B	Case C	Case D
Breeder Thermal Power, P_B^T MW_t	<u>3000</u>	5460	2680	1380
Initial Inventory, Fissile, $N_{FI,S}(0^+)$ 10^3 kg	-4.71	-7.35	-4.46	-2.98
Initial Inventory, Fertile, $N_{FE,S}(0^+)$ 10^3kg	-84.1	-126.	-80.1	-56.5
Time to Reach Minimum, Fissile, τ_{FI}^{MIN} years	5.08	4.14	5.25	40.0
Minimum Inventory, Fissile, $N_{FI,S}(\tau_{FI}^{MIN})$ 10^3 kg	-7.71	-11.7	-7.34	<u>-5.30</u>
Fissile Replacement Time, τ_{FI}^0 yr	38.3	<u>25.0</u>	40.2	--
Fertile Inventory at τ_{FI}^0, $N_{FE,S}(\tau_{FI}^0)$ 10^3 kg	-214.	-267.	-204.	--
Steady-State Change, Fissile, $(dN_{FI,S}/dt)_{SS}$ 10^3 kg/yr	0.24	0.61	<u>0.21</u>	0.0
Steady-State Change, Fertile, $(dN_{FE,S}/dt)_{SS}$ 10^3 kg/yr	-2.63	-4.00	-2.50	-1.73
Minimum Inventory, Fertile, $N_{FE,S}(\tau^{EOL})$ 10^3 kg	-218.	-327.	-208.	-147
End-of-System-Life Inventory, Fissile, $N_{FI,S}(\tau_S^{EOL})$ 10^3 kg	9.07	23.6	7.70	-0.44
End-of-System-Life Inventory, Fertile, $N_{FE,S}(\tau_S^{EOL})$ 10^3 kg	-109.	-166.	-104.	-71.8

Minimum Fissile Replacement Time, $(\tau_{FI}^0)_{MIN}$ = 16.3 years

Table 4.3-1: Some characteristics of the reference fast-fission breeder system in four operating modes. Values underlined have been used to fix P_B^T.

already been calculated using Eq(4.3-7) and is 1383 MW_t.

The most striking feature of Fig. 4.3-4 is the intersection of all four fissile inventory curves. This occurs after 16.3 years of operation at a value of -5.3×10^3 kg. In Fig. 4.3-3, the value of $(\tau^0_{FI})_{MIN}$ was found to be 16.3 years and for a reference HTGR,

$$N_{FI,S}(t_o) = -\omega_{FI,S}[\tau^D_C+\tau^R_{FI}+\ell_{FI}(t_o-\tau^R_{FI})]/\tau^D_C R_C + G_{FI,C}(1-\ell_{FI})(t_o-\tau^R_{FI})R_C, \quad \tau^R_{FI}<t_o\leq\tau^{EOL} \tag{4.3-18}$$

or using the values in Table 4.1-1,

$$N_{FI,S}(t_o) = -5.3 \times 10^3 \text{ kg}, \quad t_o = (\tau^0_{FI})_{MIN} = 16.3 \text{ years}. \tag{4.3-19}$$

Clearly, $(\tau^0_{FI})_{MIN}$ is the time needed for the breeder to replace the fissile deficit which is accrued by the breeder alone during the early years of operation. When the converter reactor is added to the system, the intersection point will no longer be at zero but at a value determined by Eq(4.3-19).

Since, from Eq(4.3-2), $N_{FI,S}(\tau^{EOL}_S)$ is a linearly increasing function of R_B, the fissile end-of-system-life inventories are in order of increasing thermal power. Thus, Case B with a breeder thermal power of 5460 MW_t has the greatest surplus while Case D, P^T_B = 1380 MW_t, has a deficit. The fertile end-of-system-life inventories will be in the opposite order as can be seen from Eq(4.3-9) so that the Case D deficit is 71.8 tonnes while the Case B deficit is 166 tonnes.

In this section, the variation of some system characteristics with breeder thermal power were investigated. It was found that any inventory at a fixed time will be a linear function of R_B and hence P^T_B.

This was confirmed numerically in Fig. 4.3-1 for the initial and end-of-system-life, fertile and fissile inventories. The existence of a minimum value of $N_{FI,S}(\tau_{FI}^{MIN})$ which is not predicted by the standard doubling time approach was also confirmed. To explain the shape of $N_{FE,S}(\tau_{FI}^{0})$ as a function of P_B^T, the variation of τ_{FI}^{0} was examined and the equations developed in Section 3.3 were used to bound the various regimes. The asymptotic value of $(\tau_{FI}^{0})_{MIN}$ was further clarified in Fig. 4.3-4 where it was found, numerically, that at this time the breeder will have replaced its own deficit.

4.4 Changes in Breeder Parameters

The reference fast-fission breeder described in Section 4.1 is a GCFR with a breeding ratio of 1.45, a fissile specific inventory of 1.1 kg/MW_t, a core mean residence period of 3.0 years and a blanket mean residence period of 6.0 years. In the following, the values of these parameters will be changed to investigate the effects on the system characteristics. The reference breeder system will be designated as Case I and some of its characteristics have been listed in Table 4.3-1. Temporal variations of the four cases described below are shown in Fig. 4.4-1 for P_B^T equal to 3000 MW_t.

The breeder in Case II is identical to the reference breeder except the breeding ratio has been reduced to 1.20. To evaluate the net generation ratios, the data used in Section 4.1 were applied, that is, breeding was split such that 60% occurs within the core and 40% within the blanket and $\gamma_{FI,FE}^{n,abs}$ was set to unity. Some characteristics of this system are listed in Table 4.4-1 for the same operating modes that were

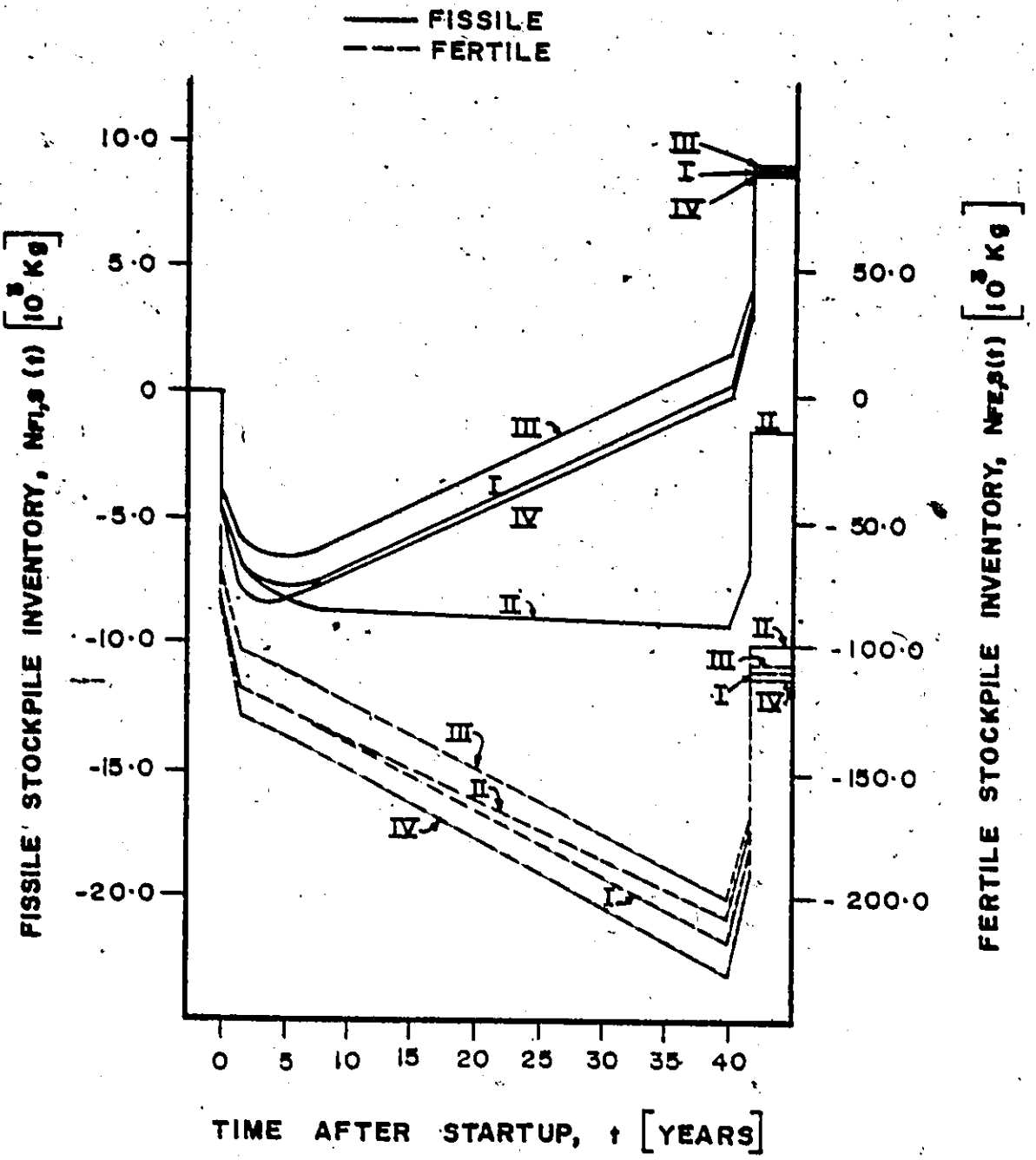

Fig. 4.4-1: Variation with time of the fissile and fertile stockpile inventories for four breeders described in the text. In all cases P_B^T is 3000 MW_t.

Parameter	Case A	B*	C	D
Breeder Thermal Power, P_B^T MW_t	<u>3000</u>	--	6510	3260
Initial Inventory, Fissile, $N_{FI,S}(0^+)$ 10^3 kg	-4.71	--	-8.48	-4.99
Initial Inventory, Fertile, $N_{FE,S}(0^+)$ 10^3kg	-84.1	--	-144.	-88.5
Time to Reach Minimum, Fissile, τ_{FI}^{MIN} years	40.0	--	6.35	40.0
Minimum Inventory, Fissile, $N_{FI,S}(\tau_{FI}^{MIN})$ 10^3 kg	-9.18	--	-14.8	<u>-9.10</u>
Fissile Replacement Time, τ_{FI}^0 yr	--	--	41.5	--
Fertile Inventory at τ_{FI}^0, $N_{FE,S}(\tau_{FI}^0)$ 10^3 kg	--	--	-167.	--
Steady-State Change, Fissile, $(dN_{FI,S}/dt)_{SS}$ 10^3 kg/yr	-0.02	--	<u>0.21</u>	0.0
Steady-State Change, Fertile, $(dN_{FE,S}/dt)_{SS}$ 10^3 kg/yr	-2.37	--	-4.04	-2.50
Minimum Inventory, Fertile, $N_{FE,S}(\tau^{EOL})$ 10^3 kg	-209.	--	-353.	-220.
End-of-System-Life Inventory, Fissile, $N_{FI,S}(\tau_S^{EOL})$ 10^3 kg	-1.46	--	6.89	-0.84
End-of-System-Life Inventory, Fertile, $N_{FE,S}(\tau_S^{EOL})$	-98.5	--	-167.	-104.

Minimum Fissile Replacement Time, $(\tau_{FI}^0)_{MIN}$ = 34.7 years

Table 4.4-1: Some characteristics of the fast-fission breeder system, Case II, with reduced breeding ratio (1.2) in three operating modes. Values underlined were used to fix P_B^T.
*$(\tau_{FI}^0)_{MIN}$ > 25 years, Mode II-B is impossible.

evaluated for Case I. The initial loadings are the same for Case I-A and Case II-A since $N_{M,S}(0^+)$ is independent of $G_{M,I}$. The value of τ_{FI}^{MIN} has been increased from 5.08 in the reference system to 40.0 years in the reduced breeding ratio system. From Table 4.4-1 $(dN_{FI,S}/dt)_{SS}$ is negative, hence Eq(3.3-31) applies. Because of the reduced breeding ratio and the longer time to reach the minimum, $N_{FI,S}(\tau_{FI}^{MIN})$ is greater than the reference value.

It might be expected that since $G_{FI,C}$ is -0.20 and $(G_{FI,BC}+G_{FI,BB})$ is 0.20, the breeder will just supply the HTGR; however, $(dN_{FI,S}/dt)_{SS}$ given by

$$(dN_{FI,S}/dt)_{SS} = \{-(\omega_{FI,C}/\tau_C^D+\omega_{FI,BC}/\tau_{BC}^D\ U_C/U_B)\ell_{FI} - G_{FI,C}(U_C/U_B-1)(1-\ell_{FI})\}R_C\ , \qquad (4.4\text{-}1)$$

is -20 kg/years. The first term in Eq(4.4-1) is due to the reprocessing losses neglecting irradiation and the other term gives the irradiation effects. From Table 4.1-1 and Table 4.1-2, $U_C/U_B = 1.04$, setting this to unity, the steady-state rate of change of the fissile stockpile will be -24 kg/year. Thus, the steady-state decrease is primarily due to reprocessing losses. After the final processing, the Case II-A system has a fertile deficit of -9.85×10^4 kg, 10% less than the reference case. This is attributable to the fertile net generation ratio being less negative than the reference case, hence less fertile material will be consumed.

At τ_S^{EOL}, the reduced breeding ratio system has a fissile deficit of 1.46×10^3 kg, hence the fissile replacement time is set to zero. The minimum fissile replacement time is 34.7 years, over twice as long as the

reference case. From Eq(4.3-14), the following proportionality can be found,

$$(\tau_{FI}^{O})_{MIN} - \tau_{FI}^{R} \underset{\sim}{\alpha} [G_{FI,BC} + G_{FI,BB}]^{-1} , \qquad (4.4\text{-}2)$$

where terms on the order of ℓ_{FI} have been neglected. Here $(G_{FI,BC}+G_{FI,BB})$ has been reduced by a factor of 2.25 from the reference value and the minimum fissile replacement time has increased by a factor of 2.52. The lack of exact proportionality is due to other terms in Eq(4.3-14) but the importance of the net generation ratio can be seen.

Because $(\tau_{FI}^{O})_{MIN}$ is greater than 25.0 years, it is not possible to operate the breeder in Mode B, that is, no breeder thermal power will give a fissile replacement time less than 34.7 years. The system operating in Mode C is required to produce, at steady-state, 210 kg/yr. The reference breeder system in Case I-C requires a breeder thermal power of 2766 MW_t compared to the reduced breeding ratio system which requires 6518 MW_t. The rate of change of the fissile inventory is calculated using Eq(4.2-12). In this equation, neglecting terms on the order of ℓ_{FI}, an approximate proportionality from Eq(4.3-17) can be found:

$$R_B \underset{\sim}{\alpha} (G_{FI,BC} + G_{FI,BB})^{-1} . \qquad (4.4\text{-}3)$$

Reducing the breeding gain, $(G_{FI,BC} + G_{FI,BB})$, by a factor of 2.25 increases the breeder thermal power in this mode by a factor of 2.4. Again, the difference in the ratios is due to the other terms in Eq(4.3-17). A reference breeder system with a breeder thermal power of 1383 MW_t, Case I-D, just supplies the converter at steady-state and provides a minimum value of $N_{FI,S}(\tau_{FI}^{MIN})$. For Case II-D, the breeder

thermal power is 3259 MW_t, 2.4 times larger than the reference. The size of the breeder is calculated using Eq(3.3-38) or Eq(4.3-7) and the proportionality given by Eq(4.4-3) is also approximately true. The minimum fissile inventory in Case II-D is 1.7 times larger than Case I-D due primarily to the increased breeder thermal power.

Many system characteristics are inversely proportional to the breeder gain: the minimum fissile replacement time, the steady-state rates of change and the breeder power required to fix the various modes. Also, from Eq(3.2-44), the fertile net generation ratio is proportional to the fissile net generation ratio. Thus, while reducing the breeding ratio decreases the fissile fuel production, fertile fuel consumption is also decreased.

The fissile specific inventory was reduced to 0.85 kg/MW_t for Case III. This was used to find the fertile specific inventory but the remainder of the parameters describing the breeder were kept constant. The average core enrichment was taken to be 12% and the ^{232}Th fuelled radial blanket was assumed to be the same size as the core. Using this, $\omega_{FE,BC}$ was calculated to be 6.23 kg/MW_t and $\omega_{FE,BB}$, 7.08 kg/MW_t. Some characteristics of this breeder-converter system are listed in Table 4.4-2 for the four operating modes described for the reference system.

In operating mode A, $P_B^T = 3000\ MW_t$, the initial fertile and fissile loadings are decreased due to the reduced fuelling requirements of the Case III breeder. The fissile specific inventory has been decreased by a factor of 1.29 which is given by

$$\frac{\left\{\left|N_{FI,S}(0^+)\right| - \omega_{FI,C} R_C\right\}_I}{\left\{\left|N_{FI,S}(0^+)\right| - \omega_{FI,C} R_C\right\}_{III}} = 1.29 . \qquad (4.4\text{-}4)$$

Parameter	Case A	B	C	D
Breeder Thermal Power, P_B^T MW_t	3000	4190	2750	1370
Initial Inventory, Fissile, $N_{FI,S}(0^+)$ 10^3 kg	-3.98	-4.97	-3.77	-2.64
Initial Inventory, Fertile, $N_{FE,S}(0^+)$ 10^3kg	-72.4	-88.1	-69.1	-51.0
Time to Reach Minimum, Fissile, τ_{FI}^{MIN} years	5.04	4.45	5.23	40.0
Minimum Inventory, Fissile, $N_{FI,S}(\tau_{FI}^{MIN})$ 10^3 kg	-6.60	-8.06	-6.29	-4.77
Fissile Replacement Time, τ_{FI}^0 yr	33.3	25.0	36.9	--
Fertile Inventory at τ_{FI}^0, $N_{FE,S}(\tau_{FI}^0)$ 10^3 kg	-184.	-198.	-184.	--
Steady-State Change, Fissile, $(dN_{FI,S}/dt)_{SS}$ 10^3 kg/yr	0.24	0.42	0.21	0.0
Steady-State Change, Fertile, $(dN_{FE,S}/dt)_{SS}$ 10^3 kg/yr	-2.59	-3.24	-2.45	-1.76
Minimum Inventory, Fertile, $N_{FE,S}(\tau^{EOL})$ 10^3 kg	-201.	-247.	-191.	-139.
End-of-System-Life Inventory, Fissile, $N_{FI,S}(\tau_S^{EOL})$ 10^3 kg	9.23	16.3	7.71	-0.43
End-of-System-Life Inventory, Fertile, $N_{FE,S}(\tau_S^{EOL})$ 10^3 kg	-107.	-134.	-101.	-70.7

Minimum Fissile Replacement Time, $(\tau_{FI}^0)_{MIN}$ = 13.7 years

Table 4.4-2: Some characteristics of the fast-fission breeder system, Case III, with $\omega_{FI,BC}$ = 0.85 kg/MW_t in four operating modes. Parameters underlined were used to fix P_B^T.

From Eq(4.2-10), decreasing the fissile specific inventory will also decrease the time to reach the minimum fissile inventory; by decreasing $\omega_{FI,BC}$ by 1.29, τ_{FI}^{MIN} is reduced by 0.8%. This reduction is due to the decreased fuelling requirements of the breeder which is given by

$$(dN_{FI,S}/dt)^{B-} = \omega_{FI,BC}/\tau_{BC}^{D} \quad . \tag{4.4-5}$$

Also, the value of $N_{FI,S}(\tau_{FI}^{MIN})$ is 14% smaller than the reference, τ_{FI}^{0} is 13% shorter than Case I-A and $(\tau_{FI}^{0})_{MIN}$ is 16% shorter for the same reason. The reduced refuelling rate also implies less losses, thus, at the end-of-system-life, the fissile surplus of the reduced inventory breeder system is 9.23×10^3 kg, 2% more than the reference. There are three effects combined here as a result of decreasing $\omega_{FI,BC}$: a smaller initial loading, reduced loss rates and smaller final addition to the stockpile.

The effects of reducing the specific inventory are most pronounced in operating mode B. Here, the system is required to have a fissile replacement time of 25 years. The Case III-B breeder thermal power is 4192 MW_t compared to 5462 MW_t for the reference Case I-B. In Eq(4.3-15) it can be seen that decreasing the value of $\omega_{FI,BC}$ will also decrease R_B. The effects in operating modes C and D are less since the changes are on the order of ℓ_M as seen in Eq(4.3-17) and Eq(4.3-7). Thus, the changes in breeder thermal power from the reference Cases I-C and I-D are only 0.8%. This is approximately the value of

$$\frac{(\omega_{FI,BC})_I}{(\omega_{FI,BC})_{III}} \frac{\ell_{FI}}{\tau_{BC}^{D}} = 0.0065 \quad . \tag{4.4-6}$$

To summarize, decreasing the specific inventory will decrease the initial

loading, the refuelling rate, the refuelling loss rate and the final stockpile addition. These effects, however, are small. It is the refuelling loss rate which produces the greatest effect and this is in the order of ℓ_{FI}/τ^D_{BC} as shown in Eq(4.4-6).

The final parameters varied were the two mean residence periods for the breeder: τ^D_{BC} and τ^D_{BB}. These were changed such that the ratio τ^D_{BC}/τ^D_{BB} was kept constant while τ^D_{BC} was reduced to 2.0 years. This case is designated Case IV and some of its characteristics are listed in Table 4.4-3 for the four operating modes of the reference case. Decreasing the mean residence periods will increase the refuelling rate as seen in Eq(4.4-5) and, in this model, shorten the time to reach steady-state. Thus, τ^{MIN}_{FI} in Case IV-A is shortened to 3.94 years since, from Eq(4.2-10),

$$(\tau^{MIN}_{FI}-\tau^R_{FI}) \underset{\sim}{\alpha} \tau^D_{BB} \quad . \qquad (4.4\text{-}7)$$

When τ^D_{BB} is decreased by 33%, the value of $(\tau^{MIN}_{FI}-\tau^R_{FI})$ is shortened by 32%. Although this system reaches the minimum fissile inventory in less time than the reference system, the increased fuelling rate during the first τ^R_{FI} years and the increased loss rates combine to produce a deeper minimum.

Increased loss rates contribute to the longer fissile replacement time and are responsible for the decrease in $(dN_{FI,S}/dt)_{SS}$ and the increase in $(dN_{FE,S}/dt)_{SS}$. The effect on the minimum fissile replacement time is an increase of 5%. During the system lifetime, the increase loss rate also reduces the value of $N_{FI,S}(\tau^{EOL}_S)$ and increase the value of $N_{FE,S}(\tau^{EOL}_S)$ by 3% of the reference values. For the other operating modes, decreasing the mean residence periods results in larger breeder powers

Parameter	Case A	Case B	Case C	Case D
Breeder Thermal Power, P_B^T MW_t	3000.	6080	2820	1410
Initial Inventory, Fissile, $N_{FI,S}(0^+)$ 10^3 kg	-4.71	-8.01	-4.52	-3.01
Initial Inventory, Fertile, $N_{FE,S}(0^+)$ 10^3kg	-84.1	-136.	-80.9	-57.0
Time to Reach Minimum, Fissile, τ_{FI}^{MIN} years	3.94	3.24	4.03	40.0
Minimum Inventory, Fissile, $N_{FI,S}(\tau_{FI}^{MIN})$ 10^3 kg	-8.32	-14.1	-7.98	-5.45
Fissile Replacement Time, τ_{FI}^0 yr	40.04	25.0	40.3	--
Fertile Inventory at τ_{FI}^0, $N_{FE,S}(\tau_{FI}^0)$ 10^3 kg	-231.	-314.	-215.	--
Steady-State Change, Fissile, $(dN_{FI,S}/dt)_{SS}$ 10^3 kg/yr	0.23	0.68	0.21	0.0
Steady-State Change, Fertile, $(dN_{FE,S}/dt)_{SS}$ 10^3 kg/yr	-2.72	-4.54	-2.62	-1.79
Minimum Inventory, Fertile, $N_{FE,S}(\tau^{EOL})$ 10^3 kg	-232.	-318.	-223.	-155.
End-of-System-Life Inventory, Fissile, $N_{FI,S}(\tau_S^{EOL})$ 10^3 kg	8.81	26.7	7.76	-0.41
End-of-System-Life Inventory, Fertile, $N_{FE,S}(\tau_S^{EOL})$ 10^3 kg	-112.	-186.	-108.	-73.9

Minimum Fissile Replacement Time, $(\tau_{FI}^0)_{MIN}$ = 17.0 years

Table 4.4-3: Some characteristics of the fast-fission breeder system, Case IV, with τ_{BC}^D = 2.0 yr and τ_{BB}^D = 4.0 yr is four operating modes. Values underlined were used to fix P_B^T.

needed to achieve specific characteristics. These changes are small since it is the increased loss rates which are primarily responsible and this effect is on the order of ℓ_{FI}. A secondary effect is to shorten the pre-steady-state period which introduces the steady-state generation ratios earlier than for the reference case.

The result of the above is to establish the importance of the net generation ratio in breeding descriptions. This result is valid for both fissile and fertile inventories; many characteristics were found to be directly proportional to the breeder gain, $G_{M,BC} + G_{M,BB}$. Changing the specific inventories and mean residence periods affect the fuelling rates but, for nearly all characteristics, this is a small effect proportional to the loss fraction, ℓ_M.

The procedure derived in Chapter III has been used in this chapter to describe a Gas-Cooled Fast Reactor coupled to a High Temperature Gas-Cooled Reactor. Since there is such a wide range of values available for parameters, a reference system was chosen which consisted of a representative GCFR-HTGR. The temporal variation of such a system with $P_C^T = P_B^T = 3000$ MW_t was described in Section 4.2. Here, the general shapes of the inventories anticipated in Section 3.3 were confirmed. In the next section, the effects of varying the breeder thermal power were investigated by two methods: (1) by directly varying P_B^T to observe the effects on the system characteristics and (2) by demanding the system operate in a specific mode and hence fix P_B^T. We find that any inventory at a fixed time is a linear function of P_B^T. Also, τ_{FI}^0 and τ_{FI}^{MIN} are functions of breeder power and the various regimes are bounded by powers calculated using the equations developed in Section 3.3. Finally, the effects of

changing some breeder parameters, the breeding ratio, the specific fissile inventory and the fuel discharge periods, were examined and related to the system equations of Chapter III. Of the variables changed, the most significant was the breeding ratio; to a lesser extent the other parameters also affect the results.

The results from this chapter have emphasized the new and detailed information which can be extracted for use in describing the breeding capabilities of a fast-fission breeder. With this bridge established between the more familiar type of breeder and the new procedure for analysis, we will proceed in the next two chapters to analyse breeders in a lesser stage of development, namely the fusion and spallation breeders.

CHAPTER V

FUSION BREEDER

The term fusion breeder is used here to refer to a fusion device which produces fissile fuel in its blanket. For the fusion breeder blanket designs presented in Section 2.3, there is considerable variation in the estimated values of total blanket generation ratio and blanket energy multiplication factor. For this reason, two reference fusion breeder systems will be investigated in this chapter rather than a single reference system and the effects of varying some parameters as in Chapter IV. Another reason for the choice of two reference systems is the distinction made in the literature between symbiotic and hybrid fusion breeders.

Lidsky[11] defines a symbiont as a fusion device with fission supressed in the breeding blanket and a hybrid as a device in which both fusion and fission reactions occur. The distinction between a symbiont and a hybrid is one of degree since there will be some fission reactions in DT fusion blankets containing fertile and fissile materials. A parameter which can be used to quantify this operational definition is the blanket energy multiplication factor defined by Eq(3.1-13). Reducing fissions will result in less energy released in the blanket, thus a fusion breeder with low blanket energy multiplication, say $M<2.0$, will be referred to as a symbiont and one with a high value, a hybrid. Another consequence of supressing fission in the blanket is to decrease neutron

multiplication, hence symbionts will tend to have a lower total blanket generation ratio than a hybrid.

The first section of this chapter will provide a description of the two reference systems chosen. Following this, the characteristics of the symbiotic and hybrid systems will be calculated using the same procedure as was used in Chapter IV for the fast-fission breeder. Applying the same method of analysis to several types of breeders and obtaining detailed results which are directly comparable is essential if valid comparisons are to be made. In the standard doubling time approach, the symbiotic breeder would be found to have a zero doubling time. As will be illustrated in Section 5.2, this is not true. Following the description of the breeding capacities, the power balance of fusion breeder systems will be presented.

5.1 Reference Systems

Since hybrids and symbionts differ only in their blanket designs, the same plasma core will be used for both cases: a DT burning TOKAMAK[79]. This plasma is maintained for long burn times, ~1000 s, by neutral beam injection of both deuterons and tritons with an injector efficiency of 0.57. The density of the plasma is 8×10^{13} cm^{-3} and, for an injector power of 575 MW, the mean discharge period for the tritons is ~2.0 s. For both the core and blankets of the fusion breeder Eq(4.1-2) is used to evaluate the initial specific inventory. The neutron wall loading is taken to be 0.74 MW/m^2 which is applicable to near term designs and the first wall is located 2.0 m from the centre of the plasma. The plasma amplification factor, Q_B^P, is defined by

$$Q_B^P = P_{fusion}/P_B^I \quad , \tag{5.1-1}$$

where P_{fusion} is the power produced by fusion in the core. This can be related to the total amplification factor, Q_B^T, defined in Eq(3.4-6) by

$$Q_B^P = \{(Q_B^T - \alpha_B)U_{fusion}/U_B \quad , \tag{5.1-2}$$

where U_{fusion} is 17.58 MeV for DT reactions and the other symbols are as defined in Section 3.4. The DT TOKAMAK plasma used here has a plasma amplification factor of 1.09. In addition, α_B is 0.95, that is, 95% of the injected beam energy is recovered in the blanket as heat.

For a fusion core, $G_{FI,BC}$, $G_{FE,BC}$ and $G_{Li,BC}$ will be zero since this is no fissile, fertile or lithium materials in the core; also, $G_{T,BC}$ will be -1.0 from Eq(3.2-32). The thermal-to-electric conversion efficiency is 0.38 and, using a ratio of auxiliary to neutron beam power of 0.20, the injector efficiency defined in Section 3.4 will be 0.475. The low values of η_B^I, Q_B^R and the wall loading reflect the possibility of earlier introduction of fusion devices if they are used to produce fissile fuel rather than as pure fusion power reactors. A load factor of 70% is assumed for the same reason. The fusion core parameters are listed in Table 5.1-1.

The parameters describing the reference symbiotic fusion breeder blanket are listed in Table 5.1-2. From Fig. 2.3-1, it can be seen that a blanket with a total generation ratio of 1.45 and an energy multiplication factor of 1.5 is representative of thorium blanket designs and satisfies our definition of a symbiont. Combining Eq(3.3-22) with Eq(3.3-30) and Eq(3.3-31), the steady-state rate of change of the

Parameter	Value
Plasma Radius	1.60 m
First Wall Radius	2.00 m
Ion Density	8×10^{13} cm^{-3}
Ratio of Deuterium to Tritium Ions	1.0
Tritium Mean Discharge Period, τ_{BC}^{D}	2.06 yr
Tritium Specific Inventory, $\omega_{T,BC}$	9.195×10^{-6} kg/MW_{fusion}
Tritium Net Generation Ratio, $G_{T,BC}$	-1.00
Plasma Amplification Factor, Q_B^P	1.09
Injector Efficiency, η_B^I	0.475
Thermal-Electric Conversion Efficiency, η_B^T	0.38
Fraction of Injected Energy Recovered, α_B	0.95
Load Factor, LF_B	0.70

Table 5.1-1: Reference fusion breeder core parameters for the DT TOKAMAK reactor[79] used in this analysis.

Parameter	Value
Fissile Net Generation Ratio, $G_{FI,BB}$	0.25
Fertile Net Generation Ratio, $G_{FE,BB}$	-0.25
Tritium Net Generation Ratio, $G_{T,BB}$	1.20
Lithium Net Generation Ratio, $G_{Li,BB}$	-1.20
Fissile Specific Inventory, $\omega_{FI,BB}$	0.0 kg/MW_{fusion}
Fertile Specific Inventory, $\omega_{FE,BB}$	26.73 kg/MW_{fusion}
Tritium Specific Inventory, $\omega_{T,BB}$	0.0 kg/MW_{fusion}
Lithium Specific Inventory, $\omega_{Li,BB}$	11.82 kg/MW_{fusion}
Energy Released per Characteristic Reaction, U_B	24.67 MeV
Fuel Mean Discharge Period, τ^D_{BB}	17.76 years

Table 5.1-2: Reference symbiotic fusion breeder blanket parameters necessary for this analysis.

tritium inventory will be given by

$$\left(\frac{dN_{T,S}}{dt}\right)_{SS} = \left\{\frac{\omega_{T,BC}}{\tau^{D}_{BC}}\ell_T + (G_{T,BB}-1)(1-\ell_T)\right\} R_B \qquad (5.1\text{-}3)$$

Thus, for $(dN_{T,S}/dt)_{SS}$ to be positive, the tritium net generation ratio in the blanket must satisfy

$$G_{T,BB} \geq \frac{\omega_{T,BB}\ell_T}{\tau^{D}_{BC}(1-\ell_T)} + 1 , \qquad (5.1\text{-}4a)$$

$$\geq 1.18. \qquad (5.1\text{-}4b)$$

With $G_{T,BB}$ fixed at 1.20 to allow production to exceed losses, $G_{FI,BB}$ will be 0.25. We also have $G_{FE,BB} = -0.25$, that is from Eq(3.2-43), there will be no neutron absorption in the fissile material produced and $Y^{n,abs}_{FI,FE}$ will be unity. In addition, the value of $G_{Li,BB}$ will be -1.20 or $Y^{n,abs}_{T,Li}$ will be unity. The ratio of tritium production to total conversion for this blanket will be 0.83 which, from Fig. 2.3-2, is a plausible design.

A blanket energy multiplication of 1.5 will result in an energy release of 24.67 MeV per DT fusion. The mean residence period of the blanket fuel elements is based on an uncollided neutron first wall exposure of 9.2 MW yr/m^2 [45,79] which results in a value for τ^{D}_{BB} of 17.76 years. Since fissions are supressed, there will be no fissile enrichment in the blanket. The calculation of $\omega_{M,BB}$ is complicated by geometric dependent factors. Using a 40 cm thick fertile zone[45] at a radius of 200.5 cm to allow for the vacuum wall, a fuel volume fraction of 63%[53] and the assumed neutron wall loading, $\omega_{FE,BB}$ will be 26.7 kg

per MW of fusion power if the density of ThC pins is 9.35 g/cm^3 (81). To calculate the lithium inventory, a 60 cm thick zone following the fertile zone is assumed. Thus, $\omega_{Li,BB}$ will be 11.82 kg/MW$_{fusion}$ where the volume fraction of lithium in this zone was also taken to be 63%.

For the hybrid blanket described in Table 5.1-3, a uranium-plutonium fuel cycle was assumed with a total blanket generation ratio of 3.5 and a blanket energy multiplication factor of 20.0. From Fig. 2.3-1, this design is well within the regime of the U-Pu blankets. To normalize the blanket results, $G_{T,BB}$ and $G_{Li,BB}$ for the hybrid will be taken to the same as the symbiont; thus, $G_{FI,BB}$ will be 2.3, 9.2 times that of the symbiont. This results in a ratio of tritium production to total conversion of 0.34, somewhat lower than the bulk of the data displayed in Fig. 2.3-2. Since the hybrid blanket will have some fusion reactions, Eq(4.1-3) is not expected to hold. Using the reaction rate ratios reported by Su et al(47) in the U-Pu region, the value of $G_{FI,BB}$ is found to be -2.61. The blanket energy multiplication factor of 20.0 results in a release of 285.5 MeV per DT fusion reaction. This is 11.57 times that of the symbiont and is greater than the energy released per neutron absorption in the thermal fission reactor of Section 4.1 by 70%. The fuel resides in the blanket until its first wall exposure reaches 4.1 MW yr/m^2 (45,80) or 7.91 years. To minimize the effects of geometry on the specific inventories, the same lithium and heavy element loading as in the symbiotic case will be used but corrected for the change from thorium to uranium-plutonium. The average fissile enrichment was taken to be 4%, hence $\omega_{FE,BB}$ will be 27.36 kg per MW of fusion power and $\omega_{FI,BB}$ will be 1.1 kg/MW$_{fusion}$.

Parameter	Value
Fissile Net Generation Ratio, $G_{FI,BB}$	2.30
Fertile Net Generation Ratio, $G_{FE,BB}$	-2.61
Tritium Net Generation Ratio, $G_{T,BB}$	1.20
Lithium Net Generation Ratio, $G_{Li,BB}$	-1.20
Fissile Specific Inventory, $\omega_{FI,BB}$	1.10 kg/MW_{fusion}
Fertile Specific Inventory, $\omega_{FE,BB}$	27.36 kg/MW_{fusion}
Tritium Specific Inventory, $\omega_{T,BB}$	0.0 kg/MW_{fusion}
Lithium Specific Inventory, $\omega_{Li,BB}$	11.82 kg/MW_{fusion}
Energy Released per Characteristic Reaction, U_B	285.5 MeV
Fuel Mean Discharge Period, τ^D_{BB}	7.91 years

Table 5.1-3: Reference hybrid breeder blanket parameters necessary for this analysis.

For the balance of the system, the values are listed in Table 5.1-4. The reprocessing times for the fissile and fertile material are 1.5 years as in Chapter IV and for lithium and tritium, 2 days since less activity and fabrication are projected. A result of this reduced processing is that the loss fraction for tritium and lithium is 0.5% rather than 1.5% for fissile and fertile material. The energy to extract fissile material is 3.35×10^3 kW_e hr/kg and for tritium, 4.50×10^3 kW_e hr/kg. Both the fission and fusion reactors are assumed to have a lifetime of 40.0 years.

5.2 Characteristics of the Symbiotic System

The model developed in Chapter III has been used to calculate the fissile, fertile, tritium and lithium inventories for the reference symbiotic fusion breeder system. In the first part of this section, a breeder thermal power of 3000 MW_t will be used. Following this, the variation of some characteristics with breeder thermal power will be presented. As stated in Section 3.3, the inventories calculated have similar general trends, hence comments for the fast-fission breeder systems in Chapter IV will be applicable here.

The fissile inventory is calculated using Eq(3.3-23) which for the symbiotic fusion breeder can be written as

$$N_{FI,S}(t) = -\omega_{FI,C}R_C H(t) + \int_o^t (D_{FI,C}(t')R_C + D_{FI,BB}(t')R_B)dt' + ((\omega_{FI,C} + 1/2\tau_C^D G_{FI,C})R_C(1-\ell_{FI}) + 1/2\tau_{BB}^D G_{FI,BB}R_B(1-\ell_{FI}))\, H(t-\tau^{EOL}-\tau_{FI}^R),\ t\geq 0 . \quad (5.2\text{-}1)$$

Parameter	Value
Reprocessing Fabrication Lags:	
Fissile, τ^R_{FI}	1.5 yr
Fertile, τ^R_{FE}	1.5 yr
Tritium, τ^R_T	2 days
Lithium, τ^R_{Li}	2 days
Loss Fractions:	
Fissile, ℓ_{FI}	0.015
Fertile, ℓ_{FE}	0.015
Tritium, ℓ_T	0.005
Lithium, ℓ_{Li}	0.005
Energy to Reprocess Fissile Fuel, W_{FI}	3.35×10^3 kW_e hr/kg
Energy to Reprocess Tritium, Fuel, W_T	4.50×10^3 kW_e hr/kg
System Reactor Lifetime, τ^{EOL}	40.0 yr

Table 5.1-4: Reprocessing-fabrication plant parameters necessary for this analysis.

The rate of change functions are given by

$$D_{FI,C}(t) = \begin{cases} 0, \ t \leq 0 , & (5.2\text{-}2a) \\ -\omega_{FI,C}/\tau_C^D, \ 0 < t \leq \tau_{FI}^R , & (5.2\text{-}2b) \\ -\omega_{FI,C}/\tau_C^D \ell_{FI} + G_{FI,C}(1-\ell_{FI}), \ \tau_{FI}^R < t \leq \tau^{EOL} , & (5.2\text{-}2c) \\ (\omega_{FI,C}/\tau_C^D + G_{FI,C})(1-\ell_{FI}), \ \tau^{EOL} < t \leq \tau^{EOL} + \tau_{FI}^R , & (5.2\text{-}2d) \\ 0, \ t > \tau^{EOL} + \tau_{FI}^R , & (5.2\text{-}2e) \end{cases}$$

for the converter reactor and

$$D_{FI,BB}(t) = \begin{cases} 0, \ t \leq \tau_{FI}^R , & (5.2\text{-}3a) \\ G_{FI,BB}(t-\tau_{FI}^R)/\tau_{BB}^D(1-\ell_{FI}), \ \tau_{FI}^R < t \leq \tau_{FI}^R + \tau_{BB}^D , & (5.2\text{-}3b) \\ G_{FI,BB}(1-\ell_{FI}), \ \tau_{BB}^D + \tau_{FI}^R < t \leq \tau^{EOL} + \tau_{FI}^R , & (5.2\text{-}3c) \\ 0, \ t > \tau^{EOL} + \tau_{FI}^R , & (5.2\text{-}3d) \end{cases}$$

for the breeder blanket. The fissile stockpile inventory, $N_{FI,S}(t)$, during the system lifetime is shown in Fig. 5.2-1.

The inventory during the first 1.5 years is completely determined by the converter reactor since the initial loading is given by

$$N_{FI,S}(0^+) = -\omega_{FI,C} R_C , \quad (5.2\text{-}4a)$$

$$= -1.5 \times 10^3 \text{ kg}; \quad (5.2\text{-}4b)$$

and the initial rate of decrease by

$$dN_{FI,S}(t)/dt = -\omega_{FI,C}/\tau_C^D R_C, \ 0 < t \leq \tau_{FI}^R , \quad (5.2\text{-}5a)$$

$$= -5.0 \times 10^2 \text{ kg/yr.} \quad (5.2\text{-}5b)$$

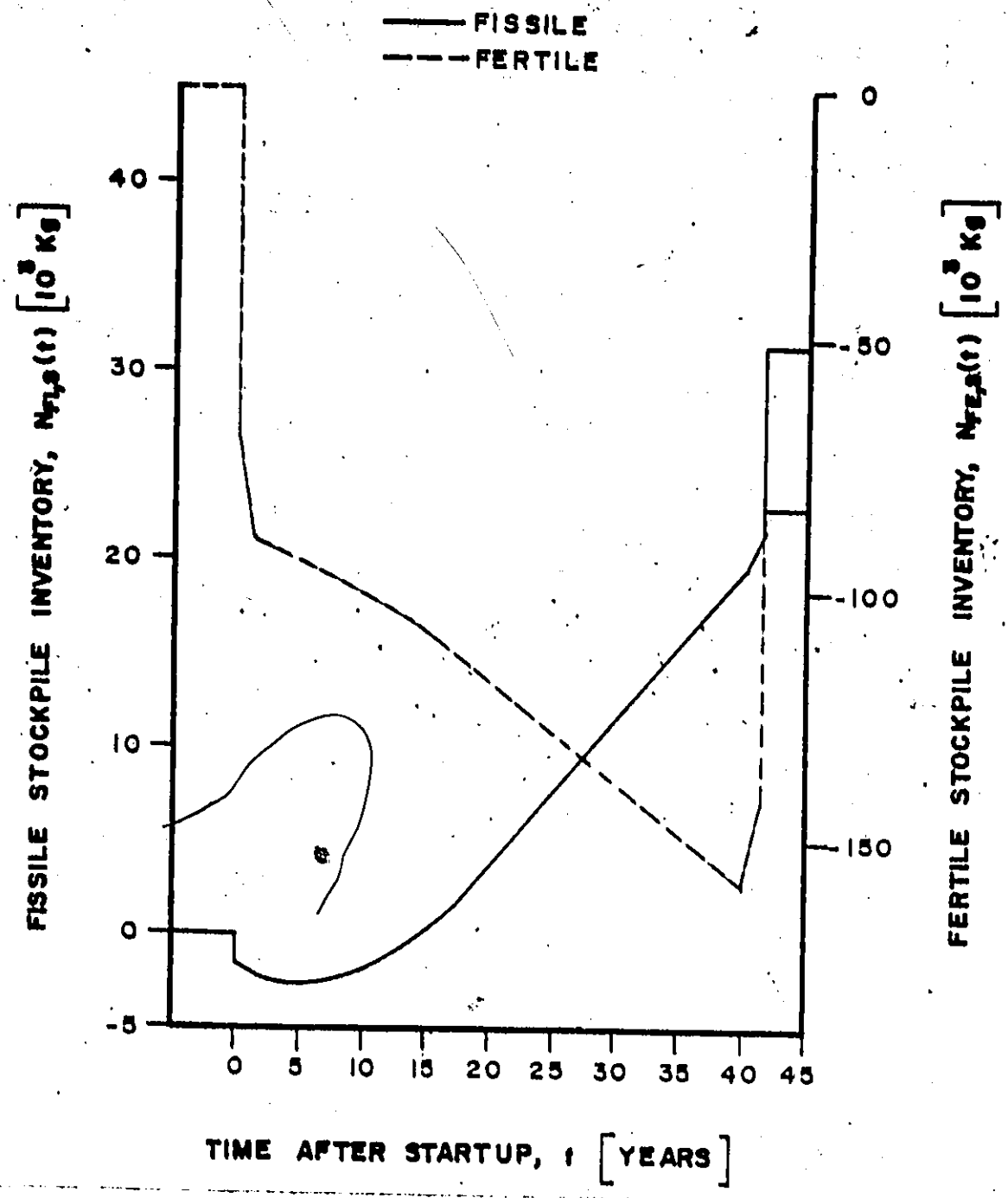

Fig. 5-2.1: Fissile and fertile stockpile inventories for the reference symbiotic fusion breeder system with P_B^T = 3000 MWt.

During the 17.76 year quadratic variation, $\tau_{FI}^R < t \leq \tau_{BB}^D + \tau_{FI}^R$, the minimum value is reached and the fissile fuel deficit replaced. The time to reach the minimum is found using Eq(3.3-33),

$$\tau_{FI}^{MIN} = \tau_{FI}^R + \{\omega_{FI,C}/\tau_C^D R_C \ell_{FI} - G_{FI,C}(1-\ell_{FI})\} \quad (5.2\text{-}6a)$$

$$X\{G_{FI,BB} R_B (1-\ell_{FI})/\tau_{BB}^D\}^{-1}, \quad \tau_{FI}^R < \tau_{FI}^{MIN} \leq \tau_{BB}^D + \tau_{FI}^R ,$$

$$= 5.22 \text{ years.} \quad (5.2\text{-}6b)$$

Substituting this into Eq(5.2-1) yields a minimum fissile inventory of -2.7×10^3 kg which is only 34% of the reference fission breeder system minimum but 75% more than the initial loading of the symbiotic system. The fissile replacement time is found using Eq(3.3-40) with the coefficients given by Eq(3.3-41). For the symbiotic system, when these equations are combined, τ_{FI}^O is calculated from

$$\tau_{FI}^O = \tau_{FI}^R + \frac{R_C}{R_B}\left[\frac{\omega_{FI,C}}{\tau_C^D}\ell_{FI} - G_{FI,C}(1-\ell_{FI}) + \left\{\left[\frac{\omega_{FI,C}}{\tau_C^D}\ell_{FI}\right]^2 + \left[G_{FI,C}(1-\ell_{FI})\right]^2 + 2\omega_{FI,C}(1-\ell_{FI})\left[\frac{G_{FI,BB}}{\tau_{BB}^D}\frac{R_B}{R_C}\left(1+\frac{\tau_{FI}^R}{\tau_C^D}\right) - \frac{G_{FI,C}}{\tau_C^D}\ell_{FI}\right]\right\}^{1/2}\right]\left[G_{FI,BB}(1-\ell_{FI})/\tau_{BB}^D\right]^{-1},$$

$$\tau_{FI}^R < \tau_{FI}^O \leq \tau_{FI}^R + \tau_{BB}^D , \quad (5.2\text{-}7a)$$

$$= 14.97 \text{ years.} \quad (5.2\text{-}7b)$$

Steady-state is established in the system at $t = \tau_{BB}^D + \tau_{FI}^R = 19.29$ years, nearly half of the reactor lifetime. The rate of increase of the fissile inventory at steady-state is given by

$$(dN_{FI,S}/dt)_{SS} = -\omega_{FI,C}/\tau_C^D \ell_{FI} R_C + [G_{FI,C}R_C + G_{FI,BB}R_B](1-\ell_{FI}) ,$$

$$\tau_{BB}^D + \tau_{FI}^R < t \leq \tau^{EOL} , \qquad (5.2\text{-}8a)$$

$$= 7.8 \times 10^2 \text{ kg/year.} \qquad (5.2\text{-}8b)$$

This rate of production is sufficient to fuel 3.7 external HTGRs which consume 3.1×10^2 kg/year at steady-state. When the final core and blanket reach the stockpile at $\tau^{EOL} + \tau_{FI}^R$, there is a discontinuous increase in the inventory given by

$$\Delta N_{FI,S}(\tau^{EOL}+\tau_{FI}^R) = \{[\omega_{FI,C} + 1/2\tau_C^D G_{FI,C}]R_C + 1/2\tau_{BB}^D G_{FI,BB}R_B\}(1-\ell_{FI}) , \qquad (5.2\text{-}9a)$$

$$= 9.9 \times 10^3 \text{ kg} , \qquad (5.2\text{-}9b)$$

which contributes to the fissile end-of-system-life inventory surplus of 3.1×10^4 kg. This value of $N_{FI,S}(\tau_S^{EOL})$ is sufficient to start up and operate 11.4 identical symbiotic systems.

The fertile inventory, also shown in Fig. 5.2-1, is calculated using

$$\begin{aligned} N_{FE,S}(t) = & -[\omega_{FE,C}R_C + \omega_{FE,BB}R_B]H(t) \\ & + \int_o^t \{D_{FE,C}(t')R_C + D_{FE,BB}(t')R_B\}dt' \\ & + \{(\omega_{FE,C} + 1/2\tau_C^D G_{FE,C})R_C \\ & + (\omega_{FE,BB} + 1/2\tau_{BB}^D G_{FE,BB})R_B\}(1-\ell_{FE})H(t-\tau^{EOL}-\tau_{FE}^R) , \end{aligned} \qquad (5.2\text{-}10)$$

where for the converter,

$$D_{FE,C}(t) = \begin{cases} 0, & t \le 0 , \quad (5.2\text{-}11a) \\ -\omega_{FE,C}/\tau_C^D, & 0 < t \le \tau_{FE}^R , \quad (5.2\text{-}11b) \\ -\omega_{FE,C}/\tau_C^D \ell_{FE} + G_{FE,C}(1-\ell_{FE}), & \tau_{FE}^R < t \le \tau^{EOL} , \quad (5.2\text{-}11c) \\ (\omega_{FE,C}/\tau_C^D + G_{FE,C})(1-\ell_{FE}), & \tau^{EOL} < t \le \tau_{FE}^R + \tau^{EOL} , \quad (5.2\text{-}11d) \\ 0, & t > \tau^{EOL} + \tau_{FE}^R ; \quad (5.2\text{-}11e) \end{cases}$$

and for the breeder blanket,

$$D_{FE,BB}(t) = \begin{cases} 0, & t \le 0 , \quad (5.2\text{-}12a) \\ -\omega_{FE,BB}/\tau_{BB}^D, & 0 < t \le \tau_{FE}^R , \quad (5.2\text{-}12b) \\ -\omega_{FE,BB}/\tau_{BB}^D \ell_{FE} + G_{FE,BB}(t-\tau_{FE}^R)/\tau_{BB}^D(1-\ell_{FE}) , & \quad (5.2\text{-}12c) \\ \qquad \tau_{FE}^R < t \le \tau_{FE}^R + \tau_{BB}^D , & \\ -\omega_{FE,BB}/\tau_{BB}^D \ell_{FE} + G_{FE,BB}(1-\ell_{FE}), & \tau_{FE}^R + \tau_{BB}^D < t \le \tau^{EOL} , \quad (5.2\text{-}12d) \\ (\omega_{FE,BB}/\tau_{BB}^D + G_{FE,BB})(1-\ell_{FE}), & \tau^{EOL} < t \le \tau^{EOL} + \tau_{FE}^R , \quad (5.2\text{-}12e) \\ 0, & t > \tau^{EOL} + \tau_{FE}^R . \quad (5.2\text{-}12f) \end{cases}$$

Using Eq(5.1-2), the fusion power is found to be 1321 MW hence $\omega_{FE,BB}$ will be 11.76 kg/MW$_t$, approximately equal to $\omega_{FE,C}$. The initial fertile loading will be given by

$$N_{FE,S}(0^+) = -(\omega_{FE,C}R_C + \omega_{FE,BB}R_B) , \quad (5.2\text{-}13a)$$

$$= -6.8 \times 10^4 \text{ kg}, \quad (5.2\text{-}13b)$$

or 18% of the initial loading of the fast-fission breeder system. At steady-state, the fertile inventory decreases linearly with a rate of changing found using

$$(dN_{FE,S}/dt)_{SS} = -(\omega_{FE,C}/\tau_C^D R_C + \omega_{FE,BB}/\tau_{BB}^D R_B)\ell_{FE} \quad (5.2\text{-}14a)$$

$$+(G_{FE,C}R_C + G_{FE,BB}R_B)(1-\ell_{FE}) ,$$

$$= -1.96 \times 10^3 \text{ kg/yr}. \quad (5.2\text{-}14b)$$

The minimum of $N_{FE,S}(t)$ occurs when the reactors are shut down and has a value of -1.6×10^5 kg. After the final core and blanket have been processed however, the fertile deficit, $N_{FE,S}(\tau_S^{EOL})$, is reduced to -8.1×10^4 kg.

In Fig. 5.2-2, the tritium inventory during the system lifetime is shown as calculated using

$$N_{T,S}(t) = -\omega_{T,BC}H(t) + \int_0^t \{D_{T,BC}(t') + D_{T,BB}(t')\}R_B dt' + (\omega_{T,BC} + 1/2\tau_{BC}^D G_{T,BC} + 1/2\tau_{BB}^D G_{T,BB})R_B \times (1-\ell_T)H(t-\tau^{EOL}-\tau_T^R) , \quad (5.2\text{-}15)$$

where here,

$$D_{T,BC}(t) = \begin{cases} 0, \ t<0 , & (5.2\text{-}16a) \\ -\omega_{T,BC}/\tau_{BC}^D, \ 0<t\leq\tau_T^R , & (5.2\text{-}16b) \\ -\omega_{T,BC}/\tau_{BC}^D\ell_T-(1-\ell_T) , \ \tau_T^R<t\leq\tau^{EOL} , & (5.2\text{-}16c) \\ (\omega_{T,BC}/\tau_{BC}^D-1)(1-\ell_T), \ \tau^{EOL}<t\leq\tau^{EOL}+\tau_T^R , & (5.2\text{-}16d) \\ 0, \ t>\tau^{EOL}+\tau_T^R; & (5.2\text{-}16e) \end{cases}$$

and

$$D_{T,BB}(t) = \begin{cases} 0, \ t\leq\tau_T^R , & (5.2\text{-}17a) \\ G_{T,BB}(t-\tau_T^R)/\tau_{BB}^D(1-\ell_T), \ \tau_T^R<t\leq\tau_{BB}^D+\tau_T^R , & (5.2\text{-}17b) \\ G_{T,BB}(1-\ell_T), \ \tau_{BB}^D+\tau_T^R<t\leq\tau^{EOL}+\tau_T^R , & (5.2\text{-}17c) \\ 0, \ t>\tau^{EOL}+\tau_T^R. & (5.2\text{-}17d) \end{cases}$$

The initial tritium inventory is small,

$$N_{T,S}(0^+) = -\omega_{T,BC}R_B, \quad (5.2\text{-}18a)$$

$$= -1.2 \times 10^{-4} \text{ kg} , \quad (5.2\text{-}18b)$$

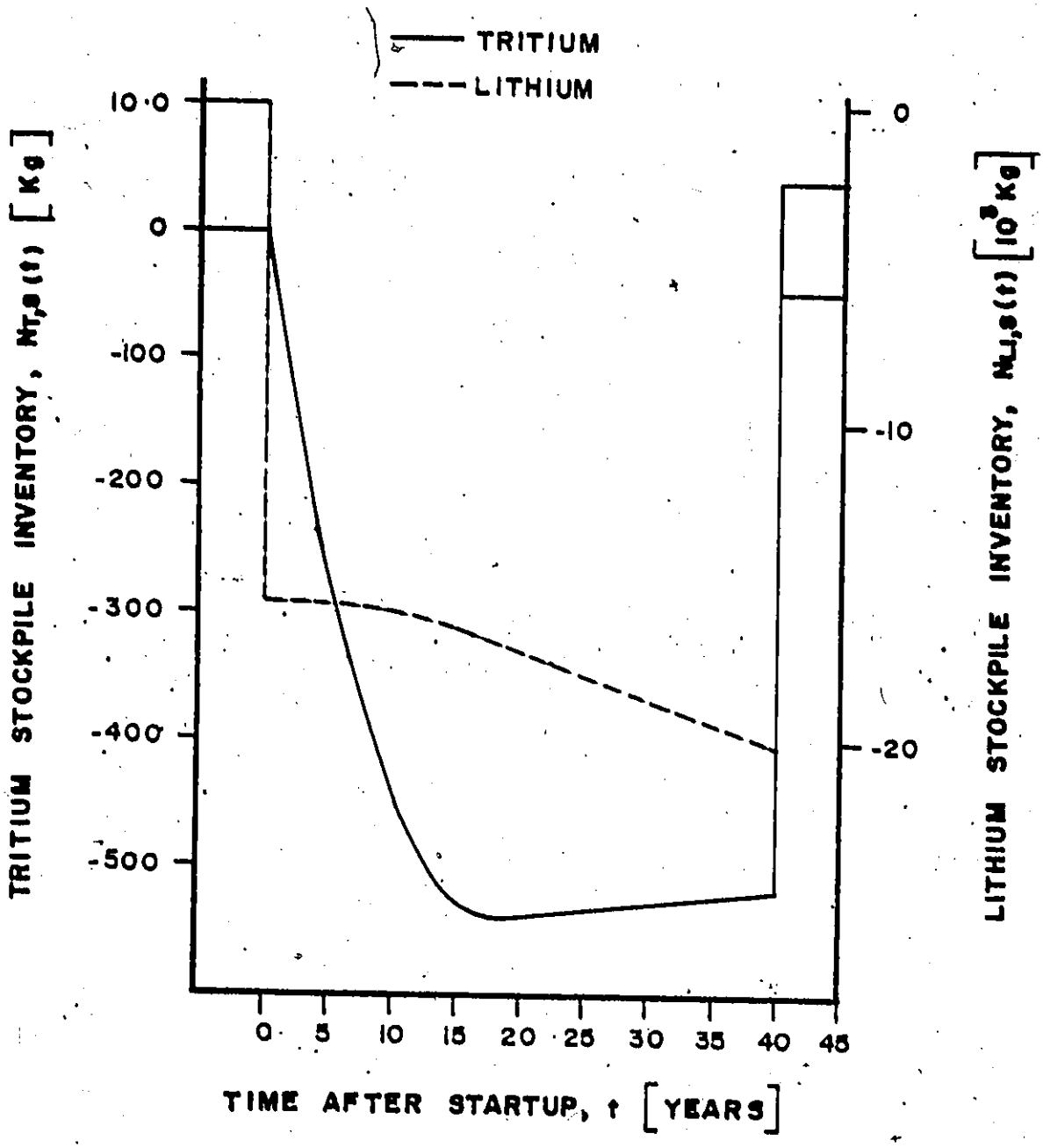

Fig. 5.2-2: Tritium and lithium stockpile inventories for the reference symbiotic fusion breeder with P_B^T = 3000 MWt.

since only the tritium in the plasma is considered. If the initial loading included a backup fuel supply, then the value of $N_{T,S}(0^+)$ would increase. Although tritium begins to reach the stockpile after two days, the tritium inventory does not reach a minimum value until 17.5 years since the tritium is assumed to be extracted from the blanket fuel elements.

During the pre-steady-state period, the rate of change of the tritium inventory is given by

$$dN_{T,S}(t)/dt = [-\omega_{T,C}/\tau_{BC}^{D}\ell_T-(1-\ell_T) + G_{T,BB}(t-\tau_T^R)/\tau_{BB}^{D}(1-\ell_T)]R_B, \quad \tau_T^R<t\leq\tau_{BB}^{D}+\tau_B^R. \tag{5.2-19}$$

Since τ_{BB}^{D} is 17.76 years, the first two terms, -42 kg/yr, will dominate until tritium production in the blanket becomes significant, about 10 years after startup. The minimum value of the tritium inventory is -5.4×10^2 kg and is reached at a time found from Eq(3.3-34). Since the converter reactor does not affect the tritium inventory for the reference symbiotic breeder, we have

$$\tau_T^{MIN} = (\tau_T^{MIN})_{MIN} = \tau_T^R+\tau_{BB}^{D}\left\{\frac{\omega_{T,BC}/\tau_{BC}^{D}\ell_T-(1-\ell_T)}{G_{T,BB}(1-\ell_T)}\right\}, \tag{5.2-20a}$$

$$= 17.49 \text{ years}, \tag{5.2-20b}$$

which can also be deduced from Eq(5.2-19) if the rate of change is set to zero. At steady-state, the system produces 0.97 kg/yr where

$$(dN_{T,S}/dt)_{SS} = \{-\omega_{T,BC}/\tau_{BC}^{D}\ell_T + (G_{T,BB}-1)(1-\ell_T)\}R_B, \quad \tau_T^R+\tau_{BB}^{D}<t\leq\tau^{EOL}. \tag{5.2-21}$$

This is nearly constant when compared with the initial rate of decrease. The increase in the tritium stockpile due to the final processing of the blanket is given by

$$\Delta N_{T,S}(\tau^{EOL}+\tau_L^R) = (\omega_{T,BC}-1/2\tau_{BC}^D+1/2\tau_{BB}^D G_{T,BB})R_B(1-\ell_T) \quad (5.2\text{-}22a)$$

$$= 5.3 \times 10^2 \text{ kg.} \quad (5.2\text{-}22b)$$

This large inventory in the blanket results in an end-of-system-life surplus of 38.8 kg but represents a radiation hazard during the reactor operating period.

The final material investigated for the 3000 MW_t symbiotic fusion breeder is the lithium stockpile as shown in Fig. 5.2-2. This inventory depends only on the breeder blanket parameters and hence will be calculated using

$$N_{Li,S}(t) = -\omega_{Li,BB}R_B H(t) + \int_0^t D_{Li,BB}(t')dt' \quad (5.2\text{-}23)$$

$$+(\omega_{Li,BB} + 1/2\tau_{BB}^D G_{Li,BB})(1-\ell_{Li})R_B H(t-\tau^{EOL}-\tau_{Li}^R) ,$$

and

$$D_{Li,BB}(t) = \begin{cases} 0, \ t\leq 0 , & (5.2\text{-}24a) \\ -\omega_{Li,BB}/\tau_{BB}^D, \ 0<t\leq\tau_{Li}^R , & (5.2\text{-}24b) \\ -\omega_{Li,BB}/\tau_{BB}^D\ell_{Li} + G_{Li,BB}(t-\tau_{Li}^R)/\tau_{BB}^D(1-\ell_{Li}), & (5.2\text{-}24c) \\ \quad \tau_{Li}^R<t\leq\tau_{Li}^R+\tau_{BB}^D, & \\ -\omega_{Li,BB}/\tau_{BB}^D\ell_{Li} + G_{Li,BB}(1-\ell_{Li}), & \\ \quad \tau_{Li}^R+\tau_{BB}^D<t\leq\tau^{EOL} , & (5.2\text{-}24d) \\ (\omega_{Li,BB}/\tau_{BB}^D+G_{Li,BB})(1-\ell_{Li}), \ \tau^{EOL}<t\leq\tau^{EOL}+\tau_{Li}^R , & (5.2\text{-}24e) \\ 0, \ t>\tau^{EOL}+\tau_{Li}^R . & (5.2\text{-}24f) \end{cases}$$

The initial lithium loading is given by

$$N_{Li,S}(0^+) = -\omega_{Li,BB} R_B \,, \tag{5.2-25a}$$

$$= -1.6 \times 10^4 \text{ kg} \,, \tag{5.2-25b}$$

but the steady-state rate of decrease is only

$$(dN_{Li,S}/dt)_{SS} = \{-\omega_{Li,BB}/\tau^D_{BB}\ell_{Li} + G_{Li,BB}(1-\ell_{Li})\}R_B \tag{5.2-26a}$$

$$= -1.5 \times 10^2 \text{ kg/yr.} \tag{5.2-26b}$$

Thus, the minimum lithium inventory, $N_{Li,S}(\tau^{EOL})$, is -2.0×10^4 kg, only 30% more than the initial loading. When the final blanket material is added to the stockpile, $N_{Li,S}(\tau^{EOL}_S)$ is -5.9×10^3 kg.

In this reference system, the thermal powers of the breeder and the converter were equal to 3000 MW_t. Using Eq(5.1-2), the total plasma amplification factor is found to be 2.48, thus, from Eq(3.4-11), the circulating energy fraction is 2.24. Since ε_B exceeds unity, electrical power must be supplied to the fusion component; 1411 MW_e in this case. The converter reactor produces only 1140 MW_e so the symbiotic system must import from outside the system 271 MW_e. Improvements in Q^T_B, η^T_B or η^I_B will reduce ε_B and improve the system power balance. Using Eq(3.4-20), the net nuclear efficiency is given by

$$\eta^N_S = \frac{(\eta^T_C(1-\varepsilon_C) + \eta^T_B(1-\varepsilon_B)Q^T_B/(Q^T_B-\alpha_B)P^N_B/P^N_C)}{(1 + P^N_B/P^N_C)} \,, \tag{5.2-27a}$$

$$= -0.0558. \tag{5.2-27b}$$

The system has a negative net power output, hence η^N_S will also be negative. The power for processing is small, 1.48 MW_e at steady-state which leads to a net system efficiency η^{NET}_S of -0.062. This value is less than η^N_S since the power needed for processing must also be brought

in from outside the system. The poor power balance of the symbiotic fusion breeder system is due to the low energy multiplication in the blanket and the low plasma amplification factor used.

As was the case for the fast-fission breeder system, the variation of some system characteristics with breeder thermal power are presented. In the following, the thermal power of the converter is fixed at 3000 MW_t. The characteristics which will be discussed are the same as in Section 4.3: the fertile and fissile startup and end-of-system-life inventories, the minimum fissile inventory and the fertile inventory at the fissile replacement time. These are shown in Fig. 5.2-3.

The initial fissile inventory, $N_{FI,S}(0^+)$, will be independent of the breeder size since the breeder has no fissile fuel requirements. The end-of-system-life fissile inventory is a linear function of breeder thermal power since, as discussed in Section 4.3, any inventory at a fixed time is a linear function of the breeder size. For the reference symbiotic system, we have

$$\partial N_{FI,S}(\tau_S^{EOL})/\partial R_B = 1/2\tau_{BB}^D G_{FI,BB}(1-\ell_{FI}) + \int_0^{\tau_S^{EOL}} D_{FI,BB}(t')dt', \quad (5.2\text{-}28a)$$

$$\partial N_{FI,S}(\tau_S^{EOL})/\partial P_B^T = 13.2 \text{ kg/MW}_t. \quad (5.2\text{-}28b)$$

This value is more than twice that of the reference fast-fission breeder. Applying Eq(4.3-3) to the symbiotic data, it is found that for $P_B^T > 653$ MW_t there will be a surplus of fissile material produced. This value can be compared with 1429 MW_t for the reference fast-fission breeder system.

The minimum fissile inventory, $N_{FI,S}(\tau_{FI}^{MIN})$, for the symbiotic fusion breeder system does not exhibit a sharp minimum. From Fig. 5.2-4, the minimum value of τ_{FI}^0 is found to be 1.5 years, thus, using Eq(3.3-49)

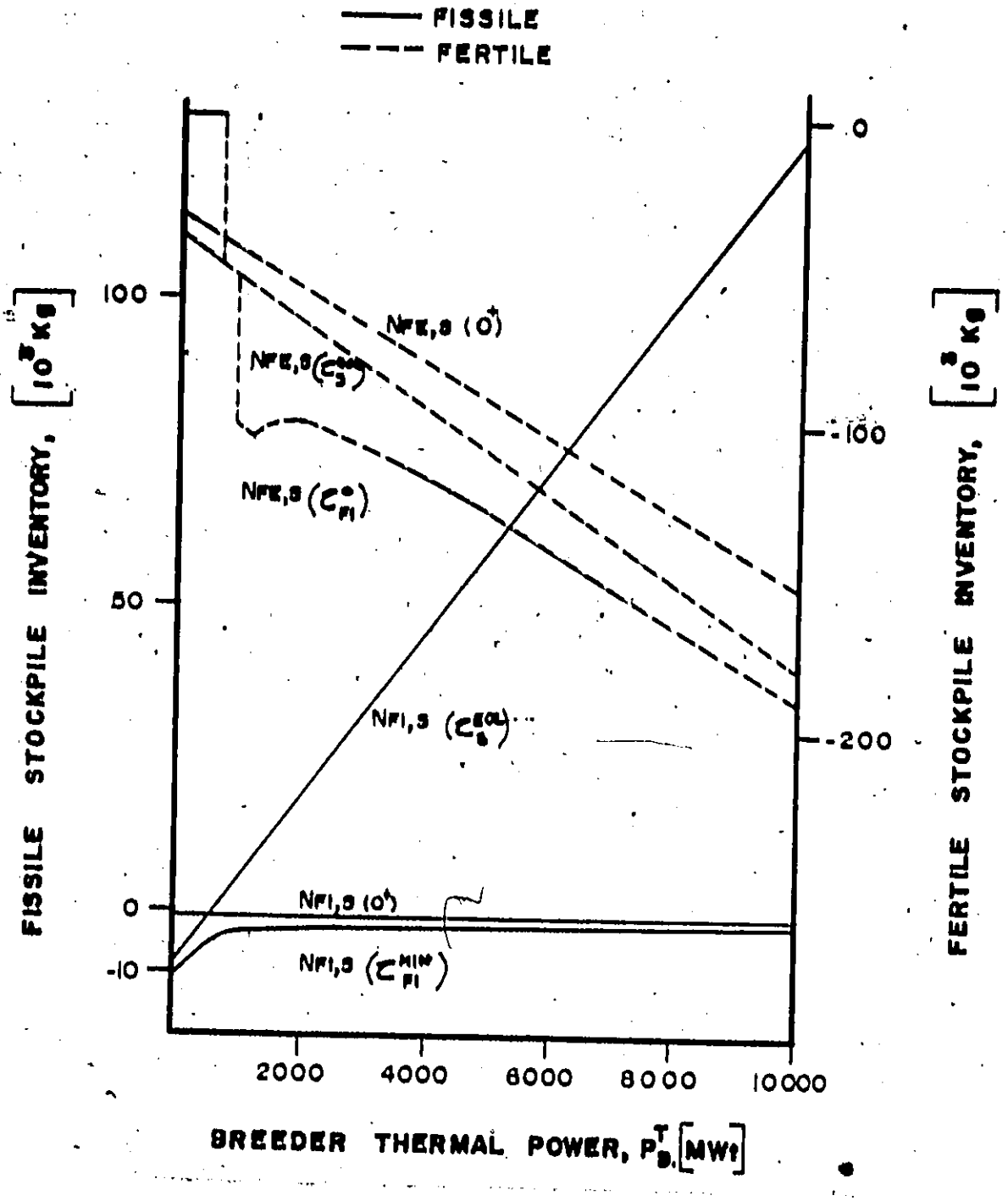

Fig. 5.2-3: Variation of the fissile and fertile stockpile inventories at certain times with breeder power for the reference symbiotic fusion breeder.

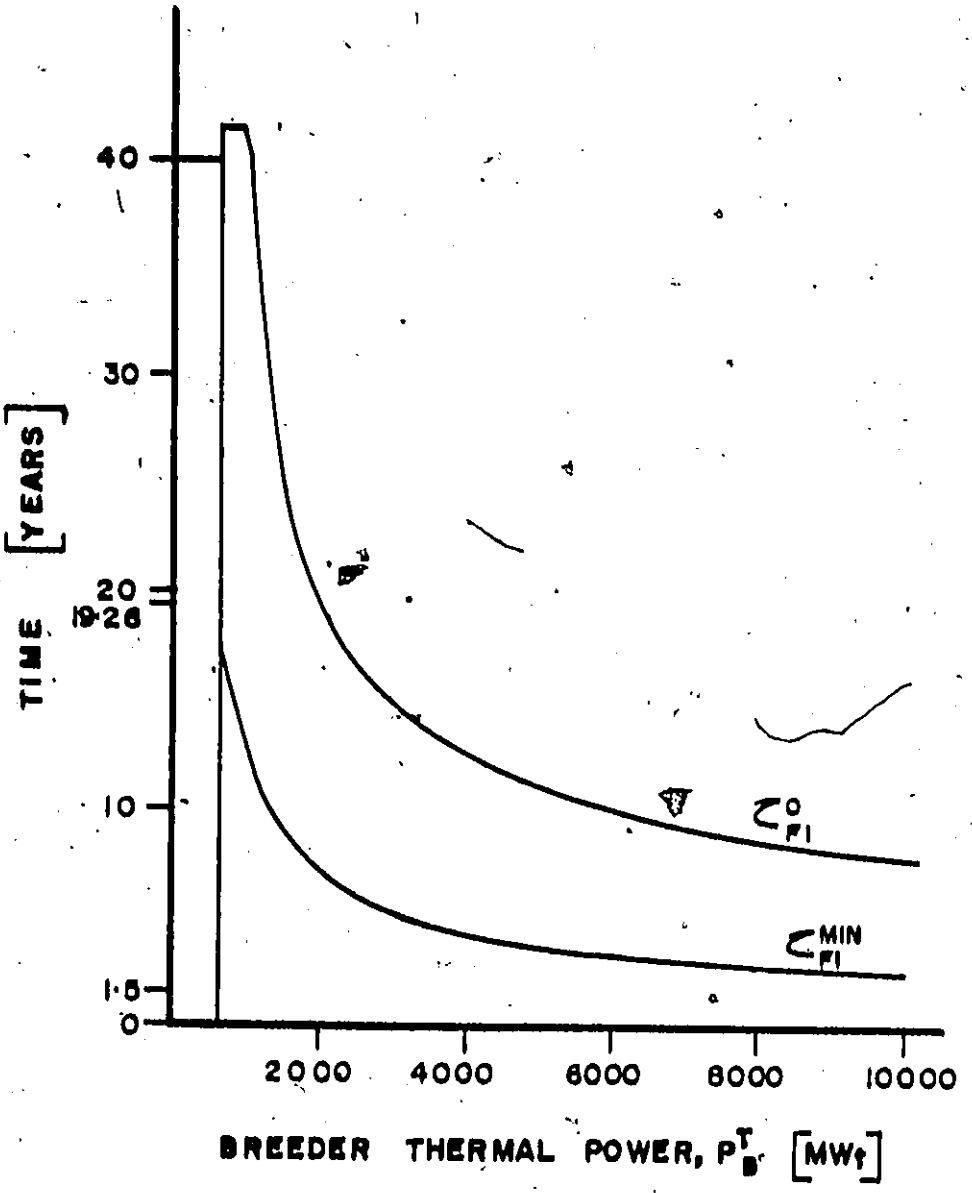

Fig. 5.2-4: Variation of fissile replacement time and time to reach minimum fissile inventory for the reference symbiotic fusion breeder system.

and Eq(3.3-50a), an infinite breeder thermal power is needed to minimize $N_{FI,S}(\tau_{FI}^{MIN})$. This minimum value will be -2.1 x 10^3 kg, the amount required by the converter alone for 1.5 years. The minimum fissile inventory, however, is nearly independent of breeder size. The change due to increasing the breeder thermal power from 3000 MW_t to infinity is only 530 kg or 20%. The minimum value of τ_{FI}^{MIN} is calculated from Eq(3.3-34)

$$(\tau_{FI}^{MIN})_{MIN} = \tau_{FI}^{R} = 1.5 \text{ yrs.} \qquad (5.2\text{-}29)$$

The fertile inventory at startup, $N_{FE,S}(0^+)$, and the inventory at the end-of-system-life, $N_{FE,S}(\tau_S^{EOL})$ are linear functions of P_B^T. The initial fertile inventory change with breeder thermal power is determined by

$$\partial N_{FE,S}(0^+)/\partial R_B = -\omega_{FE,BB} , \qquad (5.2\text{-}30a)$$

$$\partial N_{FE,S}(0^+)/\partial P_B^T = -11.76 \text{ kg/MW}_t , \qquad (5.2\text{-}30b)$$

while the end-of-system-life change is determined by

$$\partial N_{FE,S}(\tau_S^{EOL})/\partial R_B = -\omega_{FE,BB} + \int_0^{\tau_S^{EOL}} D_{FE,BB}(t')dt' + (\omega_{FE,BB} + 1/2\tau_{BB}^{D} G_{FE,BB})(1-\ell_{FE}^{-}), \qquad (5.2\text{-}31a)$$

$$\partial N_{FE,S}(\tau_S^{EOL})/\partial P_B^T = -14.6 \text{ kg/MW}_t . \qquad (5.2\text{-}31b)$$

Both of these slopes are ~50% less than the reference fast-fission breeder system slopes given by Eq(4.3-9) and Eq(4.3-10) respectively. The fertile inventory at the fissile replacement time, also shown in Fig. 5.2-3, has five regimes due to the five time periods of τ_{FI}^{0} shown in Fig. 5.2-4. For a breeder thermal power greater than 2030 MW_t, τ_{FI}^{0} is

less than $\tau_{BB}^{D}+\tau_{FI}^{R}$ which for the symbiotic blanket is 19.26 years. During this period, the fissile replacement time will be given by Eq(3.3-40) or Eq(5.2-7a). If P_B^T is between 2030 MW_t and 1049 MW_t, then τ_{FI}^{O} will be between $\tau_{BB}^{D}+\tau_{FI}^{R}$ and τ^{EOL}. The fissile replacement time in this region is given by Eq(3.3-42)

$$\tau_{FI}^{O}=\tau_{FI}^{R}+\{\omega_{FI,C}R_C(1+\frac{\tau_{FI}^{R}}{\tau_C^{D}})+G_{FI,BB}(1-\ell_{FI})R_B\frac{\tau_{BB}^{D}}{2}\}$$

$$X(-\frac{\omega_{FI,C}}{\tau_C^{D}}R_C\ell_{FI}+(G_{FI,C}R_C+G_{FI,BB}R_B)(1-\ell_{FI}))^{-1} \quad , \qquad (5.2\text{-}32)$$

$$\tau_{BB}^{D}+\tau_{FI}^{R}<\tau_{FI}^{O}\leq\tau^{EOL} \quad .$$

When P_B^T is between 955 MW_t and 1049 MW_t, then τ_{FI}^{O} is between $\tau^{EOL}+\tau_{FI}^{R}$ and τ^{EOL}. As seen from Eq(3.3-43), the equation for the fissile replacement time during this period is very similar to Eq(3.3-42) and hence Eq(5.2-32). In all three of these regimes, τ_{FI}^{O} is a function of P_B^T, hence $N_{FE,S}(\tau_{FI}^{O})$ will not vary linearly with P_B^T. If the breeder thermal power is reduced, 653 $MW_t<P_B^T<955$ MW_t, the fissile deficit is replaced only after the final core and blanket have been processed, hence, τ_{FI}^{O} is equal to τ_S^{EOL} and $N_{FE,S}(\tau_{FI}^{O})$ coincides with $N_{FE,S}(\tau_S^{EOL})$. As found above, for $P_B^T<653$ MW_t, there is no fissile surplus and τ_{FI}^{O} is set to zero.

As was the case for the fast-fission breeder system, four operating modes were investigated for the symbiotic fusion breeder. These operating modes are:

(A) P_B^T is 3000 MW_t, the breeder and converter thermal powers are equal;

(B) τ_{FI}^{O} is 25 years, a value suitable for an expanding power system;

(C) $(dN_{FI,S}/dt)_{SS}$ is such that one external HTGR is supplied;

(D) $N_{FI,S}(\tau_{FI}^{MIN})$ is minimized.

To find the breeder thermal power required for mode B, Eq(3.3-24) is used which reduces here to

$$P_B^T = U_B\{\omega_{FI,C}(1+\frac{\tau_{FI}^R}{\tau_C^D}) + [\frac{\omega_{FI,C}}{\tau_C^D}\ell_{FI} - G_{FI,C}(1-\ell_{FI})](\tau_{FI}^O-\tau_{FI}^R)\}$$

$$X\{G_{FI,BB}(1-\ell_{FI})(\tau_{FI}^O-\tau_{FI}^R)\}^{-1} \times \frac{Q_B^T}{(Q_B^T-\alpha_B)} R_C \,, \qquad (5.2\text{-}33a)$$

$$\tau_{BB}^D+\tau_{FI}^R<\tau_{FI}^O\leq\tau^{EOL} \,,$$

$$= 1480 \text{ MW}_t \,. \qquad (5.2\text{-}33b)$$

The steady-state rate of change required for Mode C is given by Eq(4.3-16) and P_B^T will be given by

$$P_B^T = -2U_B R_C\{\frac{-\omega_{FI,C}}{\tau_C^D}\ell_{FI}+G_{FI,C}(1-\ell_{FI})\}\, G_{FI,BB}(1-\ell_{FI})\}^{-1}$$

$$xQ_B^T/(Q_B^T-\alpha_B) \,, \qquad (5.2\text{-}34a)$$

$$= 1258 \text{ MW}_t \,. \qquad (5.2\text{-}34b)$$

As we have seen, the fissile inventory is minimized at an infinite breeder power. Some characteristics of these modes are listed in Table 5.2-1 and the first three modes are illustrated in Fig. 5.2-5.

From Fig. 5.2-5, it can be seen that the three fissile inventories are equal for the first 1.5 years after which the inventories increase in order of thermal power. Thus, Mode A with a breeder thermal power of

Parameter	Case A	B	C	D
Breeder Thermal Power, P_B^T	3000	1480	1250	$+\infty$
Initial Inventory, Fissile, $N_{FI,S}(0^+)$ 10^3 kg	-1.5	-1.5	-1.5	-1.5
Initial Inventory, Fertile, $N_{FE,S}(0^+)$ 10^3 kg	-68.3	-50.4	-47.8	$-\infty$
Initial Inventory, Tritium, $N_{T,S}(0^+)$, 10^{-6} kg	-121.	-59.8	-50.8	$-\infty$
Initial Inventory, Lithium, $N_{Li,S}(0^+)$ 10^3 kg	-15.6	-7.69	-6.53	$-\infty$
Time to Reach Minimum, Fissile, τ_{FI}^{MIN} yr	5.22	9.05	10.4	1.50
Minimum Inventory, Fissile, $N_{FI,S}(\tau_{FI}^{MIN})$ 10^3 kg	-2.63	-3.03	-3.17	-2.10
Time to Reach Minimum, Tritium, τ_T^{MIN} yr	17.5	17.5	17.5	17.5
Minimum Inventory, Tritium, $N_{R,S}(\tau_T^{MIN})$, kg	-539.	-266.	-226.	$-\infty$
Fissile Replacement Time, τ_{FI}^0, yr	15.0	25.0	30.2	1.5
Fertile Inventory at τ_{FI}^0, $N_{FE,S}(\tau_{FI}^0)$ 10^3 kg	-106.	-98.3	-101.	$-\infty$
Tritium Replacement Time, τ_T^0 yr	40.05	40.01	40.01	40.01
Lithium Inventory at τ_T^0, $N_{Li,S}(\tau_T^0)$ 10^3 kg	-5.9	-2.93	-2.49	$-\infty$

Table 5.2-1: Some characteristics of the symbiotic fusion breeder system in four operating modes. Values underlined were used to fix P_B^T.

Parameter	Case A	B	C	D
Steady-State Change, Fissile, $(dN_{FI,S}/dt)_{SS}$ 10^3 kg/yr	0.78	0.28	<u>0.21</u>	$+\infty$
Steady-State Change, Fertile, $(dN_{FE,S}/dt)_{SS}$ 10^3 kg/yr	-1.97	-1.46	-1.38	$-\infty$
Steady-State Change, Tritium, $(dN_{T,S}/dt)_{SS}$ kg/yr	0.97	0.48	0.41	$+\infty$
Steady-State Change, Lithium, $(dN_{Li,S}/dt)_{SS}$ 10^3 kg/yr	-0.15	-0.07	-0.06	$-\infty$
Minimum Inventory, Fertile, $N_{FE,S}(\tau^{EOL})$ 10^3 kg	-155.	-120.	-115.	$-\infty$
Minimum Inventory, Lithium, $N_{Li,S}(\tau^{EOL})$ 10^3 kg	-20.2	-9.96	-8.46	$-\infty$
End-of-System-Life Inventory, Fissile, $N_{FI,S}(\tau_S^{EOL})$ 10^3 kg	30.8	10.9	7.93	$+\infty$
End-of-System-Life Inventory, Fertile, $N_{FE,S}(\tau_S^{EOL})$ 10^3 kg	-80.9	-60.2	-57.1	$-\infty$
End-of-System-Life Inventory, Tritium, $N_{T,S}(\tau_S^{EOL})$ kg	38.8	19.1	16.3	$+\infty$
End-of-System-Life Inventory, Lithium, $N_{Li,S}(\tau_S^{EOL})$ 10^3 kg	-0.94	-2.93	-2.49	$-\infty$

Minimum Fissile Replacement Time, $(\tau_{FI}^0)_{MIN}$ = 1.5 yr

Minimum Tritium Replacement Time, $(\tau_T^0)_{MIN}$ = 573 yr ($\tau^{EOL} = \infty$)

Table 5.2-1: Some characteristics of the symbiotic fusion breeder system in four operating modes. Values underlined were used to fix P_B^T (continued).

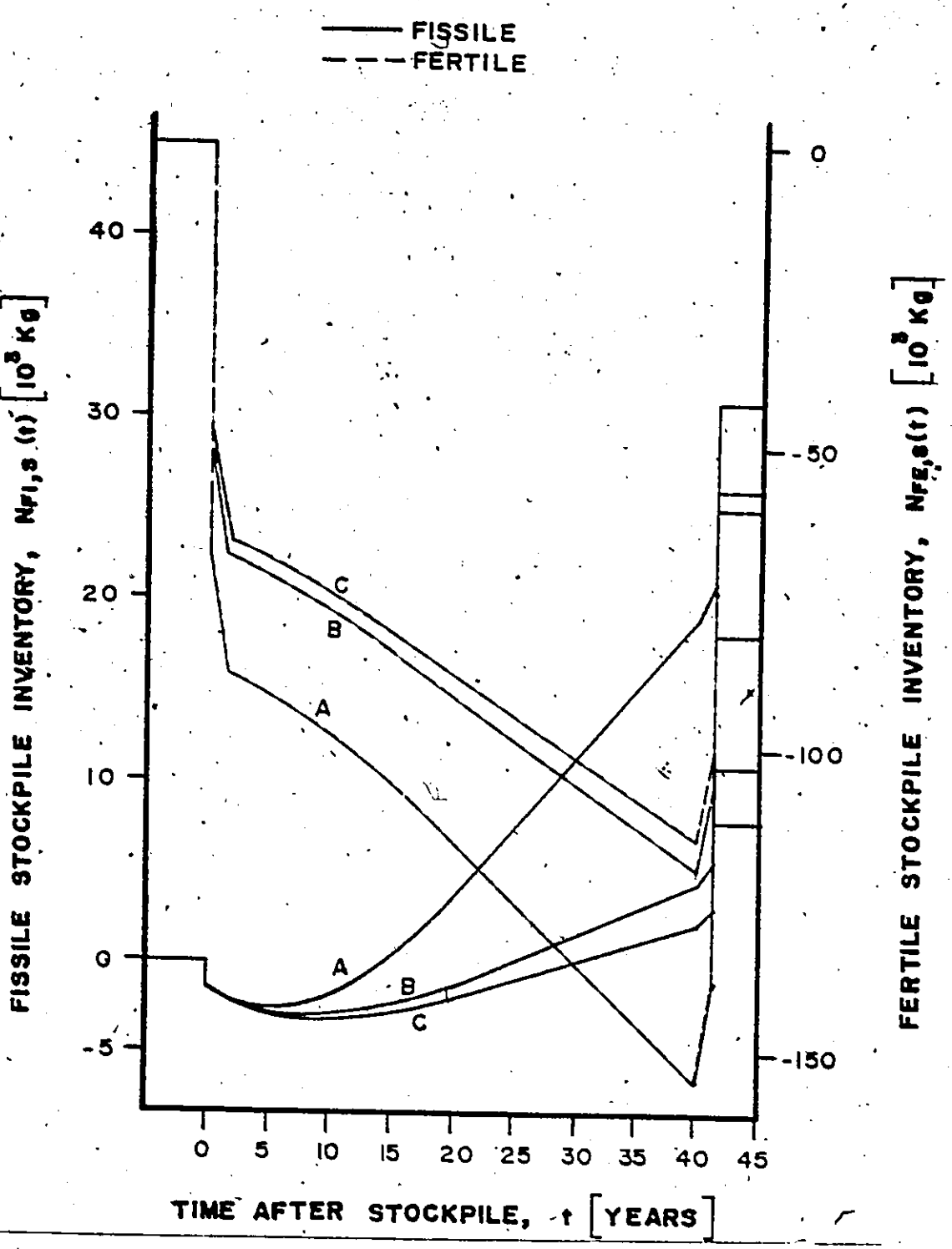

Fig. 5.2-5: Fissile and fertile stockpile inventories for the reference symbiotic fusion breeder in three operating modes described in text.

3000 MW_t has a fissile inventory greater than that of Mode C with a breeder thermal power of 1258 MW_t. The fertile inventories are in the opposite order, that is, Mode C has a smaller fertile deficit than Mode A. From Eq(5.2-20), the time to reach the minimum tritium inventory is equal for all operating modes. This is because the tritium inventory is determined solely by the breeder parameters.

The variation of symbiotic system characteristics with breeder thermal power has the same general trend as the fast-fission breeder. Since the breeder requires no fissile fuel, the initial fissile loading is independent of breeder size. For the same reason, the minimum fissile inventory does not have a sharp minimum as was the case for the fast-fission breeder system. The minimum value of $N_{FI,S}(\tau_{FI}^{MIN})$ occurs for an infinite breeder power but the variation with breeder power is small. The tritium inventory is determined only by breeder parameters, hence τ_T^{MIN} is equal to the minimum value for all breeder thermal powers. All the operating modes investigated produce a surplus of tritium but also require a large amount of tritium to operate. This deep minimum is due to the large fuelling loss rate and the long pre-steady-state period. The long mean residence period in the breeder blanket also delays full fissile fuel production but, nonetheless, this reference symbiotic fusion breeder system can produce more fissile material at a given breeder thermal power than the reference fast-fission reactor. A low blanket energy multiplication and plasma amplification factor lead to a value of $\epsilon_B>1$, thus the symbiotic breeder system has a poor power balance. In fact, by setting n_S^N to zero, we find that for $P_B^T>2419$ MW_t, the system will have a negative power output. This combination of good fissile

fuel production and low power generation is typical of symbiotic fusion breeder systems.

The symbiotic fusion breeder has been analysed in this section. Of primary interest here is the result that, although the fissile inventory of the breeder is zero, a non-zero fissile replacement time occurs. This is due to the effects of the converter. The tritium inventory goes through a deep minimum as a result of the long pre-steady-state period. This also leads to a large amount of tritium in the final blanket which could be a potential operating hazard. The fissile minimum inventory does not have a clearly defined minimum value; an infinite breeder power is required. However, $N_{FI,S}(\tau_{FI}^{MIN})$ is a slowly varying function of P_B^T. In the next section the hybrid fusion breeder will be discussed which will show the effects of changing the blanket design to increase fissions.

5.3 Characteristics of the Hybrid System

In this section, the characteristics of the reference hybrid fusion breeder will be presented. First, the temporal variation of the fissile, fertile, tritium and lithium inventories will be calculated for a 3000 MW_t fusion component. Following this, the variation of some characteristics with breeder thermal power will be found. Since the hybrid produces ^{239}Pu, the reference converter reactor data will be adjusted such that $\omega_{FI,C} = 0.51$ kg/MW_t and $\omega_{FE,C} = 11.28$ kg/MW_t.

The fissile inventory of the hybrid fusion breeder shown in Fig. 5.3-1 is calculated using

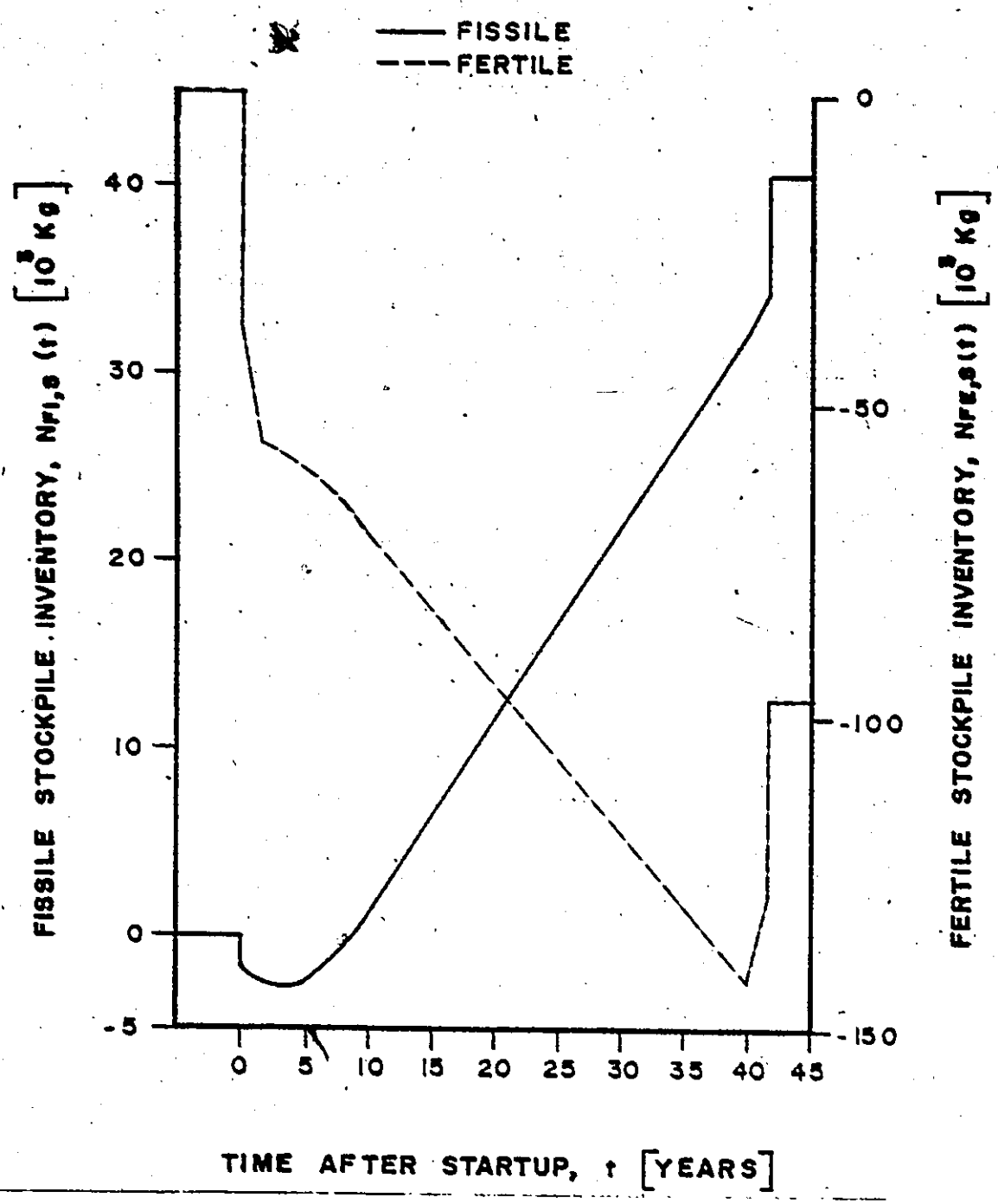

Fig. 5.3-1: Fissile and fertile inventories for the reference hybrid fusion breeder system with P_B^T = 3000 MWt.

$$N_{FI,S}(t) = -[\omega_{FI,C}R_C + \omega_{FI,BB}R_B]\,H(t)$$
$$+\int_o^t \{D_{FI,C}(t')R_C + D_{FI,BB}(t')R_B\}dt'$$
$$+\{(\omega_{FI,C} + 1/2\tau_C^D G_{FI,C})R_C(1-\ell_{FI})$$
$$+(\omega_{FI,BB} + 1/2\tau_{BB}^D G_{FI,BB})R_B(1-\ell_{FI})\}H(t-\tau^{EOL}-\tau_{FI}^R) \quad (5.3\text{-}1)$$

The rate of change functions, $D_{M,i}(t)$, for the hybrid system can be written as:

$$D_{FI,C}(t) = \begin{cases} 0, & t\le 0, \quad (5.3\text{-}2a) \\ -\omega_{FI,C}/\tau_C^D, & 0\le t\le \tau_{FI}^R, \quad (5.3\text{-}2b) \\ -\omega_{FI,C}/\tau_C^D\ell_{FI}+G_{FI,C}(1-\ell_{FI}), & \tau_{FI}^R<t\le\tau^{EOL}, \quad (5.3\text{-}2c) \\ (\omega_{FI,C}/\tau_C^D+G_{FI,C})(1-\ell_{FI}), & \tau^{EOL}<t\le\tau^{EOL}+\tau_{FI}^R, \quad (5.3\text{-}2d) \\ 0, & t>\tau^{EOL}+\tau_{FI}^R, \quad (5.3\text{-}2e) \end{cases}$$

for the reference converter HTGR and

$$D_{FI,BB}(t) = \begin{cases} 0, & t\le 0, \quad (5.3\text{-}3a) \\ -\omega_{FI,BB}/\tau_{BB}^D, & 0<t\le\tau_{FI}^R, \quad (5.3\text{-}3b) \\ -\omega_{FI,BB}/\tau_{BB}^D\ell_{FI}+G_{FI,BB}(t-\tau_{FI}^R)/\tau_{BB}^D(1-\ell_{FI}), & \tau_{FI}^R<t\le\tau_{BB}^D+\tau_{FI}^R, \quad (5.3\text{-}3c) \\ -\omega_{FI,BB}/\tau_{FI}^D\ell_{FI}+G_{FI,BB}(1-\ell_{FI}), & \tau_{BB}^D+\tau_{FI}^R<t\le\tau^{EOL}, \quad (5.3\text{-}3d) \\ (\omega_{FI,BB}/\tau_{BB}^D+G_{FI,BB})(1-\ell_{FI}), & \tau^{EOL}<t\le\tau^{EOL}+\tau_{FI}^R, \quad (5.3\text{-}3e) \\ 0, & t>\tau^{EOL}+\tau_{FI}^R, \quad (5.3\text{-}3f) \end{cases}$$

for the breeder blanket. Unlike the symbiotic fusion breeder, the hybrid fusion breeder does have an initial fissile loading. Using Eq(5.1-2),

the hybrid total amplification factor is 18.6, hence the fusion power for this 3000 MW_t breeder is 176 MW. In terms of the breeder thermal power, the fissile specific inventory of the hybrid will be 0.065 kg/MW_t.

Because the hybrid does require fissile fuel, the initial fissile inventory will be given by

$$N_{FI,S}(0^+) = -(\omega_{FI,C}R_C + \omega_{FI,BB}R_B) , \tag{5.3-4a}$$

$$= -1.73 \times 10^3 \text{ kg.} \tag{5.3-4b}$$

This value is 15% more than the initial loading of the symbiotic system but 63% less than the initial fissile inventory of the fast-fission breeder system. The quadratic variation of the inventory occurs for 1.5 years$<t\leq$9.41 years and during this period the system reaches the minimum fissile inventory and replaces the fissile deficit. Since the minimum inventory is reached during the pre-steady-state period, Eq(3.3-33) is applicable. For the hybrid, this equation can be written as

$$\tau_{FI}^{MIN} = \tau_{FI}^{R} + \left(\frac{\omega_{FI,C}R_C}{\tau_C^D} + \frac{\omega_{FI,BB}R_B}{\tau_{BB}^D}\right)\ell_{FI} - G_{FI,C}R_C(1-\ell_{FI})$$

$$\times\{G_{FI,BB}R_B(1-\ell_{FI})/\tau_{BB}^D\}^{-1} , \tag{5.3-5a}$$

$$= 2.86 \text{ yrs.} \tag{5.3-5b}$$

Three effects are combined here to produce a value of $(\tau_{FI}^{MIN})_{HY}$, the time to reach minimum inventory of the hybrid system, which is 55% of the symbiotic system, $(\tau_{FI}^{MIN})_{SY}$. Neglecting terms of order ℓ_{FI} in Eq(3.3-33), we find

$$\frac{(\tau_{FI}^{MIN}-\tau_{FI}^{R})_{HY}}{(\tau_{FI}^{MIN}-\tau_{FI}^{R})_{SY}} \simeq \frac{(\tau_{BB}^{D})_{HY}}{(\tau_{BB}^{D})_{SY}} \frac{(G_{FI,BB})_{SY}}{(G_{FI,BB})_{HY}} \frac{(R_B)_{SY}}{(R_B)_{HY}} . \tag{5.3-6}$$

The actual value of the ratio on the left hand side of Eq(5.5-6) is 0.366. From the data for the symbiotic and hybrid systems, the ratios on the right hand side will be

$$(\tau^D_{BB})_{HY}/(\tau^D_{BB})_{SY} = 7.91/17.76 = 0.445 , \quad (5.3\text{-}7a)$$

$$(G_{FI,BB})_{SY}/(G_{FI,BB})_{HY} = 0.25/2.30 = 0.109 , \quad (5.3\text{-}7b)$$

$$(R_B)_{SY}/(R_B)_{HY} = 1321/176 = 7.51 . \quad (5.3\text{-}7c)$$

Combining these, the right hand side of Eq(5.3-6) is 0.364; the difference is due to the exclusion of the hybrid fuelling requirements. This minimum fissile inventory is -2.7×10^3 kg; approximately equal to the symbiotic system value. Using Eq(3.3-40) and Eq(3.3-41), the hybrid fusion breeder system is found to replace the fissile deficit after 8.72 years, 54% of the symbiotic system value. At steady-state, the rate of increase of the fissile inventory will be found from

$$(dN_{FI,S}/dt)_{SS} = -\left(\frac{\omega_{FI,C}R_C}{\tau^D_C} + \frac{\omega_{FI,BB}R_B}{\tau^D_{BB}}\right)\ell_{FI} \quad (5.3\text{-}8a)$$

$$+(G_{FI,C}R_C + G_{FI,BB}R_B)(1-\ell_{FI}) ,$$

$$= 1.02 \times 10^3 \text{ kg/yr.} \quad (5.3\text{-}8b)$$

This value of $(dN_{FI,S}/dt)_{SS}$ is sufficient to fuel 4.9 steady-state HTGRs. At the end-of-system-life, $N_{FI,S}(\tau^{EOL}_S)$ is 4.1×10^4 kg, enough to start up and operate 15 identical hybrid systems.

The fertile inventory is also shown in Fig. 5.3-1 as calculated using Eq(5.2-10) with the hybrid data. The initial fertile loading is -3.8×10^4 kg, 56% of the symbiotic system fertile loading. This is due to the decrease in the fusion power of the hybrid compared with the

symbiont. At steady-state, the fertile inventory decreases 2.4×10^3 kg/yr and reaches a minimum value of -1.4×10^5 kg at 40 years. Although the steady-state decrease of the hybrid is greater than that of the symbiotic system, the initial inventory of the symbiont is greater, hence the depth of the minimum of the hybrid fertile stockpile inventory is 8% less than the symbiotic system. At the end-of-system-life however, the large fertile loading in the symbiotic system is added to the stockpile, thus, $N_{FE,S}(\tau_S^{EOL})$ for the hybrid system is -9.7×10^4 kg; 20% less than the symbiotic system.

In Fig. 5.3-2, the tritium and lithium inventories during the system lifetime are shown. The tritium inventory was calculated using Eq(5.2-15) with the rate of change functions given by Eq(5.2-16) and Eq(5.2-17). Because the same equations, net generation ratios and specific inventories have been used for both the hybrid and symbiotic systems, differences in the tritium inventories will be due to the changes in fusion power and blanket mean residence period. Thus, the initial tritium inventory is

$$N_{T,S}(0^+) = -\omega_{T,BC}R_B = -1.6 \times 10^{-5} \text{ kg}. \qquad (5.3\text{-}9)$$

which is 13% of the initial loading of the symbiont. From Eq(5.3-7c), the ratio of hybrid to symbiotic fusion power is also 13%. The tritium inventory reaches a minimum value of -32.7 kg after 7.79 years. The time to reach minimum is calculated using Eq(5.2-20) from which we find

$$(\tau_T^{MIN} - \tau_T^R)_{HY}/(\tau_T^{MIN} - \tau_T^R)_{SY} = (\tau_{BB}^D)_{HY}/(\tau_{BB}^D)_{SY} , \qquad (5.3\text{-}10a)$$

$$= 0.445 . \qquad (5.3\text{-}10b)$$

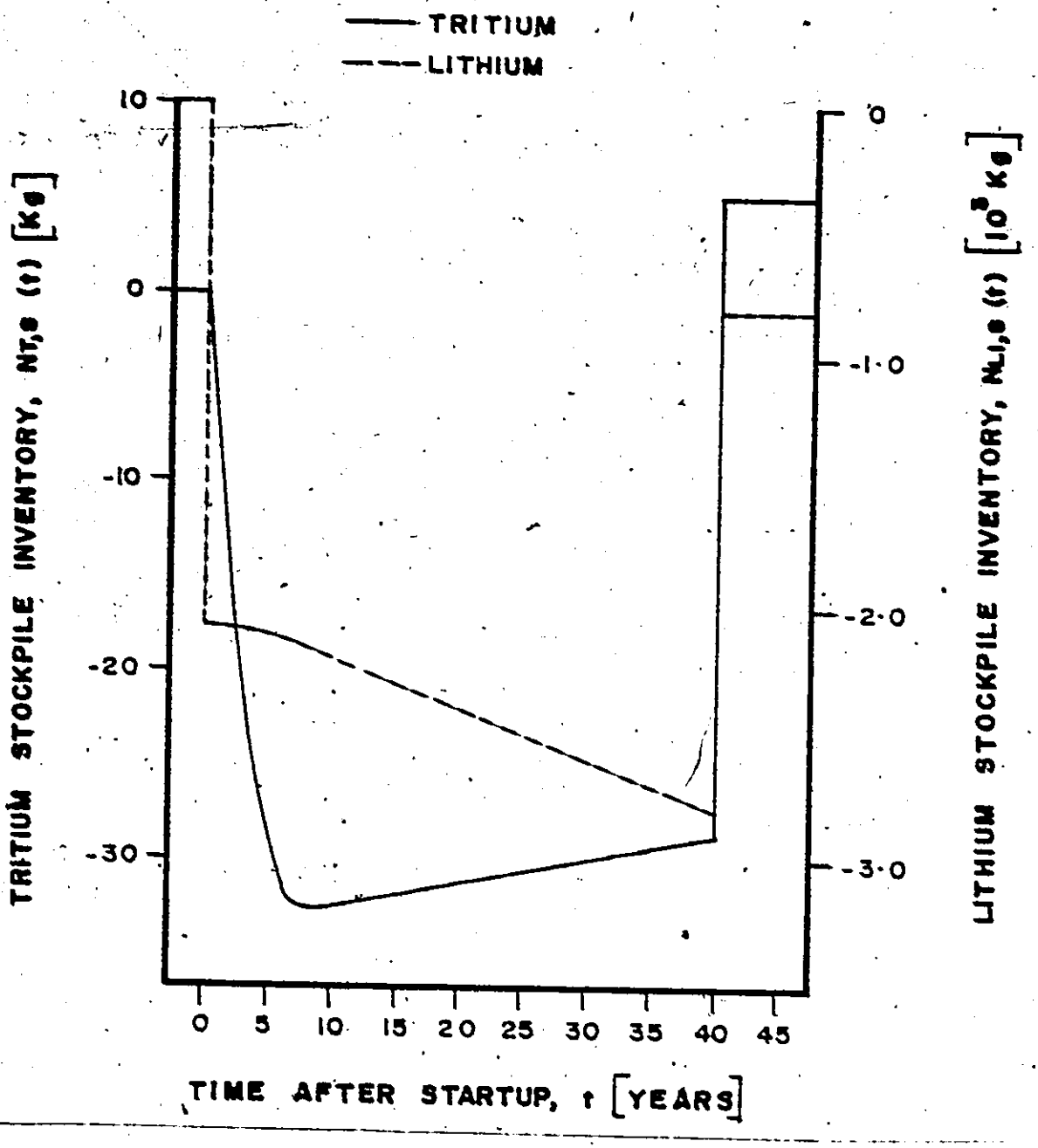

Fig. 5.3-2: Tritium and lithium stockpile inventories for the reference hybrid fusion breeder system with P_{T_R} = 3000 MWt.

At steady-state, using Eq(5.2-21), the hybrid produces 0.13 kg/yr which can be compared with the symbiotic system:

$$\frac{(dN_{T,S}/dt)_{SS,HY}}{(dN_{T,S}/dt)_{SS,SY}} = \frac{(R_B)_{HY}}{(R_B)_{SY}} = 0.13 \quad . \tag{5.3-11}$$

When the final tritium loading in the blanket is recovered, the hybrid system has a surplus of 5.2 kg, 13% of the symbiotic system value. The values for the lithium inventory, listed in Table 5.3-1 and shown in Fig. 5.3-2, will have the same relationship to the symbiotic system values as did the tritium inventory.

The hybrid reactor differs from the symbiont in the values of the parameters and the initial fissile inventory. The effects due to the changes in parameters are: (1) the increase by a factor of 9.2 in the fissile net generation ratio, (2) the decrease by a factor of 2.3 in the blanket mean residence period and (3) the decrease by a factor of 7.5 in fusion power. It is combinations of these which lead to shortened values of τ_{FI}^{MIN}, τ_{T}^{MIN} and τ_{FI}^{O} and increased fissile fuel production rates compared to the symbiont.

The increase in value of the blanket energy multiplication factor by a factor of 13 considerably improves the power balance of the hybrid compared with the symbiont. We found Q_B^T to be 18.6, hence, using Eq(3.4-11), the circulating energy fraction is 0.30. Since this is less than unity, the hybrid fusion reactor is a net power producer. For a breeder thermal power of 3000 MW_t, the hybrid produced 801 MW_e and the nuclear efficiency, η_S^N is 33%. The fuel processing energy requirement at steady-state is 0.74 MW_e, hence η_S^R will be 0.13%. The hybrid system,

Parameter	Case A	B	C	D
Breeder Thermal Power, P_B^T MW_t	<u>3000</u>	913	1028	2371
Initial Inventory, Fissile, $N_{FI,S}(0^+)$ 10^3 kg	-1.73	-1.60	-1.61	-1.69
Initial Inventory, Fertile, $N_{FE,S}(0^+)$ 10^3 kg	-38.6	-35.3	-35.5	-37.6
Initial Inventory, Tritium, $N_{T,S}(0^+)$, 10^{-6} kg	-16.0	-4.90	-5.50	-13.0
Initial Inventory, Lithium, $N_{Li,S}(0^+)$ 10^3 kg	-2.07	-0.63	-0.71	-1.64
Time to Reach Minimum, Fissile, τ_{FI}^{MIN} yr	2.86	5.95	5.46	3.22
Minimum Inventory, Fissile, $N_{FI,S}(\tau_{FI}^{MIN})$ 10^3 kg	-2.68	-2.85	-2.81	<u>-2.67</u>
Time to Reach Minimum, Tritium, τ_T^{MIN} yr	7.79	7.79	7.79	7.79
Minimum Inventory, Tritium $N_{T,S}(\tau_T^{MIN})$ kg	-32.7	-9.95	-11.2	-25.8
Fissile Replacement Time, τ_{FI}^0, yr	8.72	<u>25.0</u>	20.7	9.81
Fertile Inventory at τ_{FI}^0, $N_{FE,S}(\tau_{FI}^0)$ 10^3 kg	-68.2	-83.9	-78.9	-68.3
Tritium Replacement Time, τ_T^0 yr	40.01	40.01	40.01	40.01
Lithium Inventory at τ_T^0 $N_{Li,S}(\tau_T^0)$ 10^3 kg	-0.82	-0.25	-0.28	-0.65
Steady-State Change, Fissile, $(dN_{FI,S}/dt)_{SS}$ 10^3 kg/yr	1.02	0.16	<u>0.21</u>	0.76

Table 5.3-1: Some characteristics of the hybrid fusion breeder system in four operating modes. Values underlined were used to fix P_B^T.

Parameter	Case A	Case B	Case C	Case D
Steady-State Change, Fertile, $(dN_{FE,S}/dt)_{SS}$ 10^3 kg/yr	-2.39	-1.41	-1.46	-2.09
Steady-State Change, Tritium, $(dN_{T,S}/dt)_{SS}$ kg/yr	0.13	0.04	0.04	0.10
Steady-State Change, Lithium, $(dN_{Li,S}/dt)_{SS}$ 10^3 kg/yr	-0.02	-0.01	-0.01	-0.02
Minimum Inventory, Fertile, $N_{FE,S}(\tau^{EOL})$ 10^3 kg	-143.	-105.	-107.	-131.
Minimum Inventory, Lithium, $N_{Li,S}(\tau^{EOL})$ 10^3 kg	-2.81	-0.86	-0.96	-1.45
End-of-System-Life Inventory, Fissile, $N_{FI,S}(\tau_S^{EOL})$ 10^3 kg	40.6	6.25	8.14	30.3
End-of-System-Life Inventory, Fertile, $N_{FE,S}(\tau_S^{EOL})$ 10^3 kg	-97.2	-58.1	-60.3	-85.4
End-of-System-Life Inventory, Tritium, $N_{T,S}(\tau_S^{EOL})$ kg	5.17	1.57	1.77	4.08
End-of-System-Life Inventory, Lithium, $N_{Li,S}(\tau_S^{EOL})$ 10^3 kg	-0.82	-0.25	-0.28	-0.65

Minimum Fissile Replacement Time, $(\tau_{FI}^0)_{MIN}$ = 3.22 yr

Minimum Tritium Replacement Time, $(\tau_T^0)_{MIN}$ = 261 yr ($\tau^{EOL} = \infty$)

Table 5.3-1: Some characteristics of the hybrid fusion breeder system in four operating modes. Values underlined were used to fix P_B^T (continued).

although producing more fissile fuel than the symbiotic system, requires less energy for processing: 0.74 MW_e compared with 1.48 MW_e. This is due to the smaller fusion power of the hybrid leading to reduced tritium fuelling requirements. The importance of a large blanket energy multiplication factor can clearly be seen here.

The variation of the initial fissile and fertile inventories, the end-of-system-life fissile and fertile inventories, the minimum fissile inventory and the fertile inventory at the fissile inventory time are shown in Fig. 5.3-3. Since the hybrid fusion breeder differs from the symbiont in the values of the parameters and in the fissile fuel requirements only, the comments in Section 5.2 about the symbiotic system will be applicable to the hybrid system except for two characteristics. The initial fissile inventory for the symbiotic system is independent of breeder power but the hybrid requires some fissile fuel; hence $N_{FI,S}(0^+)$ will be a function of P_B^T,

$$\partial N_{FI,S}(0^+)/\partial R_B = -\omega_{FI,BB} \,, \tag{5.3-12a}$$

$$\partial N_{FI,S}(0^+)/\partial P_B^T = -0.065 \text{ kg/MW}_t \,. \tag{5.3-12b}$$

This variation is only 6% of the fast-fission breeder system value given in Eq(4.3-1). The minimum fissile inventory minimum value occurs at a breeder thermal power of 2371 MW_t,

$$(P_B^T)_{FI}^{MIN} = U_B R_C \frac{Q_B^T}{(Q_B^T-\alpha_B)} \left\{ \frac{\omega_{FI,C}}{\tau_C^D} \ell_{FI} - G_{FI,C}(1-\ell_{FI}) \right\}$$
$$\times \left\{ \frac{2G_{FI,BB}(1-\ell_{FI})}{\tau_{BB}^D} \omega_{FI,BB}\left(1+\frac{\tau_{FI}^R}{\tau_{BB}^D}\right) \right.$$
$$\left. + \left[\frac{\omega_{FI,BB}\ell_{FI}}{\tau_{BB}^D} - G_{FI,BB}(1-\ell_{FI}) \right]^2 \right\}^{-1/2} . \tag{5.3-13}$$

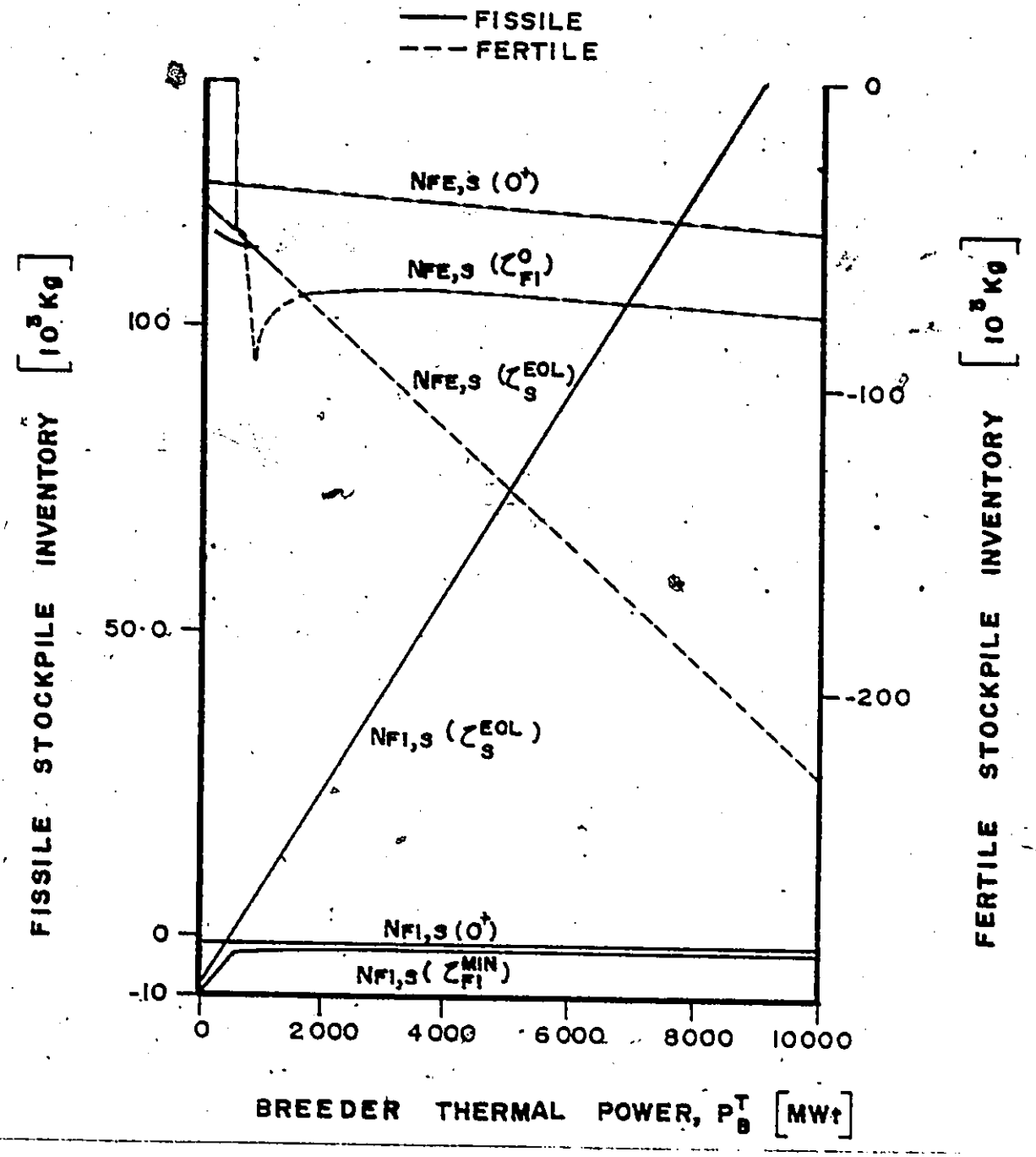

Fig. 5.3-3: Variation of fissile and fertile stockpile inventory characteristics with breeder thermal power for the reference hybrid fusion breeder system.

The minimum value of $N_{FI,S}(\tau_{FI}^{MIN})$ is -2.6×10^3 kg but, as with the symbiotic system, there is little variation with P_B^T: less than 12% from the minimum between 513 MW_t and 10,000 MW_t.

In Fig. 5.3-4, the variation of τ_{FI}^0 and τ_{FI}^{MIN} with breeder thermal power are shown. Here, because the value of $\omega_{FI,BB}$ is not zero, the asymptotes are not equal. The minimum value of the fissile replacement time, given by Eq(3.3-46) and Eq(3.3-47), is 3.22 years. The minimum value of τ_{FI}^{MIN} is 1.502 years.

The four operating modes discussed previously are illustrated in Fig. 5.3-5 and some characteristics are listed in Table 5.3-1. Due to the increased fissile breeding capacity of the hybrid, the breeder powers required for Modes B and C are less than that of the symbiotic system. Also, there is a finite value of P_B^T which gives a minimum $N_{FI,S}(\tau_{FI}^{MIN})$.

In general, the hybrid system characteristics are similar to the symbiotic system. The differences are due to different values of the parameters and a non-zero fissile fuel initial inventory in the hybrid. The three parameters which are important are the breeding blanket net generation ratio, the breeding blanket mean residence period and the breeding blanket energy multiplication factor. These combine to increase the fissile fuel production over that of the symbiotic system and to make the hybrid system a net power producer. Adding fissile fuel to the hybrid breeder blanket serves to increase the value of $(\tau_{FI}^0)_{MIN}$ so that a finite value of P_B^T will produce a minimum value of $N_{FI,S}(\tau_{FI}^{MIN})$.

5.4 Fusion Breeder Power Balance

As has been demonstrated above, the power balance in a fusion

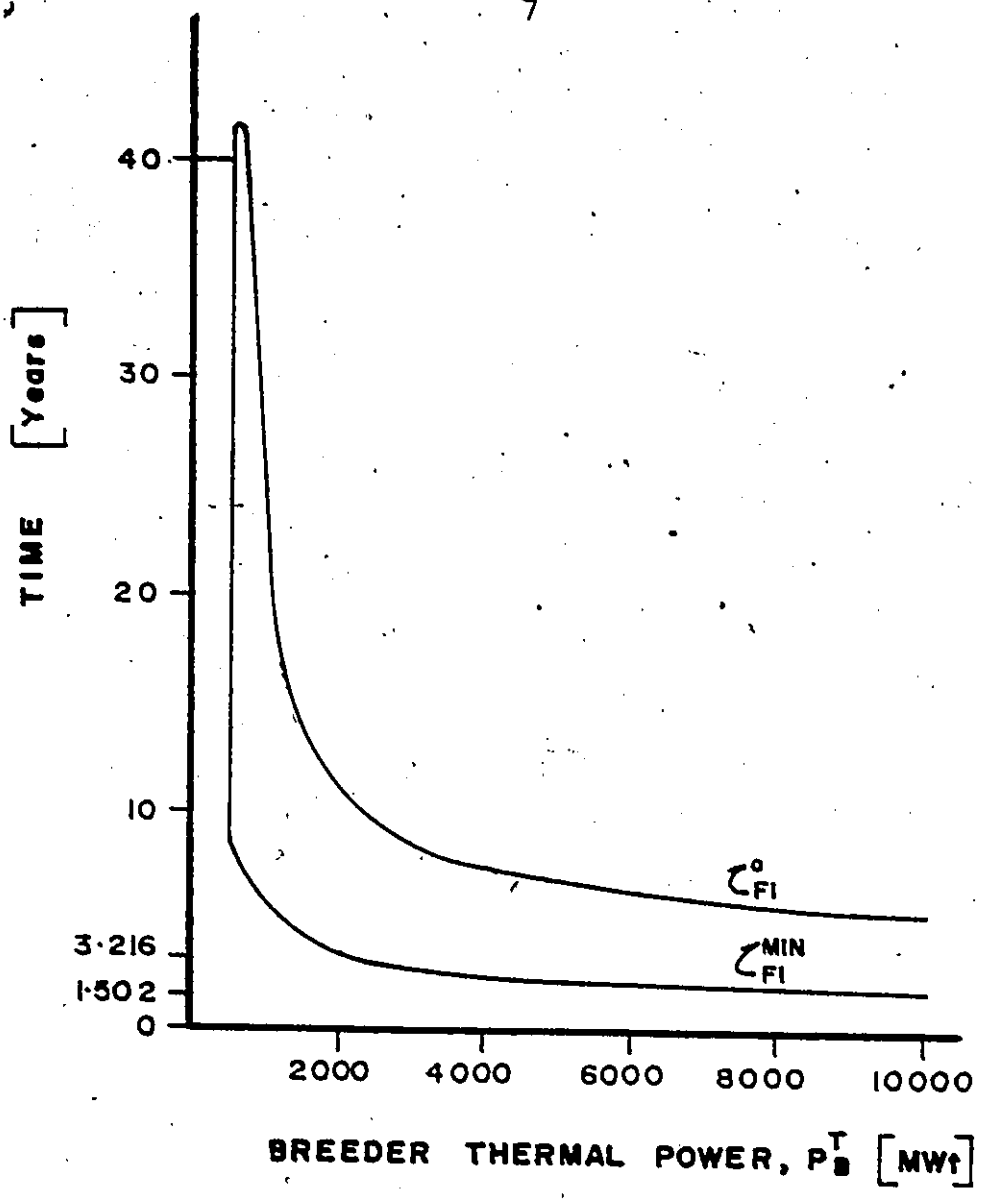

Fig. 5.3-4: Variation of the fissile replacement time and time to reach minimum fissile inventory with breeder thermal power for the reference hybrid fusion breeder system.

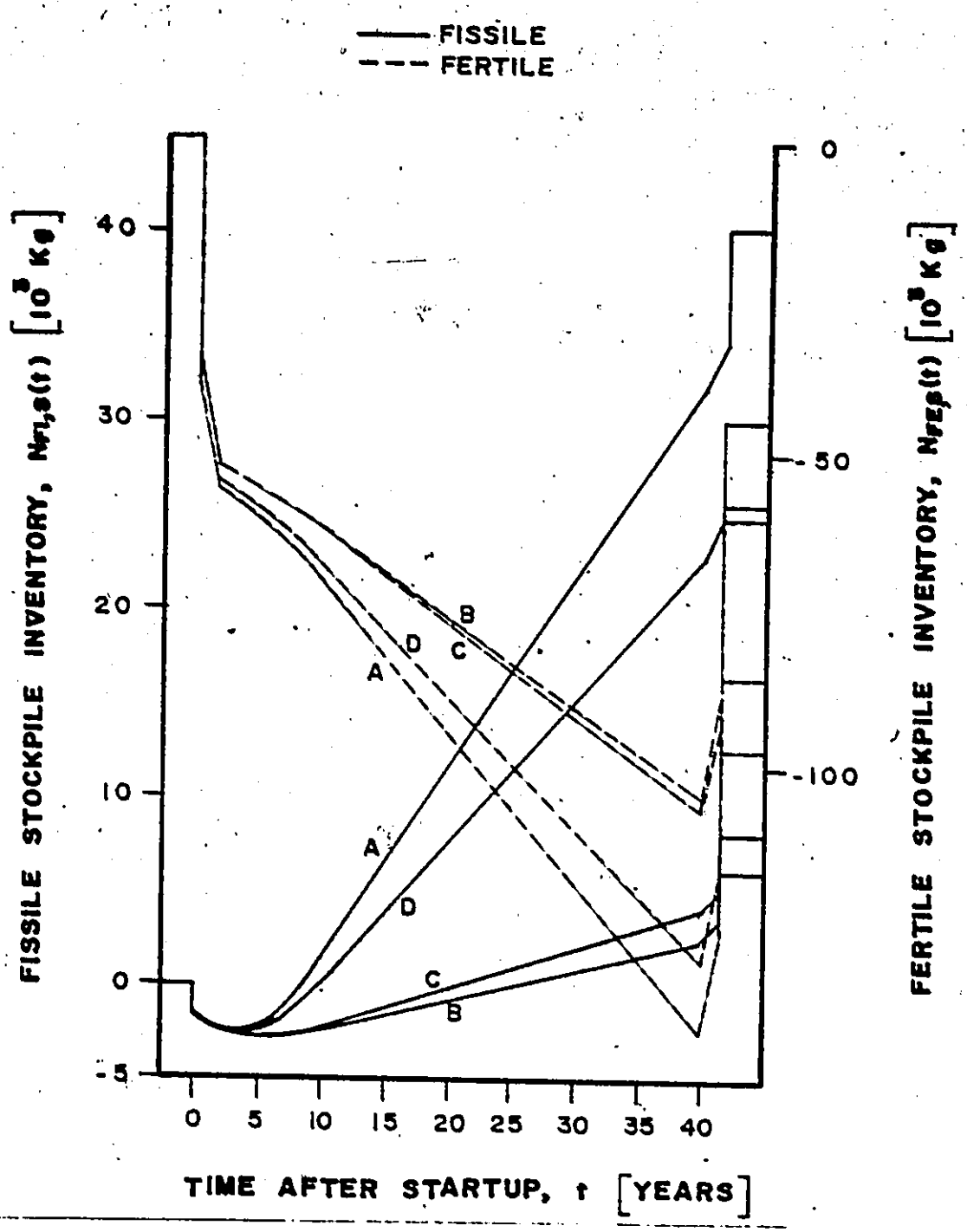

Fig. 5.3-5: Fissile and fertile stockpile inventories for the reference hybrid reactor system in four operating modes described in the text.

breeder, in particular the value of Q_B^T, is important not only to electrical power production but also to fissile fuel production. The total amplification factor defined by Eq(3.4-6) is related to the plasma amplification factor by Eq(5.1-2). This equation can be rewritten in terms of the fusion breeder blanket energy multiplication factor M so that for a DT fusion reactor,

$$Q_B^T = Q_B^P(0.20 + 0.80M) + \alpha_B \ . \qquad (5.4\text{-}1)$$

The value of Q_B^T not only fixes the ratio of breeder thermal power to the characteristic reaction rate,

$$P_B^T = \frac{Q_B^T}{(Q_B^T - \alpha_B)} U_B R_B \ , \qquad (5.4\text{-}2)$$

but also the value of the circulating energy fraction,

$$\varepsilon_B = (Q_B^T \eta_B^T \eta_B^I)^{-1} \ . \qquad (5.4\text{-}3)$$

The effects of varying Q_B^T and M will be investigated in the following.

In Fig. 5.4-1, the circulating energy fraction and the total amplification factor are shown as a function of M for two values of $(\eta_B^T \eta_B^I)$: 0.18 and 0.36. For the fusion breeders considered in Section 5.1, the value of $(\eta_B^T \eta_B^I)$ was 0.18 and the latter value is an optimistic one obtainable with $\eta_B^T = 0.40$ and $\eta_B^I = 0.90$. From Eq(5.4-1), the total amplification factor is a linearly increasing function of M, hence, from Eq(5.4-3), ε_B will decrease with increasing M. Clearly, the circulating energy fraction decreases as the efficiencies improve. Thus, increasing $(\eta_B^T \eta_B^I)$ from 0.18 to 0.36 lowers the value of M required for ε_B to be

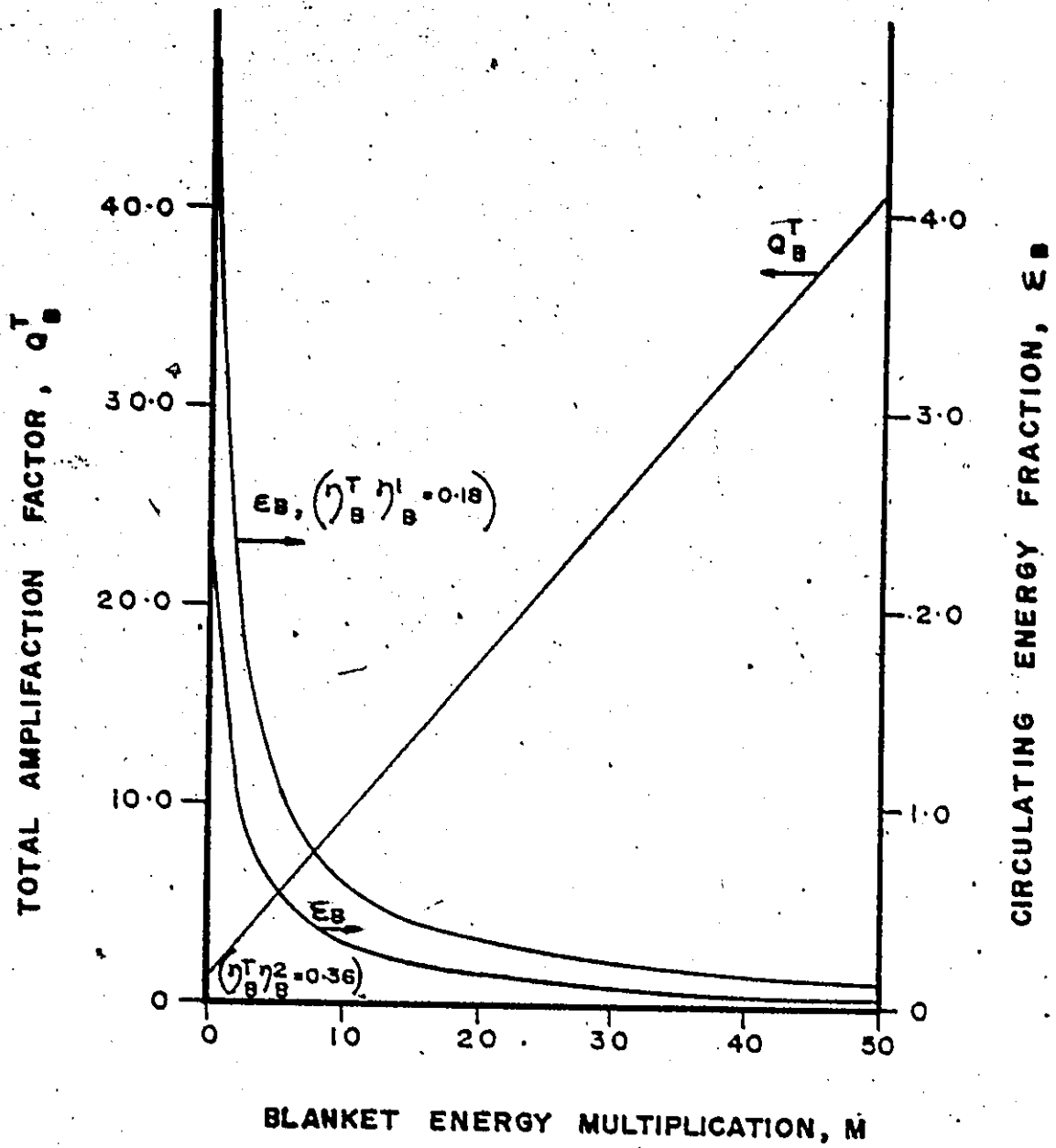

Fig. 5.4-1: Total amplification factor and circulating energy fraction as a function of blanket energy multiplication factor for a fusion breeder.

unity from 5.48 to 2.01. While such an increase would result in an improved power balance for the hybrid and symbiont, for a plasma amplification factor of 1.09, the symbiont with a blanket energy multiplication of 1.5 will require an efficiency product of 0.42 for $\varepsilon_B = 1.0$. From Eq(5.4-1) and Eq(5.4-3) we see that improving Q_B^T will also decrease the circulating energy fraction.

In Fig. 5.4-2, the nuclear efficiency is plotted as a function of the breeder thermal power of the hybrid and symbiotic systems. The nuclear efficiency is defined by Eq(3.4-20) and can be written as

$$\eta_S^N = \frac{P_C^{NET} + P_B^{NET}}{P_C^N + P_B^N} , \tag{5.4-4a}$$

$$= \frac{\{\eta_C^T(1-\varepsilon_C) + \eta_B^T(1-\varepsilon_B)P_B^T/P_C^T\}}{\{1 + (Q_B^T-\alpha_B)/Q_B^T \cdot P_B^T/P_C^T\}} , \tag{5.4-4b}$$

where we have used Eq(3.4-9) to relate P_B^T and P_B^N and Eq(4.1-1) for the fission converter reactor. At zero breeder thermal power, both curves meet at a value which gives the nuclear efficiency of the converter,

$$\eta_S^N = \eta_C^N(1-\varepsilon_C) = 0.38 . \tag{5.4-5}$$

The symbiont with $\varepsilon_B = 2.24$ has negative values of η_S^N as the breeder thermal power is increased. At a value of 2419 MW_t, η_S^N is zero, that is, neglecting processing, there is no net electrical output from the system. There is a limiting value of η_S^N as P_B^T increases to infinity. From Eq(5.4-4), we find

$$\eta_S^N \rightarrow \frac{\eta_B^T(1-\varepsilon_B)Q_B^T}{(Q_B^T-\alpha_B)} , \text{ as } P_B^T \rightarrow \infty . \tag{5.4-6}$$

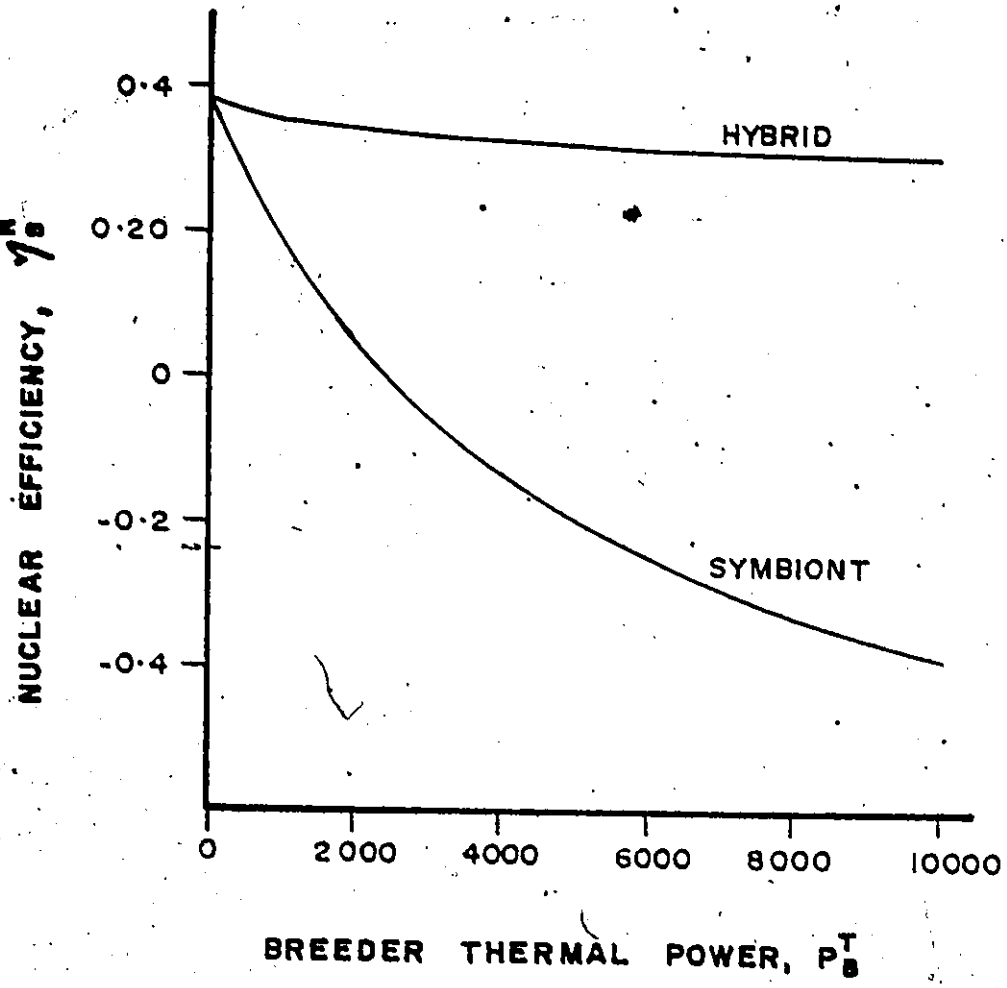

Fig. 5.4-2: Nuclear efficiency as a function of breeder thermal power for the hybrid and symbiotic fusion breeder systems.

For the symbiont, this limiting value is -0.764. Since ϵ_B is 0.30 for the hybrid, the nuclear efficiency remains positive; the limiting value being 0.280.

From this, we can see that; aside from fissile fuel production, the symbiont differs from the hybrid in its power balance. A distinguishing feature of the symbiotic system is a small, or negative, net power output since the fusion breeder will be driven by the converter produced power. The hybrid, in contrast, with its large energy multiplication factor, makes a positive contribution to the net electrical output of the system.

CHAPTER VI

SPALLATION BREEDER

The final type of breeder we shall consider is the spallation breeder. A spallation breeder produces fissile fuel and heat in a target-blanket as a result of the bombardment by high energy ions. This type of breeder has the advantage of producing fissile material without the added complexities of maintaining criticality, as in a fast-fission breeder, or of maintaining a fusioning plasma, as in a fusion breeder. It is for these reasons, as well as the anticipated high fissile fuel production rate possible, that this concept has received revived attention[6,16,17,18]. Following the pattern set in the previous two chapters, the effects of alternate breeder powers will be discussed in Section 6.3. Finally, the spallation system power balance will be discussed including the effect of the incident proton energy.

6.1 Reference System

The method proposed for producing fissile material using neutrons generated by high energy proton collisions, that is, the spallation breeder, has been outlined in Section 2.4. As a reference system, a design by Mynatt et al[16] for a gas-cooled, thorium fuelled target-blanket will be considered since such a device would couple well with the reference converter reactor. This reference reactor, described in Section 4.1, is a thorium fuelled HTGR. The breeder component of the

system consists of a proton linear accelerator which will produce a current of 1000 MeV protons and the target-blanket. The accelerator efficiency is 50%, a value projected by ORNL[16] and AECL[18] for near-term spallation breeders.

The combined target-blanket is modelled after the proposed GCFR set forth in Section 2.1, that is, a pressurized helium cooled, thorium-uranium fuelled arrangement with stainless steel structure. Moderating material is kept to a minimum to ensure a hard neutron spectrum in the blanket. With 1% fissile enrichment, the specific inventory of fissile material is expected to be 0.60 kg/MW_t and of fertile material, 59.8 kg/MW_t. Although $\omega_{FI,BB}$ is comparable to 0.50 kg/MW_t for the HTGR, the value of $\omega_{FE,BB}$ is 5.4 times larger than that for the reference converter. This is due to the combination of large inventory needed to reduce the average power density and to the low power production in the thorium blanket. This blanket is expected to produce a net 44.8 fissile atoms per incident proton or, from Fig. 2.4-1 or Eq(2.4-1), each neutron released would produce 0.99 fissile atoms. This compares favourably with the projected value of one fissile nucleus per neutron estimated by Tunnicliffe et al[18] although Eq(2.4-1) is applicable to a natural uranium target rather than thorium. In assessing the value of $G_{FE,BB}$, it was assumed that approximately one third more fertile atoms were destroyed by fast-fission and spallation reactions than fissile atoms produced, hence $G_{FE,BB}$ will be -59.7. The energy released per characteristic reaction, U_B, is calculated to be 2496 MeV for this thorium blanket; 96% of the value for uranium from Eq(2.4-4). Fuel would remain in the blanket for 242 full power days or 0.88 years if a 75% load

factor is assumed.

The energy released in the target-blanket is recovered with a thermal efficiency of 38%, the same as the fusion breeder value. The ORNL spallation breeder has a calculated total amplification factor of 2.5 so that using Eq(3.4-11), the circulating energy fraction, ε_B, will be 2.1. Since this value exceeds unity, the spallation breeder proposed here will be a net consumer of electrical energy. The value of U_B includes the incident proton energy hence the value of α_B will be zero.

The balance of the system is the same as described in Section 4.1: a HTGR converter reactor described in Table 4.1-1 combined with the reprocessing-fabrication plant described in Table 4.1-3. Since, for this concept, the core and blanket are combined, no core parameters will be required. The parameters for the spallation breeder blanket are listed in Table 6.1-1.

6.2 Characteristics of the Reference System

Following the pattern set in Chapter IV and Chapter V, the characteristics of the fissile and fertile inventories will be investigated for the reference spallation breeder. In this section, a breeder thermal power of 3000 MW_t is used to calculate the inventories of interest. By convention, as explained in Section 3.3, both inventories are set to zero prior to the initial loading.

The fissile and fertile inventories, shown in Fig. 6.2-1, are calculated using the following:

Parameter	Value
Fissile Net Generation Ratio, $G_{FI,BB}$	44.8
Fertile Net Generation Ratio, $G_{FE,BB}$	-59.7
Fissile Specific Inventory, $\omega_{FI,BB}$	0.60 kg/MW$_t$
Fertile Specific Inventory, $\omega_{FE,BB}$	59.8 kg/MW$_t$
Fuel mean Discharge Period, τ^D_{BB}	0.884 yr
Energy Released per Characteristic Reaction, U_B	2496 MeV
Thermal-Electric Conversion Efficiency, η^T_B	0.38
Injector Efficiency, η^I_B	0.50
Circulating Energy Fraction, ϵ_B	2.10
Total Amplification Factor, Q^T_B	2.50
Fraction of Injected Energy Recovered, α_B	0.0
Load Factor, LF_B	0.75

Table 6.1-1: Reference spallation breeder data necessary for this analysis.

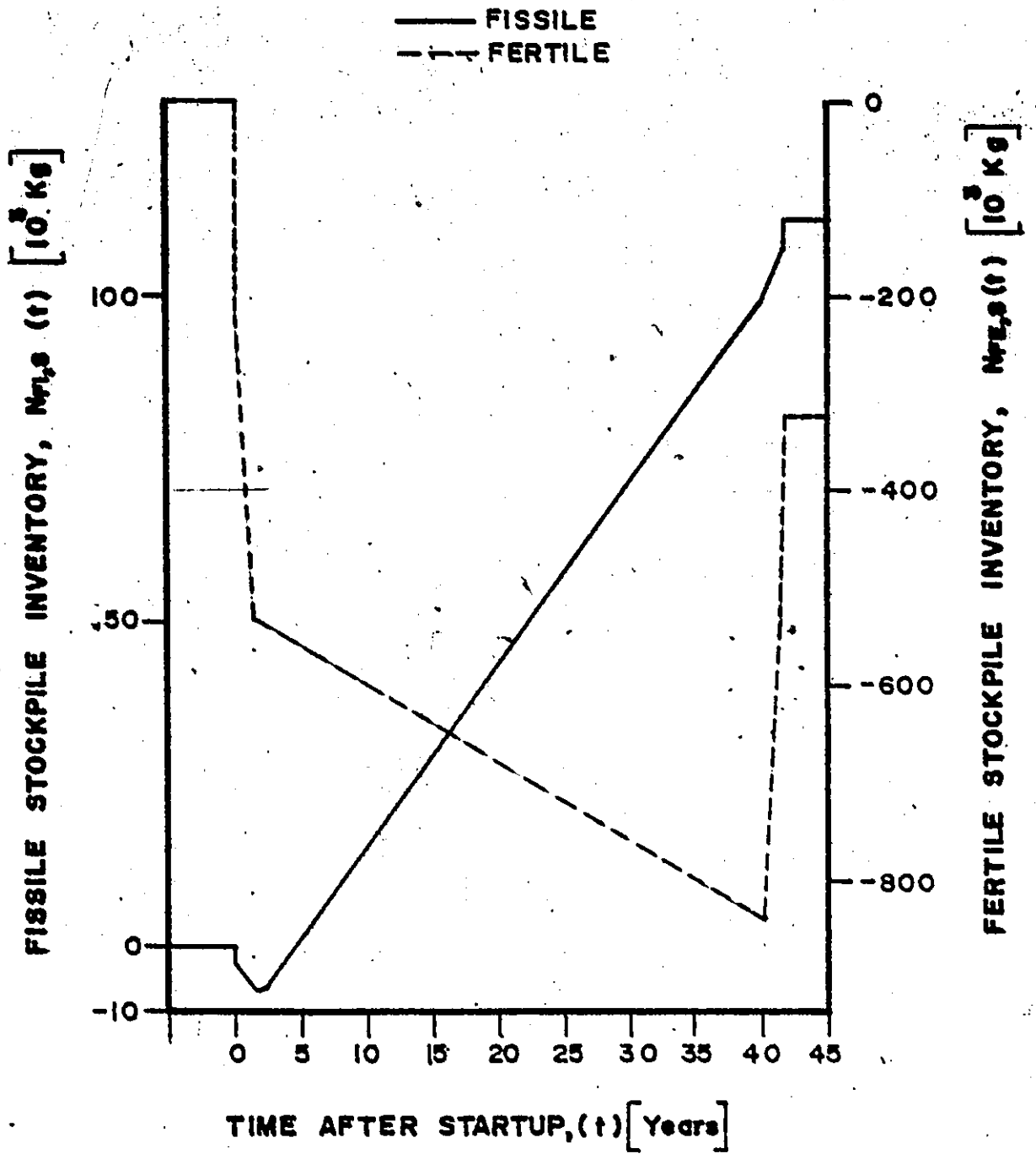

Fig. 6.2-1: Fissile and fertile stockpile inventories for the reference spallation breeder system with P_B^T = 3000 MWt.

$$N_{M,S}(t) = -[\omega_{M,C}R_C + \omega_{M,BB}R_B]H(t)$$
$$+\int_0^t [D_{M,C}(t')R_C + D_{M,BB}(t')R_B]dt'$$
$$+[(\omega_{M,C} + 1/2\tau_C^D G_{M,C})(1-\ell_M)R_C$$
$$+(\omega_{M,BB} + 1/2\tau_{BB}^D G_{M,BB})(1-\ell_M)R_B]H(t-\tau^{EOL}-\tau_M^R). \quad (6.2\text{-}1)$$

The converter reactor rate of change function, $D_{M,C}(t)$, will be found using

$$D_{M,C}(t) = \begin{cases} 0, \ t\leq 0 , & (6.2\text{-}2a) \\ -\omega_{M,C}/\tau_C^D, \ 0<t\leq\tau_M^R , & (6.2\text{-}2b) \\ -\omega_{M,C}/\tau_C^D\ell_M + G_{M,C}(1-\ell_M), \ \tau_M^R<t\leq\tau^{EOL} , & (6.2\text{-}2c) \\ (\omega_{M,C}/\tau_C^D + G_{M,C})(1-\ell_M), \ \tau^{EOL}<t<\tau^{EOL}+\tau_M^R , & (6.2\text{-}2d) \\ 0, \ t>\tau^{EOL}+\tau_M^R , & (6.2\text{-}2e) \end{cases}$$

while for the spallation breeder blanket,

$$D_{M,BB}(t) = \begin{cases} 0, \ t\leq 0, & (6.2\text{-}3a) \\ -\omega_{M,BB}/\tau_{BB}^D, \ 0<t\leq\tau_M^R, & (6.2\text{-}3b) \\ -\omega_{M,BB}/\tau_{BB}^D\ell_M + G_{M,BB}(t-\tau_M^R)/\tau_{BB}^D(1-\ell_M), & (6.2\text{-}3c) \\ \qquad \tau_M^R<t\leq\tau_M^R+\tau_{BB}^D , & \\ -\omega_{M,BB}/\tau_{BB}^D\ell_M + G_{M,BB}(1-\ell_M), & (6.2\text{-}3d) \\ \qquad \tau_M^R+\tau_{BB}^D<t\leq\tau^{EOL}, & \\ (\omega_{M,BB}/\tau_{BB}^D + G_{M,BB})(1-\ell_M) , & (6.2\text{-}3e) \\ \qquad \tau^{EOL}<t\leq\tau^{EOL}+\tau_M^R , & \\ 0, \ t>\tau^{EOL} + \tau_M^R . & (6.2\text{-}3f) \end{cases}$$

The initial fissile inventory, $N_{FI,S}(0^+)$, will be loaded into both the converter core and the spallation breeder blanket,

$$N_{FI,S}(0^+) = -(\omega_{FI,C}R_C + \omega_{FI,BB}R_B) , \qquad (6.2\text{-}4a)$$

$$= -3.3 \times 10^3 \text{ kg.} \qquad (6.2\text{-}4b)$$

Because the spallation breeder requires 45% less fissile fuel than the fast-fission breeder, the spallation breeder system loading is 70% of the fast-fission breeder. In contrast, the initial fertile inventory of the spallation system,

$$N_{FE,S}(0^+) = -(\omega_{FE,C}R_C + \omega_{FE,BB}R_B) , \qquad (6.2\text{-}5a)$$

$$= -2.12 \times 10^5 \text{ kg} , \qquad (6.2\text{-}5b)$$

is 2.5 times that of the reference fast-fission breeder system. This is due to the large fertile inventory necessary for the target-blanket.

For the time between $t=0^+$ and $t=\tau^R_{FI}$, the fissile and fertile inventories decrease linearly. The fissile inventory rate of change is given by

$$\frac{dN_{FI,S}(t)}{dt} = \frac{\omega_{FI,C}}{\tau^D_C} R_C + \frac{\omega_{FI,BB}}{\tau^D_{BB}} R_B , \quad 0<t\leq\tau^R_{FI} , \qquad (6.2\text{-}6a)$$

$$= -2.5 \times 10^3 \text{ kg/yr} . \qquad (6.2\text{-}6b)$$

This rate of decrease is 56% greater than that of the fast-fission breeder system given by Eq(4.2-7) even though the fissile specific inventory of the spallation blanket is less than that for the fast-fission breeder. As discussed in Section 4.4, the reason for the greater rate of decrease is

the short mean residence period in the spallation breeder blanket. Thus, while requiring 45% less fissile material at each loading, the spallation blanket is refuelled 3.4 times more often than the reference fast-fission breeder. The combination of a large fertile inventory and short mean discharge period results in a very steep initial decrease for the fertile inventory,

$$\frac{dN_{FE,S}(t)}{dt} = -\frac{\omega_{FE,C}}{\tau_B^D} R_C + \frac{\omega_{FE,BB}}{\tau_{BB}^D} R_B \quad , \; 0<t\leq\tau_{FE}^R \; , \tag{6.2-7a}$$

$$= -2.1 \times 10^5 \text{ kg/yr} \; . \tag{6.2-7b}$$

This is 12 times the rate of decrease for the fast-fission breeder system.

Because τ_{BB}^D is short, steady-state is reached after only 2.4 years. The minimum value of the fissile inventory occurs after 1.57 years or one month after processed fissile material begins to reach the stockpile inventory. The time to reach the minimum fissile inventory is calculated from

$$\tau_{FI}^{MIN} = \tau_{FI}^R + \{(\omega_{FI,C}/\tau_C^D R_C + \omega_{FI,BB}/\tau_{BB}^D R_B)\ell_{FI} \tag{6.2-8}$$

$$-G_{FI,C}R_C(1-\ell_{FI})\}\{G_{FI,BB}R_B(1-\ell_{FI})/\tau_{BB}^D\}^{-1} \; .$$

If terms in the order of ℓ_{FI} are neglected, the difference between $(\tau_{FI}^{MIN})_{SP}$, the time to reach the minimum fissile inventory for the spallation breeder system, and $(\tau_{FI}^{MIN})_{FF}$, the time for the fast-fission breeder system, can be related by

$$\frac{(\tau_{FI}^{MIN}-\tau_{FI}^{R})_{SP}}{(\tau_{FI}^{MIN}-\tau_{FI}^{R})_{FF}} \simeq \frac{(\tau_{BB}^{D})_{SP}}{(\tau_{BB}^{D})_{FF}} \frac{(G_{FI,BB})_{FF}}{(G_{FI,BB})_{SP}} \frac{(U_B)_{SP}}{(U_B)_{FF}} , \qquad (6.2\text{-}9a)$$

$$= 0.020 . \qquad (6.2\text{-}9b)$$

Using the data in Table 4.1-2 and Table 6.1-1, the ratios on the right hand side of Eq(6.2-9a) will be

$$(\tau_{BB}^{D})_{SP}/(\tau_{BB}^{D})_{FF} = 0.147 , \qquad (6.2\text{-}10a)$$

$$(G_{FI,BB})_{FF}/(G_{FI,BB})_{SP} = 0.013 , \qquad (6.2\text{-}10b)$$

and

$$(U_B)_{SP}/(U_B)_{FF} = 15.2 . \qquad (6.2\text{-}10c)$$

Combining these, the right hand side of Eq(6.2-9a) yields 0.029; the difference is due to neglecting the fuelling of the breeders. The value of $N_{FI,S}(\tau_{FI}^{MIN})$ is -7.1×10^3 kg, 8% less than that of the fast-fission breeder system. Although τ_{FI}^{MIN} is much shorter for the spallation system, the increased refuelling rate produces a minimum nearly as deep as that for the fast-fission system.

The fissile fuel replacement time for the reference spallation system occurs during the steady-state period. Using Eq(3.3-42), the value of τ_{FI}^{0} is found to be 4.52 years, 12% of the value obtained for the reference fast-fission breeder system. The fertile inventory at the fissile replacement time is -5.6×10^5 kg. At steady-state, the rate of change of the fissile and fertile inventories is given by

$$\left(\frac{dN_{M,S}}{dt}\right)_{SS} = -\left[\frac{\omega_{M,C}}{\tau_C^D} R_C + \frac{\omega_{M,BB}}{\tau_{BB}^D} R_B\right] \ell_M + (G_{M,C}R_C + G_{M,BB}R_{BB})(1-\ell_M) \quad (6.2\text{-}11)$$

For the fissile inventory, this steady-state rate of change is 2.8×10^3 kg/year or 11.7 times that of the fast-fission system and for the fertile inventory, -8.0×10^3 kg/year, 3.1 times greater than the fast-fission system. The minimum fertile inventory, $N_{FE,S}(\tau^{EOL})$, is -8.4×10^5 kg. After the final core and blanket have been processed and added to the stockpile, $N_{FI,S}(\tau_S^{EOL})$ is 1.1×10^5 kg and $N_{FE,S}(\tau_S^{EOL})$ is 3.3×10^5 kg. Here, the spallation breeder system has produced 12.3 times as much fissile fuel as the reference fast-fission breeder system while consuming only 3.0 times as much fertile material. Clearly, the spallation breeder concept conserves resources more efficiently than the fission breeder.

In Section 6.1, the value of the circulating energy fraction was found to be 2.10. Since this value exceeds unity, the spallation breeder proposed here will be a consumer of electrical power. For a breeder thermal power of 3000 MW_t, the net electrical demand of the breeder will be

$$P_B^{NET} = \eta_B^T(1-\epsilon_B)P_B^T = -1228 \text{ MW}_e . \quad (6.2\text{-}12)$$

The converter reactor produces 1140 MW_e, hence there is a deficit of -88 MW_e. If the steady-state processing energy requirements are included, the deficit increases to 90 MW_e. The nuclear efficiency, η_S^N, calculated by Eq(3.4-20) is -1.47% and the net efficiency at steady-state is -1.50%. The spallation breeder characteristic reaction rate, R_B, will be related

to the thermal power by

$$R_B = P_B^T/U_B \ , \qquad (6.2\text{-}13)$$

since α_B is zero. A convenient measure of this characteristic reaction rate and hence breeder size is the proton current. Using Eq(3.1-20), we find

$$I_B = q_p \ P_B^T/U_B \ . \qquad (6.2\text{-}14)$$

For this reference spallation breeder, I_B is 1.2 A, four times the size of the accelerator projected in Section 2.4.

In this section, we have found that the fissile and fertile inventories of the spallation breeder system follow the same trends as the previous breeder systems studied. Also, by comparing the spallation system with the fast-fission system, the effects of varying the system parameters discussed in Section 4.4 were confirmed. For this spallation system, the three major parameter changes from the fast-fission system are: the short blanket mean discharge period, the large fissile and fertile net generation ratios and the high value of the energy released per characteristic reaction. Although the energy released is large, the spallation breeder is a consumer of electrical energy. This poor power balance is offset, however, by the system's efficient use of resources and large fissile fuel production rate.

6.3 Alternate Operating Modes

Since the 3000 MW_t spallation breeder investigated in the previous section is four times the size projected for future use[16,18], it

is important to know how the system will scale with size. In this section, the variation of some system characteristics with breeder thermal power or proton current will be discussed. Following the example set in the previous two chapters, the six inventory characteristics investigated and shown in Fig. 6.3-1 are: the initial and end-of-system-life fissile and fertile inventories, the minimum fissile inventory and the fertile inventory at the fissile replacement time.

As discussed previously, the initial and final inventories will be linear functions of R_B. Using Eq(6.2-13) and Eq(6.2-14), we find any characteristic which is a linear function of R_B will also be a linear function of P_B^T and I_B. For the initial inventories, the rate of change with breeder power will be

$$\partial N_{FI,S}(0^+)/\partial P_B^T = -0.6 \text{ kg/MW}_t \ ; \qquad (6.3\text{-}1)$$

for the fissile inventory and for the fertile inventory,

$$\partial N_{FE,S}(0^+)/\partial P_B^T = -59.8 \text{ kg/MW}_t \ . \qquad (6.3\text{-}2)$$

The end-of-system-life inventory gives the fissile surplus or fertile deficit which can be expected during the lifetime of the system. At τ_S^{EOL}, for the fissile inventory, we have

$$\partial N_{FI,S}(\tau_S^{EOL})/\partial P_B^T = 34.8 \text{ kg/MW}_t \ , \qquad (6.3\text{-}3)$$

compared with 6.0 kg/MW_t for the reference fast-fission breeder system and for the fertile inventory

$$\partial N_{FE,S}(\tau_S^{EOL})/\partial P_B^T = -82.9 \text{ kg/MW}_t \ . \qquad (6.3\text{-}4)$$

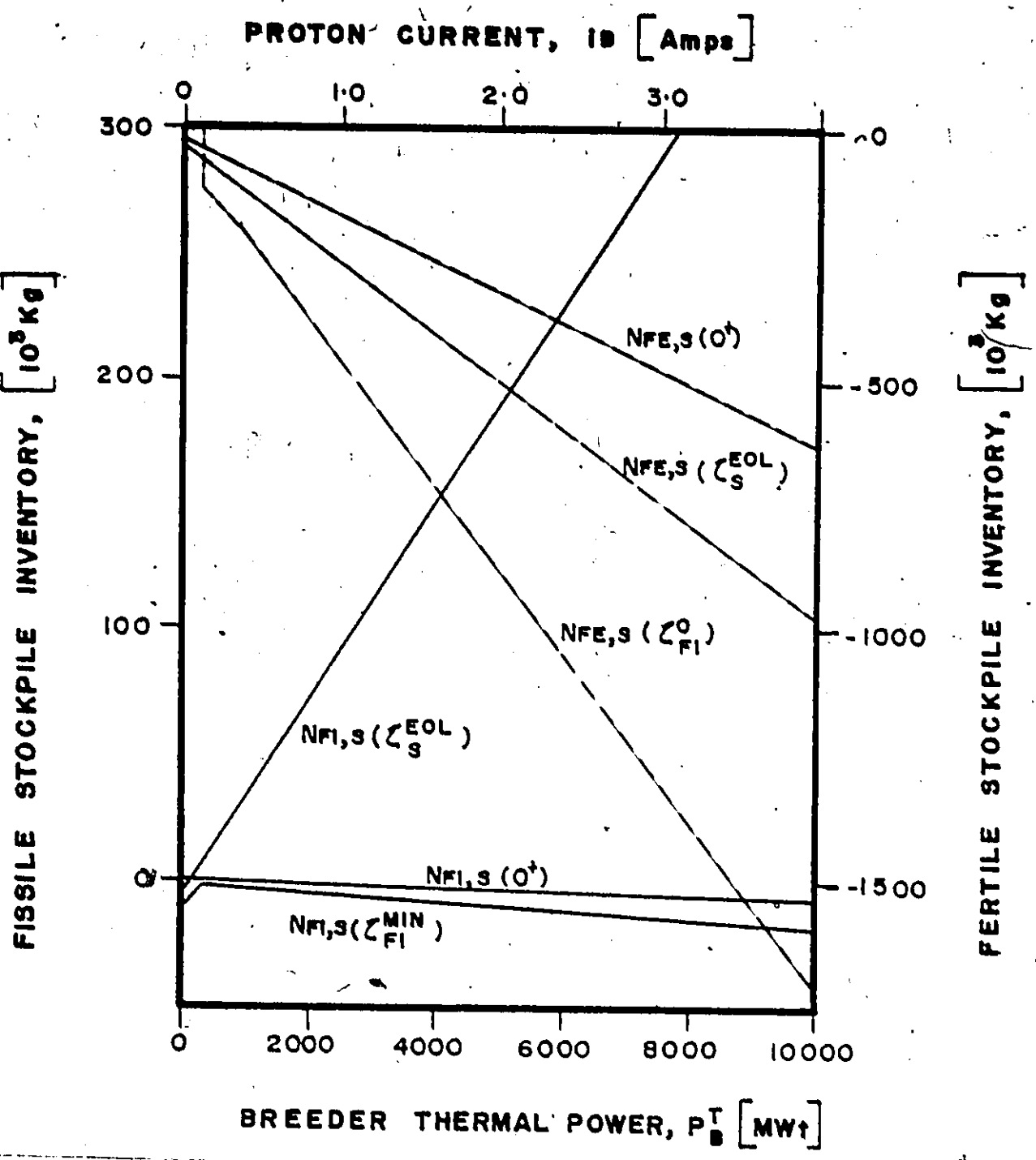

Fig. 6.3-1: Variation of some reference spallation breeder characteristics with breeder thermal power.

compared with -22.8 kg/MW_t for the reference fast-fission system. The large value of $(\partial N_{FI,S}(\tau_S^{EOL})/\partial P_B^T)$ is an incentive for operating at large breeder thermal powers. Using Eq(4.3-3), the size of the breeder which will produce no surplus at τ_S^{EOL} will be 214 MW_t. This is in contrast to the fast-fission system which required a breeder power of 1429 MW_t.

The minimum fissile inventory in Fig. 6.3-1 exhibits a sharp break in slope. From Eq(3.3-48), the minimum fissile replacement time is

$$(\tau_{FI}^O)_{MIN} = \tau_{FI}^R + \{\omega_{FI,BB}(1+\frac{\tau_{FI}^R}{\tau_{BB}^D}) + 1/2G_{FI,BB}(1-\ell_{FI})\tau_{BB}^D\}$$
$$x\{G_{FI,BB}(1-\ell_{FI})-\omega_{FI,BB}\ell_{FI}/\tau_{BB}^D\}^{-1} , \qquad (6.3\text{-}5a)$$

$$= 3.56 \text{ years} . \qquad (6.3\text{-}5b)$$

Since $(\tau_{FI}^O)_{MIN} > (\tau_{BB}^D + \tau_{FI}^R)$, the minimum fissile inventory will occur at the breeder thermal power which gives a zero steady-state rate of change, or, from Eq(3.3-37),

$$(R_B)_{FI}^{MIN} = R_C\left\{-\frac{\omega_{FI,C}}{\tau_C^D}\ell_{FI} + G_{FI,C}(1-\ell_{FI})\right\}$$
$$x\left\{\frac{\omega_{FI,BB}}{\tau_{BB}^D}\ell_{FI} + G_{FI,BB}(1-\ell_{FI})\right\}^{-1} . \qquad (6.3\text{-}6)$$

Evaluating this, we find that $N_{FI,S}(\tau_{FI}^{MIN})$ is minimized at a breeder thermal power of 206 MW_t or at a proton current of 83 mA. For breeder thermal powers less than this, τ_{FI}^{MIN} will occur at the end of the reactor life as seen in Fig. 6.3-2, hence $N_{FI,S}(\tau_{FI}^{MIN})$ will increase linearly to the minimum value. For P_B^T = 206 MW_t, Eq(6.2-8) is applicable and since τ_{FI}^{MIN} is a function of R_B, $N_{FI,S}(\tau_{FI}^{MIN})$ will be non-linear in P_B^T. The minimum inventory in this region is given by

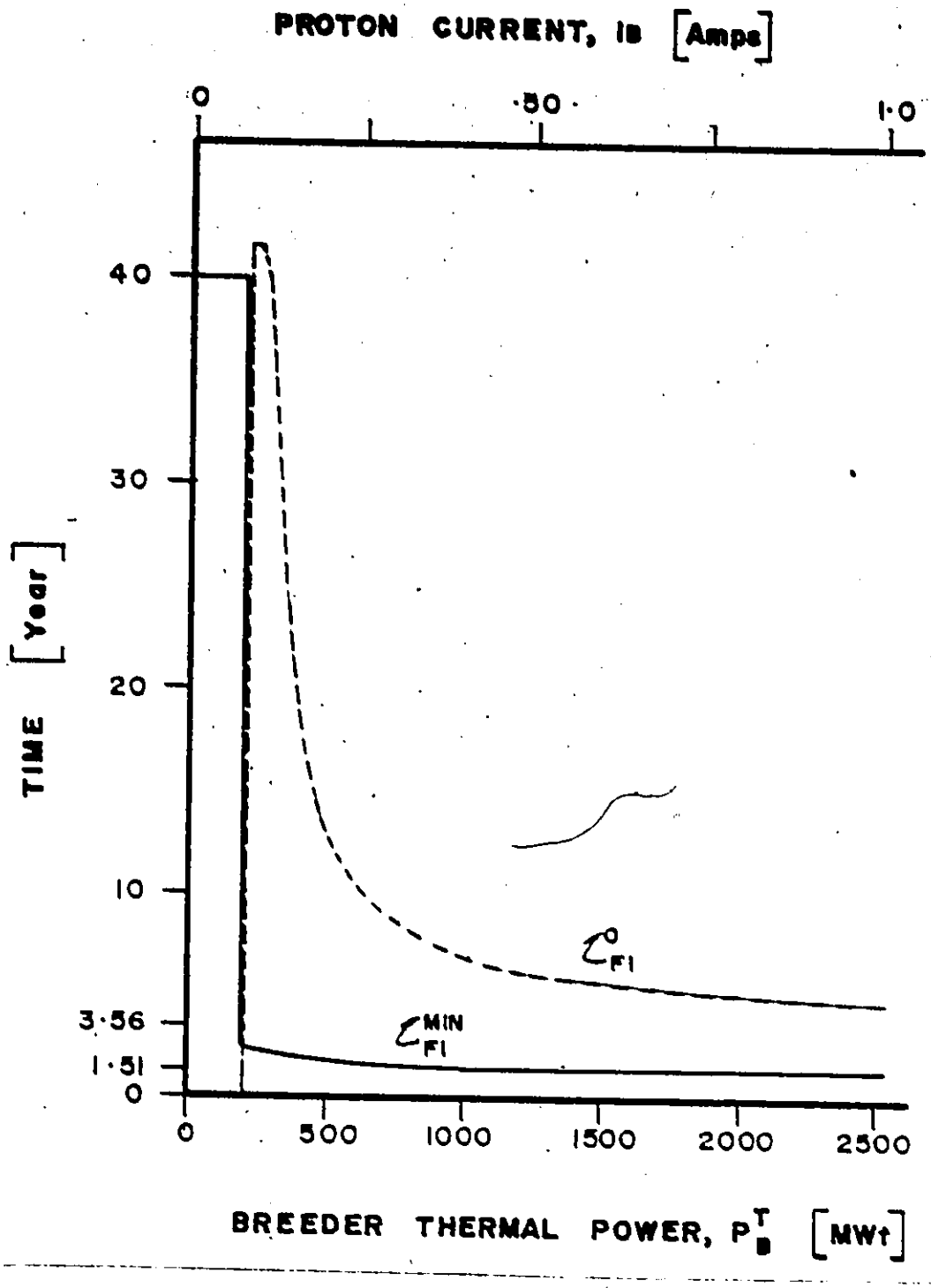

Fig. 6.3-2: Variation of the fissile replacement time and the time to reach minimum fissile inventory with breeder thermal power for the reference spallation breeder.

$$N_{FI,S}(\tau_{FI}^{MIN}) = -(\omega_{FI,C}R_C + \omega_{FI,BB}R_B)$$
$$-(\omega_{FI,C}/\tau_C^D R_C + \omega_{FI,BB}/\tau_{BB}^D R_B)\tau_{FI}^R$$
$$-1/2\tau_{BB}^D \left\{ \left(\frac{\omega_{FI,C}}{\tau_C^D} R_C + \frac{\omega_{FI,BB}}{\tau_{BB}^D} R_B \right) \ell_{FI} \right.$$
$$\left. -G_{FI,C}R_C(1-\ell_{FI}) \right\}^2 \left\{ G_{FI,BB}(1-\ell_{FI})R_B \right\}^{-1} , \qquad (6.3\text{-}7)$$
$$\tau_{FI}^R < \tau_{FI}^{MIN} \leq \tau_{BB}^D + \tau_{FI}^R .$$

In the last term on the right hand side of Eq(6.3-7), τ_{BB}^D is short and $G_{FI,BB}$ is large and as $R_B \to \infty$, Eq(6.3-7) will approach a linear function of R_B. Neglecting terms on the order of ℓ_{FI},

$$\partial N_{FI,S}(\tau_{FI}^{MIN})/\partial R_B \simeq -\omega_{FI,BB}(1+\tau_{FI}^R/\tau_{BB}^D), \; P_B^T >> 206 \text{ MW}_t . \qquad (6.3\text{-}8)$$

At $P_B^T = 3000$ MW_t, the value of $(\partial N_{FI,S}(\tau_{FI}^{MIN})/\partial P_B^T)$ is approximately -1.66 kg/MW_t while using Eq(6.3-8) we find -1.62 kg/MW_t.

The fertile inventory at the fissile replacement time for the spallation system as shown in Fig. 6.3-1 does not seem to exhibit the complexity displayed by the other three breeder systems: fast-fission in Fig. 4.3-1, symbiotic fusion in Fig. 5.2-3 or hybrid fusion in Fig. 5.3-3. This is because the fissile replacement time passes through the various regimes at much lower breeder thermal powers. Thus, as shown in Fig. 6.3-2, the value of P_B^T for a non-zero τ_{FI}^0 is 2.4 MW_t, for τ_{FI}^0 to be 41.5 years, 250 MW_t and for τ_{FI}^0 to be 40.0 years, P_B^T is 280 MW_t. These regimes are so close together that the detail in Fig. 6.3-1 is lost. The minimum fissile replacement time is given by Eq(6.3-5a) and was found to be 3.56 years.

In Fig. 6.3-3, the four operating modes of the spallation breeder are displayed for a converter thermal power of 3000 MW_t. These modes of operation are the same as were used for the previous breeder systems and are listed here for reference:

(A) $P_B^T = 3000\ MW_t$;

(B) $\tau_{FI}^O = 25.0$ years;

(C) $(dN_{FI,S}/dt)_{SS} = 210$ kg/year;

and (C) $N_{FI,S}(\tau_{FI}^{MIN})$ is minimized.

Some of the characteristics of these modes are listed in Table 6.3-1.

Operating Mode A, as we have found, corresponds to a proton current of 1.2 A. To find the breeder thermal power required for Mode B, Eq(3.3-24) is used or

$$P_B^T = U_B R_C \left\{ \omega_{FI,C}\left(1+\frac{\tau_{FI}^R}{\tau_C^D}\right) + \left[\frac{\omega_{FI,C}}{\tau_C^D}\ell_{FI} - G_{FI,C}(1-\ell_{FI})\right](\tau_{FI}^O - \tau_{FI}^R)\right\}$$

$$\times\left\{-\omega_{FI,BB}\left(1+\frac{\tau_{FI}^R}{\tau_{BB}^D}\right) + \left[\frac{\omega_{FI,BB}}{\tau_{BB}^D}\ell_{FI} + G_{FI,BB}(1-\ell_{FI})\right](\tau_{FI}^O - \tau_{FI}^R)\right\} - 1 \,,$$

$$\tau_{BB}^D + \tau_{FI}^R < \tau_{FI}^O \leq \tau^{EOL} \,, \qquad (6.3\text{-}9a)$$

$$= 331\ MW_t \,. \qquad (6.3\text{-}9b)$$

This value, which is 6% of the reference fast-fission breeder power required for the same mode of operation, corresponds to a proton current of 133 mA. For operating Mode C, Eq(3.3-25) is applicable which, for the reference spallation breeder system, becomes

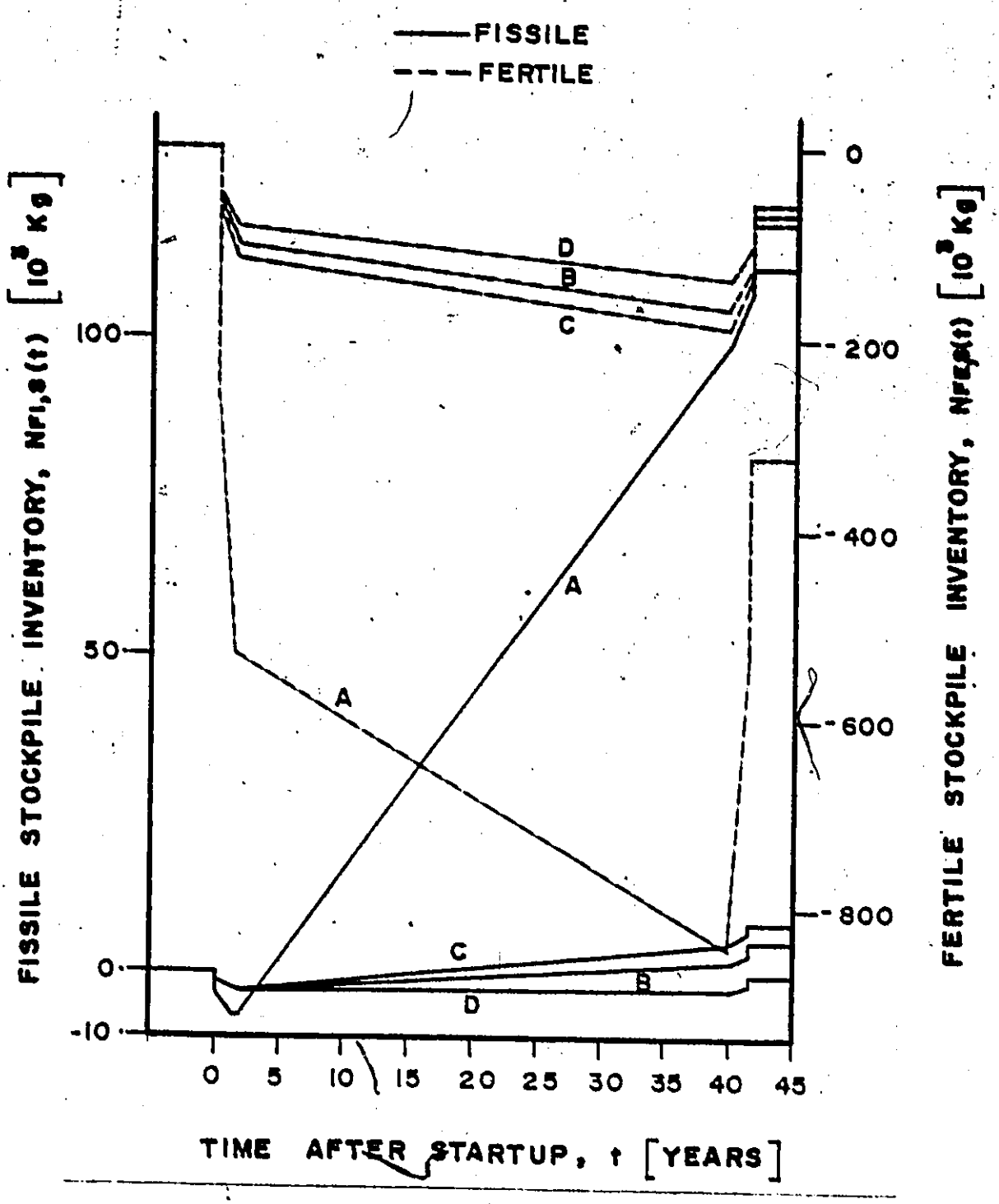

Fig. 6.3-3: Fissile and fertile inventories for the reference spallation breeder system in four operating modes described in the text.

Parameter	Case A	Case B	Case C	Case D
Breeder Thermal Power, P_B^T MW_t	3000	331	412	206
Initial Inventory, Fissile, $N_{FI,S}(0^+)$ 10^3 kg	-3.30	-1.70	-1.75	-1.62
Initial Inventory, Fertile, $N_{FE,S}(0^+)$ 10^3 kg	-212.	-52.8	-57.7	-45.3
Time to Reach Minimum, Fissile, τ_{FI}^{MIN} yr	1.57	2.05	1.95	40.0
Minimum Inventory, Fissile, $N_{FI,S}(\tau_{FI}^{MIN})$ 10^3 kg	-7.11	-2.84	-2.96	-2.68
Fissile Replacement Time, τ_{FI}^0, yr	4.52	25.0	16.5	--
Fertile Inventory at τ_{FI}^0, $N_{FE,S}(\tau_{FI}^0)$ 10^3 kg	-555.	-143.	-145.	--
Steady-State Change, Fissile, $(dN_{FI,S}/dt)_{SS}$ 10 kg/yr	2.80	0.12	0.21	0.0
Steady-State Change, Fertile, $(dN_{FE,S}/dt)_{SS}$ 10^3 kg/yr	-8.02	-1.74	-1.93	-1.44
Minimum Inventory, Fertile, $N_{FE,S}(\tau^{EOL})$ 10^3 kg	-840.	-170.	-190.	-138.
End-of-System-Life Inventory, Fissile, $N_{FI,S}(\tau_S^{EOL})$ 10^3 kg	111.	4.99	7.93	-0.32
End-of-System-Life Inventory, Fertile, $N_{FE,S}(\tau_S^{EOL})$ 10^3 kg	-325.	-71.4	-79.2	-59.6

Minimum Fissile Replacement Time, $(\tau_{FI}^0)_{MIN}$ = 3.56 yr.

Table 6.3-1: Some characteristics of the spallation breeder system in four operating modes. Values underlined have been used to fix P_B^T.

$$P_B^T = -2U_B\left\{\frac{\omega_{FI,C}\ell_{FI}}{\tau_C^D} + G_{FI,C}(1-\ell_{FI})\right\} \times\left\{\frac{\omega_{FI,BB}\,\ell_{FI}}{\tau_{BB}^D} + G_{FI,BB}(1-\ell_{FI})\right\}^{-1}, \qquad (6.3\text{-}10a)$$

$$= 412\ MW_t\ , \qquad (6.3\text{-}10b)$$

where Eq(4.3-16) has been used. The spallation breeder power required to operate in Mode C is 15% of that required for the reference fast-fission breeder and corresponds to a proton current of 165 mA. As discussed previously, for operating Mode D, a breeder thermal power of 206 MW_t or a proton current of 83 mA is required.

6.4 Spallation Breeder Power Balance

The system power balance will be important for calculating the revenues from the sale of electricity and the capital costs of the system. The total amplification factor will be related to the energy released per incident proton by

$$Q_B^T = U_B/E\ , \qquad (6.4\text{-}1)$$

where E is the energy of the incident protons. Since α_B is zero, P_B^T will be given by

$$P_B^T = R_B U_B\ , \qquad (6.4\text{-}2)$$

The circulating energy fraction, Eq(3.4-11), will also be a function of U_B,

$$\varepsilon_B = \frac{E}{U_B \eta_B^T \eta_B^I}\ , \qquad (6.4\text{-}4)$$

Clearly, U_B will be an important power balance parameter.

In Section 2.4, the following relation between incident proton energy and the total energy release was introduced for a uranium target:

$$U_B = 2.99(E - 130) \text{ MeV}, \quad 130 \text{ MeV} \leq E \leq 1000 \text{ MeV} . \tag{6.4-5}$$

This equation was found to hold to within 5% for the ORNL[16] blanket at 1000 MeV in Section 6.1. Using Eq(6.4-5), Eq(6.4-1) can be written as

$$Q_B^T = \frac{2.99U_B'}{U_B + 388.7} , \tag{6.4-6}$$

which, for the reference system, yields $Q_B^T = 2.59$ at $U_B = 2496$. This equation has been used in Fig. 6.4-1 to find Q_B^T, ε_B and I_B when P_B^T is 3000 MW_t. The total amplification factor and the circulating energy fraction are not very sensitive to changes in U_B: increasing U_B from 2000 MeV to 3000 MeV results in an increase in Q_B^T of 4% and a decrease in ε_B of 5%. The proton current required for a 3000 MW_t breeder power is, however, sensitive to changes in U_B; for a 50% increase in U_B, I_B is decreased by 41%.

The nuclear efficiency for the spallation system can be written as

$$\eta_S^N = \left\{ \eta_C^T(1-\varepsilon_C) + \eta_B^T(1-\varepsilon_B)\frac{P_B^T}{P_B^T} \right\} \left\{ 1+\frac{P_B^T}{P_C^T} \right\}^{-1} , \tag{6.4-7}$$

As with the fusion breeder system, there will be a limiting value of η_S^N as the breeder power increases. For the reference spallation system, this limit is -0.42 where

$$\eta_S^N \longrightarrow \eta_B^T(1-\varepsilon_B) \quad \text{as} \quad P_B^T \longrightarrow \infty , \tag{6.4-8}$$

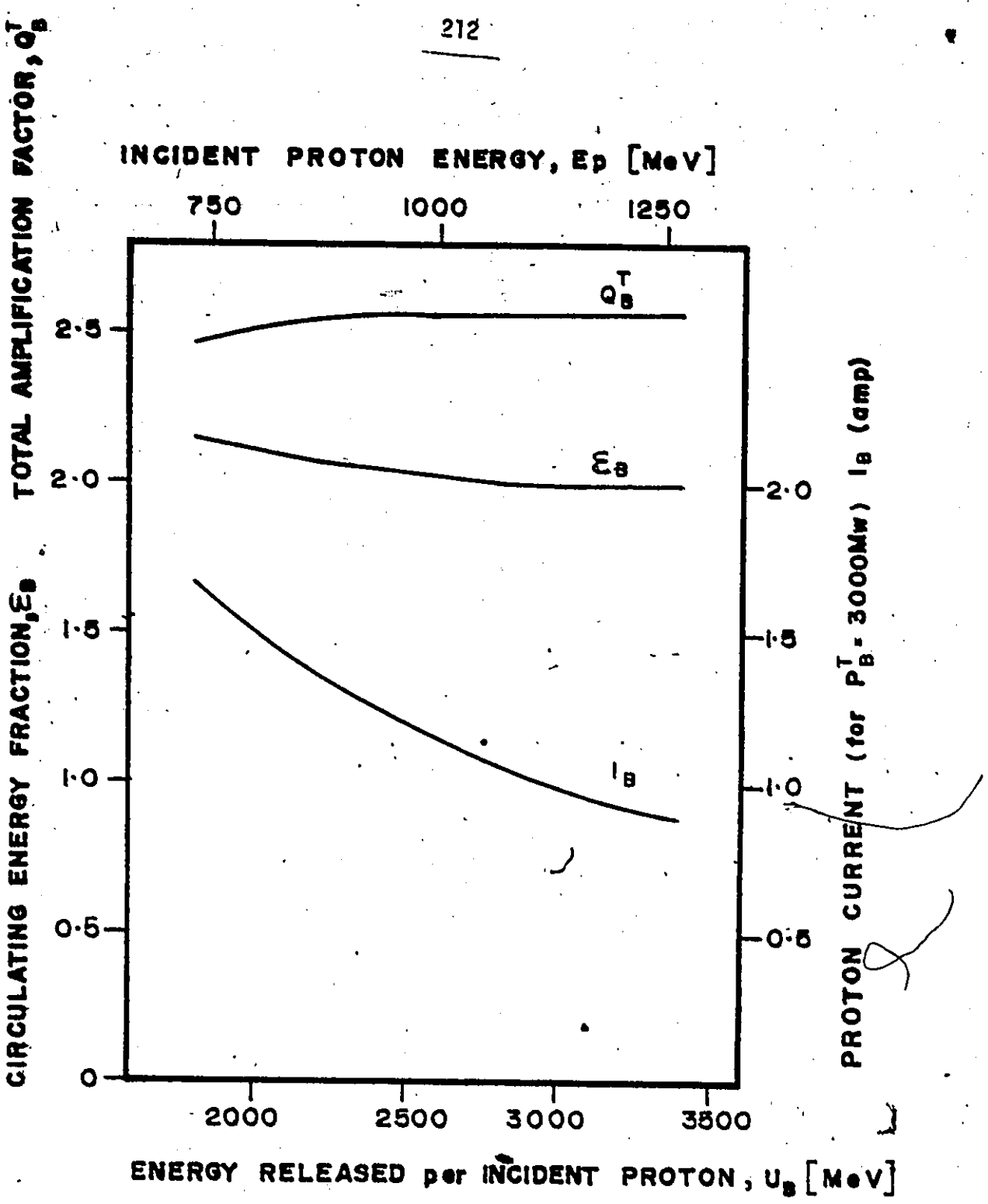

Fig. 6.4-1: Some power balance parameters as a function of energy released per incident proton for the equation assumed in text.

By setting η_S^N to zero in Eq(6.4-7), the breeder thermal power at which no net electrical power is produced is found to be 2727 MW_t. This corresponds to a proton current of 1.09 A. Thus, for breeder thermal powers less than 2727 MW_t, there will be a positive net electrical power output from the system.

CHAPTER VII

COMPARISON OF BREEDING SYSTEMS

One of the reasons advanced in Section 1.1 for introducing the system model developed here was to provide a uniform and consistent method of analysis for discussing breeding systems. In this chapter, the four reference breeder systems analysed above will be compared. First, these systems will be considered for the case where each has a breeder thermal power of 3000 MW_t. Following this, the operation of the four breeder systems in alternative operating modes will be discussed. Finally, a brief economic analysis will be presented in Section 7.3.

7.1 Reference Systems

There are many factors to consider when comparing breeders: costs, resource utilization and power production as well as fissile fuel production. In Table 7.1-1, some useful quantitative parameters for this purpose are listed. These include $N_{FI,S}(\tau_{FI}^{MIN})$, a measure of the fissile fuel investment required by the system, $N_{FE,S}(\tau^{EOL})$, an indicator of the lifetime fuelling costs, the steady-state rates of change, the fissile replacement time, the fissile fuel production in terms of $N_{FI,S}(\tau_S^{EOL})$, and the power produced or consumed. In addition, Fig. 7.1-1 shows the fissile stockpile inventory and Fig. 7.1-2, the fertile stockpile inventory for the four reference breeder systems. The HTGR converter reactor inventories are included in these figures for comparison.

Parameter	Breeder Type			
	Fast-Fission	Symbiotic	Hybrid	Spallation
Minimum Fissile Inventory, $N_{FI,S}(\tau_{FI}^{MIN})$ 10^3 kg	-7.71	-2.63	-2.68	-7.11
Minimum Fertile Inventory, $N_{FE,S}(\tau^{EOL})$ 10^3 kg	-219.	-155.	-143.	-840.
Steady-State Change, Fissile, $(dN_{FI,S}/dt)_{SS}$ 10^3 kg/yr	0.24	0.78	1.02	2.80
Steady-State Change, Fertile, $(dN_{FE,S}/dt)_{SS}$ 10^3 kg/yr	-2.63	-1.97	-2.39	-8.02
Fissile Replacement Time, τ_{FI}^{0} yr	38.3	15.0	8.72	4.52
End-of-System-Life Fissile Inventory, $N_{FI,S}(\tau_S^{EOL})$ 10^3 kg	9.07	30.8	40.6	111.
End-of-System-Life Fertile Inventory, $N_{FE,S}(\tau_S^{EOL})$ 10^3 kg	-109.	-80.9	-96.2	-325.
Net System Electrical Output Excluding Fuel Processing, P_S^{NET} MW_e	2280	-271	1941	-88
Nuclear Efficiency, η_S^N %	38.0	-5.58	33.2	-1.47
Specific Fissile Production, $N_{FI,S}(\tau_S^{EOL})/P_B^T$ 10^3 kg/MW_t	3.02	10.3	13.6	37.2
End-of-System-Life to Minimum Fissile Inventory Ratio, $\frac{N_{FI,S}(\tau_S^{EOL})}{\lvert N_{FI,S}(\tau_{FI}^{MIN})\rvert}$	1.18	11.7	15.2	15.7

Table 7.1-1: Reference breeder system data for a 3000 MW_t breeder.

Parameter	Breeder Type			
	Fast-Fission	Symbiotic	Hybrid	Spallation
Ratio of Fissile to Fertile End-of-System-Life Inventories, $\frac{N_{FI,S}(\tau_S^{EOL})}{\lvert N_{FE,S}(\tau_S^{EOL}) \rvert}$	0.08	0.38	0.42	0.34
Breeder to Converter Steady-State Change $\frac{(dN_{FI,S}/dt)_{SS,B}}{\lvert (dN_{FI,S}/dt)_{SS,C} \rvert}$	1.14	3.71	4.86	13.3
Breeder to Converter End-of-System Life Fissile Inventory Ratio $\frac{N_{FI,S}(\tau_S^{EOL})_B}{\lvert N_{FI,S}(\tau_S^{EOL})_C \rvert}$	0.89	3.02	3.99	10.9

Table 7.1-1: Reference breeder system data for a 3000 MW_t breeder (continued).

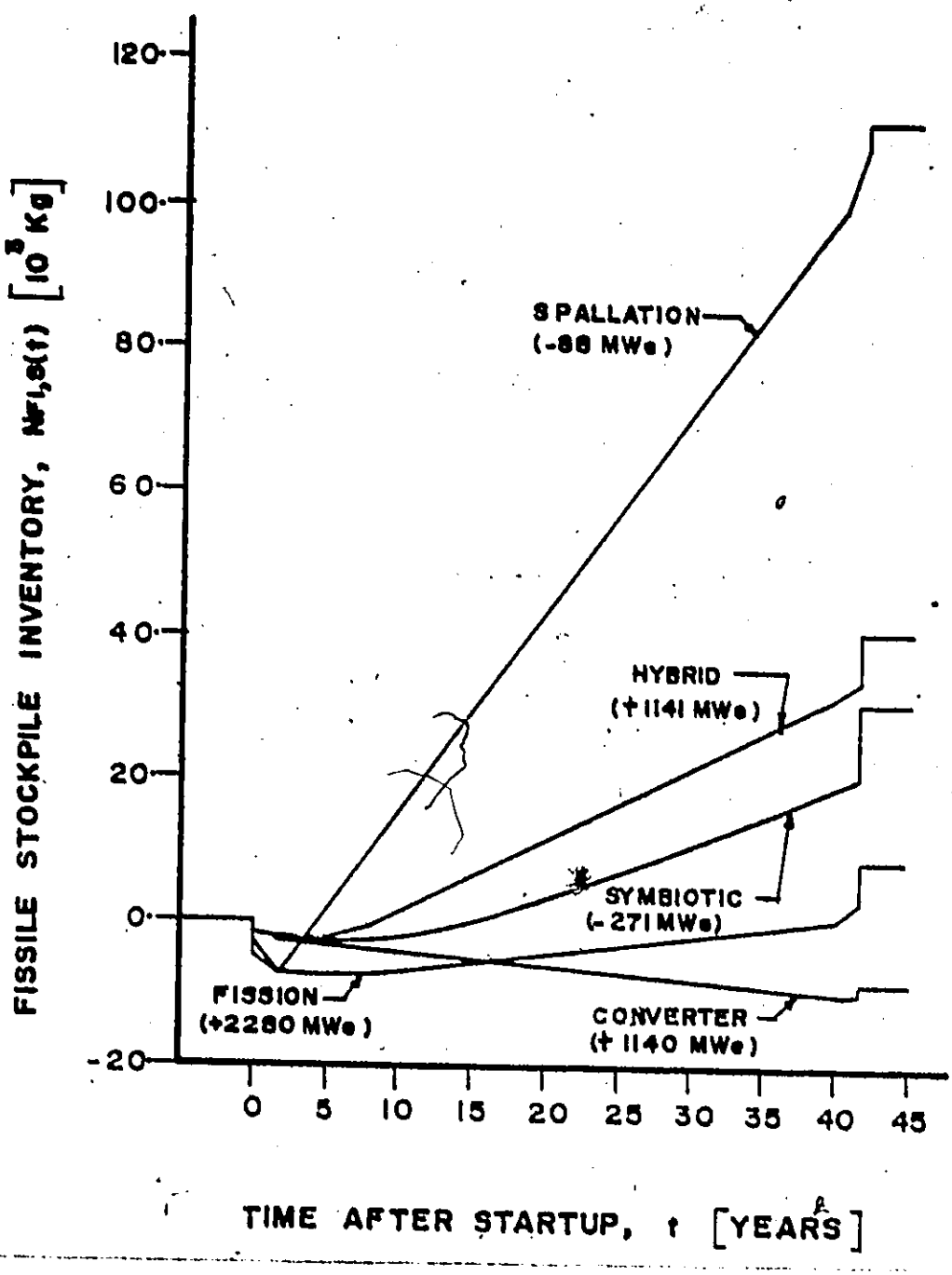

Fig. 7.1-1: Fissile stockpile inventory for the four reference breeder system with a thermal power and converter of 3000 MW_t. Number in brackets is the net power output of the system, P_S^{NET} neglecting processing.

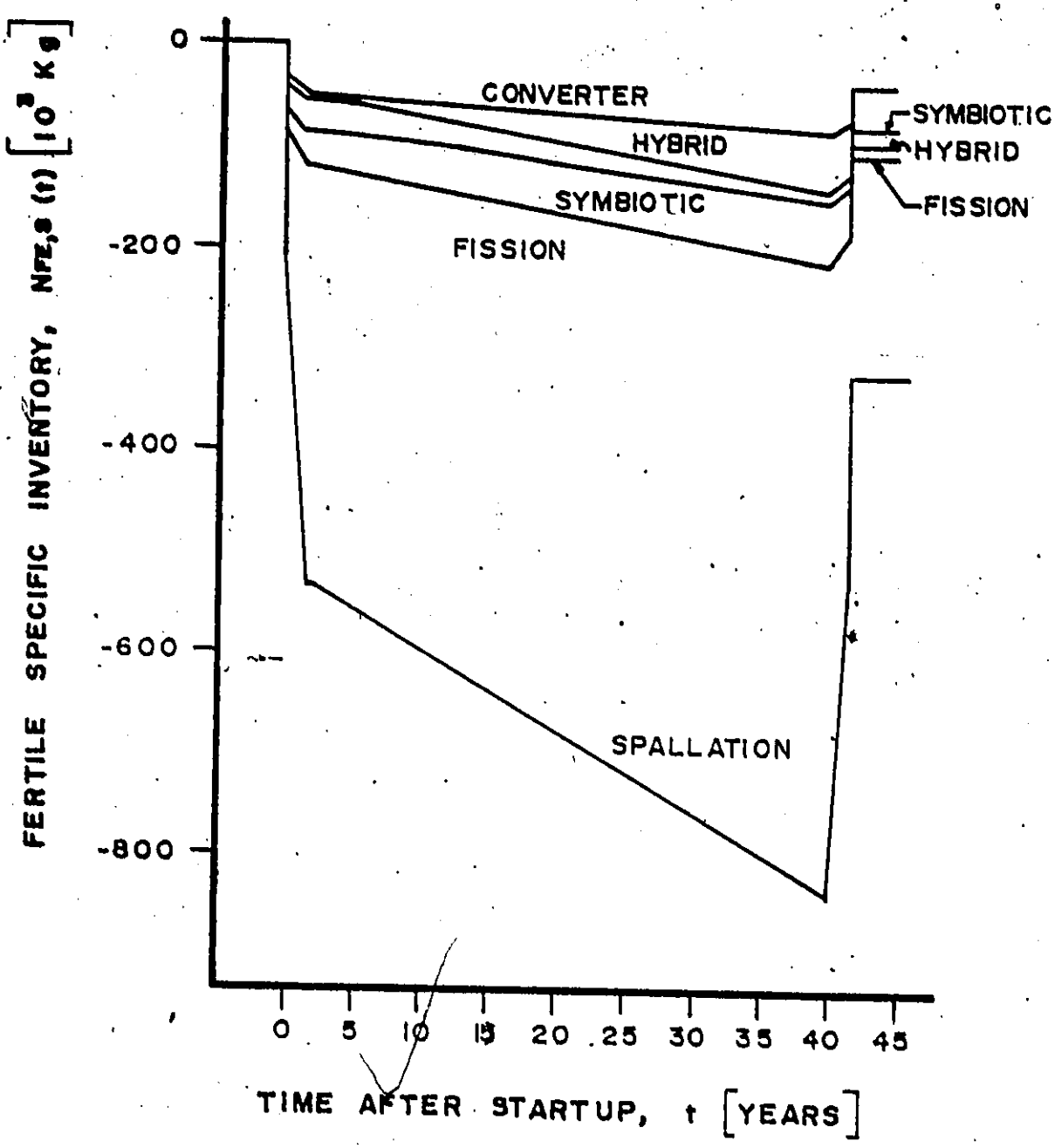

Fig. 7.1-2: Fertile stockpile inventory for the four breeders and the fission converter. The breeder and converter reactors have a thermal power of 3000 MWt.

Referring to Fig. 7.1-1, the end-of-system-life fissile inventories may be ranked in the following order: spallation, hybrid, symbiotic and fast-fission. There are several measures which can be used to assess fissile fuel production. The end-of-system-life inventory, $N_{FI,S}(\tau_S^{EOL})$, may be taken as an absolute value. The ratio of this to the minimum fissile inventory, $N_{FI,S}(\tau_{FI}^{MIN})$, will give the number of identical breeder systems which can be fuelled by the system. For the four reference breeder systems, it can be seen from Table 7.1-1 that the spallation breeder is the "best" using this criterion. The hybrid, however, because of its low minimum inventory is very close; only 3.3% less than the spallation system. Since all breeders have the same thermal power, the ratio of $N_{FI,S}(\tau_S^{EOL})$ to P_B^T preserves the relative ranking of $N_{FI,S}(\tau_S^{EOL})$ however the large value for the spallation breeder shows the incentive for using a large spallation system for fissile fuel production. Another measure of the lifetime fissile fuel production by a breeder system is the number of converters which can be fuelled. This is given by the ratio of $N_{FI,S}(\tau_S^{EOL})_B$ to $\left|N_{FI,S}(\tau^{EOL})\right|_C$. Here, the effectiveness of the spallation and fusion breeders for fissile fuel production is emphasized.

In Fig. 7.1-2, the fertile stockpile inventories are shown for the same systems. Here, the order of $N_{FE,S}(\tau^{EOL})$ is hybrid, symbiotic, fast-fission and spallation. This reflects the increasing value of $(\omega_{FE,BC} + \omega_{FE,BB})$ of the breeders: 1.61 kg/MW$_t$ for the hybrid, 11.76 kg/MW$_t$ for the symbiont, 17.3 kg/MW$_t$ for the fast-fission breeder and 59.8 kg/MW$_t$ for the spallation breeder. The amount of fertile fuel required by the breeder system, either $N_{FE,S}(\tau^{EOL})$ which must be

guaranteed, or $N_{FE,S}(\tau_S^{EOL})$ which is consumed over the life-time, is an indicator of the fuelling costs and resource utilization of the system. It is interesting to note that although more fertile fuel must be invested in the symbiotic than the hybrid fusion breeder, at the end-of-system-life, more fertile fuel is consumed in the hybrid. This can be attributed to the fact that, at final processing, the large fertile inventory of the symbiont is recovered while during operation the rate of decrease of the fertile inventory is less than that of the hybrid system. A measure of the overall breeding gain or resource utilization efficiency of the breeding system is the ratio of fissile to fertile end-of-system-life inventories. From Table 7.1-1, it can be seen that the hybrid outranks the others in this respect with a ratio of 0.42; the symbiotic and spallation systems with 0.38 and 0.34 come next followed by the fast-fission breeder with 0.08. The low value of the fast-fission system is due to the large amount of fertile and fissile material consumed by the breeder to maintain criticality.

The symbiotic system requires the least amount of fissile fuel of any of the four systems; 2.62 tonnes followed by the hybrid, spallation and fast-fission breeder systems. No fissile material is used in the symbiotic blanket hence the only requirement for fissile material is to fuel the converter reactor. The hybrid, although the blanket contains 4% fissile material, has a low value of R_B and this serves to decrease the fissile fuel demand. It might be expected that since $\omega_{FI,BC}$ for the fast-fission breeder is nearly twice the value of $\omega_{FI,BB}$ for the spallation breeder, the minimum would be twice as deep. However, the minimum value for the spallation system is 92% that of the fast-fission breeder system.

Since τ_{BB}^{D} for the fast-fission breeder is 3.4 times that of the spallation breeder, there is a rapid decrease in $N_{FI,S}(t)$ during the first τ_{FI}^{R} years which leads to a deep fissile minimum for the spallation system.

Recovery of a breeder system from the initial deficit can be measured by the steady-state rate of increase of the fissile inventory or the fissile replacement time. The order of the values of $(dN_{FI,S}/dt)_{SS}$ is the same as for $N_{FI,S}(\tau_S^{EOL})$. These steady-state rates of increase of the fissile inventory range from 2.8 tonnes/year for the spallation system to 0.24 tonnes/year for the fast-fission system. In terms of how many reference converter reactors can be fuelled at steady-state, the fast-fission system can supply 1.14 while the spallation system can fuel 13.3. The fertile steady-state rate of decrease, $|(dN_{FE,S}/dt)_{SS}|$, follows the order of the end-of-system life fertile inventories. The fissile replacement time, τ_{FI}^{0}, can be thought of as a doubling time as used in reactor physics: the length of time needed for the system to replace the initial fissile inventory and hence be capable of starting up an identical system. For the reference breeder systems, there is a factor of 8.5 between the fast-fission system value of 38.3 years and the spallation system value of 4.52 years. The hybrid system at 8.72 years and the symbiotic system at 15.0 years falls between the two extremes.

Although a breeder can be operated primarily as a fissile fuel factory, that is, solely to produce fuel, the amount of electricity produced or consumed will be important to the system economics. Electrical power will be either a source of revenue or an operating cost depending upon whether $n_S^N > 0$ or $n_S^N < 0$. Here, the importance of large values of Q_B^T and small values of ε_B enter. The fast-fission breeder system, which

has an infinite value of Q_B^T, produced the most electrical power of the four systems: 2280 MW_e with a nuclear efficiency of 38%. The hybrid which has a value of ε_B of 0.30 due to the large energy multiplication in the breeder blanket, is also a net producer of electricity; 1941 MW_e with a nuclear efficiency of 33%. This is in contrast to both the symbiotic and spallation breeder systems which are consumers of power. The symbiont has a value of Q_B^T which is 7.5 times less than the hybrid and, as a result, the symbiotic system consumes 271 MW_e. This leads to a nuclear efficiency of -5.6%. For the spallation breeder, Q_B^T is 8% larger than for the symbiont and the system consumes 88 MW_e from the outside. The spallation system has a nuclear efficiency of -1.5%. For power production, the systems can be ranked in the following order: fast-fission, hybrid, spallation and symbiotic.

In summary then, it is clear that no single breeder system excells in all aspects. The spallation system produces the most fissile fuel. For resource utilization, the hybrid excells. In terms of fissile fuel investment, the symbiotic system requires less than the other three breeding systems. The fast-fission system, although outranked in all other aspects of fissile fuel production, is superior in terms of power produced. Clearly, additional considerations will be necessary to assess the systems in a particular context.

7.2 Alternate Operating Modes

In the analysis of the various breeding systems, the breeder thermal power was varied in order to examine the changes in certain characteristics of the system. This has been used, for example, to set

the fissile replacement time and the steady-state rate of change of the fissile inventory in what has been termed alternate operating modes. The value of P_B^T which leads to, say, a specific value of τ_{FI}^0 can be used as a measure of the fissile fuel production capabilities of the breeder. Thus, a good breeder will require a low thermal power to achieve the value of τ_{FI}^0. In addition to specifying τ_{FI}^0, it is also possible to find P_B^T such that: (1) $N_{FI,S}(\tau_S^{EOL})$ is zero, or, the system does not consume or produce fissile fuel; (2) $(dN_{FI,S}/dt)_{SS}$ is zero, or, the system does not consume fissile fuel at steady-state; and (3) $(dN_{FI,S}/dt)_{SS}$ is sufficient to fuel an external HTGR which in this case requires 210 kg/year. To estimate the breeder capabilities without the accompanying converter reactor, $(\tau_{FI}^0)_{MIN}$ or $(\tau_{FI}^{MIN})_{MIN}$ which are applicable when P_B^T is infinite, can be examined. These parameters are listed in Table 7.2-1 for the four reference breeder systems previously discussed.

The breeder thermal power which is required for the system to have a specified fissile replacement time is calculated using Eq(3.3-24) or

$$P_B^T = R_C U_B \left(\frac{Q_B^T}{Q_B^T - \alpha_B}\right)\left\{\omega_{FI,C}\left(1+\frac{\tau_{FI}^R}{\tau_C^D}\right) + \left[\frac{\omega_{FI,C}}{\tau_C^D}\,\ell_{FI} - G_{FI,C}(1-\ell_{FI})\right](\tau_{FI}^0-\tau_{FI}^R)\right\}\left\{-\omega_{FI,BC}\left(1+\frac{\tau_{FI}^R}{\tau_{BC}^D}\right)\right.$$
$$\left. -\omega_{FI,BB}\left(1+\frac{\tau_{FI}^R}{\tau_{BB}^D}\right) + \left[-\left(\frac{\omega_{FI,BC}}{\tau_{BC}^D}+\frac{\omega_{FI,BB}}{\tau_{BB}^D}\right)\ell_{FI} + (G_{FI,BC}+G_{FI,BB})(1-\ell_{FI})\right](\tau_{FI}^0-\tau_{FI}^R)\right\}^{-1} \qquad (7.2\text{-}1)$$

From Eq(7.2-1), it can be seen that a breeder with a large value of

Parameter	Breeder Type			
	Fast-Fission	Symbiotic	Hybrid	Spallation
Breeder thermal power for a 25 year fissile replacement time, τ_{FI}^{0}, MW_t	5462	1480	913	331
Breeder thermal power for a zero end-of-system-life fissile inventory, $N_{FI,S}(\tau_S^{EOL})$, MW_t	1429	653	534	214
Breeder thermal power for a zero fissile steady-state rate of change, $(dN_{FI,S}/dt)_{SS}$, MW_t	1383	629	514	206
Breeder thermal power for the fissile steady-state rate of change necessary to fuel a HTGR at 210 kg/year, MW_t	2767	1258	1028	412
Breeder thermal power for a minimum fissile inventory to be minimum, MW_t	1383	∞	2371	206
Minimum fissile replacement time, $(\tau_{FI}^{0})_{MIN}$, year	16.3	1.50	3.22	3.56
Minimum time to reach fissile minimum, $(\tau_{FI}^{MIN})_{MIN}$, year	3.010	1.500	1.502	1.509

Table 7.2-1: Data for alternate operating modes for the four reference breeder systems.

($G_{FI,BC} + G_{FI,BB}$) will have a small power. The spallation breeder requires the smallest thermal power, 331 MW_t, and has the largest net fissile generation ratio, 44.8. Next in order of increasing breeder power we have the hybrid, 913 MW_t, 2.8 times as large as the spallation system. The symbiotic system with a net generation ratio of 0.25 requires a breeder power of 1480 MW_t, 4.5 times that of the spallation system. The fast-fission breeder system requires a breeder thermal power 16.5 times that of the spallation system, 5462 MW_t. Also from Eq(7.2-1) we see that the greater the fissile specific inventories and the greater the value of U_B, the greater the thermal power required. Because of these two effects, the symbiotic system requires a smaller thermal power to achieve a 25 year fissile replacement time than the fast-fission breeder system even though the fissile net generation ratio is less.

To find the breeder power which involves no fissile fuel consumption, that is, $N_{FI,S}(\tau_S^{EOL}) = 0$, we use Eq(4.3-3),

$$\frac{\partial N_{FI,S}(\tau_S^{EOL})}{\partial P_B^T} P_B^T = -N_{FI,C}(\tau_S^{EOL}) \quad . \qquad (7.2\text{-}2)$$

Clearly, the larger the value of $(\partial N_{FI,S}(\tau_S^{EOL})/\partial P_B^T)$, the smaller the breeder power required. Here again, the spallation breeder requires the smallest power, 214 MW_t, and the fast-fission breeder, the largest, 1429 MW_t. The equation which gives the breeder power for a specific rate of change at steady-state is

$$P_B^T = U_B \left(\frac{Q_B^T}{Q_B^T - \alpha_B}\right)\left\{\left(\frac{dN_{FI,S}}{dt}\right)_{SS} + \left[\frac{\omega_{FI,C}\ell_{FI} + G_{FI,C}(1-\ell_{FI})}{\tau_C^D}\right] R_C\right\}$$

$$\times\left\{-\left[\frac{\omega_{FI,BC}}{\tau_{BC}^D} + \frac{\omega_{FI,BB}}{\tau_{BB}^D}\right]\ell_{FI} + (G_{FI,BC}+G_{FI,BB})(1-\ell_{FI})\right\}^{-1}. \qquad (7.2\text{-}3)$$

The importance of a large fissile net generation ratio is again shown. The spallation system for a zero steady-state fissile rate of change needs a breeder thermal power of 206 MW_t and for 210 kg/year production, 412 MW_t. For these same modes of operation, the fast-fission breeder requires 1383 MW_t and 2767 MW_t respectively. The hybrid and symbiotic systems fall between these two values.

For minimum fissile minimum inventory, $(P_B^T)_{FI}^{MIN}$ depends, not only on the net fissile generation ratio, but also on the fissile specific inventory. Thus, the symbiotic system requires an infinite breeder power for a minimum fissile investment since $\omega_{FI,BB}$ is zero. The hybrid with a low fissile specific inventory requires a breeder power of 2371 MW_t. The fast-fission and spallation breeders have larger specific inventories but, since $(G_{FI,BB})_{SP} > (G_{FI,BC}+G_{FI,BB})_{FF}$, the spallation breeder size to minimize $N_{FI,S}(\tau_{FI}^{MIN})$ is 206 MW_t compared with 1383 MW_t for the fast-fission system. This same relative order occurs for both $(\tau_{FI}^0)_{MIN}$ and $(\tau_{FI}^{MIN})_{MIN}$.

In Fig. 7.2-1 and Fig. 7.2-2, an attempt has been made to summarize the fissile fuel production, resource utilization and electrical power production of the four breeder systems for varying breeder thermal power. The ratio of the fissile inventories at the end-of-system-

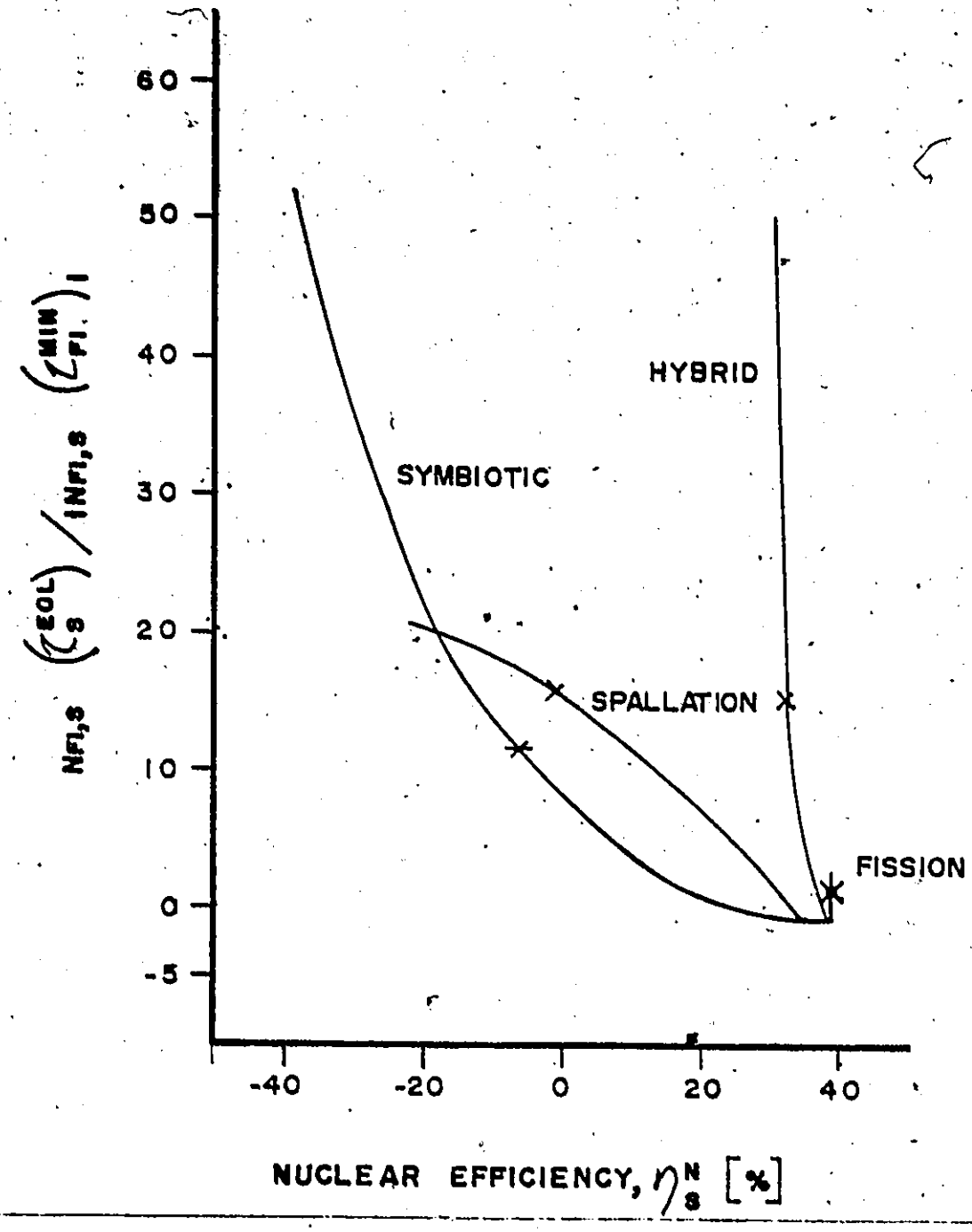

Fig. 7.2-1: Ratio of fissile inventory at the end-of-system-life to the minimum fissile inventory for four types of breeders for power ranging from 200 MWt to 10,000 MWt. Crosses indicate reference, 3000 MWt, breeder systems.

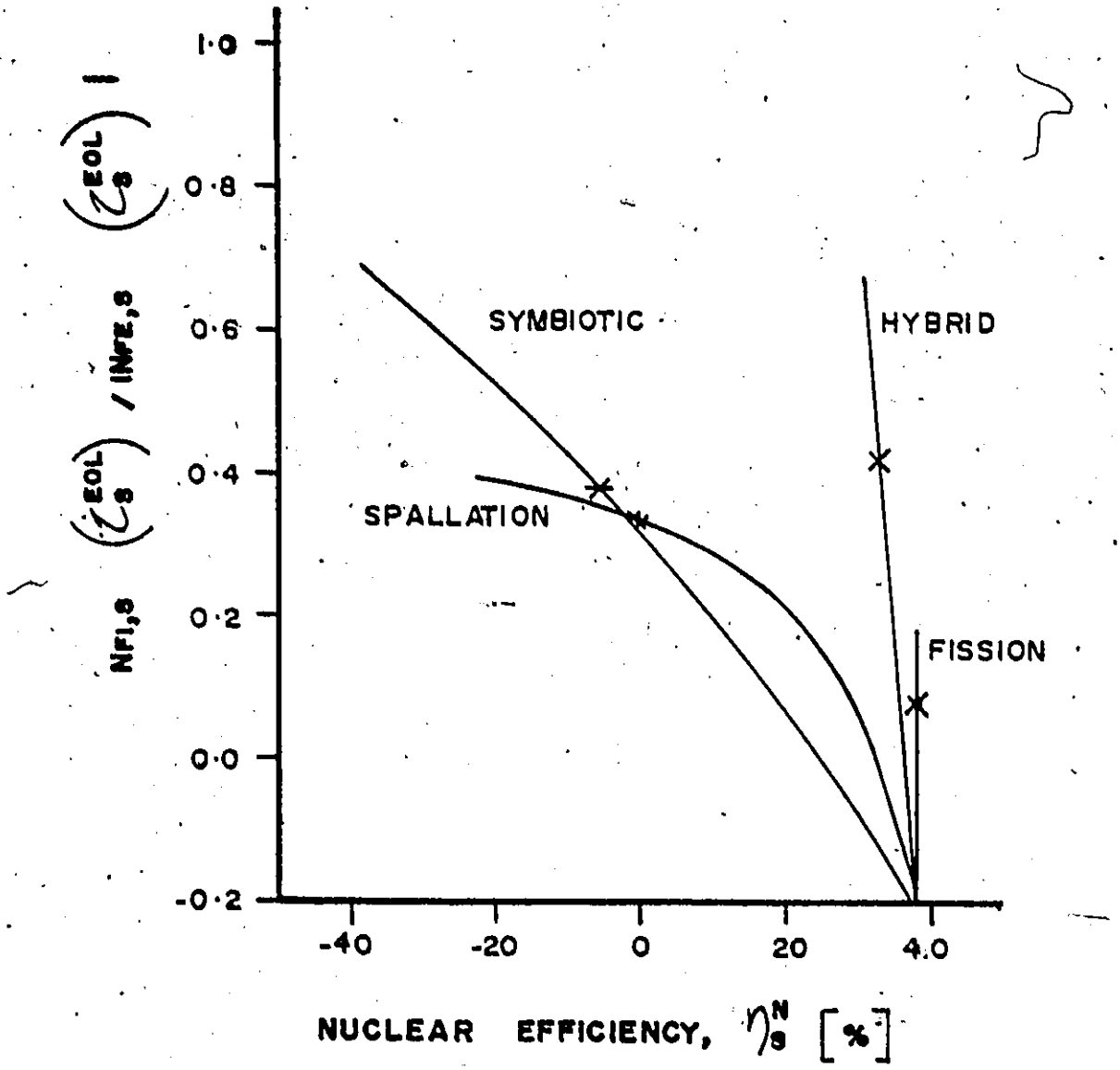

Fig. 7.2-2: Ratio of fissile to fertile end-of-system-life inventories for the four reference breeder systems for breeder thermal powers from 0 to 10,000 MWt. Crosses indicated refer 3000 MWt breeder systems.

life to the minimum value and the nuclear efficiency are plotted in Fig. 7.2-1 such that higher electrical output is to the right of the figure and higher fissile output at the top. The thermal powers of the breeders range from zero where the four curves converge at the value determined by the converter alone, to 10000 MW_t. Crosses have been marked at P_B^T = 3000 MW_t for reference.

The fission breeder curve is a straight, vertical line since η_S^N is constant and increasing P_B^T increases the production to minimum ratio. Although it cannot be seen on the plot, there is a limiting value of $N_{FI,S}(\tau_S^{EOL})/|N_{FI,S}(\tau_{FI}^{MIN})|$ as $P_B^T \rightarrow \infty$ since for large breeder thermal powers, both $N_{FI,S}(\tau_S^{EOL})$ and $N_{FI,S}(\tau_{FI}^{MIN})$ are linear functions of P_B^T as seen in Fig. 4.3-1. The hybrid nuclear efficiency decreases slightly as P_B^T increases and from Eq(5.4-6), the limiting value of η_S^N will be $\eta_B^T(1-\epsilon_B)$ or 0.28. As mentioned in Section 5.3, the minimum fissile inventory curve for the hybrid is very flat and as a result, the limit of the ratio plotted here will be very large. For the symbiont, the limiting value of η_S^N will be -0.76 since ϵ_B is greater than unity. The limit of fissile fuel production to minimum inventory will be infinite since the minimum value of $N_{FI,S}(\tau_{FI}^{MIN})$ occurs at an infinite breeder power. The spallation breeder in contrast, has both a limiting value of nuclear efficiency, -0.41, and the production to minimum ratio, ~23. This causes the spallation breeder curve in Fig. 7.2-1 to turn over.

In Fig. 7.2-2, resource utilization is plotted against nuclear efficiency where resource utilization is measured by $N_{FI,S}(\tau_S^{EOL})/|N_{FE,S}(\tau_S^{EOL})|$. As was the case in Fig. 7.1-1, all curves converge at P_B^T = 0 at a value for the converter alone, -0.21. The fission breeder

curve is again a straight, vertical line since n_S^N is constant. The maximum value for the resource utilization can be estimated in the limit of $P_B^T \rightarrow \infty$,

$$\frac{N_{FI,S}(\tau_S^{EOL})}{|N_{FE,S}(\tau_S^{EOL})|} \rightarrow \left\{-\left[\frac{\omega_{FI,RC}}{\tau_{BC}^D} + \frac{\omega_{FI,BB}}{\tau_{BB}^D}\right] \ell_{FI} + (G_{FI,BC}+G_{FI,BB})(1-\ell_{FI})\right\} \times \left\{-\left[\frac{\omega_{FE,BC}}{\tau_{BC}^D} + \frac{\omega_{FE,BB}}{\tau_{BB}^D}\right] \ell_{FE} + (G_{FE,BC}+G_{FE,BB})(1-\ell_{FI})\right\}^{-1} \tag{7.2-4}$$

which assumes that the initial and final core loadings and the pre-steady-state and steady-state rates of change are equal. In these assumptions there are errors which cancel so the value obtained will be accurate to within $\tau_{BB}^D/2\tau^{EOL}$. For the fission converter, the value obtained using Eq(7.2-4) is -0.214 and for the fast-fission breeder system, 0.266. The hybrid curve is also nearly vertical since n_S^N varies little with breeder thermal power. For an infinite breeder thermal power, the limiting value of the fissile to fertile ratio is 0.875. An even higher value of resource utilization limit is obtained for the symbiotic breeder, 0.971. The spallation breeder because of the small value of τ_{BB}^D and $G_{FI,BB}/G_{FE,BB}$ has a limiting value of 0.423. Because this is lower than the symbiotic fusion breeder limit and the nuclear efficiency limit is less, the two curves cross over in Fig. 7.2-2. In terms of this measure of resource utilization, the order of the breeders is: symbiotic, hybrid, spallation and fast-fission.

7.3 Some Economic Considerations

Up to this point little has been said about how to combine the above results in order to select the most desirable breeder-converter system. One possible method is an economic analysis where costs of, and revenues from, the system are used as a basis of comparison. This allows one to assess economic penalties against untried technologies and discounts if, for example, the device is to be used as a stepping stone to future technologies, such as fusion breeders. In this section, it will be shown, briefly, how the system characteristics found from the model developed in Chapter III can be used in such an analysis. Numerical results presented will be tentative due to the lack of definitive data for proposed breeders.

There are two types of costs associated with power reactors: (1) capital which involve the construction expenses of the plant and (2) operating which involve the expenses after the plant has been constructed. These two can be combined into a single cost parameter, the capitalized cost[82] which can be written as

$$C = P + \int_0^{\tau_S^{EOL}} (1 + r)^{-1}[F(t)+I(t)+O(t)+M(t)]dt, \qquad (7.3\text{-}1)$$

where P is the plant capital cost, r is the discount rate, F(t) is the fuel cycle expenses not including nuclear material, I(t) is the interim capital replacement costs, O(t) is the operational costs and M(t) is the nuclear material costs. Nuclear plant component and material costs are usually given on a per unit power or per unit weight basis. The capitalized cost can be separated into terms due to each component,

$$C = c_C P_C^T + c_B P_B^T + c_R (P_C^T + P_B^T)$$

$$+ \int_0^{\tau_S^{EOL}} (1+r)^{-1} [F(t)+I(t)+O(t)+M(t)]dt, \qquad (7.3\text{-}2)$$

where the lower case parameters, c_i, refer to the specific capital costs and C, B and R refer to the converter, breeder and reprocessing-fabrication plant respectively.

The plant costs, interim capital costs and operational expenses will be proportional to the size of the components as measured by the thermal power. For the nuclear material costs, the following will hold:

$$\int_0^{\tau_S^{EOL}} M(t)dt = \sum_J \left| N_{J,S}(\tau_S^{EOL}) \right| c_{N,J} , \qquad (7.3\text{-}3)$$

where $c_{N,J}$ is the price of nuclear fuel J. For fertile material a better estimate of costs, as can be seen from the fertile inventory curves generated by this analysis, may be found using the inventories evaluated at τ^{EOL} which give the maximum amount of material to be purchased. Some credit for the final core discharged can be made in the capitalized cost. Since we are dealing with breeders, there is no need to include fissile or tritium material in Eq(7.3-3), but rather an amount equal to the minimum value of these inventories should be included as a plant cost rather than in fuelling costs. Fuel cycle expenses, F(t), include fabrication and reprocessing costs. For our system, the following will be used,

$$\int_0^{\tau_S^{EOL}} F(t)dt = \sum_J \sum_i \frac{(\omega_{J,i})}{\tau_i^D} \tau^{EOL} P_i^T LF_i c_{N,R} , \qquad (7.3\text{-}4)$$

where the sum over J includes fertile and fissile material and LF_i is the load factor of component i. The cost of processing is given here on a per unit weight basis, $c_{N,R}$.

Revenues from the combined system will come from two sources: (1) fissile fuel and (2) electrical power. The revenue can be written as

$$S = \sum_J s_{N,J} N_{J,S}(\tau_S^{EOL}) + s_p \tau^{EOL}(P_C^{NET} LF_C + P_B^{NET} LF_B) , \qquad (7.3\text{-}5)$$

where here $s_{N,J}$ is the price of bred fuel, fissile or tritium, and s_p, of electrical power. In order for the system to be economically attractive, revenues must exceed costs, or

$$S - C > 0. \qquad (7.3\text{-}6)$$

The difference between revenues and costs can be used as a figure of merit for a breeder system.

To give some numerical results, economic data is needed. Breeder system economic data, however, are not well defined at this time. Therefore, the economic comparison presented here would be viewed as showing trends rather than definitive results. Because of this, Eq(7.3-2) will be simplified further. Since all four systems will have the same reprocessing-fabrication plant and, for a fixed thermal power, this is a constant term, we will not include this in the capital cost explicitly but rather charge it to the fuel cycle expenses. Also, for simplicitly, operating costs other than for nuclear fuel will be excluded. For nuclear fuel costs, the cost of fertile fuel and processing will be considered. We note that if fertile recycle is not included, the price of processing may be reduced but more fertile fuel must be purchased.

For the two fusion breeder systems, the lithium costs and the sale of tritium will be excluded although some allowance for the lithium costs have been incorporated into the capital costs below. In addition, no allowance for inflation or interest will be considered, that is, capital and operating costs are given equal weight.

Using the above, the capitalized cost used here will be

$$C = c_C P_C^T + c_B P_B^T + c_{N,FE} N_{FE,S}(\tau^{EOL}) + c_{N,R}\left[\left(\frac{\omega_{FE,C}+\omega_{FI,C}}{\tau_C^D}\right)\right.$$

$$\left. xP_C^T LF_C + \left(\frac{\omega_{FE,BC}+\omega_{FI,BC}}{\tau_{BC}^D} + \frac{\omega_{FE,BB}+\omega_{FI,BB}}{\tau_{BB}^D}\right)P_B^T LF_B\right]\tau^{EOL} \quad (7.3\text{-}7)$$

For revenues we will use

$$S = s_{N,FI} N_{FI,S}(\tau_S^{EOL}) + s_P(P_C^{NET} LF_C + P_B^{NET} LF_B)\tau^{EOL} \quad (7.3\text{-}8)$$

If $n_S^{NET}<0$, then power must be purchased and it is assumed that the buying and selling prices are equal.

The economic analysis data from conceptual designs will be used. These are listed in Table 7.3-1 for the converter and the four proposed breeder reactor types. Here, the converter reactor has the lowest specific capital cost since the technology is well developed. The fast-fission breeder has the next largest value; the GCFR is a direct advance on HTGR technology and hence the costs will not be much greater than for the converter. The hybrid has a specific capital cost of 490 \$/kW$_t$. The fusion breeder is a new technology and the costs will be greater than for fission reactors. The symbiont has a specific capital cost 40% greater

Specific Capital Costs			
Component	Symbol	Cost ($/kW$_t$)	(Reference)
Converter	c_C	215	(34)
Fast-Fission Breeder	$(c_B)_{FF}$	260	(29)
Symbiotic Fusion Breeder	$(c_B)_{SY}$	680	(45)
Hybrid Fusion Breeder	$(c_B)_{HY}$	490	(45)
Spallation Breeder	$(c_B)_{SP}$	500	(16)
Fuel Costs			
Component	Symbol	Cost ($/kg)	(Reference)
Material: ThO_2			
Cost of Material	$c_{N,FE}$	40	(35)
Cost of Processing	$c_{N,R}$	161	(25)
Material: UO_2			
Cost of Material	$c_{N,FE}$	80	(35)
Cost of Processing	$c_{N,R}$	100	(25)

Table 7.3-1: Costs used for converter and breeder reactors and the fuel costs used in economic analysis.

than the hybrid since, for a given breeder thermal power, a greater fusion power is required in the symbiont than in the hybrid. The spallation system requires an extension of accelerator technology and a large facility, hence its specific capital costs, although comparable to the hybrid, is twice as large as the fast-fission breeder. The cost of ThO_2 in Table 7.3-1 is half that of UO_2 but processing is expected to be more difficult due to the more active product to be handled.

In Fig. 7.3-1, the prices of fissile fuel and electricity such that

$$C = S \ , \tag{7.3-9}$$

are shown for the four reference systems where both the breeder and converter thermal powers are 3000 MW_t. For the fast-fission breeder, equal amounts of thorium and uranium fertile material have been assumed. Using Eq(7.3-7) and Eq(7.3-8), Eq(7.3-9) can be rewritten as

$$s_p = \frac{C - s_{N,FI} N_{FI,S}(\tau_S^{EOL})}{\tau^{EOL}(P_C^{NET} LF_C + P_B^{NET} LF_B)} \ . \tag{7.3-10}$$

In Fig. 7.3-1, any price pair (s_p, $s_{N,FI}$) in the hatched region will satisfy Eq(7.3-6), that is, revenues will exceed costs. Since the net electrical power of the symbiont and spallation breeder is negative, the slope of these lines are opposite that of the fast-fission and hybrid systems. The converter reactor must purchase fissile fuel, hence the price of electrical power must increase with increasing fissile fuel costs. The price of fissile fuel from the spallation and symbiotic systems is relatively insensitive to the price of electricity since the amount of power purchased is not great. In fact, of all four breeders,

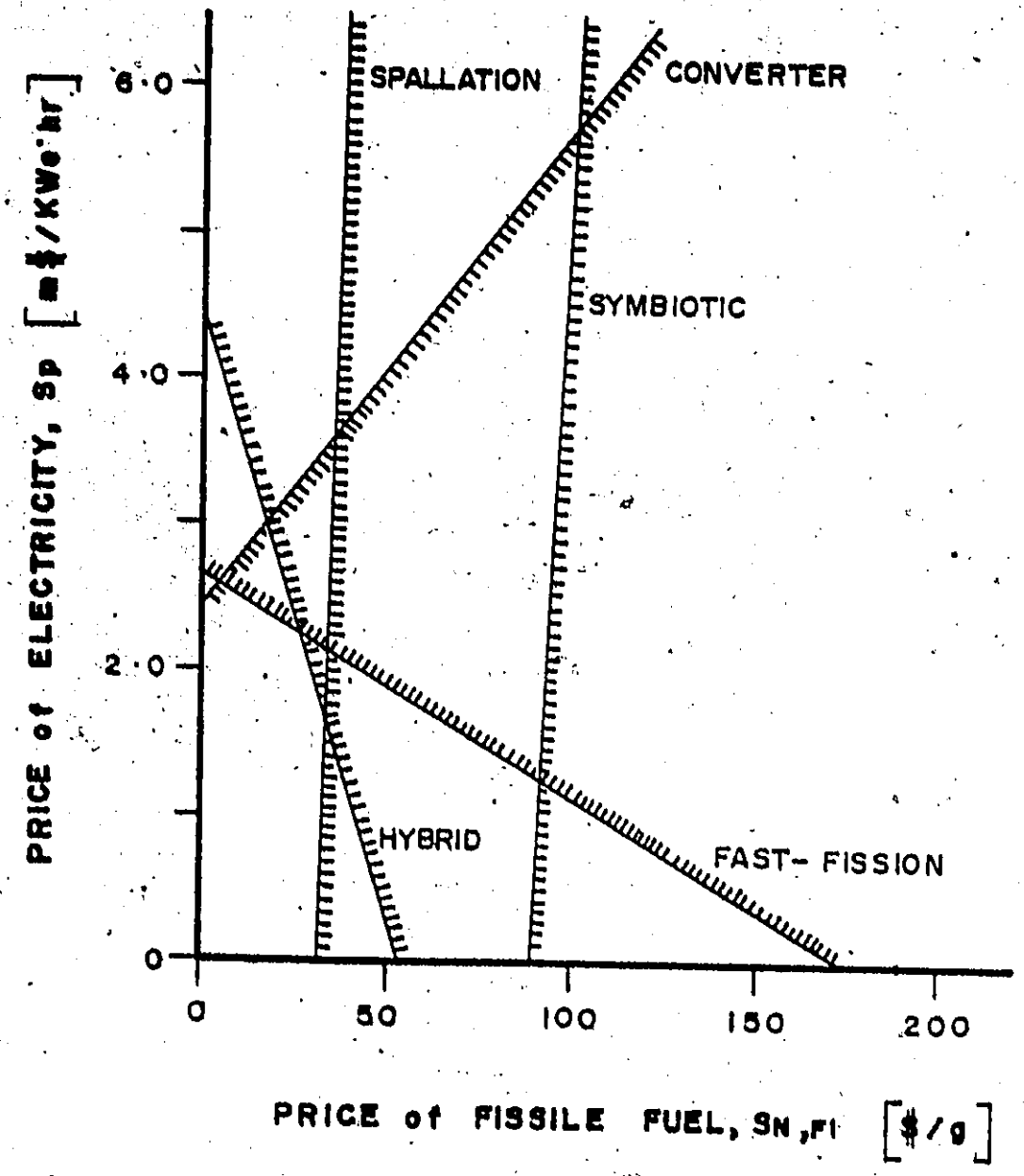

Fig. 7.3-1: Price of electricity and fissile fuel for revenues to exceed costs for the four reference breeder systems. In the hatched area, s>c.

the price of fissile fuel from the fast-fission breeder is most sensitive to the price of electricity since this sytem produces the most electrical power and the least fissile fuel.

To obtain a single parameter to gauge the effectiveness of a breeder system, we will use the price of electricity from a converter reactor fuelled with fissile material from the breeder system. This can be found from Fig. 7.3-1 by the intersection of the converter price curve with the breeder system curves. Thus, a HTGR fuelled with fissile material from the fast-fission breeder can break even economically at s_p = 2.56 m\$/kW$_e$·hr and $s_{N,FI}$ = 4.27 \$/g. The hybrid gives the next cheapest price: s_p = 2.98 m\$/kW$_e$·hr and $s_{N,FF}$ = 16.5 \$/g. Because the cost of the spallation breeder is comparable to that of the hybrid, the price of electricity from the converter is close to that of the hybrid fuelled system: s_p = 3.06 m\$/kW$_e$·hr and $s_{N,FI}$ = 34.0 \$/g. The symbiotic system produces a price of electricity of 8.72 m\$/kW$_e$·hr at a fissile fuel cost of 98 \$/g. These results are very sensitive to the capital costs of the components since the capital cost is ~\$10^9 compared with the fuelling costs of ~\$10^8. It is the low capital cost of the fast-fission breeder and its electrical power producing capabilities which give a low price for electricity. Changing the specific capital costs will greatly affect the prices produced here.

From this analysis we find that the price of nuclear fuel will be determined by the price of electricity. If power is cheap, the spallation system will be the most economical breeder and the fast-fission system the most expensive. Using the cost of electricity from a converter reactor fuelled with fissile fuel from a breeder system, the breeder

systems have been ranked using the above cost data: fast-fission, hybrid, spallation and symbiotic. Thus, with these values, the hybrid is a good breeder at nearly all fissile fuel prices because it produces both fissile fuel and electricity. The spallation system, because of its large fissile output, is relatively insensitive to electricity prices. The high capital costs of the symbiotic system are found to be prohibitive.

CHAPTER VIII

SUMMARY AND CONCLUSIONS

The need for rigorous and comprehensive analysis of different nuclear breeders was identified in the Introduction. The problem was identified as the establishment of a general and tractable basis for assessing (1) the fissile fuel production, (2) the necessary fissile investment and (3) the resource utilization along with the power produced by any type of breeder. Previous research had been based primarily on the unique characteristics of the fast-fission breeder and were not readily adaptable to the more recent nuclear breeding concepts. The research presented in this thesis fulfills these requirements.

Central to this analysis is the concept of synergism; this term implies the interaction of the components of the entire system. To this end, both the breeder and converter reactors along with the associated reprocessing-fabrication plant were included. To eliminate costly computer simulations while still allowing extensive evaluations, a lumped parameter analysis was chosen. Lumped parameters are based on space and energy integrated values which can be reliably estimated from the existing literature, or, if required, calculated from detailed designs. Also, the concept of a stockpile inventory was employed as a means of accounting for the flow of materials throughout the system in a realistic manner. Based on these concepts, a suitable procedure for analysis of breeding systems was derived.

Prior to developing the mathematical description, the physics and engineering aspects of some types of breeders and thermal fission converter reactors were presented. The breeder types considered were fast-fission, symbiotic fusion, hybrid fusion and spallation. In addition to providing the necessary physical description of the systems, data to be used was assembled from a wide range of sources. The large range of breeding capabilities and designs justified the choice of using lumped parameters. In the analysis which followed, reference systems based on typical parameters were used and some sensitivity studies to estimate the effects of varying these selected values was done. However, with such a wide range of possible design choices for each of the components, the analysis presented could not be exhaustive. Further studies might involve varying the converter reactor parameters so as to best match the breeder; in particular, a coupled system of fast-fission breeder reactors could be investigated. Also, the effects of fission reactor produced tritium on the fusion reactor system[5] could be considered.

The mathematical description was developed in Chapter III. First, a notation for describing the important nuclear reactions was set up. One of the distinctive parameters introduced at this point was the concept of a characteristic reaction rate for each of the reactor types. For the fission reactors, the characteristic reaction rate used was the neutron absorption rate in fissile fuel. The characteristic reaction rate for a deuterium-tritium fuelled fusion breeder was the DT fusion reaction rate while for the spallation breeder, the rate at which the incident particles strike the target was used. These characteristic reaction rates correspond to an intuitive notion of the size of each

reactor type and were found to be easily related to the fissile fuel production and thermal power of the reactors. Also in this section, it was shown that the DD and D^3He reaction rates in a DT fuelled fusion breeder could be neglected.

Using this notational system, a general equation for the isotope balance in a reactor was developed. This was integrated over space, energy and time in accordance with the choice of lumped parameters to define a net generation ratio. The net generation ratio of a material in a reactor times the characteristic reaction rate of the reactor gives the change in the number of atoms of that material during the period it is in the reactor divided by the refuelling interval. At steady-state, the space and energy integrated reaction rates and the inventories in the core or blanket of a reactor is periodic with respect to the refuelling interval. Because of this, a "refuelling interval averaged" description was used to arrive at a continuous, analytical expression for the variation of the reactor stockpiles as a function of time.

Fissile fuel net generation ratios can be extracted from the literature but to describe the fertile fuel inventory, the fertile net generation ratio is needed. Based on the decay equations for thorium and plutonium fuel cycles, a relationship between the fissile and fertile net generation ratios was obtained. This relationship in general is flux and time dependent, but for reasonable values of flux and for times sufficiently long for intermediate decay products to reach equilibrium, a constant expression can be obtained. The lithium net generation ratio was also related to the tritium net generation ratio in a fusion breeder blanket. This expression is simpler since there are no intermediate

decay products. The concept of isotope weights was introduced so that fissile and fertile materials could be discussed without reference to the specific isotopes involved. This is not seen as a limitation on the procedure since we can describe the stockpile of any isotope if required but was employed to emphasize the analytical procedure.

Having derived a description of the stockpile variation for a component reactor, the system stockpile inventory variation was derived. The system, as we have said, consists of a breeder reactor, a thermal fission converter reactor and the necessary reprocessing-fabrication plant. The stockpile is used as a means of accounting for material flows into and out of the system. By setting the initial value to zero, we know that if the inventory at any time is negative, then material must be brought into the system while if it is positive, material can be sent out of the system. The equations developed are applicable to any material within the system and explicitly incorporates effects due to pre-steady-state and lags and losses due to fuel processing. Pre-steady-state is described by two generalized functions: $h_1(t)$ which accounts for any pre-steady-state fuelling schemes and $g_1(t)$ which accounts for pre-steady-state net generation ratios. The stockpile inventory equations also include the initial loading and final discharge of the cores and blankets.

Simple, physically reasonable estimates of $h_1(t)$ and $g_1(t)$ were found for the cores and blankets of the various reactor components. If a more detailed fuel management scheme is known for a given design, this can be readily incorporated into the analysis using these pre-steady-state functions. Since such a fuelling scheme is not known at present for the proposed breeder concepts, the values used were developed and

and this allowed us to evaluate the system stockpile inventory variation during the reactor lifetime without recourse to devising detailed fuel management schemes. These simplifications introduce an error of less than 10% when compared with fast-fission breeder reactor data but since the uncertainty in the data presented in Chapter II is approximately 20%, the estimates for the pre-steady-state functions were thought to be reasonable for the parametric studies presented here.

The inventory variations calculated by this procedure will of course depend upon the specific values of the parameters used but the shapes produced will be similar. As noted above, prior to startup, all inventories are set to zero. The initial loading of the reactors results in a step decrease for all materials. Following this initial loading there will be a further decrease in the inventory as the cores and blankets are refuelled until material begins to reach the stockpile from the reprocessing-fabrication plant. This is an effect attributable to the processing lag. The pre-steady-state blanket net generation ratio used here results in a quadratic variation of the inventories until steady-state is reached. At steady-state, the rate of change of the material stockpile will be constant until the reactor is shut down. Following this, there will be an increase in the stockpile inventory due to the addition of material already in the processing plant. Finally the processed final cores and blankets are added to the stockpile causing a step increase. Sometime during the system life, every material will reach a minimum value which will be the maximum amount of the material which must be supplied from outside the system.

A result obtained from the equations for the stockpile variation

is that we can find the value of the breeder power of the breeder characteristic reaction rate which will give a specified inventory or rate of change at a given time. For example, the fissile replacement time has been defined as the time needed by the system to replace the initial fissile investment, that is, at the fissile replacement time, the system fissile inventory will be zero. We can find a breeder power which is necessary to obtain a given fissile replacement time and hence necessary to maintain a given rate of increase of nuclear power. Another result is that there will be a value of the breeder characteristic reaction rate which minimizes the fissile investment in the system. We have called this means of choosing breeder size alternate operating modes.

The system power balance is calculated in a manner similar to the stockpile inventory; the individual components are considered first then the complete system....Two parameters which are important to a power balance are the total amplification factor which is the ratio of thermal power generated to injected energy and the circulating energy fraction which is the ratio of electrical energy recycled back into the reactor to the gross electrical output. Note that for a fission reactor, the total amplification factor will be infinite but the circulating energy fraction will be non-zero. The higher the amplification factor and the smaller the circulating energy fraction, the larger the net electrical power output. In defining the net electrical output, we explicitly include the electrical power required for reprocessing. The power balance of the system can be quantified by two efficiencies: the nuclear efficiency which is the ratio of electrical power output of the reactors to the nuclear power generated, and the reprocessing efficiency which is

the ratio of electrical power used for reprocessing to the nuclear power generated. The net system efficiency will be the difference between these.

With this procedure we analysed four breeder types. Since the fast-fission breeder is in the most advanced state of development and is the most familiar concept, a fast-fission breeder represented by a GCFR coupled to a thermal fission converter reactor represented by a HTGR was considered first. The temporal variation of the system fissile and fertile stockpiles for a system with both reactors having a thermal power of 3000 MW_t and the effects on some characteristics of varying the breeder thermal power were investigated. We also found that (1) decreasing the breeder fissile net generation ratio decreases the fissile fuel production; (2) reducing the breeder fissile specific inventory increases fissile fuel production and (3) decreasing the fuel mean discharge periods in the breeder decreases fissile fuel production. The latter two effects are smaller compared with the first and all these are equally applicable to the other breeders.

Two types of fusion breeders are identified in the literature: symbionts which have fissions in the blanket suppressed and hybrids in which both fission and fusion reactions occur. The hybrid has a larger fissile net generation ratio and blanket energy multiplication factor than the symbiont because of the increased fission reaction rate. Both reactors used a tokamak as its fusion concept and the inventories of heavy elements and lithium were set equal to normalize the results somewhat. Similarly, for comparison with the fast-fission reactor, the reference HTGR was used as the thermal fission converter reactor. Both of the fusion breeder systems were found to be superior fissile fuel

producers than the fast-fission breeder system. The tritium and lithium inventories were also calculated and it was found that due to the short mean discharge period in the fusion core, a very deep tritium minimum occurred although both systems generated a surplus after the final blanket was processed. An interesting effect due to having no initial fissile specific inventory in the symbiont was that an infinite breeder power is necessary to minimize the fissile investment in the system. From the power balance calculations, we found that the symbiotic system was a net consumer of electricity while the hybrid was a net producer. This is a result of the larger blanket energy multiplication factor in the hybrid compared to the symbiont.

The final breeder system considered was the spallation breeder. Here a proton linear accelerator and a gas-cooled thorium fuelled target-blanket was coupled with the reference HTGR. A very high fissile net generation ratio led to a very large fissile fuel production rate. This of course also led to a large fertile fuel consumption over the lifetime of the system. Unfortunately, the large circulating energy fraction required to operate the accelerator resulted in the system being a net power consumer for a breeder thermal power of 3000 MW_t. Since the spallation breeder is an excellent fissile fuel producer, however, it is possible to operate as a fissile fuel factor at smaller breeder powers than the other three breeder systems.

In comparing the four breeder systems we find that no single breeder excells in all aspects. At a breeder thermal power of 3000 MW_t, the relative ranking of the fissile fuel production capabilities is: spallation, hybrid, symbiotic and fast-fission. For fertile resource

utilization, the relative ordering is: symbiotic, hybrid, fast-fission and spallation. In terms of fissile investment, the symbiotic fusion breeder system requires the least and for power produced, the fast-fission breeder system excells. To obtain a single figure of merit to gauge the different systems, the result of this method of analysis were combined with economic data. Here, the cost of electricity produced by a thermal fission converter fuelled with fissile fuel produced by a breeder system was used. Because of its high electrical output and lower capital cost, it was found that for fast-fission breeder was "best". The hybrid which produces both fissile fuel and electricity was next followed by the spallation breeder system. Both of these had similar specific capital costs. The high capital cost of the symbiont was found to be prohibitive. We stress the tentative nature of this economic data and note that the ordering of the system is strongly influenced by specific capital costs.

In the above comparison, we have not explicitly included some considerations. We implicitly assumed the technological feasibility of the various concepts although economic penalties were assessed against both fusion breeders and the spallation breeder. The difficulty of maintaining a fusioning plasma within a fissioning blanket may preclude the hybrid as a viable concept. Similarly, there will be great difficulty in confining a proton beam accelerated over distances of a kilometer. The environmental impact of large breeders with low thermal efficiency must be considered. Here the spallation breeder because of its good fissile production capabilities may be a forerunner since smaller breeders could be employed as fissile fuel factors. Use of plutonium in fast-fission breeders may not be allowed if proliferation constraints are

imposed and the already poor fissile fuel production may be further reduced. Finally, in a rapidly accelerating nuclear reactor economy, the low fissile investment characteristics of the symbiotic system cannot be overlooked. Clearly, further engineering development will serve to clarify these points and the economic data will reflect these concerns. This of course may alter the choice of the breeder system from that which we have found. The above is summarized in the following table.

	Fast Fission	Symbiotic	Hybrid	Spallation
Fissile Production	Poor	Good	Better	Best
Fertile Utilization	Poor	Better	Best	Good
Power Production	Best	Poorest	Good	Poor
Cost	Best	Poorest	Good	Poor

The procedure for analysing different fissile fuel breeding systems derived in this thesis has been found to be a useful tool for comparing on an equal basis, different conceptual breeding devices. The built-in flexibility and the use of lumped parameters further extends the usefulness since it can be used for scoping calculations if data is uncertain and also can incorporate detailed designs and operational fuelling schemes if these are known. The fact that any material can be so analysed means that fertile fuel utilization and tritium consumption can be calculated. Essential to the procedure is the inclusion, at the outset, of all system components in a synergetic manner.

REFERENCES

1. L.M. Lidsky, "Fission-Fusion Symbiosis: General Considerations and a Specific Example", British Nuclear Energy Society Nuclear Fusion Conference, Culham Laboratory, U.K., Sept. (1969).
2. E. Klein, A Comprehensive Etymological Dictionary of the English Language, Elsevier Publishing Co., Amersterdam (1971).
3. R.W. Hardie, W.W. Little and R.P. Omberg, "A Comprehensive Expression for the Doubling Time of Fast Breeder Reactors", Nucl. Tech., 26,115 (1975).
4. M. Heindler and A.A. Harms, "Fissile Fuel Doubling Time Characteristics for Reactor Life-Time Fuel Logistics", Nucl. Sci. Eng., 66,167 (1978).
5. C.W. Gordon and A.A. Harms, "Comparative Energetics of Three Fusion-Fission Symbiotic Nuclear Reactor Systems", Nucl. Eng. Design, 54,269 (1975).
6. A.A. Harms and C.W. Gordon, "Parametric Analysis of the Spallation Breeder", Nucl. Sci. Eng., 63,336 (1977).
7. E.L. Draper, Jr. and S.J. Gage, "The Fusion-Fission Breeder: Its Potential in a Fuel-Starved Thermal Reactor Economy", Conf. 721111, Texas Symposium on the Technology of Controlled Thermonuclear Fusion Experiments and the Engineering Aspects of Fusion Reactors, Austin Texas, 20-22 Nov., (1972).
8. R.R. Leonard, Jr., "A Review of Fusion-Fission (Hybrid) Concepts", Nucl. Tech., 20,161 (1973).

9. P. Fortescue, "The Fusion Breeder Concept", Annals of Nucl. Energy, 2,29 (1975).

10. F.H. Tenney, "A Brief Review of the Fusion-Fission Hybrid Reactor", Conf. 760935, Proceedings of the 2nd Topical Meeting on the Technology of Controlled Nuclear Fusion, Richland, Wash., 21-23 Sept. (1976).

11. L.M. Lidsky, "Fission-Fusion Systems: Hybrid, Symbiotic and Augean", Nucl. Fusion, 15,151 (1975).

12. G. Lavergne, J.E. Robinson and J.G. Martel, "On the Matching of Fusion Breeders to Heavy Water Reactors", Nucl. Tech., 26,12 (1975).

13. W. Seifritz, "The Symbiosis Between Beam-Driven Hybrid DT-Fusion Reactors and Near Breeder HTGR's", Trans. Am. Nucl. Soc., 23,27 (1976).

14. W.C. Gough, "The EPRI Viewpoint on Fusion-Fission", Conf. 760733, Proceedings of the US-USSR Symposium on Fusion-Fission Reactors, Livermore, Calif., 13-16 July (1976).

15. V.G. Vasil'kov, V.I. Gol'danskii, V.P. Dzhelepov and V.P. Dmitrievskii, "The Electronuclear Method of Generating Neutrons and Producing Fissionable Materials", Soviet Atomic Energy, 29,858 (1970).

16. F.R. Mynatt, R.G. Alsmiller, J. Barish, T.A. Gabriel, D.E. Bartine, J.J. Burns, J.A. Martin, M.J. Saltmarsh and E.S. Bettis, "Preliminary Report on the Promise of Accelerator Breeding and Converter Reactor Symbiosis (ABACS) as an Alternative Energy System", ORNL/TM-5750, Oak Ridge National Laboratory, Feb. (1977).

17. M. Steinberg, "Nuclear Power Without Nuclear Bombs", New Scientist, 75,14 (July 7, 1977).

18. P.R. Tunnicliffe, B.G. Chidley and J.S. Fraser, "High Current Proton Linear Accelerator and Nuclear Power", AECL-5622, Atomic Energy of Canada Ltd., Chalk River, Ont. (1976).

19. A.A. Harms and C.W. Gordon, "Fissile Fuel Breeding Potential with Paired Fusion-Fission Reactors", Annals Nucl. Energy, 3,213 (1976).

20. C.W. Gordon and A.A. Harms, "The Basic Characteristics of an Efficient Fusion Breeder", Atomkernenergie, 29,213 (1977).

21. A.A. Harms and M. Heindler, "The Matching of Dense Plasma Focus Devices with Fission Reactors", Nucl. Sci. Eng., 66, 1 (1978).

22. P. Fortescue, "Comparative Breeding Characteristics of Fusion and Fast Reactors", Science, 196,1326 (1977).

23. D.R. Marr, R.W. Hardie and R.P. Omberg, "An Expression for the Compound Doubling Time which Explicitly Includes the Approach to Equilibrium", Trans. Am. Nucl. Soc., 26,587 (1977).

24. J.J. Duderstadt and L.J. Hamilton, Nuclear Reactor Analysis, John Wiley and Sons, Inc., New York (1976).

25. S. Banerjee, S.R. Hatcher, A.D. Lane, H. Tamm, and J.I. Veeder, "Some Aspects of the Thorium Cycle in Heavy-Water-Moderated Pressure Tube Reactors", Nucl. Tech., 34,58 (1977).

26. M. Silverstri, I. Casgrande, A. Broggiato, C. Manicini, and A. Pedretti, "The CIRENE Project", Proceedings of the 4th International Conference on the Peaceful Uses of Atomic Energy, Geneva, 6-16 Sept., 5,269 (1971).

27. K. Wirtz, "Development of Advanced Power Reactors in the Federal Republic of Germany", in (J.M. Kallfetz and R.A. Karam, Ed.), Advanced Reactors: Physics, Design and Economics, Pergamon Press, New York, 1975.

28. G. Melese-d'Hospital, and M. Simnad, "Status of Helium-Cooled Nuclear Power Systems", Energy, 2,211 (1977).

29. M.M. El-Wakil, Nuclear Energy Conversion, Intext Educational Publishers, Scranton, Pa. (1971).

30. P. Engelmann, and W. Häfele, "The Base Program of the DeBeNeLux Fast Breeder Project", Proceedings of the 4th International Conference on the Peaceful Uses of Atomic Energy, Geneva, 6-16 Sept., 5,63 (1971).

31. R.J. Cerbone, "Physics of Gas Cooled Fast Breeder Reactors", in (J.M. Kallfetz and R.A. Karam, Ed.), Advanced Reactors: Physics, Design and Economics, Pergamon Press, New York, 1975.

32. A.F. Fritzsche, L.A. Lys, and G. Sarlos, "The Gas Cooled Fast Breeder Reactor", Proceedings of the 4th International Conference on the Peaceful Uses of Atomic Energy, Geneva, 6-16 Sept., 5,409 (1971).

33. J.W. Landis, E.W. O'Rorke, C.L. Rickard, P. Fortescue, A. Goodjohn, J.L. Everett, R.F. Walker, and D.B. Trauger, "Gas-Cooled Reactor Development in the United States of America", Proceedings of the 4th International Conference on the Peaceful Uses of Atomic Energy, Geneva, 6-16 Sept., 5,345 (1971).

34. Power Reactors '76, Nuclear Engineering International Supplement, April, 1976.

35. S. Banerjee, E. Critoph, and R.G. Hart, "Thorium as a Nuclear Fuel for CANDU Reactors", Can. J. Chem. Eng., 53,291 (1975).

36. W.B. Lewis, M.F. Duret, D.S. Craig, V.I. Veeder, and A.S. Bain, "Large-Scale Nuclear Energy from the Thorium Cycle", Proceedings of the 4th International Conference on the Peaceful Uses of Atomic Energy, Geneva, 6-16 Sept., 9,239 (1971).

37. L. Massimo, Physics of High Temperature Reactors, Pergamon Press, Oxford (1976).

38. J.A. Lake, R.A. Doncals, R.W. Rathburn, and H.C. Robinson, "Breeding Ratio and Doubling Time Characteristics of the Clinch River Breeder Reactor", in (J.M. Kallfetz and R.A. Karem, Ed.), Advanced Reactors: Physics, Design and Economics, Pergamon Press, New York, 1975.

39. N.C. Paik, R.A. Doncals and J.A. Lake, "Fuel and Blanket Management of the Clinch River Breeder Reactor", in (J.M. Kallfetz and R.A. Karam, Ed.), Advanced-Reactors: Physics, Design and Economics, Pergamon Press, New York, 1975.

40. F.L. Ribe, "Fusion Reactor Systems", Rev. Mod. Phys., 47,7 (1975).

41. D. Steiner, "The Technological Requirements for Power by Fusion", Nucl. Sci. Eng., 58,107 (1975).

42. R.L. Hirsch, "Status and Future Directions of the World Program in Fusion Research and Development", Ann. Rev. Nucl. Sci., 25,79 (1975).

43. E.T. Cheng, M.M.H. Rogheb and R.W. Conn, "Neutronics and Photonics Studies for the University of Wisconsin Laser Fusion Reactor Blanket", Trans. Am. Nucl. Soc., 26,504 (1977).

44. A.G. Cook and J.A. Maniscalco, "^{233}U Breeding and Neutron Multiplying Blankets for Fusion Reactors", Nucl. Tech., 30,5 (1976).

45. D.J. Bender and J.D. Lee, "The Potential for Fissile Breeding with the Fusion-Fission Hybrid Reactor", Trans. Am. Nucl. Soc., 23,24 (1976).

46. J.D. Lee, "Blanket Design for the Mirror Fusion-Fission Hybrid Reactor", Conf.-760733, Proceeding of the US-USSR Symposium on Fusion-Fission Reactors", Livermore, Calif., 13-16 July (1976).

47. S.F. Su, G.L. Woodruff and N.J. McCormick, "A High-Gain Fusion-Fission Reactor for Producing Uranium-233", Nucl. Tech., 29,392 (1976).

48. J.D. Lee, "Neutronics of Sub-Critical Fast-Fission Blankets for D-T Fusion Reactors", Proceedings of the Intersociety Energy Conversion Engineering Conference, San Diego, Calif., 25-29 Sept. (1972).

49. R.A. Krakowski, D.J. Dudziak, T.A. Oliphant and K.I. Thomassen, "An Engineering Design of a Linear Theta-Pinch Hybrid Reactor (LTPHR)", Trans. Am. Nucl. Soc., 21,61 (1975).

50. T.A. Parish and R.S. Spangler, "The Production of ^{233}U in Hybrid Fusion Reactor Blankets", Trans. Am. Nucl. Soc., 21,59 (1975).

51. A.G. Cook and J.A. Maniscalco, "^{233}U Breeding and Neutron Multiplying Blankets for Fusion Reactors", Trans. Am. Nucl. Soc., 23,25 (1976).

52. J.D. Lee, D.J. Bender, R.W. Moir and K.R. Schultz, "Mirror Hybrid-A Status Report", Conf. 760935, Proceedings of the 2nd Topical Meeting on the Technology of Controlled Nuclear Fusion, Richland, Wash., 21-23 Sept. (1976).

53. J.A. Maniscalco, "Fusion-Fission Hybrid Concepts for Laser Induced Fusion", Nucl. Tech., 28,98 (1976).

54. S.S. Rozhkov and G.E. Shatalov, "Thorium in the Blanket of Hybrid Thermonuclear Reactor", Conf. 760733, Proceeding of a US-USSR Symposium on Fusion-Fission Reactors, Livermore, Calif., 13-16 July (1976).

55. R.N. Horoshko, H. Hurwitz and H. Zmora, "Applications of Laser Fusion to the Production of Fissile Materials", Annals of Nucl. Ssci. and Eng., 1,64 (1975).

56. D.J. Bender and J.D. Lee, "Neutronics and Thermal-Hydraulic Analysis of a Fast Fission Blanket for a Fusion Reactor", Trans. Am. Nucl. Soc., 21,64 (1975).

57. E. Greenspan, "Fusion-Fission Hybrid Reactors for Tritium Breeding", Trans. Israeli Nucl. Soc., 3,20 (1975).

58. V.V. Kotov and G.E. Shatolov, "Gas-Cooled Blanket for a Hybrid Thermonuclear Reactor with Solid Lithium Containing Materials", Conf. 760733, Proceedings of a US-USSR Symposium on Fusion-Fission Reactors, Livermore, Calif., 13-16 July (1976).

59. J.A. Maniscalco, "A Conceptual Design for a Laser Fusion Hybrid", Conf. 760935, Proceedings of the 2nd Topical Meeting on the Technology of Controlled Nuclear Fusion, Richland, Wash., 21-23 Sept. (1976).

60. G.L. Woodruff and D.C. Quimby, "Fusion-Fission Neutronic Calculations for the Laser Solenoid", Conf. 760935, Proceedings of the 2nd Topical Meeting on the Technology of Controlled Nuclear Fusion, Richland, Wash., 21-23 Sept. (1976).

61. M. Steinberg, J. Powell, K. Batchelor, H. Takechashi, J. Blewett, T. Sheedan, H. Ludwig, V. Dang, P. Grand, O. Lazereth and H. Kont, "Linear Accelerator Breeder (LAB): A Preliminary Analysis and Proposal", BNL-50592, Brookhaven National Laboratory (Nov. 1976).

62. M. Bervovitch, H. Cormichael, G.C. Hanna and E.P. Hincks, "Yield of Neutrons per Interaction in U, Pb, W, and Sn by Protons of Six Energies Between 250 and 900 MeV Selected from Cosmic Radiation", Phys. Rev. C, 6,660 (1972).

63. D. West and E. Wood, "Neutron Yields from Protons and Deuterons of Momenta between 0.85 and 1.7 GeV/c Totally Absorbed in Lead", Can. J. Phys., 49,2061 (1971).

64. V.A. Barashenkov and V.D. Toneev, "Neutron Fluxes Generated by High Energy Protons in Thick Blocks of Uranium", Soviet Atomic Energy, 35,798 (1972).

65. V.A. Barashenkov, V.D. Toneev and S.E. Chigrinov, "Interaction of High Energy Deuteron Beams in Matter", Soviet Atomic Energy, 37,1256 (1974).

66. G.C. Tillet and A.R. Buhl, "Clinch River Breeder Reactor Breeding Characteristics", Nucl. Tech., 28,92 (1976).

67. C.J. Joseph, E. Datilleux, J. Contono, H. Eschrich, E. Schneider and J. Van Geel, "Operating Experience and Planned Improvements in Eurochemic Reprocessing Plant", Proceedings of the 4th International Conference on the Peaceful Uses of Atomic Energy, Geneva, 6-16 Sept., 8, 349 (1971).

68. K. Ehlers, J. Schlösser, K.G. Hackstein and E. Mertz, "Comparison of Uranium Fuel Cycles Using High and Low Enrichment in High Temperature Reactors", Proceeding of the 4th International Conference on the Peaceful Uses of Atomic Energy, Geneva, 6-16 Sept., 9,287 (1971).

69. H.L. Wyckoff and P. Greebler, "Definition of Breeding Ratio and Doubling Time", Nucl. Tech., 21,158 (1974).

70. C.T. Rombough and B.V. Koen, "Total Energy Investment in Nuclear Power Plants", Nucl. Tech., 26,5 (1975).

71. V.A. Maroni, R.D. Wilson and G.E. Staahl, "Some Preliminary Considerations of a Molten-Salt Extraction Process to Remove Tritium from Liquid Lithium Fusion Reactor Blankets", Nucl. Tech., 25,83 (1975).

72. A. Fodero, The Elements of Neutron Interaction Theory, MIT Press, Cambridge, Mass. (1961).

73. D.J. Rose and M. Clark, Jr., Plasmas and Controlled Fusion, MIT Press, Cambridge, Mass. (1961).

74. T. Kammash, Fusion Reactor Physics, Ann Arbor Science Publishers, Inc., Ann Arbor, Mich. (1976).

75. A.F. Henry, Nuclear Reactor Analysis, MIT Press, Cambridge, Mass. (1975).

76. K.O. Ott and R.C. Borg, "Derivation of Consistent Measures for the Doubling Time of Fast Breeder Fuel", Nucl. Sci. Eng., 62,243 (1977).

77. J. Darvas, P.A. Davenport, S. Forster, A. Knobloch, J.T.D. Mitchell and B. Sack, "Energy Balance and Efficiency of Power Stations with a Pulsed Tokamak Reactor", Jül-1304, Kernforshungsanlage, Jülich GmbH (1976).

78. J.R. Lamarsh, Introduction to Nuclear Reactor Theory, Addison-Wesley Publishing Co., Inc., Reading, Mass. (1972).

79. F.H. Tenney, "A Tokamak Hybrid Study", Conf. 760733, Proceedings of a US-USSR Symposium on Fusion-Fission Reactors, Livermore, Calif., 13-16 July (1976).

80. D.J. Bender, "Mirror Hybrid Reactor Optimization Studies", Conf. 760733, Proceedings of a US-USSR Symposium on Fusion-Fission Reactors, Livermore, Calif., 13-16 July (1976).

81. T.A. Parish, "Fusion Fission Studies at the University of Texas at Austin", Conf. 760733, Proceedings of a US-USSR Symposium on Fusion-Fission Reactors, Livermore, Calif., 13-16 July (1976).

82. D.E. Doonigi and R.L. Engel, "The Economics of Fusion-Fission Systems", Conf. 760733, Proceedings of a US-USSR Symposium on Fusion-Fission Reactors, Livermore, Calif., 13-16 July (1976).